



Springer Series in Synergetics

Editor: Hermann Haken

Synergetics, an interdisciplinary field of research, is concerned with the cooperation of individual parts of a system that produces macroscopic spatial, temporal or functional structures. It deals with deterministic as well as stochastic processes.

- Volume 1 **Synergetics** An Introduction 2nd Edition
By H. Haken
 - Volume 2 **Synergetics** A Workshop
Editor: H. Haken
 - Volume 3 **Synergetics** Far from Equilibrium
Editors: A. Pacault and C. Vidal
 - Volume 4 **Structural Stability in Physics**
Editors: W. Güttinger and H. Eikemeier
 - Volume 5 **Pattern Formation** by Dynamic Systems and **Pattern Recognition**
Editor: H. Haken
 - Volume 6 **Dynamics of Synergetic Systems**
Editor: H. Haken
 - Volume 7 **Problems of Biological Physics**
By L. A. Blumenfeld
 - Volume 8 **Stochastic Nonlinear Systems**
in Physics, Chemistry, and Biology
Editors: L. Arnold and R. Lefever
 - Volume 9 **Numerical Methods in the Study of Critical Phenomena**
Editors: J. Della Dora, J. Demongeot, and B. Lacolle
 - Volume 10 **The Kinetic Theory of Electromagnetic Processes**
By Y. L. Klimontovich
 - Volume 11 **Chaos and Order in Nature**
Editor: H. Haken
 - Volume 12 **Nonlinear Phenomena in Chemical Dynamics**
Editors: C. Vidal and A. Pacault
-

Nonlinear Phenomena in Chemical Dynamics

Proceedings of an International Conference
Bordeaux, France, September 7-11, 1981

Editors: C. Vidal and A. Pacault

With 124 Figures

Springer-Verlag Berlin Heidelberg New York 1981

Professeur Dr. *Christian Vidal*
Professeur Dr. *Adolphe Pacault*

Centre de Recherches Paul Pascal, Domaine Universitaire
F-33405 Talence Cédex, France

Series Editor

Professor Dr. Hermann Haken

Institut für Theoretische Physik der Universität Stuttgart, Pfaffenwaldring 57/IV
D-7000 Stuttgart 80, Fed. Rep. of Germany

ISBN-13:978-3-642-81780-9 e-ISBN-13:978-3-642-81778-6
DOI: 10.1007/978-3-642-81778-6

This work is subject to copyright. All rights are reserved, whether the whole or part of the material is concerned, specifically those of translation, reprinting, reuse of illustrations, broadcasting, reproduction by photocopying machine or similar means, and storage in data banks. Under § 54 of the German Copyright Law where copies are made for other than private use, a fee is payable to "Verwertungsgesellschaft Wort", Munich.

© by Springer-Verlag Berlin Heidelberg 1981
Softcover reprint of the hardcover 1st edition 1981

The use of registered names, trademarks, etc. in this publication does not imply, even in the absence of a specific statement, that such names are exempt from the relevant protective laws and regulations and therefore free for general use.

2153/3130-543210

Preface

An international conference titled *Nonlinear Phenomena in Chemical Dynamics* was held in Bordeaux on September 7-11, 1981. The present volume contains the text of lectures and abstracts of posters presented during the meeting.

This conference is part of a series of scientific multidisciplinary meetings in which chemistry is involved at various levels. Amongst the most recent ones let us mention Aachen 1979, Bielefeld 1979, New York 1979, Elmau 1981. In addition, this meeting is a direct extension of the first one that took place in Bordeaux in 1978 on the topic "Far from equilibrium: instabilities and structures," at the conclusions of which we could write (cf. *Far from Equilibrium*, Springer Series in Synergetics, Vol.3):

"The three key words, *far from equilibrium*, *instabilities* and *structures*, best illustrate the new concepts which emerge from the description of the dynamics of various systems relevant to many different research areas."

The present proceedings show how much these remarks have remained true, even though substantial progress has been achieved during the three last years. To get a deeper experimental knowledge of open reacting systems, to model and simulate reaction-diffusion systems, to develop the mathematical theory of dynamical systems, these are the main directions in current investigations. They give evidence for general behaviours that are related to the influence of the system's surroundings rather than the specific nature of the population forming the system: instabilities, non-equilibrium transitions, periodicity of evolution, hysteresis and multistability, chaotic behaviour, etc. For this reason many conclusions of the studies published in this volume have a far-reaching effect beyond the scope of chemical systems, to which this conference has voluntarily been restricted to preserve deeper discussions.

In spite of this beautiful harvest of results, it seems to us that one field of investigation is still standing back, namely the study of spatial structures that emerge spontaneously in non-equilibrium reacting systems. It is most likely that the forthcoming years should bring new lights on the various aspects of this important question.

We would like to thank the Centre National de la Recherche Scientifique for financial support, without which this meeting would have not been held. We express special thanks to Mrs Maurat, who helped us so efficiently in the organization of the meeting and preparation of the proceedings.

Bordeaux, September 1981

C. Vidal · A. Pacault

Preface

Du 7 au 11 Septembre 1981 s'est tenu à Bordeaux un Colloque International du C.N.R.S. intitulé *Phénomènes non-linéaires de la dynamique chimique*. Le présent volume rassemble le texte des conférences et le résumé des affiches qui y furent présentées.

Cette réunion fait partie d'un ensemble de manifestations scientifiques pluridisciplinaires où la Chimie est partie prenante à des degrés divers. Parmi les plus récentes, citons par exemple : Aix-la-Chapelle 1979, Bielefeld 1979, New-York 1979, Elmau 1981. En outre, ce Colloque est dans le prolongement direct d'une première réunion, organisée à Bordeaux en 1978 sur le thème : Loin de l'équilibre : instabilités et structures. A l'issue de celle-ci nous écrivions (cf. *Far from equilibrium*, Synergetics vol 3) :

"L'élaboration d'une description dynamique - et non plus statique - des phénomènes fait surgir peu à peu des concepts communs à la plupart des disciplines traditionnelles, pour autant que les évolutions considérées aient lieu *loin de l'équilibre*, auquel cas des *instabilités* peuvent apparaître et donner naissance à des *structures*."

Les comptes-rendus présentés ici montrent combien de tels propos demeurent d'actualité, même si - et qui pourrait s'en étonner - des progrès substantiels ont été réalisés durant ces trois dernières années. L'approfondissement de notre connaissance expérimentale des milieux ouverts sièges de transformations chimiques, la modélisation et la simulation numérique de l'évolution des systèmes où interviennent simultanément réactions et diffusion, le développement de la théorie mathématique des systèmes dynamiques constituent les axes de recherche principaux. Ils débouchent sur la mise en évidence de comportements généraux, plus liés à l'environnement qu'à la nature de la population étudiée : instabilités, transitions de non équilibre, périodicités, hystérèses et multistabilités, évolutions chaotiques, etc. C'est pourquoi le caractère général et la portée de certaines conclusions des travaux publiés dans cet ouvrage vont bien au-delà du seul domaine des *systèmes chimiques*, auquel le thème de ce Colloque était volontairement restreint afin de permettre des discussions en profondeur.

En face d'une belle moisson de résultats que ce volume engrange, il est un secteur de recherche qui semble, pourtant, marquer le pas aujourd'hui : celui des structures spatiales prenant spontanément naissance au sein d'un milieu réactionnel hors d'équilibre. Les années à venir devraient, sans nul doute, apporter des éclaircissements sur les différents aspects de cette importante question.

Nous tenons à remercier le Centre National de la Recherche Scientifique sans le concours financier duquel ce Colloque n'aurait pu avoir lieu. Nous exprimons notre reconnaissance à notre secrétaire, Mme Maurat, qui nous a efficacement aidés à organiser cette réunion et à en préparer les actes.

Contents

Part I. General Nonlinear Behavior

Phenomenes nonlineaires de la dynamique chimique: allocution d'ouverture By P. Glansdorff	2
La Chimie à la croisée des disciplines traditionnelles. Comportements identiques de populations différentes. By A. Pacault, F. Carmona and J.J. Piau (With 7 Figures)	5
Dynamical Systems Described by Discrete Maps with Noise By H. Haken and A. Wunderlin	15
Thermokinetic Oscillations and Multistability in Gas-Phase Oxidations By P. Gray, J.F. Griffiths, and S.M. Hasko	20

Part II. Weak Turbulence

Chemical Kinetics and Differentiable Dynamical Systems By D. Ruelle	30
Topology of Chaos in a Chemical Reaction By J.C. Roux and H.L. Swinney (With 5 Figures)	38
Experiments on Chaos in a Continuous Stirred Reactor By J.L. Hudson, J. Mankin, J. McCullough, and P. Lamba (With 9 Figures)	44
Chemical Kinetics as an Experimental Field for Studying the Onset of Turbulence. By C. Vidal (With 7 Figures)	49
Transition vers la turbulence par intermittence. By Y. Pomeau	63
Bifurcation of <i>Motifs</i> in Families of <i>Mixed Two-Vector Fields</i> By C. Lobry and R. Lozi (With 7 Figures)	67
Bifurcations élémentaires—successions et interactions By G. Iooss (With 2 Figures)	71
Chaos and Chemistry. By O.E. Rössler	79
Evolution of Chaos and Power Spectra in One-Dimensional Maps By H. Mori (With 6 Figures)	88
Tests of the Period-Doubling Route to Chaos. By M.J. Feigenbaum	95

Part III. Stochastic Analysis

Thermal Fluctuations in Nonlinear Chemical Systems By G. Nicolis, F. Baras, and M. Malek Mansour (With 2 Figures)	104
Fluctuations in Non-Equilibrium Phase Transitions: Critical Behavior By P. Hanusse	115
Critical Exponents of a Pure Noise Induced Transition, Nonlinear Noise and Its Effect on an Electrohydrodynamic Transition in Nematics By R. Lefever and W. Horsthemke	120

Part IV. Critical Phenomena

Critical Slowing Down of Chemical Reactions Near Thermodynamic Critical Points. By I. Procaccia	128
Metastability and Nucleation in Chemical Systems with Multiple Steady States. By J. Boissonade (With 4 Figures)	134

Part V. Coupling of Oscillators

Synchronization of a Chemical Oscillation by Periodic Light Pulses By E. Dulos (With 13 Figures)	140
Electrically Coupled Belousov-Zhabotinsky Oscillators: A Potential Chaos Generator. By M.F. Crowley and R.J. Field (With 6 Figures)	147

Part VI. Reaction-Diffusion Problems

The Rotor as a Phase Singularity of Reaction-Diffusion Problems and Its Possible Role in Sudden Cardiac Death. By A.T. Winfree (With 1 Figure)	156
Chemical Waves in the Iodate-Arsenous Acid System By A. Hanna, A. Saul, and K. Showalter (With 7 Figures)	160
Mécanisme réactionnel fondé sur une étude expérimentale expliquant des instabilités interfaciales liées à des réactions chimiques By E. Nakache and M. Dupeyrat (With 3 Figures)	166

Part VII. Biochemical Processes

Complex Dynamic Structures By B. Hess, E.M. Chance, A.R. Curtis, and A. Boiteux (With 2 Figures)	172
Two Topics in Chemical Instabilities: I. Periodic Precipitation Processes; II. Resonances in Oscillatory Reactions and Glycolysis By J. Ross	180

Part VIII. From Bistability to Oscillations

Bistability in a C.S.T.R.: New Experimental Examples and Mathematical Modeling. By I.R. Epstein, C.E. Dateo, P. De Kepper, K. Kustin, and M. Orbán (With 4 Figures)	188
Chlorite Oscillators: A Result of the Cross-Shaped Phase Diagram Technique By P. De Kepper (With 4 Figures)	192

A New Type of Chemical Oscillator: Potential Oscillation and Bistability on a Platinum Electrode in some Aqueous Hydrogen-Halogen (ATE) Pumped Systems. By M. Orbán and I.R. Epstein (With 2 Figures)	197
Constrained and Continuously Pumped Chemical Systems with Emphasis on Conditions for Bistability. By R.M. Noyes (With 1 Figure)	201
Perturbation of Bromate Oscillators By E. Körös, M. Varga, and G. Putirskaya (With 4 Figures)	207
Periodic Reactions with Bromate II: Verification of Selection Criteria of Organic Radicals Oscillating Without Catalysts By J. Chopin-Dumas and P. Richetti (With 3 Figures)	213
<i>Part IX. Mathematical Modeling</i>	
On Scaling the Oregonator Equations By J.J. Tyson (With 3 Figures)	222
The Behaviour of a Multistable Chemical System Near the Critical Point By K. Bar-Eli (With 9 Figures)	228
Recent Developments in the Theory of Stoichiometric Networks and Application to the Belousov-Zhabotinsky System By B.L. Clarke (With 4 Figures)	240
<i>Part X. Poster Abstracts</i>	
Stratification Phenomena in Corrosion Scales: Towards a Nonlinear Interpretation. By G. Bertrand, J.-M. Chaix, K. Jarraya, and J.-P. Larpin (With 2 Figures)	248
Nucleation Process in the Two-Dimensional X^3 Schlögl Model By A. Blanché and P. Hanusse	250
From Bistability to Oscillations: A Phase Diagram Approach. Application to the Belousov-Zhabotinsky Reaction By J. Boissonade and P. De Kepper	251
Numerical Simulations of Surface Reactions By M. Bouillon, R. Dagonnier, P. Dufour, and M. Dumont	252
On the Preoscillatory Period of the Belousov-Zhabotinsky Reaction: A Search for Intermediates. By M. Burger and K. Rácz	253
Non-Equilibrium Phase Transition of the Intercalation Process By T. Butz, A. Hübler, and A. Lerf (With 1 Figure)	254
Pseudo-Steady States in Solid-Liquid Systems By M. Cournil, P. Galtier, and F. Conrad	255
$A + 2B = 3B$ Kinetics Producing all or Flip or None Stimulus Response in a Cell Model, and Strategies for a Chemical Implementation of such Kinetics By P. Decker and O. Saygin (With 1 Figure)	256
Topological Order in 2D Chemical Systems By C. Dewel, D. Walgraef, and P. Borckmans	257
Bifurcation of Multiple Limit Cycles in Plane Quadratic Mass-Action Systems By C. Escher	258

Belousov-Zhabotinsky System: Mechanism of the Ce^{3+} /Bromate Reaction By H.D. Försterling, H.J. Lamberz, and H. Schreiber	259
The Legitimacy of the Quasi-Steady State Approximation in Enzyme Kinetics: A Singular Perturbation Approach. By G. Fritzsche and M.S. Seshadri ...	260
Nonlinear Phenomena in Stirred Flow Systems of Mn^{2+} and Acidic Bromate By W. Geiseler	261
On Phase Transitions in Schlögl's Second Model. By P. Grassberger	262
A Nonlinear Phenomenon of Chemical Dynamics in Geology: The Case of Skarns By B. Guy	263
The Prepattern Theory of Mitosis: Spatial Dissipative Structures in the 3-Dimensional Sphere. By A. Hunding	264
Mechanistic Study of the Briggs-Rauscher Reaction By P. De Kepper and I. Epstein (With 1 Figure)	265
Multiwavelength Analysis of Linear and Nonlinear Kinetics in the CSTR By H. Lachmann	266
Inhomogeneous Fluctuations and Bifurcations in Nonlinear Chemical Systems By H. Lemarchand and G. Nicolis	267
Temperature-Compensated Epigenetic Oscillations: Timing of Cell Division Cycles and Circadian Rhythms? By D. Lloyd and S.W. Edwards (With 1 Figure)	268
Chaotic Behavior of E.H.D. Instability for an Insulating Liquid Subjected to Unipolar Injection. By B. Malraison and P. Atten	269
Effect of Light Intensity Fluctuations on a Real Photochemical Reaction: The Thermoluminescence of Fluorescein in Boric Acid Glass By J.C. Micheau, W. Horsthemke and R. Lefever (With 1 Figure)	270
Bifurcation Theoretic Approach for Strong Field Photodissociation Phenomenon By N.K. Rahman	271
A Linear Method to Analyze a Nonlinear Oscillator: Driving the Glycolytic Oscillator by Sinusoidal Temperature Cycles By K.A. Rinast, R. Heringer, R. Joerres, T. Kreuels, W. Martin and K. Brinkmann	272
Bursting Phenomena in the Belousov-Zhabotinsky Reaction By J. Rinzel and W.C. Troy	273
Experimental Investigations and Model Simulations for Studying the Influence of Noise and External Disturbances on the Behavior of the Belousov- Zhabotinsky Reaction. By P.G. Sørensen (With 1 Figure)	274
Linearization Procedure and Nonlinear Systems of Differential and Difference Equations. By W.-H. Steeb	275
Reversible and Non-Reversible Modifications of Enzyme Systems Activity by Electric Field. By J.M. Valleton, E. Selegny, and J.C. Vincent	276
A Dynamic Regime with Structured Fourier Spectrum By C. Vidal and A. Rossi (With 1 Figure)	277
<i>Index of Contributors</i>	279

Part I

General Nonlinear Behavior

Phénomènes nonlinéaires de la dynamique chimique: allocution d'ouverture

Paul Glansdorff

Faculté des Sciences
Université Libre de Bruxelles

Nombreux sont ceux qui, dans cette assemblée, ont eu le privilège d'assister au précédent colloque intitulé : "Loin de l'équilibre. Instabilités et Structures" et en ont conservé un souvenir durable. Comme pour la présente réunion, ce colloque avait été organisé par le Centre National de la Recherche Scientifique, mieux connu par son sigle C.N.R.S., à l'initiative des mêmes animateurs, les professeurs Pacault et Vidal. On trouverait difficilement meilleure garantie de succès. Au surplus, pour ceux qui n'ont pas eu ce privilège, on peut présumer que la publication accélérée des compte-rendus les aura aussi édifiés. C'était non loin d'ici, au Centre Paul Pascal, il y aura déjà trois ans dans quelques jours.

Mais faut-il dire : "Déjà" avec la nostalgie des instants heureux révolus, ou, tout au contraire, "Seulement", en témoignage de la diversité et de l'abondance des progrès accomplis dans le monde, depuis cette initiative exemplaire de stimulation scientifique? Reconnaissons qu'en cette circonstance au moins, la sagesse nous impose le second terme de l'alternative.

Tout avait commencé, comme on dit aujourd'hui, avec un nouvel essor de la Thermodynamique des phénomènes irréversibles, dès qu'il fut possible d'en déduire un critère d'évolution suffisamment général pour contribuer à l'étude du comportement dans le domaine régi par des lois non linéaires. Il devait en résulter directement une extension de la notion de stabilité aux processus physico-chimiques hors d'équilibre, dans un état stationnaire ou oscillant. L'unification de ce concept devait bientôt être suivie par celle des méthodes d'application avec l'emploi des propriétés de la production d'entropie d'excès et de l'énergie cinétique d'excès comme fonctions de Liapounoff, représentatives respectivement des effets dissipatifs et convectifs. La découverte par ces méthodes des états critiques de stabilité marginale, générateurs de bifurcations, ou parfois simplement leur redécouverte, mais assortie d'une signification physique clarifiée, devait aboutir finalement au concept thermodynamique nouveau et unifié de structure dissipative.

Depuis l'exemple en hydrodynamique des cellules de Bénard engendrées par l'apparition d'effets convectifs, jusqu'à celui du cycle limite provoqué par catalyse en cinétique chimique et en particulier dans les réactions d'intérêt biologique, les causes d'instabilité accompagnées de changement de branche relèvent désormais d'un mécanisme commun. Ce dernier se manifeste régulièrement sous la forme d'un conflit entre deux tendances opposées. L'une est stabilisante et représentative d'effets dissipatifs déjà connus par la théorie linéaire, tandis que l'autre est déstabilisante et directement responsable des effets de non linéarité.

Ces différents résultats provoquèrent bientôt un regain d'intérêt envers les problèmes d'évolution sous leurs diverses formes mathématiques, physiques, chimiques et biologiques prolongées parfois jusqu'à des aspects écologiques ou épistémologiques.

Mais fondamentalement, il semble que l'actualité du sujet provient surtout de la perspective offerte par l'étude du comportement des structures dissipatives, d'observer la manifestation spontanée d'un ordre d'origine dynamique, donc issu des lois du monde physique, et qui soit compatible avec l'ordre biologique.

A considérer le développement actuel dont le présent Colloque apporte un témoignage direct, il est permis d'affirmer que du côté de la dynamique chimique, ce fut une explosion. Le terme n'est pas exagéré puisque toutes les évocations qui précèdent appartiennent déjà au passé, et font maintenant partie du patrimoine commun de la Science.

Les problèmes qui se posent à présent vont beaucoup plus loin, car ils concernent les lois qui régissent la succession des bifurcations, leur multiplicité, leur classification sous le rapport de la stabilité, leurs interactions et leur aptitude à engendrer tantôt des structures stables de plus en plus élaborées, tantôt à provoquer au contraire un retour au chaos.

C'est qu'en effet, après la découverte des structures dissipatives est apparue celle des états attracteurs chaotiques de non équilibre, sous l'influence d'effets sous harmoniques, mis notamment en évidence dans les travaux récents de Feigenbaum. Après cela faudra-t-il encore distinguer entre différentes catégories de chaos et procéder à leur classement. Jusques à quand enfin, le terme d'une telle entreprise?

Je me contenterai sur ce point d'évoquer la remarquable anticipation inspirée en 1909 au Directeur de l'Académie Française Frédéric Masson, dans sa réponse au discours de réception de Henri Poincaré, l'authentique et génial inventeur de nos cycles limites : "Est-ce à dire, Monsieur, que vous doutiez plus de la Science que de la Vérité? Ni de l'une, ni de l'autre : mais celle-ci s'éloigne constamment devant celle-là et, à proportion que l'homme franchit une étape, les espaces qu'il devra parcourir reculent devant lui; par delà la steppe dont son regard embrasse l'étendue, d'autres l'attendent, et toujours d'autres, car celui-là seul est assuré d'arriver à son but qui en est resté au rudiment et qui l'a appris par coeur....".

Assurément, nous n'en sommes pas restés aux rudiments, mais les nombreux progrès que ces Journées vont nous faire connaître, ne pourront pas m'empêcher de constater que dans le domaine des applications à la biologie, l'époque est encore bien lointaine, où notre Science permettra de découvrir si, finalement, l'homme descend du singe, ou au contraire si, politiquement au moins, il y remonte.

Mis à part, l'orgueil d'une telle exigence, nous aurons encore l'occasion d'apprécier une autre catégorie de progrès importants dans le domaine de l'analyse stochastique, appliquée à l'étude des fluctuations dans le domaine voisin d'un état de non équilibre. Le principal souci consiste à établir une théorie de l'instabilité qui permette d'interpréter le mécanisme d'apparition d'un ordre à l'échelle macroscopique.

L'étude de l'influence des fluctuations extérieures, celle des transitions de phase de non équilibre, avec élaboration de diagrammes de phases, relatifs cette fois à la dynamique chimique loin de l'équilibre, l'influence de la non-linéarité dans l'étude des processus biochimiques, sont autant de sujets en pleine évolution dont nous attendons d'importants résultats.

On aura sans doute observé dans cette brève allocution, un souci de mettre en relief la rapidité exceptionnelle des progrès accomplis au cours d'une période aussi courte. Pour terminer je voudrais accentuer davantage encore ce caractère en l'opposant à l'évolution exceptionnellement lente du progrès lorsqu'il se rapporte à l'homme dans la Société.

Il y a déjà bien longtemps que le biologiste Pasteur, ayant à congratuler un mathématicien de sa génération Joseph Bertrand, ainsi qu'un chimiste Jean-Baptiste Dumas - vous voyez que nous restons ainsi devant des figures particulièrement éminentes des spécialités qui nous occupent - s'exprima en ces termes :

"S'il m'était permis de terminer par une de ces idées générales qu'aimait Monsieur Dumas, je dirais que vous et lui vous êtes la personnification de ce que peuvent atteindre à notre époque les existences laborieuses. Le vrai mérite dans la vraie démocratie, voilà ce que vous représentez tous deux. La vraie démocratie est celle qui permet à chaque individu de donner son maximum d'efforts dans le monde.....Pourquoi faut-il qu'à côté de cette démocratie féconde, il en soit une autre stérile et dangereuse qui, sous je ne sais quel prétexte d'égalité chimérique rêve d'absorber et d'anéantir l'individu dans l'Etat? Cette fausse démocratie a le goût, j'oserais dire le culte de la médiocrité. Tout ce qui est supérieur lui est suspect...On pourrait définir cette démocratie : la ligue de tous ceux qui veulent vivre sans travailler, consommer sans produire, arriver aux emplois sans y être préparés, aux honneurs sans en être dignes".

Mesdames et Messieurs, il y a à peu près cent ans que ces paroles ont été prononcées par Pasteur et notre question se pose à nouveau : Faut-il dire "Déjà" ou "Seulement". Je vous laisse juges.

La Chimie à la croisée des disciplines traditionnelles. Comportements identiques de populations différentes

A. Pacault, F. Carmona, J.J. Piaud

Centre de Recherche Paul Pascal (C.N.R.S.)
Domaine Universitaire F-33405 Talence Cédex

"L'amour de l'étude de la Nature suppose dans l'esprit deux qualités qui paraissent opposées, les grandes vues d'un génie ardent qui embrasse tout d'un coup d'oeil, et les petites attentions d'un instinct laborieux qui ne s'attache qu'à un seul point".

BUFFON [1] 1749

1. Introduction

Deux attitudes philosophiques président au développement des recherches en discussion au cours de ce colloque.

- L'une est analytique et spécifique. Elle conduit à une description de plus en plus précise à mesure que s'affinent les techniques d'analyse ; elle privilégie l'objet dont la connaissance est d'autant meilleure qu'il est plus réduit et qui, étant de mieux en mieux connu, est de moins en moins facile à classer. Cette attitude favorise la connaissance du particulier.

- L'autre est synthétique et totalisante. Elle conduit à la définition de comportements indépendants des populations qui les présentent, c'est-à-dire que le rôle des contraintes est plus important que le choix des réponses*. Cette attitude favorise la connaissance du général.

Ces deux attitudes sont complémentaires et leur adoption dépend à la fois de l'objectif poursuivi et de la psychologie de l'observateur. Elles permettent de classer en deux grandes catégories les résultats des recherches entreprises pour mieux comprendre donc pour mieux prévoir les phénomènes non linéaires.

Illustrons par des exemples limités, ou presque, à la dynamique chimique les phrases trop lapidaires qui précèdent.

La première attitude est celle des cinéticiens. Un exemple en est donné par l'analyse fine et réussie de la réaction de Belousov-Zhabotinskii conduisant au schéma réactionnel F.K.N. [2]. A partir de 4 réactants (bromate de potassium, acide malonique, sulfate de cérium, acide sulfurique), on observe ou on imagine 14 espèces chimiques qui réagissent les unes avec les autres en 13 étapes réactionnelles. Ce schéma compliqué est en accord avec les observations. On peut cependant le simplifier sous le nom d'Oregonator [3] et le ramener à cinq étapes et 3 espèces intermédiaires, sans pour autant perdre beaucoup d'informations.

Une étude du même genre a été faite pour expliquer la réaction entre les espèces chimiques : iodate de potassium, eau oxygénée, acide malonique, acide sulfurique, sulfate de manganèse [4,5].

Ainsi, une démarche réunissant les ressources de l'analyse chimique avec ses moyens les plus perfectionnés et celles de l'imagination enrichies par une bonne pratique de la cinétique réactionnelle, permet de connaître de manière de plus en plus approfondie une réaction chimique bien particulière.

*Le vocabulaire utilisé est défini en 76-2 et 76-6.

La deuxième attitude, qui est plutôt celle des thermodynamiciens, sous-tend les travaux que j'ai dirigés ou encouragés. Elle est illustrée ici par des exemples pris pour simplifier parmi ces derniers* et résumés dans le tableau I. Il réunit quelques comportements généraux (dont l'appellation seule montre bien qu'ils ne sont pas spécifiquement chimiques) et les références des travaux s'y rapportant, en spécifiant le type de population ayant ces comportements.

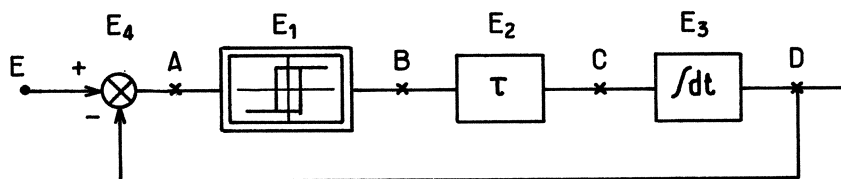
2. Analogie entre les comportements de populations de molécules et de populations d'électrons

Les comportements généraux des systèmes chimiques rassemblés dans le tableau qui suit sont analogues à ceux d'asservissements possédant une non linéarité qu'ils soient mécanique, hydraulique, pneumatique, fluïdique, thermique, électronique [6]. Des systèmes électroniques, sièges de certains de ces comportements, sont classiques. Certains ont déjà été décrits à propos de systèmes chimiques [7,8,9,10].

Nous proposons, ici, un circuit électronique (Fig. 1 et annexe) ayant la particularité de n'avoir *qu'un seul élément non linéaire* - plus ou moins avec hystérèse - associé à des éléments linéaires classiques - constante de temps, intégrateur, sommateur. Ces éléments sont eux-mêmes constitués de selfs, capacités, résistances, diodes et transistors dont les valeurs sont ajustables. Ce sont autant de contraintes imposées par l'observateur à une population d'électrons du circuit commandée par un potentiel imposé - autre contrainte - en un point bien déterminé du circuit. La réponse est un potentiel** mesuré en un point défini du circuit.

Décrivons quelques-uns des comportements observables avec ce montage.

The circuit (Fig. 1) involves the following elements : a nonlinear element E_1 ; followed by a first-order element E_2 with time constant τ , and an integrator E_3 . The complete circuit involves a negative feedback and a sommatior E_4 .



The following behaviours can be observed :

2.1 Bistability

The nonlinear element (E_1) is first considered alone. The constraint is the voltage at point A and the response is the voltage at point B. The relationship between those two voltages is given in the next figure.

* L'occasion m'est ainsi donnée de rappeler à des lecteurs monolingues que les publications en anglais ne sont pas les seules intéressantes.

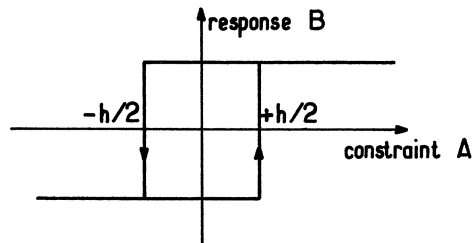
** Qu'un potentiel soit à la fois réponse et contrainte n'étonnera pas ceux habitués à considérer la variable température - contrainte constante imposée par un thermostat au réacteur, siège d'une réaction chimique périodique dont la réponse est une température temporellement périodique.

- TABLEAU I -

Quelques grandes classes de comportements	Type de populations		
	Molécules	Molécules et photons	Bactéries
Stationnarité. Multistationnarité. Transitions entre états	<u>72-2</u> ; 76-1 ; 76-3 ; <u>77-1</u> ; <u>77-4</u> ; 78-4 ; <u>80-8</u> ; <u>81-12</u> ;		
Périodicité temporelle, cycle limite	<u>72-1</u> ; <u>73-1</u> ; <u>73-2</u> ; 75-1 ; 76-4 ; 77-2 ; 77-3 ; 78-5 ; <u>79-3</u> ; 80-1 ;		76-8
Origine des oscillations temporelles ; thermique, chimique	77-5 ; 78-6 ; 79-2 ; 80-6 ;		
Critères d'existence des réactions chimiques périodiques	81-11		
Diagramme d'états dans l'hyperespace des contraintes	75-2 ; 76-5 ; 78-3 ;		
Diagramme croisé : prévision des états stationnaires et des cycles limites	80-3 ; 81-9 ;		
Excitabilité	76-3		
Régulation	78-4		
Rythmes - synchronisation	75-1 ; 75-3 ; 81-8 ;	79-1	81-8
Bruit		78-7 ; 78-12	
Turbulence chimique	<u>76-7</u> ; 79-4 ; 80-2 ; 80-5 ; 80-7 ; 81-2 à 81-7 ;		
Fluctuations	<u>78-8</u> ; <u>78-14</u> ; <u>81-1</u> ;		
Interaction, réaction-diffusion	<u>78-11</u> ; <u>81-10</u> ;		

- Les références non soulignées sont relatives à des travaux expérimentaux

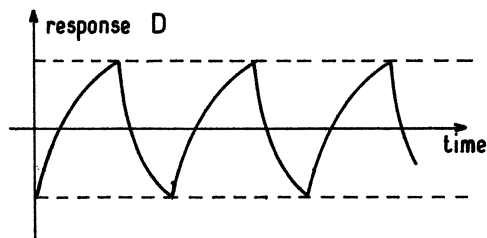
- Les références soulignées sont relatives à des travaux de simulation sur ordinateur.



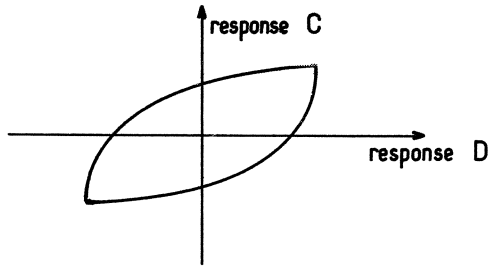
There is a bistability when the constraint is between the values $-h/2$ and $+h/2$.

2.2 Temporal periodicity, limit cycle

The nonlinear element is associated to the integrator (E_3 ; B and C connected) with the negative feedback. The constraint is now the voltage at point E and the response is the voltage at D. Relaxation oscillations are then observed whatever the constraint is.

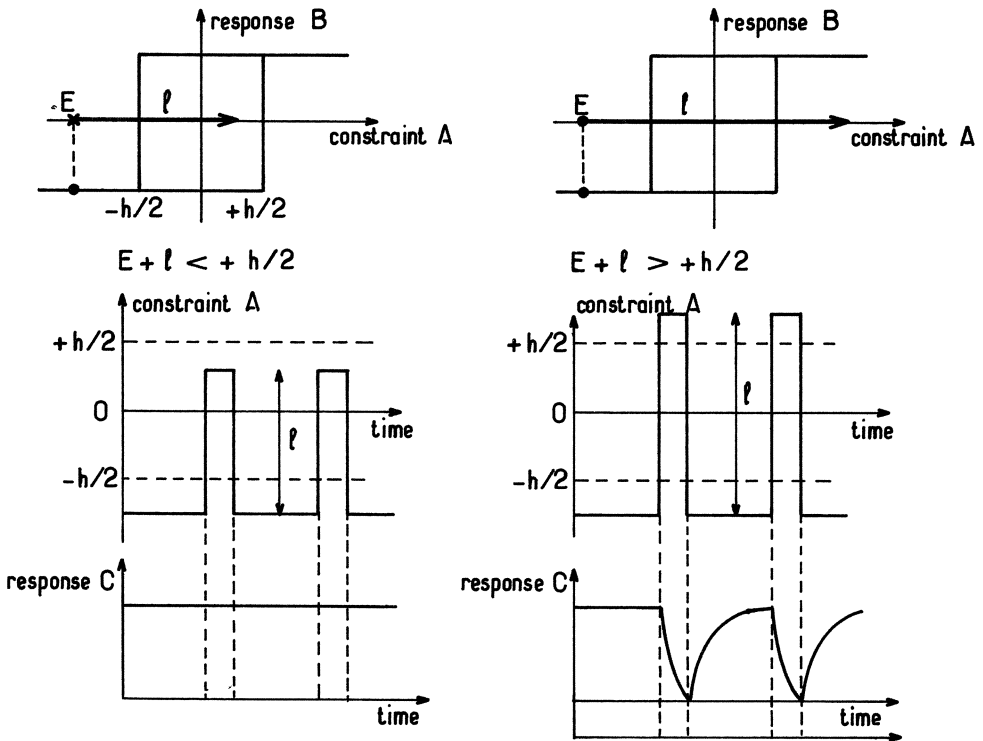


Inserting the first order element E_2 between B and C, the system still oscillates at frequency ω_0 and a limit cycle is observed in the plane defined by the response at C, which is the time derivative of the response D.



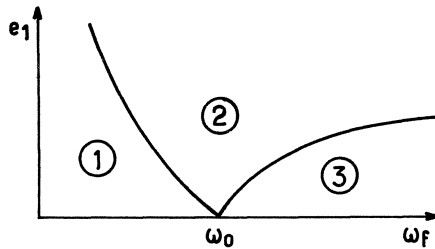
2.3 Excitability

The nonlinear element is associated to the first-order element and there is no feedback. The constraint is the voltage at point A and the response is the voltage at point C. The constraint is a pulse of height l superposed on a continuous voltage E such that the nonlinear element shows single stability. E being constant, the response depends on the value of l .



2.4 Synchronization

The complete circuit is used with the negative feedback. The constraint is a sine voltage at E and the response is the voltage at point D. Let e_1 and ω_f be the amplitude and the frequency of the constraint : the response depends on both e_1 and ω_f . Its behaviour is described in the next figure.



- In region ① : the response is a combined oscillation (beats), the shape of which depends on ω_f and e_1 .
- In region ② : the response is an oscillation with frequency ω_f : there is synchronisation between the oscillating constraint and the oscillating response.
- In region ③ : the response is an oscillation at free oscillation frequency ω_0 , whatever ω_f and e_1 of the constraint are.

3. Conclusion

On observe des comportements identiques - bistabilité ; oscillations de relaxation, cycle limite ; excitabilité, synchronisation -* avec des populations différentes - molécules ou électrons. La nature de la population s'efface donc devant la prépondérance de son environnement contrôlé (ensemble des contraintes qui lui sont imposées). On comprend une telle conclusion lorsque les populations ne se transforment pas, ne changent pas de nature, ce qui est le cas des électrons dans un circuit électrique ou des molécules d'un fluide dans une conduite (phénomènes hydrodynamiques). On la comprend moins lorsque les espèces chimiques en présence se transforment en réagissant.

En effet, la transformation de molécules différentes par réaction entre elles dépend souvent de leur nature, de leur structure, "de leur hérédité", plus que du milieu réactionnel. Il faut sans doute voir dans la nature ionique des espèces intervenant dans les réactions étudiées au cours de ce Colloque, la raison de la prépondérance de l'environnement. En effet, la nature de l'ion (Ce^{+4} , Mn^{+2} , BrO_3^- ...) conditionne surtout ses propriétés électriques globalement résumées par le potentiel d'oxydation ou d'oxydo-réduction. Ceci est confirmé par le choix qu'on peut en faire comme critère de sélection des ions susceptibles des comportements précédemment décrits [81-11]. On constate donc que l'environnement joue un rôle d'autant plus grand que la molécule est moins structurée.

Au niveau de description macroscopique des comportements de populations moléculaires susceptibles de se transformer, apparaissent déjà les aspects complémentaires héréditariste et environnementaliste.

Peut-on, enfin, espérer tirer de l'analogie de comportements de populations de molécules et d'électrons une représentation générale susceptible de les prévoir ?

Chaque élément électronique des montages présentés est décrit par une équation contenant les variables caractéristiques des circuits. Faisons abstraction de leur sens physique et ne considérons plus ces équations que comme des représentations mathématiques d'un bistable, d'une rétroaction, d'une constante de temps etc., dont l'association judicieuse conduit, comme on l'a vu, aux comportements recherchés.

Considérons alors un phénomène quelconque - hydrodynamique, électrique, chimique, biologique - ayant qualitativement les comportements déjà décrits, faisons correspondre aux variables mathématiques les variables physiques pertinentes représenta-

* Cette liste n'est pas exhaustive, le circuit électronique présentant encore d'autres comportements.

tives du phénomène ; les équations ainsi obtenues pourraient avoir un caractère de prévision telle qu'on pourrait les considérer comme une représentation quantitative satisfaisante.

L'analogie originelle disparaîtrait alors, ayant joué son rôle unificateur car l'efficacité de l'analogie se mesure à sa disparition [11].

Cette démarche, relativement classique en automatique, ne semble pas avoir été utilisée en chimie.

Cette voie de recherche, conforme à la seconde attitude évoquée dans l'introduction, mérite peut-être d'être suivie.

References

- ¹ Buffon, *Histoire naturelle, générale et particulière*, t.1, 4 (1749)
- ² R.F. Field, E. Körös, R.M. Noyes, J.A.C.S. 94, 1394 ; 8649 (1972)
- ³ R.F. Field, R.M. Noyes, J. Chem. Phys. 60, 1877 (1974)
- ⁴ P. de Kepper, I.R. Epstein, J.A.C.S. (1981) à paraître
- ⁵ R.M. Noyes, S.D. Furrow, J.A.C.S. (1981) à paraître
- ⁶ J.Ch. Gille, P. Decaulne, M. Pelegrin, *Systèmes asservis non linéaires*, Dunod (1975)
- ⁷ J.P. Gollub, T.O. Brunner, B.G. Dauly, Science 200, 48 (1978)
- ⁸ J.P. Gollub, E.J. Romer, J.E. Socolar, J. Statistical Physics 23, 321 (1980)
- ⁹ U.F. Franck, *Angewandte Chemie* 17, 1 (1978)
- ¹⁰ U.F. Franck, *Kinetics of Physicochemical Oscillations*, Aachen III, 675 (1979)
- ¹¹ *L'analogie*, t.I (1980) et t.II Recherches interdisciplinaires (1981), Maloine Doïn Edit.

1972

- 1 P. HANUSSE - "De l'existence d'un cycle limite dans l'évolution des systèmes ouverts" - C.R. Acad. Sc. Paris, t.274C, 1245 (1972)
- 2 C. VIDAL - "Sur une structure d'états stationnaires multiples" - C.R. Acad. Sc. Paris, t.274C, 1713 (1972)
- 3 C. VIDAL - "Sur un nouveau type de structure dissipative spatiale" - C.R. Acad. Sc. Paris, t.275 C, 523 (1972)

1973

- 1 P. HANUSSE - "Etude des systèmes dissipatifs chimiques à deux et trois espèces intermédiaires" - C.R. Acad. Sc. Paris, t.277 C, 263 (1973)
- 2 P. HANUSSE - "Simulation des systèmes chimiques par une méthode de Monte-Carlo" - C.R. Acad. Sc. Paris, t.277 C, 93 (1973)

1975

- 1 A. PACAULT, P. DE KEPPER, P. HANUSSE - "Description d'un système chimique dissipatif. Illustration d'un temps thermodynamique" - C.R. Acad. Sc. Paris, t.280 B, 157 (1975)

- 2 A. PACAULT, P. DE KEPPER, P. HANUSSE et A. ROSSI - "*Etude d'une réaction chimique périodique. Diagramme des états*" - C.R. Acad. Sc. Paris, t.281 C, 215 (1975)
- 3 A. PACAULT, P. DE KEPPER et P. HANUSSE - "*Aspect expérimental des réactions chimiques périodiques. Le temps thermodynamique*" - Proceedings of the 25th International Meeting of the Société de Chimie-Physique, Dijon 8-12 July 1974 (1975)

1976

- 1 P. DE KEPPER, A. PACAULT et A. ROSSI - "*Etude d'une réaction chimique périodique, multistationnarité et transitions*" - C.R. Acad. Sc. Paris, t.282 C, 199 (1976)
- 2 A. PACAULT, P. HANUSSE, P. DE KEPPER, C. VIDAL et J. BOISSONADE - "*Les réactions chimiques périodiques*" - Fundamenta Scientiae - Séminaire sur les fondements des sciences. Université Louis Pasteur, n° 52 (1976)
- 3 P. DE KEPPER - "*Etude d'une réaction chimique périodique. Transitions et excitabilité*" - C.R. Acad. Sc. Paris, t.283 C, 25 (1976)
- 4 J.C. ROUX, S. SANCHEZ et C. VIDAL - "*Etude expérimentale des structures dissipatives temporelles*" - C.R. Acad. Sc. Paris, t.282 B, 451 (1976)
- 5 P. DE KEPPER, A. ROSSI et A. PACAULT - "*Etude expérimentale d'une réaction chimique périodique. Diagramme d'état de la réaction de Belousov-Zhabotinskii*" - C.R. Acad. Sc. Paris, t.283 C, 371 (1976)
- 6 A. PACAULT, P. HANUSSE, P. DE KEPPER, C. VIDAL, J. BOISSONADE - "*Phenomena in homogeneous Chemical Systems far from Equilibrium*" - Accounts of Chemical Research, 9, 438 (1976)
- 7 J. BOISSONADE - "*Aspects théoriques de la "double-oscillation" dans les systèmes dissipatifs chimiques*" - J. Chim. Phys. n° 5, 540 (1976)
- 8 E. DULOS, A. MARCHAND - "*Variations périodiques de populations dans un système proie-prédateur : E. Coli-Bdellovibrio Bactériovorus*" - C.R. Acad. Sc. Paris, t.282 D, 1645 (1976)

1977

- 1 P. HANUSSE - "*Fluctuations around non equilibrium steady states*" - Physics Let. 59A, n° 6, 421 (1977)
- 2 J.C. ROUX et C. VIDAL - "*Etude spectroscopique d'une réaction chimique oscillante*" - C.R. Acad. Sc. Paris, t.284 C, 293 (1977)
- 3 C. VIDAL, J.C. ROUX et A. ROSSI - "*Analyse cinétique d'une réaction chimique oscillante entretenue*" - C.R. Acad. Sc. Paris, t.284 C, 585 (1977)
- 4 P. HANUSSE - "*Monte-Carlo simulation of finite fluctuations*" - J. Chem. Phys. 67, n° 2, 1282 (1977)
- 5 C. VIDAL, P. DE KEPPER, A. NOYAU, A. PACAULT - "*Phénomènes thermiques et structures dissipatives*" - C.R. Acad. Sc. Paris, t.285 C, 357 (1977)

1978

- 1 C. VIDAL - "Sur l'analyse cinétique d'un schéma réactionnel" - Actualité Chimique, n° 1, 30 (1978)
- 2 C. VIDAL et J.C. ROUX - "Etude expérimentale d'une structure dissipative temporelle" - Sciences et Techniques n° 50, 19 (1978)
- 3 A. PACAULT - "La tentation de l'homogène" - Nouv. J. de Chim., 2, n° 1, 3 (1978)
- 4 P. DE KEPPEL et A. PACAULT - "Les réactions chimiques périodiques : bistabilité et régulation ; tristabilité" - C.R. Acad. Sc. Paris, t.286 C, 5 (1978)
- 5 J.C. ROUX and C. VIDAL - "Quantitative study of a chemical oscillation", in *Synergetics-Far from Equilibrium*, ed. by A. Pacault, C. Vidal, Springer Series in Synergetics, Vol. (Springer, Berlin Heidelberg, New York 1979) p. 47
- 6 C. VIDAL and A. NOYAU - "Thermal properties of oscillating reactions : two examples", in *Synergetics-Far from Equilibrium*, ed. by A. Pacault, C. Vidal, Springer Series in Synergetics, Vol. (Springer, Berlin, Heidelberg, New York 1979) p. 152
- 7 P. DE KEPPEL and W. HORSTHEMKE - "Experimental evidence of noise induced transitions in an open chemical system", in *Synergetics-Far from Equilibrium*, ed. by A. Pacault, C. Vidal, Springer Series in Synergetics, Vol. (Springer, Berlin, Heidelberg, New York 1979) p. 61
- 8 P. HANUSSE - "Stochastic simulation of chemical systems out of equilibrium" - in *Synergetics-Far from Equilibrium*, ed. by A. Pacault, C. Vidal, Springer Series in Synergetics, Vol. (Springer, Berlin, Heidelberg, New York 1979) p. 70
- 9 A. PACAULT - "Réel et modèles", in *Synergetics-Far from Equilibrium*, ed. by A. Pacault, C. Vidal, Springer Series in Synergetics, Vol. (Springer, Berlin, Heidelberg, New York 1979) p. 128
- 10 J.C. ROUX et A. ROSSI - "Effet de l'oxygène sur la réaction de Belousov-Zhabotinskii" - C.R. Acad. Sc. Paris, t.287 C, 151 (1978)
- 11 J. BOISSONADE and W. HORSTHEMKE - "Molecular dynamics studies of the role of diffusion in chemical models with absorbing boundary states" - Physics Letters 68A, n° 2, 283 (1978)
- 12 P. DE KEPPEL et W. HORSTHEMKE - "Etude d'une réaction chimique périodique. Influence de la lumière et transitions induites par un bruit externe" - C.R. Acad. Sc. Paris, t.287 C, 251 (1978)
- 13 J. CHOPIN-DUMAS - "Diagramme d'état de la réaction de Bray" - C.R. Acad. Sc. Paris, t.287 C, 553 (1978)
- 14 P. HANUSSE, J. ROSS and P. ORTOLEVA - "Instability and far from equilibrium states of chemically reacting systems" - Advances in Chemical Physics, 38, 317 (1978)

1979

- 1 E. DULOS, P. DE KEPPEL, A. MARCHAND - "Entraînement d'une réaction chimique oscillante par des excitations lumineuses périodiques de fréquences variables" - C.R. Acad. Sc. Paris, t.289 C, 113 (1979)
- 2 C. VIDAL et A. NOYAU - "Oscillations chimiques et oscillations thermochimiques" - Nouv. J. Chim. 3, n° 2, 83 (1979)

- 3 J.C. ROUX et C. VIDAL - "Sur une méthode d'étude expérimentale des réactions périodiques" - *Nouv. J. Chim.* 3, n° 4, 247 (1979)
- 4 C. VIDAL, J.C. ROUX, A. ROSSI et S. BACHELART - "Etude de la transition vers la turbulence chimique dans la réaction de Belousov-Zhabotinsky" - *C.R. Acad. Sc. Paris*, t.289 C, 73 (1979)
- 5 J. BOISSONADE - "Molecular dynamics studies of long range and short range fluctuations in non-equilibrium chemical systems" - *Physics Letters* 74A, n° 3-4, 285 (1979)

1980

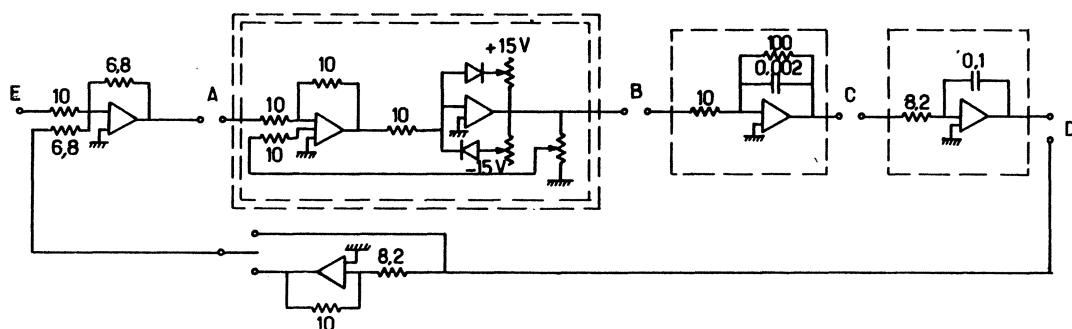
- 1 C. VIDAL, J.C. ROUX and A. ROSSI - "Quantitative measurement of intermediate species in sustained Belousov-Zhabotinsky oscillations" - *J. Amer. Chem. Soc.* 102, 1241 (1980)
- 2 C. VIDAL et J.C. ROUX - "La turbulence existe-t-elle ?" - *La Recherche*, n° 107, 66 (1980)
- 3 J. BOISSONADE and P. DE KEPPEL - "Transitions from bistability to limit cycle oscillations. Theoretical analysis and experimental evidence in an open chemical system" - *J. Phys. Chem.* 84, 501 (1980)
- 4 A. PACAULT - "Au-delà de la thermodynamique des états d'équilibre" - "De Carnot à Prigogine" - *Cahiers de Fontenay* (1980)
- 5 J.C. ROUX, A. ROSSI, S. BACHELART and C. VIDAL - "Representation of a strange attractor from an experimental study of chemical turbulence" - *Physics Letters* 77A, n° 6, 391 (1980)
- 6 C. VIDAL et A. NOYAU - "Some differences between thermokinetic and chemical oscillating reactions" - *J. Am. Chem. Soc.* 102, 6666 (1980)
- 7 C. VIDAL, J.C. ROUX, S. BACHELART, A. ROSSI - "Experimental study of the transition to turbulence in the Belousov-Zhabotinskii reaction" - *Ann. N.Y. Acad. Sci.* 357, 377 (1980)
- 8 P. HANUSSE et A. BLANCHE - "Simulation study of the critical behaviour of a chemical model system", in *Systems Far from Equilibrium*, ed. by L. Garrido (Springer, Berlin, Heidelberg, New York 1980) p. 337
- 9 A. MARCHAND et E. DULOS - "La règle d'affinité et d'indépendance des processus cinétiques : cas de la diauxie" - *C.R. Acad. Sc. Paris*, t.291 C (1980)
- 10 J.C. ROUX - "Réactions chimiques oscillantes : perspectives en biochimie" - *La Morphogénèse : de la biologie aux mathématiques*. Maloine (1980) Editeur Y. Bouligand.

1981

- 1 J. BOISSONADE - "A molecular dynamics technique to study fluctuations in non equilibrium chemical systems" - "Modelling of Chemical Reaction Systems", ed. by K. H. Ebert, P. Deuflhard, W. Jäger, Springer Series in Chemical Physics, Vol.18 (Springer, Berlin, Heidelberg, New York 1981)
- 2 C. VIDAL, J.C. ROUX - "Comment naît la turbulence ?" - *Pour la Science* 39, 50 (1981)
- 3 J.C. ROUX, A. ROSSI, S. BACHELART et C. VIDAL - "Experimental observations of complex dynamical behavior during a chemical reaction" - *Physica* 2D, 395 (1981)

- 4 C. VIDAL - "Dynamic instabilities observed in the Belousov-Zhabotinsky system" - dans "Proceedings of the International Symposium on Synergetics Elmaü 1981"(sous presse)
- 5 Y. POMEAU, J.C. ROUX, S. BACHELART, A. ROSSI et C. VIDAL - "Intermittent behaviour in the Belousov-Zhabotinsky reaction" - J. Phys. Lett. 42, L.271 (1981)
- 6 C. VIDAL, S. BACHELART et A. ROSSI - "Bifurcations en cascade conduisant à la turbulence dans la réaction de Belousov-Zhabotinsky" - J. Phys. (sous presse)
- 7 S. BACHELART, A. ROSSI, J.C. ROUX et C. VIDAL - "Mise en évidence de la turbulence chimique" dans "Symmetries and broken symmetries in condensed matter physics"(sous presse).
- 8 E. DULOS - "Des rythmes chimiques aux rythmes biologiques" dans "Analogie et connaissance", tome II (sous presse)
- 9 P. DE KEPPEL et J. BOISSONADE - "Theoretical and experimental analysis of phase diagrams and related dynamical properties in the B.Z. system" - J. Chem. Phys. 75, 189 (1981)
- 10 P. HANUSSE et A. BLANCHE - "A Monte-Carlo method for large reaction-diffusion systems" - J. Chem. Phys. 74, 6148 (1981)
- 11 J. CHOPIN-DUMAS - "Reactions périodiques avec le bromate. I. Critères de sélection de réducteurs organiques oscillants sans catalyseurs" - J. Chim. Phys. 78, 461 (1981)
- 12 P. HANUSSE - "A simulation technique for studying critical properties of chemical dissipative systems" - Springer Series in Chemical Physics (sous presse)

ANNEXE I



Values of resistors in kΩ

Values of capacitances in μF

Dynamical Systems Described by Discrete Maps with Noise

H. Haken and A. Wunderlin

Institut für Theoretische Physik der Universität Stuttgart, Pfaffenwaldring 57/IV,
D-7000 Stuttgart 80, Fed. Rep. of Germany

Some General Remarks

Since this contribution is one of the first in this volume and this conference is a truly interdisciplinary one, it might be useful to begin with a few general comments before entering the more technical part of our contribution.

When we ask ourselves where nonlinear phenomena are of greatest importance in chemistry, we are certainly led to the large class of nonequilibrium phenomena. In the first part of our contribution we want to discuss the question whether one might find general aspects or general principles which allow us to deal with nonequilibrium processes. When we look for theories which allow for a universal treatment, especially in chemistry, we are first led to thermodynamics. Its laws are indeed universal, being independent of the substances. Thermodynamics uses the concept of macroscopic variables such as temperature, entropy, free energy. It finds its microscopic foundation by statistical mechanics and this approach shows us that when going from microscopic to macroscopic descriptions, we need new concepts referring to new qualities. Temperature or entropy, e.g., are concepts alien to a single atom or molecule. There is a price to be paid for the generality of thermodynamics, however. First of all we are dealing here with closed systems. Furthermore when quantitative formulas are derived, they refer to systems in thermal equilibrium which, as we shall see below, is a very strong condition.

When dealing with systems away from thermal equilibrium in a next step, we may resort to irreversible thermodynamics. It should be stressed that its methods in general allow us to treat systems which are close to thermal equilibrium. The main phenomena we are dealing with here are relaxation and transport. General concepts used are entropy production, thermodynamic forces and fluxes. It might be necessary, however, to point out that the usual methods of irreversible thermodynamics are still too rough to cope with the new kind of phenomena we encounter in systems far from equilibrium. Here we find in chemical reactions the formation of macroscopic patterns, e.g. spiral waves or coherent oscillations. In other words, we find ordered structures on macroscopic scales. Here we may repeat the fundamental question we have asked at the beginning of this introduction. Is the formation of these patterns governed by universal principles, and can we deal with them by general concepts? It is worth mentioning that the formation of coherent patterns under nonequilibrium conditions can be observed in quite other fields also. For instance in physics (fluids, plasmas, lasers) in biology (morphogenesis, population dynamics, neural networks) etc. Indeed more than a decade ago it was suggested that the formation of such patterns be studied within an interdisciplinary field of research to be called SYNERGETICS. It was pointed out at that time that there

exist universal principles governing these processes. Here again we study the behavior of systems composed of many subsystems, the emergence of new qualities and their description by macroscopic variables.

In a way, the situation is similar to phase transitions of systems in thermal equilibrium, for instance in the ferromagnet whose order can be described by the magnetization which then serves as a so-called order parameter.

In the following we shall make a few comments on how to obtain order parameters for nonequilibrium phenomena. Over the past decade several paradigms (to use a word in vogue) have evolved.

First paradigm: Evolution equations

We describe nonequilibrium processes even for steady states by evolution equations which in chemistry are called kinetic equations. For a set of adequate variables \underline{q} , such as densities of molecules, evolution equations of the form

$$\dot{\underline{q}} = \underline{N}(\underline{q}) \quad (1)$$

are used. They apply, for instance, to processes in a continuously stirred tank reactor. If space dependence is to be taken into account, a typical class of equations is given by reaction diffusion equations of the form

$$\dot{\underline{q}} = \underline{R}(\underline{q}) + D\Delta\underline{q} \quad (2)$$

or in fluid dynamics, for instance, by the Navier-Stokes equations. In many cases fluctuations play a role which may be taken into account by adding fluctuating forces to eqs. (1) and (2) or by other stochastic treatments based on the master equation or the Fokker-Planck equation. The processes described by the equations (1) or (2) are immense and it would not make much sense to look for the general solutions of these equations. Rather a

Second paradigm: instabilities

has evolved, namely to look for such situations in which by change of external conditions (or control parameters) nonequilibrium phase transitions or bifurcations occur. It should be noted that these two concepts are still too narrow. Usually bifurcation theory neglects fluctuations which, as we know from chemistry and physics, play a crucial role just at the bifurcation point. On the other hand the phenomena occurring are much richer than we would encounter by phase transitions alone. We have described the way to cope with these instabilities, etc. in previous contributions to these series and we shall confine ourselves to some general comments. One studies in a mathematically rigorous fashion qualitative changes in macroscopic behavior, for instance the transition from monostability to bistability to the onset of oscillations, that means occurrence of limit cycles, the bifurcation of limit cycles to limit cycles with double period, or the bifurcation of a limit cycle to so-called quasiperiodic motion, i.e. a motion governed by several fundamental frequencies. Such a motion can be geometrically described as motion of the systems vector \underline{q} on a torus. The motion on a torus can also collapse again into a limit cycle or give rise to chaos. The conditions for the occurrence of these various possibilities are of delicate nature and we refer the reader to some more detailed comments made elsewhere [1].

Before going on to the second point of our presentation, a few general comments should be added. There are still some discussions going on in chemistry whether concepts of thermodynamics, such as

free energy, are capable of dealing with nonequilibrium phenomena, e.g. chemical oscillations. In a field which is in a way parallel to chemical processes, namely in laser physics, it was shown nearly 15 years ago that in nonequilibrium processes rate constants play the dominant role. Such rate constants are inherent only in kinetic equations but cannot be derived from concepts as free energy. Our quantum statistical treatment has revealed quite clearly that conventional thermodynamics is indeed inadequate to cope with open systems, whose state is kept far from thermal equilibrium. The general approach of synergetics has further shown that quite different "elementary" mechanisms may give rise to the same macroscopic phenomena, e.g. a chemical oscillation. Thus quite generally speaking, scientific study can proceed along two lines (or a combination of both of them). Either we want to study the detailed mechanism of a process or we are looking for universal features, shared by many otherwise different systems. Both approaches seem to us to be of equal importance and the present meeting gives us beautiful examples of both.

In particular, in the spirit of synergetics we find that analogies between different systems may be a useful guide to find new features. For instance, while chaos was first observed in fluid dynamics, we now find quite the same phenomenon in chemical reactions, as shown by Vidal [2] and other contributors to the present volume. On the other hand, in chemistry it has become possible to find the alternating sequence between chaos and periodic motion and it will be a challenge to other fields to find a similar phenomenon within their corresponding systems. Over the past years a

Third paradigm: discrete maps

has emerged, namely treating processes going on by discrete time intervals. Such a procedure may be useful for mathematical reasons as was first shown by Poincaré, but it may also be of practical importance for complicated processes in chemistry and biology. (For a more detailed motivation of such procedures see [1]).

In order not to duplicate too much of what we have stated before, we refer the reader to [1] and present a few general results of discrete maps with noise.

If \underline{x}_k is a n-dimensional vector, the discrete map with noise is described by an equation

$$\underline{x}_{k+1} = \underline{f}(\underline{x}_k) + G(\underline{x}_k)\underline{\eta}_k \quad (3)$$

analogous to a Langevin equation. If $W(\underline{\eta})$ describes the distribution of the noise, a Chapman-Kolmogorov equation belonging to (3) can be derived in the form [3]

$$\underline{P}(\underline{x}, k+1) = \int d^n \underline{\xi} D(\underline{\xi})^{-1} W(G^{-1}(\underline{\xi})(\underline{x} - \underline{f}(\underline{\xi}))) \underline{P}(\underline{\xi}, k) \quad , \quad (4)$$

where $D = \det G$. To (4) an eigenvalue equation of the form

$$\underline{P}_\lambda(\underline{x}) = \lambda \int d^n \underline{\xi} K(\underline{x}, \underline{\xi}) \underline{P}_\lambda(\underline{\xi}) \quad (5)$$

may be attached, where the kernel K is the same as that of (4).

Depending on parameter values, critical points can be defined in which the system vector can be decomposed into order parameters and amplitudes of slaved modes. In order to eliminate the slaved modes in the case of a discrete map we first consider a case of eq.(1) in

which $\underline{f}(\xi) = A\xi$ is a linear map. We have found the explicit solution of eq. (4) in this case, provided the distribution function of the noise is a Gaussian,

$$W(\eta) = N \exp(-\frac{1}{2}\eta\beta\eta).$$

Then P reads

$$\underline{P}(\underline{x}, k) = N_k \exp(-\frac{1}{2}(\underline{x} - \underline{x}(k)) B_k (\underline{x} - \underline{x}(k))),$$

where N_k is the normalization constant, $\underline{x}(k)$ obeys the linear eq. (3) without noise and B_k obeys

$$B_{k+1} = \beta - A(B_k + A^T \beta A)^{-1} A^T \beta.$$

Our result can be considered as a generalization of the Orenstein-Uhlenbeck process to the case of discrete noisy maps.

In order to generalize the slaving principle, which contains the center manifold theorem or adiabatic elimination techniques, to the present case, we write the probability density P in the form

$$\underline{P}(\xi_u, \xi_s, k) = h(\xi_s | \xi_u, k) g(\xi_u, k),$$

where ξ_u are the order parameters and ξ_s the slaved modes. Then two coupled integral equations may be derived for h and g.

$$h(\xi_s | \xi_u, k+1) = \iint \hat{K} h(\xi'_s | \xi'_u) d\xi'_u d\xi'_s,$$

$$g(\xi_u, k+1) = \int \tilde{K}(\xi_u, \xi'_u) g(\xi'_u, k) d\xi'_u,$$

where \hat{K} and \tilde{K} contain g and h, respectively. We have devised an iteration procedure for the solution of these two equations which in particular allows us to eliminate the ξ_s .

In a number of cases the Chapman-Kolmogorov equation can be simplified to a Fokker-Planck equation, e.g. in the case of intermittency treated [4] or, more recently, in the case of the logistic model [5]. We found that often the process can be well approximated by a Fokker-Planck equation whose stationary solution is given by

$$f(x) = N \exp(\alpha x + \beta x^2 + \gamma x^3).$$

The Fokker-Planck equation can be transformed into a Schrödinger equation and therefore direct contact with bound states, metastable states and tunneling states of quantum mechanics can be made.

Concluding Remarks

We think that with respect to the mathematics of discrete noisy maps we are just at the beginning. It should be mentioned, however, that the inclusion of noise into discrete maps [6] has been already proven to be a very valuable tool, for instance in the derivation of scaling laws for Ljapunov exponents [7].

References

- 1 H. Haken, in *Chaos and Order in Nature*, Springer Series in Synergetics, Vol. 11 (Springer, Berlin Heidelberg, New York 1981) p.2
- 2 C. Vidal, in *Chaos and Order in Nature*, Springer Series in Synergetics, Vol.11 (Springer, Berlin Heidelberg, New York 1981)p.69
- 3 H. Haken and G. Mayer-Kress, *Z.Physik* 43, 185 (1981)
- 4 P. Manneville and Y. Pomeau, *Physica* 1D, 219 (1980)
- 5 G. Mayer-Kress and H.Haken, *Phys.Lett.* 82A, 151 (1981)
- 6 e.g. G. Mayer-Kress and H. Haken, preprint, August 1980
- 7 B. Shraiman, C.E. Wayne, P.C.Martin, *Phys.Rev.Lett.* 46, 935 (1981)

Thermokinetic Oscillations and Multistability in Gas-Phase Oxidations

Peter Gray, John F. Griffiths, and Stephen M. Hasko

School of Chemistry, University of Leeds
Leeds, LS2 9JT, U.K.

1. Introduction

Although chemical interest in oscillatory inorganic reactions [1] goes back more than sixty years to LOTKA (1910, 1920), MORGAN (1916) and BRAY (1921), its renaissance dates from the discovery [2] by ZHABOTINSKII (1964+) that "spatial periodicity" was a possibility. Hopes that there might be worthwhile implications for biochemistry (and biological systems generally) catalyzed and influenced the direction of subsequent developments. This meant that the subject grew up rapidly but unevenly, and with very imperfect contact with other disciplines where similar phenomena had been already studied extensively and deeply.

The science of combustion is one of these disciplines. In its general sense, combustion relates not only to the oxidation of fuels, but to many vigorous reactions that are related by their responsiveness to temperature and their ability to generate heat. Nonlinear kinetics, propagating waves, and discontinuous responses to slowly varying conditions are not unusual in such systems [3]. Also familiar are the phenomena of ignition, extinction, hysteresis, multi-stability, and oscillations - whether stable or unstable. It is one purpose of this invited lecture to sketch some of this development and to present recent results for two gas-phase oxidations - those of ethane and acetaldehyde. Another purpose is to stress the rewards of working in well-stirred, open systems.

1.1 Advantages of well-stirred, open systems

In a closed system, chemical reaction proceeds to the point of thermodynamic equilibrium. The final state achieved is independent of the path taken towards it, and a stable equilibrium is finally approached in a non-oscillatory manner. In an open system, permanent stationary states far from thermodynamic equilibrium and sustained oscillatory states are both possible. When reactions are kinetically complex or non-isothermal (or both, as in hydrocarbon oxidation), they may show a duality or a multiplicity of states. Now the state finally achieved depends on the path taken towards it. In the same circumstances, sudden jumps can occur in response to a steadily varying change and can also be studied properly. Theoretical interpretation is made easier in several ways. For example, in stationary states, Bodenstein's quasi-stationary-state hypothesis ceases to be an approximation, and its demands for qualitative distinctions where only quantitative differences exist are not necessary. Sustained oscillations can similarly be properly represented by limit cycles in the phase plane. The artifices of 'neglecting reactant consumption' or 'keeping pool chemicals constant', which often may imply deep differences in principle, or have to be regarded as modelling very impractical systems, are done away with.

The use of an open system [4] can thus confer benefits on both experiment and theory. When the particular open system chosen for experimental use is the well-stirred, capacity-flow reactor (CSTR), another marvellous simplification can be achieved or closely approached: uniformity in temperature and concentration fields. Partial differential equations in spatial coordinates are replaced by

ordinary ones, and powerful theorems strengthen theory's grasp. In stationary states, algebraic equations are often sufficient.

These advantages and simplifications are not bought at a heavy price, for whilst the amount of experimentation required is always greater than in closed systems - flow-rate being an added variable and responses to transient perturbations an additional enquiry - the actual variety of interesting behaviour encountered is much enhanced [5].

1.2 Stable and unstable behaviour

At constant temperature, deceleratory reactions are the conventional norm of behaviour. It has become a habit to regard this behaviour as stable, loosely transferring the notion of stability from the final equilibrium state to which it properly belongs. Autocatalysis is thus a mild exception to normality; explosion constitutes a strong exception. By similar habits of mind, and in view of the violence of an explosive event, we tend to regard both the explosion and the exploded state before cooling as the instability : certainly the state of maximum reaction rate cannot be maintained for more than an instant. Topologically, however the course of events in a closed system is similar to those in non-explosive changes : temperatures remain bounded and end at ambient, where they began. Moreover if the system is open, then in a sufficiently fast flow, even the rapidly burning state can be maintained indefinitely, and we now see that both slow and explosively fast modes are stable possibilities. It is not helpful to label one stationary state as more stable than another of the same character, though they may have different ranges of existence, and attempts to do so do not seem to have led anywhere. Where ranges of physical conditions for their existences overlap we have hysteresis, and at the ends of these ranges, jumps are possible between them.

2. Reactions in the CSTR

The well-stirred reactor has been the subject of continuous investigations by chemical reactor engineers since the mid 1950s when BILOUS & AMUNDSON'S stability analysis (1955) showed the path to follow.

Activity remains intense, and it is a measure of the subject that it is only in the years 1976-80 that agreement seems to have been reached [6] on the systematic enumeration of the variety of patterns of behaviour that can be shown in a CSTR by the simplest non-isothermal prototype : a single, exothermic, irreversible reaction that is kinetically first order and that obeys the Arrhenius law.

We outline some of the important results [6,7] and the paths to them, because the behaviour of ethane oxidation with respect to ignition and extinction as residence time is varied does not fit the standard pattern in the simplest way.

2.1 Thermal diagrams

Before sketching the equations it is useful to comment on the "thermal diagram", familiar since SEMENOV (1928) and VAN HEERDEN (1953) and affording a very helpful way of looking at systems such as these. When rates of heat generation and heat removal can be represented as functions of reactant temperature, then their points of intersection represent stationary states of the system. Their gradients at the points of intersection govern the nature of the singular points that they describe. Although in a CSTR two such diagrams can be drawn, one for matter and one for energy, they are not independent of one another, and at the points of intersection they are closely connected. The connections are simplest under "adiabatic" conditions (when none of the heat released in exothermic reaction is lost through the vessel walls). Adiabatic and non-adiabatic conditions are compared below.

2.2 The equations of CSTR operation

The conventional equations for conservation of matter and energy and their equivalents in terms of reduced concentrations and temperatures are :

$$\begin{array}{l} V(dc/dt) \\ \text{accumulation} \end{array} = \begin{array}{l} vc_0 \\ \text{inflow} \end{array} - \begin{array}{l} vc \\ \text{outflow} \end{array} - \begin{array}{l} Vkc \\ \text{reaction} \end{array} \quad (1A)$$

$$\Rightarrow \frac{d\lambda}{dt} = \frac{1 - \lambda}{t_{res}} - \frac{\lambda}{t_{chem}} \exp \frac{\theta}{1 + \epsilon\theta} \quad (1B)$$

$$\begin{array}{l} \rho c_p V(dc/dt) \\ \text{self} \\ \text{heating} \end{array} = \begin{array}{l} qVkc \\ \text{exothermic} \\ \text{reaction} \end{array} - \begin{array}{l} XS(T - T_w) \\ \text{loss via} \\ \text{walls} \end{array} - \begin{array}{l} \rho c_p (T - T_0) \\ \text{heated} \\ \text{outflow} \end{array} \quad (2A)$$

$$\Rightarrow \frac{1}{B} \frac{d\theta}{dt} = \frac{\lambda}{t_{chem}} \exp \frac{\theta}{1 + \epsilon\theta} - \frac{\theta}{B} \left(\frac{1}{t_{res}} + \frac{1}{t_n} \right) \quad (2B)$$

In these expressions, most symbols have their conventional meanings [7]. The time t_n is the Newtonian cooling time for heat loss through the walls : in our circumstances t_n is about 0.2 to 0.6 s. Dimensionless temperatures θ are based on the reference temperature T_a that would prevail in the absence of exothermic reaction : $\theta = (T - T_a)/(RT_a^2/E)$. The group $\epsilon = RT_a/E$; the term B is the dimensionless adiabatic temperature increase.

2.3 Adiabatic operation

If no heat is lost through the walls, the term $1/t_n$ disappears from (2B) yielding

$$(1/B) d\theta/dt = (\lambda/t_{chem}) \exp[\theta/(1 + \epsilon\theta)] - \theta/Bt_{res} \quad (2C)$$

At the stationary points, we have $\theta_s/B = 1 - \lambda_s$. For a fixed value of T_a but varying residence time, the stationary state solutions $\theta(t_{res})$ and $\lambda(t_{res})$ either (i) vary monotonically with residence time, λ falling steadily from unity to zero and (θ/B) rising from zero to unity or (ii) they show an S- or Z-bend with a region of three solutions, the middle one physically unrealizable. Concentrations again fall to zero and temperatures eventually rise to adiabatic values. The possibility of multiple solutions disappears when

$$\frac{1}{B} + \frac{1}{\epsilon} \leq \frac{1}{4} \quad \text{or} \quad \Delta T_{max} \leq \frac{4RT_a T_{ad}}{E} \quad \text{or} \quad \epsilon \geq \frac{1}{4} \left(1 - \frac{T_a}{T_{ad}} \right)$$

As residence times are varied continuously, discontinuous jumps occur at the points when the curves turn round. Ignitions can only accompany lengthening residence times. Extinctions can only accompany shortening residence times. Stable oscillatory behaviour is impossible in adiabatic operation.

2.4 Non-adiabatic operation - heat losses to and through walls

When oxygen and ethane react in glass vessels like those used here, heat-losses through the vessel walls greatly exceed the heat transported by the outflow. In these circumstances the dependence of temperature excess on residence time must end at zero excess at $t \rightarrow \infty$, and quite different curves are possible. The full variety of behaviour has only been recognized recently, though some of the recent results [6] are rediscoveries of ZEL'DOVICH & ZYSIN'S pioneering study [8].

Equations of identical structure can still be written if the term B is replaced by B' , a time-dependent term $B' = B/(1 + t_{res}/t_n)$. Four consequences follow :

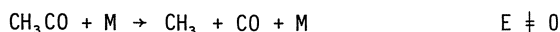
(i) for simple kinetics there is still a choice between one or three solutions, not more; (ii) ignitions can accompany decreasing residence times and vice versa; (iii) detached regions (isolas) exist, only accessible by artificial ignition; (iv) oscillatory solutions become possible.

The reactions that follow are not as simple as this prototype, and they show oscillations in closed systems. But the versatility of the simplest model must always be born in mind.

3. Kinetic aspects of ethane and acetaldehyde oxidation : the n.t.c.r.

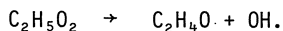
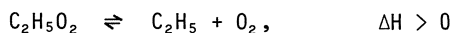
Both these oxidations have been extensively studied [5,10,11,12]. They follow rather different pathways and mechanistic differences may be illustrated by current interpretations of the negative temperature coefficient of reaction rate (ntcr) that they both possess. We do not otherwise plan to discuss detailed chemistry here.

In acetaldehyde oxidation, the ntc r arises from competition between oxidation and decomposition of acetyl radicals :



Since CH_3 radicals participate only in a straight-chain mechanism, whereas CH_3CO_3 can give rise to chain branching (via $\text{CH}_3\text{CO}_2\text{OH} \rightarrow \text{CH}_3 + \text{CO}_2 + \text{OH}$), the fact that decomposition is favoured by higher temperature at the expense of oxidation means that the overall reaction rate can fall as temperature increases.

In ethane oxidation, a different competition is invoked. Ethyl radicals can associate with oxygen, and the resulting RO_2 can either dissociate again or (by a cyclic transition state) open the route to faster oxidation by forming ethylene oxide and hydroxyl :



Once again, increased temperature increases the rate of elementary steps, but nevertheless has an adverse overall effect.

4. Apparatus and procedure for gas-phase oxidations

4.1 Apparatus

The reaction vessel is a Pyrex glass bulb about 10 cm in diameter and 0.5 dm³ in volume. It is kept at a steady (± 0.1 K), uniform (± 1 K) temperature in a recirculating air oven.

Reactants enter at the bottom of the vessel after passing separately through pre-heating coils; products leave at the top. Mixing in the vessel and hence uniformity of temperature and composition is achieved by an internal, ceramic-coated, stainless-steel stirrer magnetically driven at constant speeds up to 1200 rpm.

Flow rates (and hence reactant compositions at entry and mean residence times) are controlled by critical-flow orifices made from watchmakers' artificial ruby. Holes down to 125 μm diam. are drilled mechanically; smaller holes (down to 12.5 μm diam.) are made with a laser. So long as there is a sufficient pressure ratio across the orifice, flow rates depend only on the upstream pressure.

To monitor reaction, simultaneous, continuous measurements are made of emitted light intensity (I), species concentrations (c) and reactant temperature rise (ΔT). Concentrations of stable species are measured by mass spectrometry (from these rates of reaction can be derived). Temperature measurements are made with a very fine thermocouple : they reveal extents of self-heating and yield overall rates of heat release.

4.2 Procedure

Satisfactory experiments are not difficult to plan but they are demanding to carry out and they can be hazardous. Current procedures are derived from the experience of many thousands of observations. Details are given elsewhere [5,9].

The ranges of conditions investigated may be summarized as follows :

	Reactant proportions	Reactant pressure	Vessel temperature	Residence time
Acetaldehyde	1 : 1	3 - 25 kPa	400-620 K	2 - 10 s
Ethane	6:1 to 2:1	100 kPa	650-800 K	15-150 s

It is usually convenient to fix pressures and mass flow rates, and to vary the reaction-vessel temperature continuously or in steps. A stepwise sequence of temperatures permits the indefinite stabilisation of conditions at each step; "scanning" a temperature range by continuous variation allows quick recognition of discontinuous behaviour, such as ignition or the sudden onset of oscillations. Small perturbations (e.g. transient alterations in flow rate) allow the nature of a stationary state to be diagnosed, an oscillatory return to normal signifying a stable focus and so on.

5. Ethane oxidation in a CSTR

Ethane is less reactive than acetaldehyde and requires higher temperatures (650 to 800 K), higher pressures (1 atm) and longer residence times (15 to 150 sec). At these pressures, reactant proportions must be kept remote from stoichiometric to reduce danger and avoid destructive explosion : we study $6 \text{ C}_2\text{H}_6 + \text{O}_2$, $4 \text{ C}_2\text{H}_6 + \text{O}_2$ and $2 \text{ C}_2\text{H}_6 + \text{O}_2$. Four distinct types of behaviour are displayed, of which two are oscillatory and two are not. Investigation is by no means complete, but findings to date may be summarized as follows :

Régime I-e : Slow, dark reaction and jumps to régime V-e

There is a wide range of vessel temperatures T_a over which reaction proceeds rather slowly, without any emission of light, and without any oscillations. Self-heating (ΔT) is very small below ambient temperatures of 740 K, but around these values ΔT becomes appreciable for all mixtures and residence times. The extent of reaction and the rate of heat release increase with increasing residence time until the high-temperature end of this régime.

As vessel temperatures increase, reaction in régime I-e grows stronger and a sudden jump ("ignition") occurs to régime V-e (see below). There is normally an overshoot on the temperature record (ΔT vs T_a).

The return path from régime V-e to régime I-e shows no overshoot, but there is hysteresis : ignition occurs at $T_a = 770 \text{ K}$ and extinction at $T_a = 750 \text{ K}$.

Régime V-e : rapid, luminous reaction

The second non-oscillatory régime is found at vessel temperatures in excess of 750 K. It is luminous and markedly more rapid than that in régime I-e. Over the

temperature range studied (750 - 820 K), steady temperature excesses are typically around 40 K. Reactant consumption and reaction rates are markedly greater, and increase with increased residence time. Little if any oxygen remains, even in the 2 : 1 mixture. The reaction stoichiometry is approximately $\Delta(C_2H_6) = 0.83 \Delta(O_2)$.

Régime IV-e : Oscillatory cool flame

At the shorter residence times, and in the mixture $2 C_2H_6 + O_2$, an oscillatory, luminous reaction occurs - over a temperature range $759 < T_a < 788$ when the residence time is 15 s. This oscillatory behaviour can only be generated in a decreasing temperature traverse.

At the point of entry ($T_a = 788$ K) to the region, a steady temperature excess of 80 K gives place to an oscillation that grows in amplitude to about 70 K as T_a falls. When $T_a = 763$ K, temperature excesses at the peaks are ca 95 K above ambient, and they fall in the valleys to about 25 K. The period is about 2.5 s.

Régime II-e : Oscillatory "ignition"

A further region of oscillatory behaviour is found in an equimolar mixture at somewhat higher temperatures ($T_a \approx 795$ K) - the least remote from stoichiometric equivalence of the mixtures studied. Here the system exhibits quite violent pressure and temperature pulses accompanied by bright yellow flashes of light. They are periodic, and at 795 K there is a time of about 1 minute between successive pulses when the residence time is 15 s.

This region also can only be entered by a decreasing temperature traverse : strong oscillations do not build up gradually, but set in with a finite amplitude. As the region is traversed (T_a diminishing) the transition to the stationary mode of behaviour happens by the reaction "dropping out" on the last cycle. We cannot characterize the form or location of the reverse transition because it is too violent for our system to survive.

6. Acetaldehyde oxidation in a CSTR

More than 12 different patterns of behaviour have been encountered. Some of them extend over very narrow regions of the $p - T_a$ plane, but reproducible boundaries between the regions over which they occur have been mapped for 9 of them. They may be grouped into 5 major areas, one of these containing many subdivisions :

- I steady reaction without light emission
- II oscillatory ignition
- III oscillatory multistage ignitions
(five types observed and mapped : others only observed)
- IV oscillatory cool flames
- V steady reaction with chemiluminescence

We first describe the stationary states (I, V) then the oscillations with simpler wave forms (II, IV) and finally the hybrid, complex ignitions (III). To make points simpler, we sometimes stress the visual and thermal aspects, but it is the continuous mass-spectrometric sampling that provides the foundations of stoichiometry, reaction rates and thermochemistry on which thermokinetic interpretations are built. For more detailed descriptions, see [5,9,10].

6.1 Steady dark reaction (I) and steady cool flames (V)

Over a large, low-temperature range there is steady reaction without light emission (I). The system exhibits a normal dependence of rate on temperature and the typical maximum value of $\Delta T = 40$ K corresponds to a heat release rate of about 9 W, i.e. 18 W dm^{-3} .

The other stationary state (V) occurs at higher temperatures and moderate pressures : any upper boundary to the (p,T) region over which it occurs lies beyond the experimental limits of the apparatus.

This is a much more reactive state. Excess temperatures exceed 80 K. Increases in vessel temperature cause ΔT to diminish, indicating a negative temperature dependence of heat-release rate. This diminution is due more to shifting stoichiometry (away from CO_2 and towards CO) than to varying reaction rate.

Table 1 Stationary states (I & V) compared

	Régime I	Régime V
(a) pressure range/kPa	0 - 20	5 - 20
(b) temperature range T_a /K	430 - 500	600 - 650
(c) light emission	none	steady weak blue glow
(d) self-heating ΔT /K	0 - 30 (ΔT rises with T_a)	100 - 60 (ΔT falls)
(e) heat release rate W dm^{-3}	0 - 20 (rising)	80 - 50 (falling)
(f) extent of reaction	$\leq 20\%$	$\geq 60\%$
(g) $\Delta(\text{CH}_3\text{CHO})/\Delta(\text{O}_2)$	0.9	1.10
(h) abundant product	CO_2	CO
(j) $(-\Delta H)/\text{kJ mol}^{-1}$	≈ 370	≈ 320
(k) nature of stationary state (response to disturbance)	stable nodal point monotonic	stable nodal focus oscillatory

6.2 Oscillatory cool flames (oscillatory luminescent reactions) IV

As the vessel temperature is raised, slow dark reaction (I) changes suddenly into spiky oscillatory luminescence. These pulses look exactly like the repetitive cool flames of hydrocarbons, but here oscillations can be indefinitely prolonged.

Temperature excesses can be as much as 200 K and the oscillations in light output and excess temperature show sharp peaks separated by shallow minima.

The chemistry of oscillations is very significant : the major products that are formed are CO , H_2O , CH_4 , CH_2O and CH_3OH ; hydrogen peroxide and peracetic acid are minor products.

6.3 Oscillatory ignitions with simple waveform (region II)

These oscillations are successive violent, pulsed ignitions accompanied by an orange flash and by an audible click. Values for $\Delta T > 400$ K are measured; between ignition spikes, temperature excesses and light intensities fall to zero. Periods are typically 10 to 20 s for a 6 s residence time.

The chemistry of ignition differs from the chemistry of cool flames; CH_2O , CH_3OH and CH_4 are all destroyed at ignition - they were formed at cool flames.

The description above oversimplifies the ignition peaks : they are not featureless spikes. Each spike has a small premonitory rise that slackens and may briefly become stationary before the main leap upward. Chemical analysis shows that this stage is characteristic of a cool flame : CH_2O , CH_3OH , CH_4 build up, only to be destroyed at ignition. Repetitive ignitions could thus be reclassified as repetitive, two-stage events and regarded as the extreme part of region III (see below).

6.4 Oscillatory multi-stage ignitions III

This is the region in which stable oscillatory ignition shows a complex wave form, and it accordingly can be subdivided into numerous zones each occupied by its characteristic type. Broadly speaking, régime III lies between régimes II and IV and is occupied by hybrid wave forms having II and IV as extremes of behaviour.

Thus at the low temperature end of III, we see successive ignitions separated by one, detached cool flame. As the vessel temperature is increased and the region is traversed, the number of cool flames that separate successive ignitions increases in steps. We have been able to map five sub-regions, the last showing patterns of five detached cool flames per ignition. These regions get narrower and narrower, and we have seen still more without being able to draw precise boundaries.

So long as conditions (T_0 , p , t_{res}) are kept constant, each wave pattern is repeated. If T_0 is stepped up a little and then caused to return gradually, there is a jump from 4-stage ignition to 7-stage followed by 6-stage and 5-stage patterns before the 4-stage pattern is produced again.

These are not the only hybrids. Other forms also show up especially in the neighbourhood where regions II, III and IV merge. There we have found patterns in which n cool flames + 1 ignition and $(n + 1)$ cool flames + 1 ignition alternate.

It should be emphasized that these hybrid ignitions of complex wave form are not merely sequences of similar light and temperature pulses of different amplitude. Their chemistry is different. The mass-spectrometric analysis again permits the large and small amplitude pulses to be assigned to qualitatively different categories - one consuming and the other producing the intermediate species CH_4 , CH_2O and CH_3OH .

6.5 Chaotic behaviour

Chaotic behaviour has not been encountered : we believe that this is because it has not been generated. That is not to say that some forms of chaos might not be expected, but there are forms that could arise as a consequence of imperfect mixing and turbulent flow. If a sensor is geometrically small and has a rapid response, then it senses conditions in small elements of fluid passing by. A hypothetical thermocouple yet faster and smaller than ours might seem to reveal chaotic behaviour (it is a well-known hazard in experimental thermochemistry) that stems not from exotic chemistry but from turbulent stirring. Small electrodes may be able to act in this way. Firstly they are not always immersed in a perfectly homogeneous medium at rest or in smooth unchanging flow. Secondly, their surfaces are neither always uniform nor unchanging. Thirdly in unfriendly or hostile media they are not always behaving reversibly.

6.6 Thermokinetic mechanism

The interpretation of oscillatory cool flame and related behaviour has a long history [4] but is now based with confidence on thermal feedback and a supple kinetic mechanism of a system that shows both normal and abnormal responses to temperature [4,12,13]. The unification of chain branching and self-heating was achieved by B.F. GRAY & C.H. YANG [13] and the first detailed scheme for acetaldehyde was put forward soon after [12]. The present experimental results will form the

base for improvements to the existing models. It remains the case that no other system outside the biological field shows the richness of variety displayed here, and it is fair to say that at present discovery has outstripped modelling.

References

1. A.J. Lotka J. Phys. Chem. 14 271 (1910); J.A.C.S. 42 1595 (1920)
J.S. Morgan J. Chem. Soc. 109 274 (1916); W.C. Bray 43 1262 (1921).
2. A.M. Zhabotinskii Dokl. Akad. Nauk. S.S.S.R. 157 392 (1964);
Biofizika 9 306 (1964).
3. B.F. Gray in "Oscillatory Reactions" Spec. Per. Rep. Chem. Soc. Lond.
1 309 (1975).
4. P. Gray Ber. Bunsen. Phys. Chem. 84 309 (1980); see also Sixteenth Symp.
(Int.) Comb. p. 919 : Pittsburgh (1977).
5. P. Gray, J.F. Griffiths, S.M. Hasko & P-G. Lignola Proc. Roy. Soc. Lond.
A 374 313 (1981); Comb. & Flame (in press).
6. A. Uppal, W.H. Ray & A.B. Poore Chem. Eng. Sci. 29 967 (1974); 32 205 (1976);
W. Kauschkus, J. Demont & K. Hartmann Chem. Eng. Sci. 33 1283 (1978);
D.A. Vaganov, N.G. Samoilenko & V.G. Abromov Chem. Eng. Sci. 33 1133 (1978);
M. Golubitsky & B.C. Keyfitz S.I.A.M. J. Math. Anal. 11 316 (1980).
7. L. Lapidus & N.R. Amundson "Chemical Reactor Theory" New York : Prentice
Hall (1977).
8. Ya. B. Zel'dovich and Yu. A. Zysin Zh. Tekh. Fiz. 11 493, 501 (1941).
9. P. Gray, J.F. Griffiths & S.M. Hasko Comb. & Flame (in press): Colloque
Int. Comb. Bordeaux : Comb. Inst. (1981).
10. S.M. Hasko Ph.D. diss., University of Leeds (1980).
11. M. Cathonnet & H. James J. Chim. phys. 74 158 (1977).
12. M.P. Halstead, A. Prothero & C.P. Quinn Proc. Roy. Soc. Lond. A 322
377 (1977); Comb. & Flame 20 211 (1973).
13. B.F. Gray & C.H. Yang J. Phys. Chem. 69 2747 (1965); 75 3395, 3407 (1969).

Part II

Weak Turbulence

Chemical Kinetics and Differentiable Dynamical Systems

David Ruelle

I.H.E.S., F-91440 Bures-sur Yvette, France

1. Introduction

According to traditional physical views, the frequencies present in the time evolution of a system correspond to the excitation of various modes or degrees of freedom of the system. Following these views, hydrodynamical turbulence is due to the excitation of a large number of modes of a fluid which, being a continuous system, has indeed an infinite number of degrees of freedom. This is the theory of Landau [9] and Hopf [8]. It has however been realized now that dynamical systems with low-dimensional phase space (dimension ≥ 3) may already have a "continuous spectrum", i.e. a continuous superposition of different frequencies. Systems with a small number of degrees of freedom may thus exhibit a "turbulent" time behavior. It is now understood that fluid systems at the onset of turbulence exhibit a great wealth of phenomena involving only a small number of degrees of freedom^{*)}. Homogeneous chemical systems have a priori only a finite number of degrees of freedom at their disposal. In view of what has just been said, they might in principle show the same variety of behavior as weakly turbulent fluids.

I made this suggestion [19] at a time when such ideas were still viewed as somewhat heretical. In fact the existence of a periodic chemical reaction (Belousov-Zhabotinsky) had already shocked many chemists when it was discovered. Now, of course, the beautiful experiments by Vidal and his group [24], [25] have definitely shown that non-periodic chemical reactions exist, even though the exact dynamics is not completely clear.

In the elucidation of the time dependence of chemical reactions, there are two different aspects. One is chemical, and deals with the kinetics of the many partial reactions which take place simultaneously in the system. The other aspect is the discussion of the global nature of the solution of the equations of motion. We shall, in what follows, discuss only this second aspect which, contrary to naive expectation, is surprisingly rich. We shall first discuss quiet dynamical systems, then truly turbulent systems.

*) See Lorenz [11], Ruelle and Takens [22], McLaughlin and Martin [12], and the experimental work of Ahlers [1], and Gollub and Swinney [6].

2. Quiet Time Evolutions (stationary, periodic and quasiperiodic systems)

$$\frac{dx}{dt} = F_{\mu}(x) \quad (1)$$

where $x = (x_1, \dots, x_n)$ and μ is a parameter. The simplest type of asymptotic behavior for solutions of such an equation is given by a stationary solution $x = x_0$. Such a solution is visible of course only if it is attracting. When μ is increased, an attracting stationary solution may lose its attracting character and give rise to a periodic solution for $\mu > \mu_c$ by the Hopf bifurcation. The newly created oscillations have an amplitude $\approx \sqrt{\mu - \mu_c}$ and a frequency ω_1 which depends only weakly on μ . It is tempting to believe that as μ is further increased new frequencies $\omega_2, \omega_3, \dots$ successively appear. This is essentially the Landau-Hopf idea, and it gives rise to quasiperiodic solutions, i.e. solutions of the form

$$x(t) = f(\omega_1 t, \omega_2 t, \dots, \omega_k t) \quad (2)$$

where f is separately periodic of period 2π in each argument, and $\omega_1, \dots, \omega_k$ are independent frequencies. Notice that for $k = 0, 1$ the quasiperiodic motions reduce to stationary and periodic. A small change $\delta x(0)$ in the initial condition amounts to replacing $\omega_1 t, \dots, \omega_k t$ by $\omega_1 t + \alpha_1, \dots, \omega_k t + \alpha_k$ with small $\alpha_1, \dots, \alpha_k$. Therefore $\delta x(t)$ remains small at all times. We do not have here sensitive dependence on initial condition, this is why we say that quasiperiodic systems are quiet dynamical systems.

Using (2) we see that the quasiperiodic solutions form a k dimensional manifold. This is the image by f of the cube $[0, 2\pi]^k$ with opposite faces identified, and is therefore a k -dimensional torus.

Quasiperiodic time evolutions are detected experimentally by their frequency spectrum which contains instrumentally sharp peaks at the frequencies $\omega_1, \dots, \omega_k$ and their linear combinations with integer coefficients. In this manner the case $k = 2$ is frequently observed in hydrodynamical experiments. The case $k = 3$ is observed only rarely, and $k > 3$ has not been seen. The reason why higher quasiperiodic motions are not observed is that they are very unstable under small changes of the right hand side $F_{\mu}(x)$ of the evolution equation (1).

A way in which a quasiperiodic motion may be destroyed is by frequency locking. In practice it means that the frequencies ω_1, ω_2 (and possibly ω_3) which had irrational ratios become replaced by integral multiples of the same frequency, and a periodic motion is obtained. For instance if ω_1 and ω_2 were nearly equal, they will become synchronized. The synchronization of biological chemical oscillations in cells suspended in a common medium is probably due to frequency locking. Circadian rhythms may also use this phenomenon. It would be good to have detailed studies of frequency locking in nonbiological systems.

Another way for a quasiperiodic motion to be destroyed is through the formation of a strange attractors. This is an unconventional phenomenon, first studied in [22]. It can be expressed in conventional language by saying that the nonlinear coupling between different oscillations (or "modes") produces intrinsic noise. We come now to the study of these "intrinsically noisy" or "turbulent" systems.

3. Turbulence Time Evolutions (Strange Attractors)

Computer studies have in recent years provided many examples of strange attractors. An attractor is an asymptotic locus of solutions of the evolution equation (1) ^{*)}. A strange attractor is an attractor such that if $x(0)$ is on the attractor (or near it) and $\delta x(0)$ is a small perturbation of the initial condition, then $\delta x(t)$ grows exponentially with t . We have thus sensitive dependence on initial condition. The rate of exponential growth is called characteristic exponent. It should be remarked that some very special perturbations will in fact decrease, but it is required that most small perturbations will increase with time. Of course the exponential increase will last only for a while : until the perturbed and the unperturbed solutions have become completely unrelated. Intuitively it is clear that for many time evolutions there are special initial conditions such that a small perturbation has important consequences, it is less obvious that this can occur for all initial conditions. This is probably why the role of strange attractors has come to light in dissipative systems only recently (Lorenz [11], Ruelle and Takens [22]), even though they have been known mathematically for some time ^{**)}.

Some strange attractors are well understood mathematically (see Smale [23]) but most are not. We shall discuss here an attractor which is poorly understood mathematically, but important because of its simplicity and frequent occurrence. This attractor has been found by Rössler [16] and Pomeau in computer studies, and modeled by Hénon [7]. It consists of a ribbon of solutions of an evolution equation in three dimensions which forms a loop with a cross section like the following



Turning round the loop corresponds to a map of the above figure to itself which flattens it, stretches it, and folds it :

^{*)} To be more definite, one should allow small random perturbations of the solutions, to "shake them away" from non-attracting fixed points. A precise definition can be obtained along those lines.

^{**)} For an elementary discussion of strange attractors and their role in turbulence see Ruelle [21].



The stretching is the feature which causes sensitive dependence on initial condition.

A numerical study of the frequency spectrum associated with strange attractors shows the presence of a continuous spectrum, i.e. broadband noise is present and/or peaks are not instrumentally sharp. This has to be viewed as a fact of life rather than a mathematical result ^{*}). It is however an important fact because the frequency spectrum can be measured fairly easily while the experimental measurement of characteristic exponents is difficult (it has been obtained in an electric system by Gollub et al [5]).

4. Diagnosis of Turbulence

When one observes nonperiodic chemical oscillations, one would like to know if they are quasiperiodic or "turbulent", and to analyse the transition from quasiperiodicity to turbulence.

First, let the system be quasiperiodic : the frequency spectrum contains only linear combinations of a finite number of frequencies. Suppose (for simplicity) that the spectrum is generated by linear combinations of two frequencies ω_1 and ω_2 with ω_2/ω_1 irrational. The evolution of the system then takes place on a two-dimensional torus, which can be visualized as a circle by a cross section (Poincaré map). To be more specific let $x(t), y(t), z(t)$ be three observables of the system. Plotting $(x(t_n), y(t_n))$ where the t_n are determined by $z(t_n) = \text{constant}$ will yield points on a closed curve C . This curve will be a circle C' if the observables x, y, z are suitably chosen.



Let now the quasiperiodic system bifurcate to a turbulent one. The circle will be transformed into another set, and this transformation will be indicative of the nature of the bifurcation which has taken place. A study of this sort has been made by Curry and Yorke [2], obtaining curves similar to those of Pomeau-Hénon discussed above.

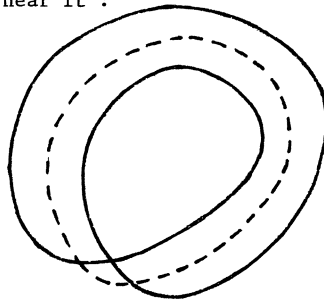
Suppose that only one observable $x(t)$ is known (often only one quantity is monitored in experiments - a concentration in chemical experiments). Time shifts will then produce other observables $y(t) = x(t+\beta), z(t) = x(t+\gamma)$. The above analysis may thus still be performed.

5. Other Pathways to Turbulence

Turbulent behavior may arise from quasiperiodic behavior as we have discussed above ^{*)}. It is also possible for a steady state or periodic solution to become unstable and make a finite jump to turbulence which is difficult to analyse. There are however two more ways to go to turbulence which are to some extent understood, and which we would like to discuss briefly (for a general review see Eckmann [3]).

In the intermittent transition to turbulence, apparently regular periodic oscillations are interrupted at irregular intervals by puffs of irregular, turbulent, behavior. When some parameter μ is increased, the puffs become more and more frequent and coalesce into continuous turbulence. This phenomenon has received a beautiful explanation from Pomeau and Manneville [14]. Starting from an attracting periodic orbit, they argue that in one of the instabilities which may develop when μ increases, the solutions of the time evolution equation still make many turns near the now unstable periodic orbit, before making an excursion away from it. These excursions are the turbulent puffs.

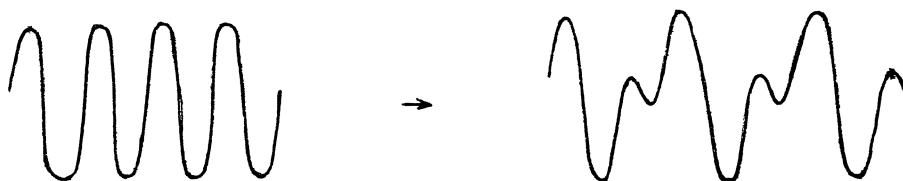
Another way a periodic orbit may become unstable is by period doubling. A periodic orbit of period T becomes non-attracting for $\mu = \mu_1$, while a periodic orbit of period $\approx 2T$ is created near it :



*) See Ruelle and Takens [22], Newhouse, Ruelle and Takens [13].

This phenomenon may occur repeatedly, an attracting periodic orbit of period $\approx 2^{n-1}T$ being replaced at μ_n by an attracting periodic orbit of period $\approx 2^n T$. Feigenbaum [4] has discovered that the points μ_n accumulate to a limit μ_∞ according to a universal geometric law (i.e. $\frac{\mu_{n+1} - \mu_n}{\mu_n - \mu_{n-1}}$ tends to a universal constant). After μ_∞ , turbulent behavior is predicted. This succession of events has apparently been seen in hydrodynamic experiments by Libchaber and Maurer [10].

I feel that there is no reason why such events could not also be seen in chemical experiments. It appears indeed that a period doubling bifurcation has been



observed by Pye and Chance [15] in their study of oscillations in cell-free extracts of brewer's yeast.

6. A Chemical Attractor

We now briefly discuss the picture of a strange attractor obtained from a chemical experiment by the group in Bordeaux (see [17]). We have in first approximation a closed orbit, which spreads out near one point to make little turns. The amount of turning depends on the position. We shall describe this situation by an approximate Poincaré map, which will be one dimensional and non-invertible (it can thus only be approximate). It is convenient to consider that the real variable x is mapped into the complex plane to

$$Ax + B + Ce^{idx}$$

(A,B,C complex, d real) and then the complex plane linearly projected back to the real line (the projection may be oblique). Notice that Ce^{idx} describes turns proportional to x . We have thus a real map of the form

$$x \mapsto ax + b + |C| \sin d(x-x_0) \tag{3}$$

By a change of variable $\xi = ax + \beta$, we transform (3) into the normal form

$$\xi \mapsto f(\xi) = a\xi + c \sin(\xi - \xi_0) \tag{4}$$

with real a, c, ξ_0 . To have an attractor we need $|a| < 1$, and we may take $c > 0$, $\xi_0 \in [0, 2\pi)$.

When $c > |a|$, the map (4) does not have a unique inverse; it resembles the well-studied $\xi \rightarrow a\xi(1-\xi)$, but with several maxima. In fact the roots of $\pm f(\xi) = \xi$ are contained in $[\frac{-c}{1-|a|}, \frac{c}{1-|a|}]$ and it is easy to see that iterates of f map the whole of \mathbb{R} into this interval. Furthermore

$$(f''/f')' = -(1 + \frac{a}{c} \cos(\xi - \xi_0)) (\frac{a}{c} + \cos(\xi - \xi_0))^{-2} < 0$$

so that f has negative Schwarzian derivative.

The picture in [17] corresponds to $a > 0$. Qualitatively, (4) appears to explain the facts discussed in [17]: existence of periodic and nonperiodic behavior, possible coexistence of different types of behavior depending on initial condition^{*}). The Feigenbaum cascade should also be observable with suitable choice of parameters.

Bibliography

1. G. Ahlers. Low-temperature studies of the Rayleigh-Bénard instability and turbulence. *Phys. Rev. Lett.* 33, 1185-1188 (1974).
2. J.H. Curry and J.A. Yorke. A transition from Hopf bifurcation to chaos: computer-experiments with maps on \mathbb{R}^2 , in The Structure of Attractors in Dynamical Systems, ed. by N.G. Markley, J.C. Martin, W. Perrizo, *Lecture Notes in Mathematics*, Vol. 668 (Springer, Berlin, Heidelberg, New York 1978)
3. J.-P. Eckmann. Roads to turbulence in dissipative dynamical systems. *Rev. Mod. Phys.* to appear.
4. M. Feigenbaum. Quantitative universality for a class of nonlinear transformations. *J. Statist. Phys.* 19, 25-52 (1978). The universal metric properties of nonlinear transformations. *J. Statist. Phys.* 21, 669-706 (1979). The transition to periodic behavior in turbulent systems. *Commun. math. Phys.* 77, 65-86 (1980).
5. J.P. Gollub, E.J. Romer, and J.E. Socolar. Trajectory divergence for coupled relaxation oscillators: measurements and models. *J. Statist. Phys.* To appear.
6. J.P. Gollub and H.L. Swinney. Onset of turbulence in a rotating fluid. *Phys. Rev. Lett.* 35, 927-930 (1975).
7. M. Hénon. A two-dimensional mapping with a strange attractor. *Commun. Math. Phys.* 50, 69-77 (1976).
8. E. Hopf. Abzweigung einer periodischen Lösung von einer stationären Lösung eines Differentialsystems. *Ber. Math.-Phys. Kl. Sächs. Akad. Wiss. Leipzig* 94, 1-22 (1942).
9. C.D. Landau. Turbulence. *Dokl. Akad. Nauk SSSR* 44, 339-342 (1944).
10. A. Libchaber et J. Maurer. Une expérience de Rayleigh-Bénard de géométrie réduite; multiplication, accrochage et démultiplication de fréquences. *J. Physique* 41, Colloques C3, 51-56 (1980).

^{*}) Equation (4) seems also to be in qualitative agreement with a recent study by J.-C. Roux, J.S. Turner, W.D. McCormick, and H. Swinney [18].

11. E.N. Lorenz. Deterministic nonperiodic flow. J. atmos. Sci. 20, 130-141 (1963).
12. J.B. McLaughlin and P.C. Martin. Transition to turbulence of a statistical stressed fluid. Phys. Rev. Lett. 33, 1189-1192 (1974). Transition to turbulence in a statically stressed fluid system. Phys. Rev. A 12, 186-203 (1975).
13. S. Newhouse, D. Ruelle, and F. Takens. Occurrence of strange axiom A attractors near quasiperiodic flows on T^m , $m \geq 3$. Commun. Math. Phys. 64, 35-40 (1978).
14. Y. Pomeau and P. Manneville. Intermittent transition to turbulence in dissipative dynamical systems. Commun. Math. Phys. 74, 189-197 (1980).
15. K. Pye and B. Chance. Sustained sinusoidal oscillations of reduced pyridine nucleotide in a cell-free extract of Sacharomyces Carlsbergensis. Proc. Nat. Acad. Sci. 55, 888-894 (1966).
16. O.E. Rössler. An equation for continuous chaos. Phys. Lett. 57 A, 397-398 (1976).
17. J.C. Roux, A. Rossi, S. Bachelard, and C. Vidal. Representation of a strange attractor from an experimental study of chemical turbulence. Phys. Lett. 77 A, 391-393 (1980).
18. J.C. Roux, J.S. Turner, W.D. Mc Cormick, and H.L. Swinney. Experimental observations of complex dynamics in a chemical reaction. Preprint.
19. D. Ruelle. Some comments on chemical oscillations. Trans. N.Y. Acad. Sci. II, 35, 66-71 (1973).
20. D. Ruelle. What are the measures describing turbulence ? Progr. Theoret. Phys. Suppl. 64, 339-345 (1978).
21. D. Ruelle. Les attracteurs étranges. La Recherche 11, 132-144 (1980); English translation : Strange attractors. Math. Intelligencer 2, 126-137 (1980).
22. D. Ruelle and F. Takens. On the nature of turbulence. Commun. Math. Phys. 23, 343-344 (1971).
23. S. Smale. Differentiable dynamical systems. Bull. Amer. Math. Soc. 73, 747-817 (1967).
24. C. Vidal, J.C. Roux, S. Bachelard and A. Rossi. Experimental study of the transition to turbulence in the Belousov-Zhabotinsky reaction. Ann. N.Y. Acad. Sci. 357, 377-396 (1980).
25. C. Vidal, J.C. Roux, A. Rossi and S. Bachelard. Etude de la transition vers la turbulence chimique dans la réaction de Belousov-Zhabotinsky. C.R. Acad. Sci. Paris, Série C, 289, 73-76 (1979).

Topology of Chaos in a Chemical Reaction

J.C. Roux* and Harry L. Swinney

Department of Physics, The University of Texas at Austin,
Austin, TX 78712, USA

1. Introduction

The authors and coworkers (TURNER et al. [1]; ROUX et al. [2]) have investigated the dynamics of the Belousov-Zhabotinskii reaction in a stirred flow reactor. These experiments, which were motivated by the numerical modeling studies of TURNER [1,3] described elsewhere in this volume, have revealed a sequence of periodic and chaotic regimes that alternate as a function of the flow rate. The periodic regimes are characterized by power spectra (of the bromide ion potential) that consist of a single fundamental frequency component and its harmonics, as Fig. 1a illustrates, while the chaotic regimes are characterized by broadband power spectra, as Fig. 1b illustrates. The observed periodic-chaotic sequence will be compared with the numerical modeling predictions and with other experiments in this section. The remainder of the paper will be devoted to an analysis of the phase space portraits and Poincare maps for the data obtained in the first chaotic regime in the sequence.

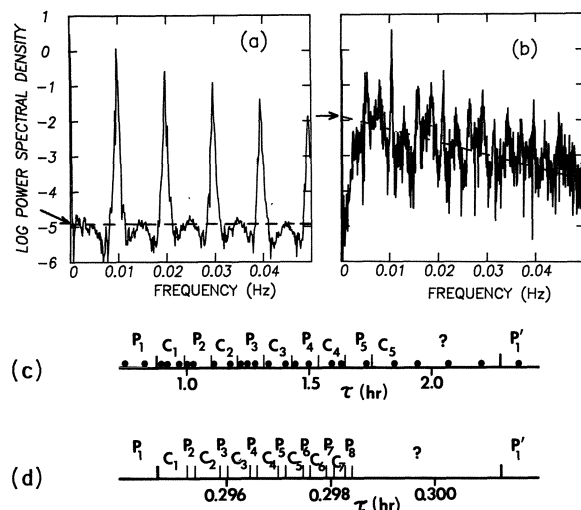


Fig. 1 Power spectra obtained in (a) periodic regime P_1 with $\tau = 0.49$ hr and (b) chaotic regime C_1 with $\tau = 0.90$ hr. The arrows on each ordinate indicate the intercepts at zero frequency of the broadband background noise level. The observed and predicted periodic-chaotic transition sequences are shown in (c) and (d), respectively (from [1,2])

* Permanent address : Centre de Recherche Paul Pascal
Université de Bordeaux I
Domaine Universitaire
33405 Talence Cédex (France)

The reaction was studied for a range of residence times τ , where τ = reactor volume/flow rate; all other variables were held fixed [1,2]. One way in which we have distinguished the periodic and chaotic regimes is by comparing the zero-frequency intercepts of the background noise level in the power spectra. In the periodic regimes the background noise level, which is presumably due to instrumental noise, is typically three orders of magnitude lower than the broadband spectral intensity at low frequencies for the chaotic regimes; this is illustrated for the first periodic regime ("P₁") in Fig. 1a and the first chaotic regime ("C₁") in Fig. 1b. The sequence of dynamical regimes distinguished in this way is summarized in Fig. 1c, which can be compared with Fig. 1d, which shows the sequence predicted [1] in a numerical study of a four variable model of the Belousov-Zhabotinskii reaction. The qualitative agreement between the model predictions and the experimental observations is excellent. It is expected that refinements of the model will improve the quantitative agreement.

The transition sequence that we have observed is similar to that observed earlier by Hudson et al. [4-5] and by the Bordeaux group [6], except that our sequence has the opposite dependence on residence time. This difference reflects the fact that the experiments of Hudson and the Bordeaux group were conducted for shorter residence times ($0.06 < \tau < 0.2$ hr) than our experiments ($0.5 < \tau < 4$ hr); these two ranges in τ are on the opposite borders of the oscillating domain (in terms of τ) of the parameter region in which oscillations are found.

We conclude this discussion of the transition sequence by noting that the sequence in Fig. 1c undoubtedly has a rich fine structure that could be studied if the flow rate control and stability were better than the few percent level we have achieved thus far. As an example of the underlying fine structure, a period doubling sequence (FEIGENBAUM [7]) apparently occurs in the P₁ regime as C₁ is approached. We have observed time series with periods 2, 4, and 8, but the system drifts uncontrollably through the different 2ⁿ regimes. The reverse (noisy) period doubling sequence probably occurs just beyond the onset of C₁, and, in fact, Fig. 1b can be seen to correspond to noisy period 4, where $f = 0.0105$ Hz is fairly sharp and $f/2$ and $3f/4$ are broadened.

2. Phase Portraits, Poincaré Sections, Maps, and Perturbations

Phase portraits have been constructed from the bromide ion time series records $B(t_i)$ [$i = 1, \dots, 32768$] following a procedure suggested by RUELLE [8]: an n -dimensional (nD) portrait can be obtained by plotting successive points [$B(t_i), B(t_i+T), \dots, B(t_i+(n-1)T)$]. If n is sufficiently large, this procedure is justified by the embedding theorem of TAKENS [9]. A 2D portrait illustrating the strange attractor that characterizes regime C₁ is shown in Fig. 2.

Two-dimensional projections of the attractor such as that in Fig. 2 show only that the trajectories are nonperiodic and that they are limited to some specific portion of the phase space. In order to learn more about this subset we can look at the $(n-1)D$ Poincaré sections of nD portraits. Consider, for example, a 3D portrait with the third dimension normal to the two shown in Fig. 2. Figure 3a shows the 2D Poincaré section obtained for a plane that passes, perpendicular to the paper, through the dashed line in Fig. 2. Clearly the points of intersection lie on a smooth curve, indicating that the trajectories lie on a well-defined 2D surface. Almost all the Poincaré sections obtained in this way gave curves that were more or less straight lines, except those obtained in the constricted part of the attractor (see the discussion and diagrams at the end of this section). Although all of the trajectories appear to merge in the constricted part of the attractor, this of course does not mean that a trajectory entering this part of the attractor can emerge in an arbitrary direction. In fact, when looking at the attractor as it evolves (see movie [10]), one can see, for instance, that trajectories lying on the inside of the attractor emerge from the constriction on the outside. Thus, the observed merging of the trajectories is simply a limitation of the method we used to construct them [11].

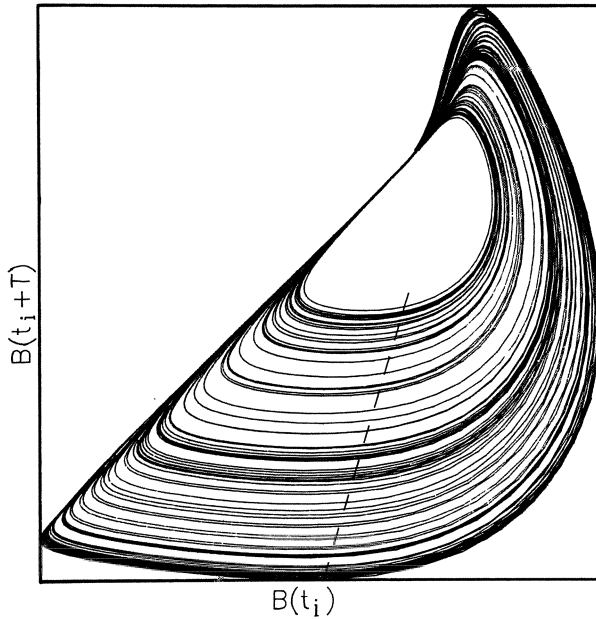


Fig. 2
A 2D phase portrait obtained
(with $T = 8.8$ s) for regime C_1
($\tau = 0.90$ hr)

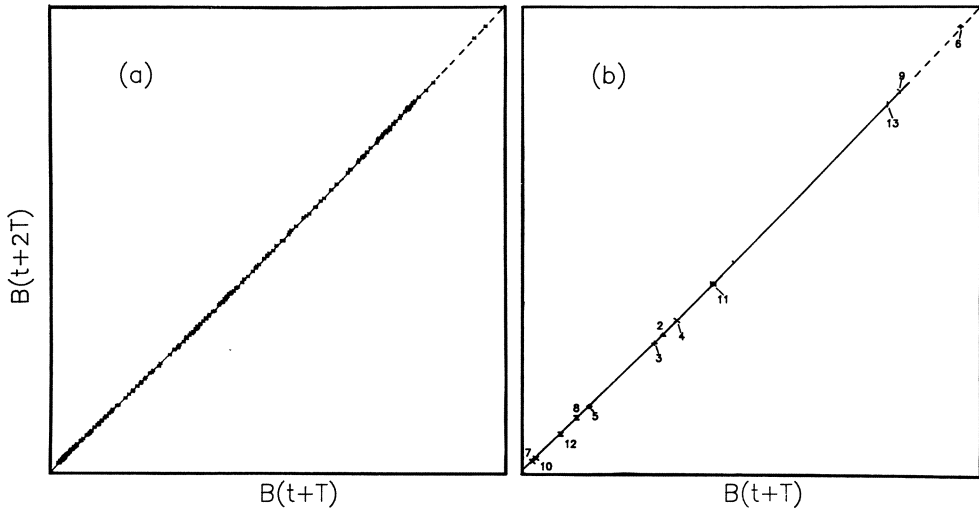


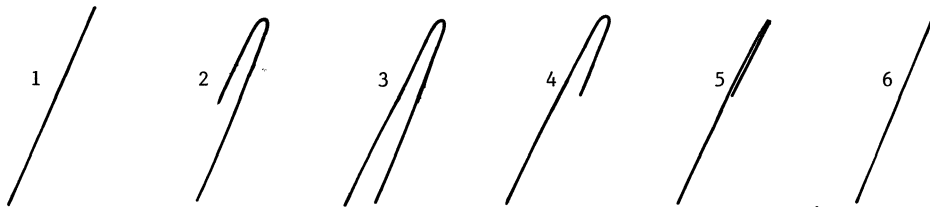
Fig. 3 (a) Poincaré section for C_1 , formed by the intersection of the 3D trajectories with the plane (normal to the paper) passing through the dashed line in Fig. 2. (b) The Poincaré section after a perturbation that occurred about when the trajectory passed through the point numbered 4 (see text). The unstable manifold is shown by the solid line and its extension by the dashed line.

We can look closer at the structure of the attractor by constructing the first return map for the Poincaré section as shown in Fig. 4a. The points can be seen to lie on a well-defined curve, indicating that the trajectories on the attractor have some kind of order. Some points are clearly off of this line; they are the results of some spontaneous perturbations of the chemical system. Although we cannot ascertain the precise origin of these perturbations (gas bubbles,

impurities, etc.), we can take advantage of their occurrence to understand some of the properties of the attractor. The chronology of one of these perturbations is shown Fig. 4b and the corresponding points of the Poincaré section are shown in Fig. 3b.

After the perturbation, the trajectories rapidly return to the attractor, indicating that the attractor has some kind of stability. Furthermore, one can see (Fig. 3b) that all the perturbed trajectories lie on the unstable manifold (the solid line) or on its extension (the dashed line), thus indicating that the stable manifold is strongly contracting. Note that points 5, 7, and 8, which appear to be on the Poincaré section (Fig. 3b), are actually off the map (Fig. 4b); this again illustrates the usefulness of the Poincaré map for the description of a chaotic state.

Figures 3b and 4b give insight into the way the attractor evolves: the "upper" trajectories, appearing as points 6 and 9, reappear on the lower part as points 7 and 10, which themselves are mapped into the central part of the attractor (points 8 and 11). So, although we have not yet been able to resolve folding in the Poincaré section, we can propose the following scheme, inspired by the behavior of one of the Rössler attractors [12]:



This figure represents schematically the evolution of the Poincaré sections at different locations on the attractor. Diagrams 2, 3, 4, and 5 represent the probable form of the Poincaré sections at successive positions along the constricted portion of the attractor, while diagrams 1 and 6, which are similar to Fig. 3a, represent, respectively, the Poincaré sections at locations preceding

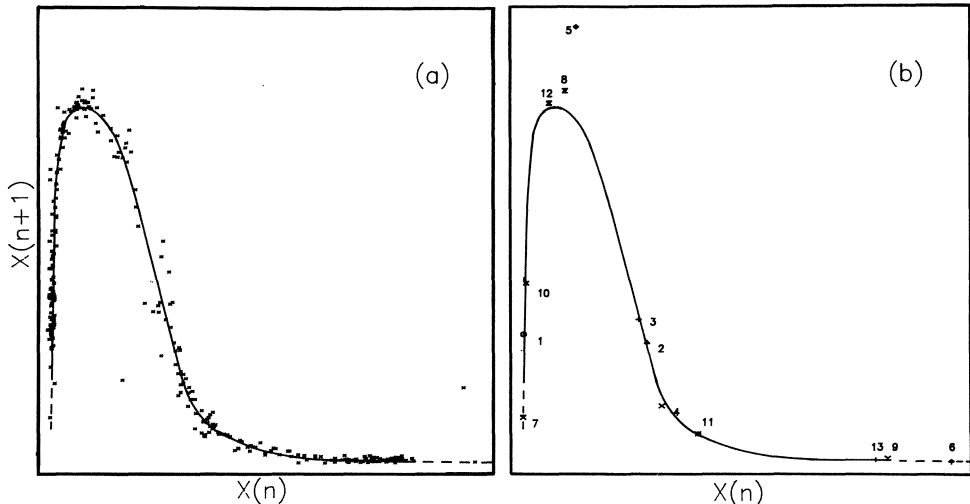


Fig. 4 (a) Poincaré return map for C_1 , formed by plotting as ordered pairs $[X(n), X(n+1)]$ the successive values of the bromide ion potential $B(t+2T)$ for phase space trajectories when they cross the plane (normal to the paper) through the dashed line in Fig. 2. (b) The Poincaré return map after a perturbation that occurred about when the trajectory passed through the point numbered 4 (see text)

and following the constricted part of the attractor. Although the present method of constructing the attractor fails to show the folding indicated in diagrams 2 through 5, it may be possible to see the folding with other attractor construction methods [11].

3. Sensitivity to Initial Conditions and Phase Coherence

Figure 5a shows 64 trajectories evolving from a very small cube at the tip of the arrow near the lower left corner. The minimum time delay between two trajectories entering the small cube is $400\Delta t$ (more than three turns), where $\Delta t = 0.88$ s. After $105\Delta t$ the initial distribution is spread over the attractor, the dispersion becoming greater as time passes. However, notice that even after almost 2 turns, the points are widely spread in space but not that widely spread in time (Fig. 5b indicates the time scale on the attractor). It thus appears that, even in this chaotic state, the attractor maintains some kind of "phase coherence" [13], which is the origin of the sharp peaks that remain in the power spectrum in the chaotic state (Fig. 1b).

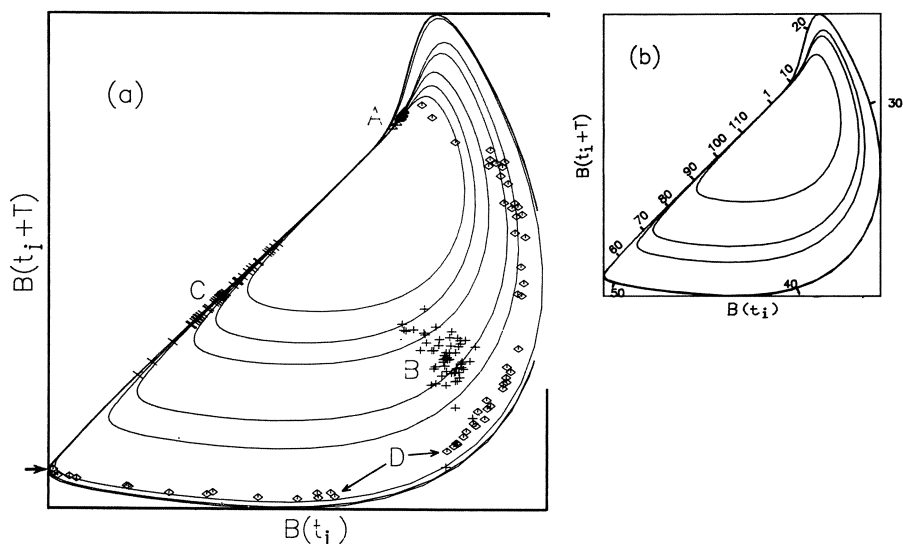


Fig. 5 (a) The evolution of a set of points that were initially all within a very small phase space volume located at the tip of the arrow on the left: A(Δ), $80\Delta t$: B(+), $105\Delta t$: C(\backslash), $140\Delta t$: D(\diamond), $210\Delta t$. (b) The speed of traversal of an orbit is illustrated by points plotted for different times (expressed in units of Δt). [$\Delta t = 0.88$ s]

Acknowledgements

We thank Robert Shaw for helpful discussions. J.-C. Roux gratefully acknowledges the granting of a leave of absence by the Centre Recherche Paul Pascal for the period September 1980 - August 1981. This research, conducted at The University of Texas at Austin in collaboration with J. S. Turner and W. D. McCormick, was supported by National Science Foundation Grant CHE79-23627 and The Robert A. Welch Foundation Grant F-805.

References

1. J. S. Turner, J.-C. Roux, W. D. McCormick, and H. L. Swinney, *Phys. Lett.* **85A**, 9, (1981)
2. J.-C. Roux, J. S. Turner, W. D. McCormick, and H. L. Swinney, in Nonlinear Problems: Present and Future, ed. by A. R. Bishop (North Holland, Amsterdam, 1981).
3. J. S. Turner, this volume: Discussion Meeting, Kinetics of Physicochemical Oscillations, Aachen, 1979: 1980 Solvay Conference in Chemistry, to be published.
4. J. L. Hudson, M. Hart, and D. Marinko, *J. Chem. Phys.* **71**, 1601 (1979).
5. J. L. Hudson and J. C. Mankin, *J. Chem. Phys.* **74** 6171 (1981).
6. C. Vidal, J.-C. Roux, S. Bachelart, and A. Rossi, *N. Y. Acad. Sci.* **357**, 377 (1980).
7. M. J. Feigenbaum, *J. Stat. Phys.* **19**, 25 (1978).
8. D. Ruelle, private communication.
9. F. Takens, in Dynamical Systems and Turbulence: Proceedings of the 1978-1980 Warwick Symposium, Springer Lecture Notes in Mathematics, ed. by D. Rand and L.-S. Young (Springer Berlin, Heidelberg, New York 1981)
10. J.-C. Roux, H. L. Swinney, and R. S. Shaw, Attracteur Etrange dans un Systeme Chimique (un film, 1981).
11. R. S. Shaw, J.-C. Roux, and H. L. Swinney, to be published.
12. O. E. Rossler, in Synergetics, A Workshop, ed. by H. Haken, (Springer, Berlin, Heidelberg, New York, 1977), p. 184.
13. Farmer, J. Crutchfield, H. Froehling, N. Packard, and R. Shaw, *N. Y. Acad. Sci.* **357**, 453 (1980).

Experiments on Chaos in a Continuous Stirred Reactor

J.L. Hudson, J. Mankin, J. McCullough, P. Lamba

Department of Chemical Engineering
University of Virginia
Charlottesville, VA 22901, USA

1. Introduction

The Belousov-Zhabotinskii reaction can undergo a variety of oscillation types in an open system as has been demonstrated by means of experiments [1] and mathematical models [2,3]. There is also evidence that chaotic behavior can occur in this reaction system [4-12]. Recent theories support the proposition that chaos can be produced by chemical reactions and flow [11, 13-17] and that the observed behavior is not an artifact of the experiments.

We have shown that with the variation of a single parameter (flow rate or residence time) in a continuous stirred reactor, there is a sequence of well-defined oscillatory states [5]. Over most of the range the behavior is periodic, but in three reproducible bands chaotic behavior is observed. This chaotic behavior is an irregular mixture of the periodic oscillations which bound it. More recently a similar sequence has been observed by researchers at the University of Texas in a different region of parameter space [10, 11].

Return maps have been constructed from our experimental data [9, 18] and we have recently calculated a positive Liapunov characteristic exponent for one apparent chaotic region [9]. Tomita and Tsuda [18-20] have constructed a model of the series of bifurcations and have analyzed the transitions from periodic n peak to periodic $n + 1$ peak oscillations. They predict a transition region containing both periodic and chaotic mixtures of n peak and $n + 1$ peak oscillations. Tomita and Tsuda have also compared this type of transition to the period doubling bifurcations discussed by Feigenbaum [21].

In this paper we reinvestigate in detail one of these transitions, viz., that from two peak periodic to three peak periodic oscillations. Between the two and three peak periodic regions is a mixed (2-3) region which can be either periodic or chaotic as predicted by Tomita and Tsuda. We characterize the chaotic behavior by means of return maps. Finally we investigate the rate of convergence of transient trajectories toward the stable two peak oscillations.

2. Experiments

The experiments were carried out in a continuous stirred reactor of volume 26.4 ml at a temperature of 25°C. The mixed feed concentrations of the malonic acid, sodium bromate, sulfuric acid and cerous ion are 0.3, 0.14, 0.2 and 0.001 M respectively. Details are given in earlier publications [5, 9].

3. Results

The dependence of the reactor behavior on reciprocal residence time (flow rate/reactor volume) is shown in Fig. 1. This is a portion of the series of transitions presented in [5]. Between the two peak and three peak periodic regions is a mixed region of width 0.005 min^{-1} . This mixed region always

occurs and its width is very reproducible. The behavior in the mixed region is usually chaotic as shown in Fig. 2 (half of a stereoplot, variables Pt, Br⁻, and Pt (t-10 sec) potentials). The coordinates of Fig. 2 are on scales of 0 to 255 corresponding to the output of an 8 bit analog to digital converter used to interface to a microcomputer. Occasionally, however, the mixed mode behavior is a 2-3 periodic oscillation as shown in Fig. 3. Tomita and Tsuda have developed a model which yields both chaotic and periodic mixed mode oscillations between the period two peak and three peak oscillations [18-20].

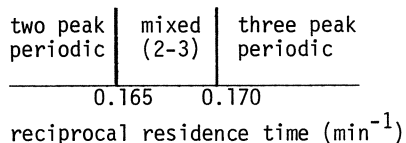


Fig. 1 Transition from two peak to three peak oscillations

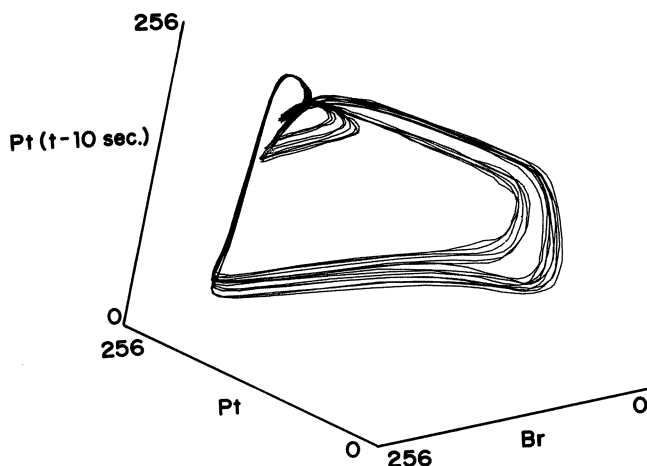


Fig. 2 Mixed 2-3 chaotic behavior

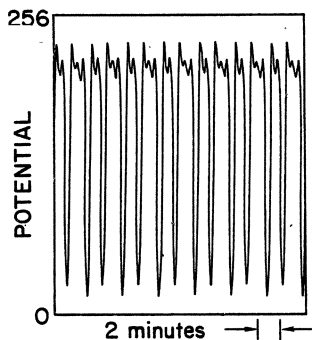


Fig. 3 Mixed 2-3 periodic behavior

Their model is based on a return map constructed from our earlier experimental data [5]. By adding a parameter b to the return map as shown in (1) Tomita

$$x_{n+1} = f(x_n) + b \tag{1}$$

and Tsuda demonstrate how the series of transitions seen in our experiments could arise. This form was chosen because the return maps constructed from the experimental data for the 2-3 and 3-4 chaotic regions appear to differ only

by a constant. This model predicts that the 2-3 chaotic behavior should be bracketed by periodic oscillations which are mixtures of two and three peaks. In our earlier work we observed only chaotic behavior in the mixed 2-3 region. It is now evident that a periodic 2-3 oscillation exists. Both the periodic and chaotic 2-3 modes are stable as evidenced by their persistence and their insensitivity to perturbations. However, we have not been able to determine the locations of the periodic and chaotic behaviors within the mixed 2-3 regions. Usually the entire range is chaotic. Occasionally it is entirely periodic. We have also observed 2-3 periodic behavior bracketed by chaotic behavior. We have not yet observed the 2-3 chaotic bracketed by 2-3 periodic suggested by the model. The exact behavior in the mixed region is thus unknown, and the variability in the results is probably caused by slight variations from day to day in feed concentrations or flow rates. It should be stated, however, that in a given series of experiments the results are reproducible.

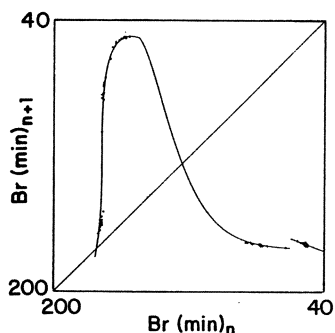


Fig. 4 $n + 1$ return map

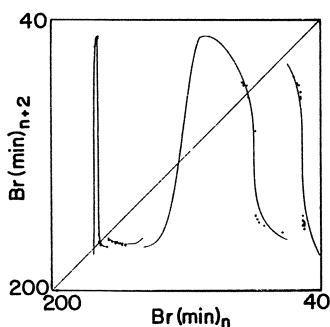


Fig. 5 $n + 2$ return map

A return map for the 2-3 chaotic region minima in bromide ion potential is shown in Fig. 4. The + are experimental data and the curve is a function fitting the data [9]. The $n + 2$ and $n + 3$ maps constructed with both the data and the function are shown in Figs. 5 and 6, respectively. The fit is reasonable but is clearly not as good as for the $n + 1$ map. We investigated the effect of varying the parameter b in (1). A sufficiently large negative value of b ($b = -2.4$) causes two additional crossings of the 45° line in the $n + 2$ map at the two outside discontinuities. These crossings are stable and therefore a periodic two peak cycle has been created. A sufficiently positive value of b ($b = 0.5$) produces three points of tangency in the $n + 3$ map and the subsequent creation of a stable 3 peak cycle.

In order to investigate the reasonableness of the $n + 2$ map, particularly the creation of stable two peak cycles by means of new crossings of the 45° line rather than by the transition from unstable to stable of an already existing 2 peak, we performed the following experiment. We jumped from a two peak periodic cycle to the chaotic region by means of a change in flow rate. From this we constructed the $n + 2$ map of Fig. 7. The points start at the 45° line and diverge from it, alternating from one side to the other. This implies the existence of an unstable two cycle at conditions where the system is chaotic. The model, i.e., using the fit of Fig. 4 and varying b in (1), is not consistent with that observation. The discrepancy could very well be in the expression used to fit the return map. We plan to use such information to develop a more reasonable fit.

Transient experiments can also be done by sudden changes into the periodic region. An $n + 2$ map constructed from a jump into the two peak periodic region is shown in Fig. 8. Here the points converge to the 45° line and

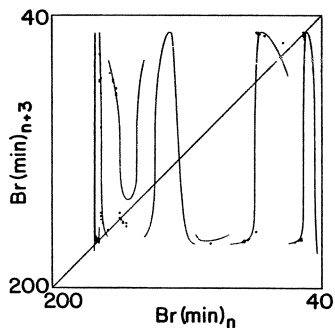


Fig. 6 $n + 3$ return map

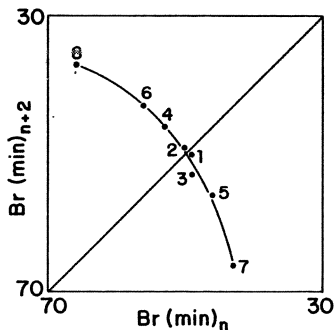


Fig. 7 Divergence from an unstable two peak cycle

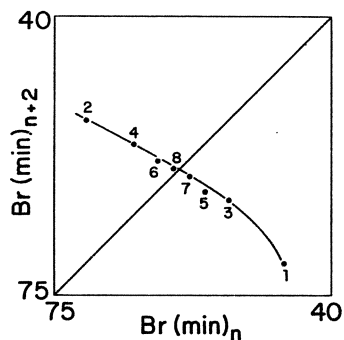


Fig. 8 Convergence to a stable two peak cycle

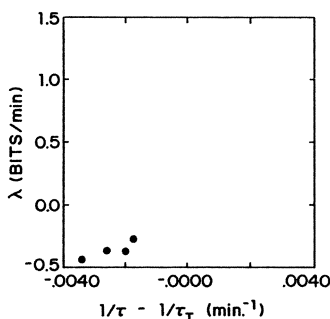


Fig. 9 Dependence of Liapunov characteristic exponent on residence time

alternate sides. From such a plot a value for the Liapunov characteristic exponent can be obtained for periodic behavior. For the conditions of Fig. 8 it is $\bar{\lambda} = -0.39$ bits/min.

The Liapunov characteristic exponent is shown in Fig. 9 as a function of $\tau^{-1} - \tau_T^{-1}$ where τ^{-1} is the reciprocal residence time and τ_T^{-1} is its value at the transition between the periodic two peak region and the 2-3 mixed region. Its value in the chaotic region was calculated from the fit shown in Fig. 4 as done in our earlier work [9]. $\bar{\lambda}$ is of course negative in the periodic region and positive for chaos [22]. Since it appears that a two peak cycle exists on both sides of the transition point, the value of $\bar{\lambda}$ passes continuously through zero at $\tau^{-1} = \tau_T^{-1}$.

Acknowledgement

This work was supported in part by the National Science Foundation through grant CPE 80-21950.

1. K. R. Graziani, J. L. Hudson, and R. A. Schmitz, Chem. Eng. J. **12**, 9 (1976).
2. K. Showalter, R. M. Noyes, and K. Bar-Eli, J. Chem. Phys. **69**, 2514 (1978).
3. Richard M. Noyes and N. Ganapathisubramanian, "A discrepancy between experimental and computational evidence for chemical chaos", to be published J. Chem. Phys.
4. R. A. Schmitz, K. R. Craziani, and J. L. Hudson, J. Chem. Phys. **67**, 3040 (1977).

5. J. L. Hudson, M. Hart, and D. Marinko, *J. Chem. Phys.* 71, 1601 (1979).
6. J. L. Hudson, D. Marinko, and C. Dove, Discussion meeting, "Kinetics of Physicochemical Oscillations," Aachen, September 1979.
7. O. E. Rössler and K. Wegmann, *Nature (London)* 271, 89 (1978).
8. C. Vidal, J.-C. Roux, S. Bachelart, and A. Rossi, *Annals N.Y. Acad. Sci.* 357, 377 (1980).
9. J. L. Hudson and J. C. Mankin, *J. Chem. Phys.* 74, 6171-6177 (1981).
10. J.-C. Roux, Jack S. Turner, W. D. McCormick and Harry L. Swinney, to be published, Proceedings Conf. Los Alamos, A. R. Bishop, ed. (North-Holland, 1981).
11. Turner, Jack S., J.-C. Roux, W. D. McCormick and Harry L. Swinney, *Physics Letters*, to be published.
12. J. C. Roux, A. Rossi, S. Bachelart, and C. Vidal, *Phys. Lett. A* 77, 391 (1980).
13. O. E. Rössler, *Z. Naturforsch. Teil A* 31, 259 (1979).
14. Kazuhisa Tomita and Ichiro Tsuda, *Physics Lett. A* 71, 489 (1979).
15. Jack S. Turner, Discussion meeting, "Kinetics of Physicochemical Oscillations", Aachen, September 1979.
16. K.-D. Willamowski and O. E. Rössler, Discussion meeting, "Kinetics of Physicochemical Oscillations," Aachen, September 1979.
17. J. J. Tyson, *J. Math. Biol.* 5, 351 (1978).
18. Kazuhisa Tomita and Ichiro Tsuda, *Prog. Theor. Phys.* 64, 1138 (1980).
19. Ichiro Tsuda, "On the abnormality of period doubling bifurcations in connection with the bifurcation structure in the Belousov-Zhabotinsky reaction system", preprint (1981).
20. Ichiro Tsuda, "Self-similarity in the Belousov-Zhabotinsky reaction", preprint (1981).
21. Mitchell J. Feigenbaum, *Los Alamos Science* 1, 4 (1980).
22. Robert Shaw, *Z. Naturfor. A* 36(1), 80 (1981).

Chemical Kinetics as an Experimental Field for Studying the Onset of Turbulence

C. Vidal

Centre de Recherches Paul Pascal
F-33405 Talence

1. Introduction

The temporal evolution of chemically reacting systems has been known for a long time to obey nonlinear differential equations, according to the so-called kinetic mass-action law. Therefore nonlinear effects, such as periodic or non-periodic time dependence, may, in principle, be displayed by these systems, when a suitable set of experimental conditions is selected. This elementary remark leads us to the conclusion that chemical systems could and should be used i) to study nonlinear phenomena, ii) to check the relevance of the dynamical systems theory and iii) perhaps to discover some unobserved or unexpected behaviour. Though this conclusion may appear quite obvious nowadays, the situation was really different a few years ago and I should like to point out that this idea first appears in a paper by RUELLE [1] in 1973.

I shall draw a parallel between experiments belonging to hydrodynamics and chemistry, so as to point out their similarity from the analytical viewpoint. Then, once the results on the transition to turbulent flows in Rayleigh-Bénard convection have been briefly recalled, I shall review what we have learnt during the last three years from the study of the onset of chemical turbulence.

2. Hydrodynamic and chemical experiments

In the wide field of hydrodynamic research, three geometries have been more thoroughly studied than any other, namely the shear flow, the Couette flow and the Rayleigh-Bénard convection problems*. One example is, of course, enough to establish a comparison between hydrodynamics and chemistry. To this end we shall take the Rayleigh-Bénard (RB) convection, mainly because the transition to turbulence is best known in that case, thanks to the great number of investigations devoted to it.

2.1 Mathematical description

The mathematical approach of thermal convection is based on the equations of motion and heat transport. Considering an infinitely extended layer of a (neutral) incompressible fluid heated from below, with time and space-independent tempera-

* A complete review being out of the scope of this paper, the reader interested in more details is referred to a recently issued monograph [2].

tures fixed at its lower and upper boundaries, one can derive the following set of dimensionless equations [3] :

$$\begin{aligned}
 P^{-1} \left(\frac{\partial \vec{v}}{\partial t} + \vec{v} \cdot \nabla \vec{v} \right) &= - \nabla \pi + \vec{\lambda} \theta + \nabla^2 \vec{v} \\
 \nabla \cdot \vec{v} &= 0 \\
 \frac{\partial \theta}{\partial t} + \vec{v} \cdot \nabla \theta &= R \vec{\lambda} \cdot \vec{v} + \nabla^2 \theta
 \end{aligned}
 \tag{1}$$

- \vec{v} : velocity vector
- $\vec{\lambda}$: unit vector in the direction opposite to gravity
- θ : deviation from the static temperature distribution
- $\nabla \pi$: all terms which can be expressed as gradients in the Navier-Stokes equation
- t : time

The dependence of the problem on the physical properties of the fluid and the external conditions applied to the layer is expressed through two dimensionless parameters :

- i) the Prandtl number $P = \frac{d^2/K}{d^2/\nu} = \frac{\nu}{K}$
- ii) the Rayleigh number $R = \frac{\alpha g \Delta T d^3}{\nu K}$

- ν : kinematic viscosity
 - K : thermal diffusivity
 - α : isobaric thermal expansion coefficient
 - g : acceleration of gravity
 - d : thickness of the layer
 - ΔT : temperature difference between the lower and upper boundaries
- } of the fluid

To get these dimensionless equations one has to introduce the thickness d as the length scale, the thermal diffusion time d^2/K as the time scale and the ratio $\Delta T/R$ as the temperature scale. Moreover all the properties of the fluid are assumed to be temperature independent, with the exception of the density in the gravity term (the so-called Oberbeck-Boussinesq approximation). The relative influence of the two nonlinear advection terms of (1), $\vec{v} \cdot \nabla \vec{v}$ and $\vec{v} \cdot \nabla \theta$, will depend on the Prandtl number, the first (second) being dominant at low (high) P values. Accordingly one expects to be different the nonlinear effects provided by mercury ($P \sim 0.03$), liquid helium ($P \sim 1$), water ($P \sim 5$) or silicon oils ($P \sim 130$). Now, given a fluid layer (i.e. ν , K , α and d fixed, and therefore P) the only one parameter, involved in equations (1), which can be changed is the Rayleigh number R . Since it does not look quite easy to achieve this goal through g , the temperature difference ΔT is thus the experimental parameter used to this end. To summarize, the RB convection provides us with a simple physical system governed by a set of nonlinear differential equations ; according to the bifurcation theory, the Rayleigh number R , monitored through the temperature difference ΔT , is the bifurcation parameter under experimental control.

Consider now an open reacting medium of constant volume V , through which a stream of chemicals is forced at a volume flow J . This medium is furthermore assumed to be homogeneous in temperature and composition. Let X_{ℓ}^o and X_{ℓ} be the concentrations of chemical species X_{ℓ} in the input and output flows. If N species,

including intermediates, are involved, the mass-balance equations will be :

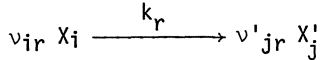
$$\frac{d X_{\ell}}{dt} = F_{\ell}(X) + \frac{J}{V} (X_{\ell}^{\circ} - X_{\ell})$$

$$\ell = 1, \dots, N$$

X : $(X_1, \dots, X_{\ell}, \dots, X_N)$

F_{ℓ} : concentration change of X_{ℓ} species due to the chemical reaction

When the chemical reaction is known (or at least assumed) to take place through a set of R elementary steps :



$$i, j = 1, \dots, N \quad ; \quad r = 1, \dots, R$$

then the functions F_{ℓ} can be further calculated. The rate of each step being given by the kinetic mass-action law, it comes out [24] as :

$$F_{\ell}(X) = \sum_r (v'_{\ell r} - v_{\ell r}) k_r \prod_i X_i^{v_{ir}}$$

$v_{\ell r}, v'_{\ell r}$: stoichiometric factors of the X_{ℓ} species in step r

k_r : rate constant of step r

Hence, the evolution of such a medium is described by the set of nonlinear differential equations :

$$\frac{d X_{\ell}}{dt} = \sum_r (v'_{\ell r} - v_{\ell r}) k_r \prod_i X_i^{v_{ir}} + \frac{1}{\tau} (X_{\ell}^{\circ} - X_{\ell}) \quad (2)$$

$$i, \ell = 1, \dots, N \quad ; \quad r = 1, \dots, R$$

where $\tau = \frac{V}{J}$ is the mean residence time of the chemicals inside the reacting volume V . The usual way to get a real system evolving according to (2) calls for a continuous stirred tank reactor (CSTR), a very common chemical engineering device.

From this analytical point of view a RB cell and a CSTR are both real physical systems whose evolution is governed by nonlinear differential equations. Therefore, each of them may be used, as well, in experimental investigations of nonlinear phenomena. Amongst many differences, it is noteworthy that a CSTR offers several bifurcation parameters, namely : τ (or $\mu = \frac{1}{\tau}$), X_{ℓ}° and even the temperature T since the rate constants k_r are temperature dependent (Arrhénus law). Only ΔT is available with an RB cell. Up to now, however, the mean residence time τ has always played this role in the reported chemical experiments [15-31]. This does not mean at all that the other variables should be neglected. On the contrary, from some preliminary attempts undertaken in our laboratory, we expect interesting results to appear from experiments bringing the temperature into play.

2.2 Experimental techniques

The number of techniques developed to investigate these two physical situations is not so great, at least if we pay attention to experiments where a time-dependent variable has been quantitatively measured. These techniques are displayed in table 1, together with some references where the corresponding experimental devi-

Table 1

	Experimental techniques	Measured Variables	References
RB convection	Local temperature variation at a boundary of the cell	T	4 5
	Doppler shift of a laser beam (Laser Doppler anemometry)	v	6 7
BZ reaction	Br ⁻ electrode potential	log [Br ⁻]	12 15 23
	Redox potential	E = f(X)	12
	Optical density at 340 nm	[Ce ⁴⁺]	16 17

ces are fully described. The RB convection has been studied in several liquids : H_e |8|, H₂O |6,9|, H_g |5|, silicon oils |10|. The bifurcation parameter has always been the Rayleigh number, scanned step by step changing the temperature difference ΔT .

All the reported chemical experiments |12-31| dealt with the same reaction, i.e. BELOUSOV-ZHABOTINSKY (BZ). As a matter of fact this reaction exhibits fascinating nonlinear effects (e.g. oscillations, chemical waves), which have been widely studied during the last twenty years*. The same bifurcation parameter, τ or μ changed by varying the volume flow J, is involved in all these studies. With the exception of some experimental conditions (temperature, inlet concentrations) these studies differ only by the physical property chosen to monitor the reaction. Compared to potentiometric techniques (see table 1), the optical density measurement at 340 nm offers at least two advantages : the spectrophotometric signal is i) linearly proportional to the concentration of a single intermediate species, Ce⁴⁺, and ii) without any time-delay. On the contrary, an ion-selective electrode has a response time of several seconds and its output varies on a logarithmic scale within the finite concentration range where the Nernst equation is valid ($\geq 5 \cdot 10^{-6}M$ for Br⁻).

2.3 Data analysis

The most common way to look at the main features of a dynamic regime is to get the Fourier transform of the time series records. This can be done either with a Fourier analyzer or by computing the Cooley-Tukey FFT algorithm of data points equally spaced in time. In addition, phase-space portraits are very helpful, particularly when irregular regimes are encountered. Here we are faced with a serious

* A detailed mechanism ("FKN" |32|) and a simplified model ("Oregonator" |33|) have been derived to account for the main features of the BZ reaction. A thorough analysis by TYSON can be found in reference |34|.

problem ; because only 1, or sometimes 2 independent variables are being measured, the true phase-space trajectories can never be drawn. Nevertheless it is conjectured that the salient topological properties of these trajectories would be preserved in some phase-space pictures reconstructed from the time record of a single variable $X(t)$. Two 3D-coordinate systems have been suggested : i) $X(t)$, $X(t+t_1)$, $X(t+t_2)$, t_1 and t_2 being arbitrary values of time [35], or ii) $X(t)$ and its first $\dot{X}(t)$ and second $\ddot{X}(t)$ derivatives with respect to time [36]. Whereas I am aware of only two recent representations of this type in the field of RB experimentation [8,9], several phase-space portraits have been obtained in chemistry [19,20,23] since the first one published [18].

3. Onset of turbulence in RB convection

To point out the original results obtained from chemical kinetics, it would seem useful as a first step to review briefly the observations yielded by RB experiments. Taking advantage of the recent theoretical progress [37], we shall focus our attention on systems with a few degrees of freedom. This is the reason why the bar graphs of table 2 only sketch the sequences of dynamic regimes observed in "little boxes", i.e. in RB cells where no more than 3 rolls are allowed to develop. The set of abbreviations introduced is quite simple :

S : stationary
P : periodic time dependence
 P_2, P_4, \dots : periodic regimes generated by successive subharmonic bifurcations of a periodic state (period doubling)
 QP_2, QP_3 : quasi-periodic regimes with 2 or 3 incommensurate basic frequencies
L : quasi-periodic regime where the basic frequencies are locked to a rational ratio (thus the regime actually looks periodic)
NP : non-periodic (or chaotic, or turbulent) state
IN : intermittent regime involving a switch at irregular time intervals between 2 different states

It must be remembered that the identification of a regime is based on the characteristics of its Fourier spectrum. As the sequence of bifurcations leading to an NP motion dependson the whole set of experimental conditions, the same liquid may exhibit several bifurcation diagrams. Nevertheless, we can disregard these details at the moment. Even at a glance at table 2, there are two major facts which cannot escape attention, taking into account the variety of fluids concerned :

i) only a few bifurcations are needed to reach a chaotic state ; this is in accordance with the new understanding of turbulence introduced ten years ago by RUELLE and TAKENS [37]

ii) the roads to turbulence may take three different paths or "scenarios" [38] :

- the Ruelle-Taken-Newhouse scenario (Hopf bifurcation)
- the Feigenbaum cascade (pitchfork bifurcation)
- the Pomeau-Maneville intermittency (inverse saddle-node bifurcation)

It is worth noting that the theoretical approach of these scenarios is already fairly well achieved [38]. As a consequence, it is time to set up a quantitative comparison between theoretical predictions and experimental results. The first attempts [8,9] dealing with the Feigenbaum cascade (universal scaling of bifurca-

Table 2

Liquid Prandtl number (authors)	Observed sequences of bifurcations leading to non-periodicity (R axis not scaled)	R value at the onset (*)
Mercury P = .03 (LIBCHABER, FAUVE)		5 - 6
Helium P = 0.4 - 0.8 (LIBCHABER, MAURER)		40 - 80
Water P = 2.5 - 5. (GOLLUB, BENSON)		50 - 120
Silicon oil P = 130. (BERGE, DUBOIS)		300

(*) Order of magnitude in R_C units (R_C : critical value of the Rayleigh number at which convection sets in)

tion points, subharmonics lowering in the Fourier spectrum) do not show any great discrepancy, even though the measurements are not yet accurate enough to ensure full agreement.

4. Dynamic patterns of the BZ reaction

Since its discovery by BELOUSOV [39] in 1958, the BZ reaction is known to undergo oscillations. Any chemical system being dissipative, these oscillations are damped and cancel after a while, when conducted in a closed vessel. They become self-sustained if they are performed in a CSTR with a suitable feed of reagents [40]. Thus, in such a chemical system, the nonlinear terms of equation (2) are important enough to give rise to a periodic behaviour. The experimental search for non-periodic (nor stationary) patterns began nearly four years ago, with the pioneering

work of SCHMITZ et al. [12]. The chronological list* of the papers issued or in press since that time is displayed in Fig.1, which is, in a way, an historical survey of this new field of experimental research. The transition from qualitative to quantitative investigations took place in the middle of 1979 when we published the first Fourier analysis [16]. Whereas 8 papers appear from 1977 to 1980, there are 13, including this one, which will have appeared at least during 1981, a promising (and perhaps somewhat disturbing) growth.

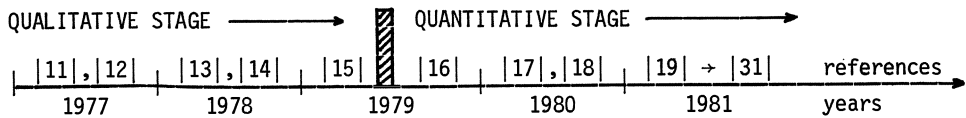


Fig.1 The short story of experimental search for NP flows in chemical systems

Let us now review the main results coming from these studies. For simplicity the symbols A, B, C will refer to the contributions of the groups working in Austin (A), Bordeaux (B) and Charlottesville (C). First of all the very existence of NP regimes has been unambiguously established by A, B and C. To illustrate this point by an example, the time dependence of the optical density, together with the corresponding noisy Fourier spectrum of this kind of regime, are presented in Fig.2 [24,28]. Many others are given in [26] and similar pictures appear too in A [23,25, 27] and C [20] publications. Then a bifurcation diagram, completely new with respect to those of table 2, has been discovered : this is a sequence of P and NP regimes which alternate regularly as the bifurcation parameter, τ or μ , varies. This kind of sequence, first recognized in C [15], has been more thoroughly investigated in A and B. The Fig.3 presents the two bifurcation diagrams thus obtained, which appear very similar, even though the experimental conditions were not identical.

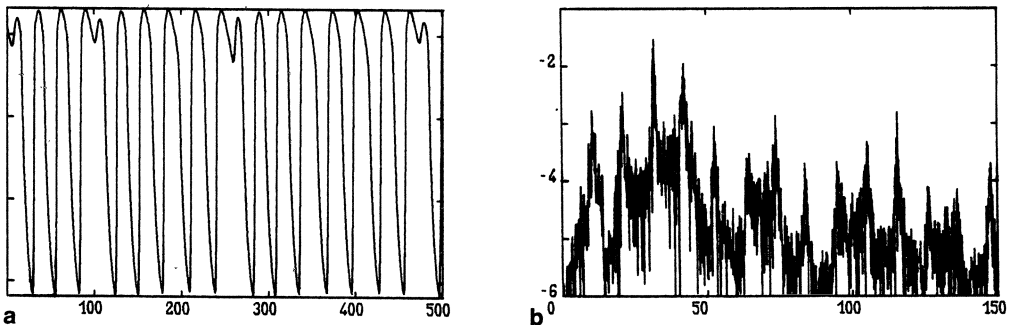


Fig.2 The BZ reaction in a chaotic state [24,26]

- (a) the optical density record (arbitrary units) versus time (sec.). When M high amplitude oscillations are followed by m oscillations of lower amplitude, the pattern is noted as M^m . Here is an example of an M^1 ($M \geq 3$) pattern
- (b) the corresponding power spectral density (Hz^{-1}) versus frequency (10^{-3}Hz) in the usual semi-logarithmic plot.

* This list, only devoted to experiments, does not include the numerical analysis and computer simulations which have also been carried out on this problem.

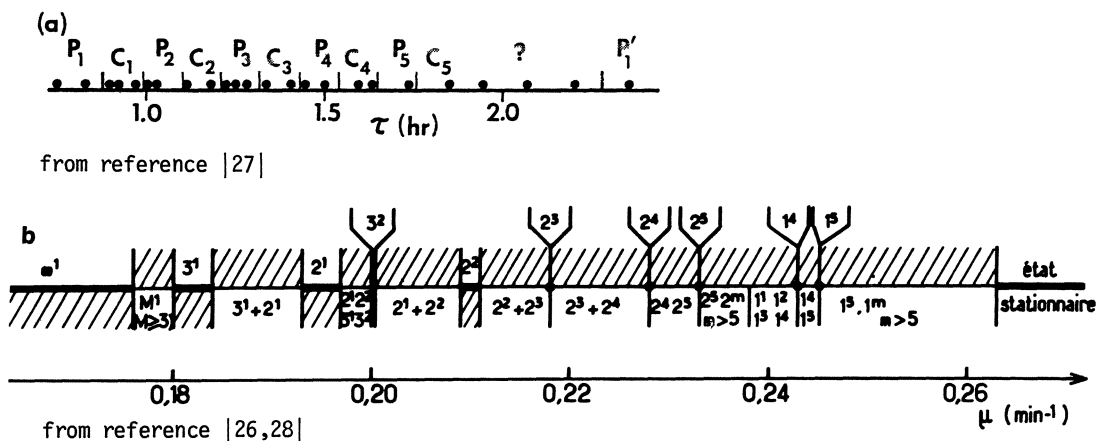


Fig.3 The bifurcation diagrams obtained in A(a) and B(b) (a) for purposes of illustration, successive experimental regimes are shown to be of equal width, although the widths have not been measured (P = periodic, C = chaotic) (b) the P regimes (above the axis) and NP regimes (under the axis) involve a limited number of patterns displayed in the M^m notation (see legend of Fig.1). The width of P regimes becomes narrower and narrower as μ increases.

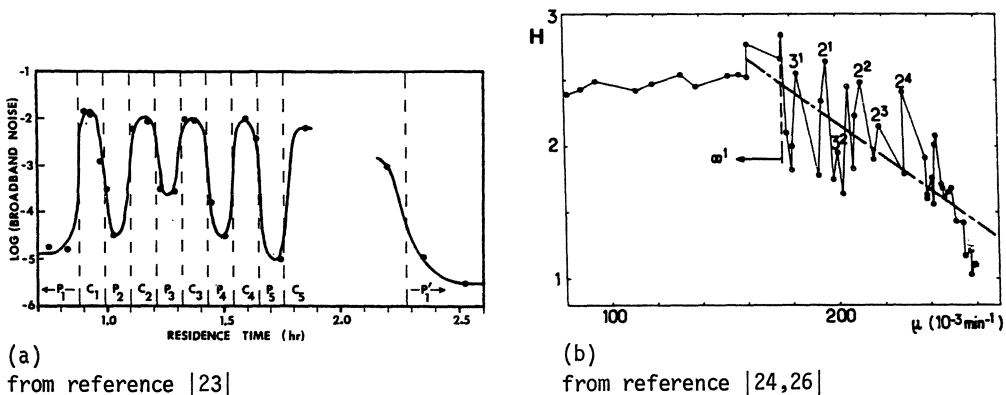


Fig.4 Evolution of the noise level content (a) the noise in the chaotic regimes (C) is several orders of magnitude larger than in the periodic regimes (P). The curve is drawn to guide the eye (b) the H function (see text for definition) remains fairly constant at the beginning and then, beyond $\mu = 0,17 \text{ min}^{-1}$, it evolves towards white noise ($H = 4.2$ for a pure sine wave ; $H = 0$ for white noise). The dashed line is drawn to show the general trend of increasing noise.

One can note however a difference in the evolution of the noise level content of the Fourier spectra. Whereas all the chaotic states of the sequence exhibit a fairly constant broadband noise in the A experiment (Fig.4a), we found that this noise increases continuously from one NP regime to the next along the bifurcation axis (Fig.4b). Thus we detect an evolution towards more and more turbulent states. Perhaps this difference might be ascribed to the different ways in which the noise le-

vel content is estimated : in the A work [23], the intercepts at zero frequency of the lines drawn through the broadband background noise were used, while we computed [24,26] the function :

$$H = \sum_{i=1}^n P_i \log P_i$$

P_i : power spectral density at frequency $i \cdot \Delta f$
 n : number of frequencies in the Fourier spectrum

In these chemical experiments, the signal to noise ratio is good enough to allow a draft of phase-space trajectories, in the framework of the above mentioned conjectures. The first picture to be obtained [18], shown in Fig.5, seems to present this sensitive dependence on initial conditions which characterizes a strange attractor. Chemistry would thus have led to an experimental illustration of this mathematical concept. The usefulness of the phase-space portraits is further demonstrated by the Poincaré (or first return) maps which can be deduced from them. For instance, Fig.6 shows the maps obtained in A and C experiments, when the re-

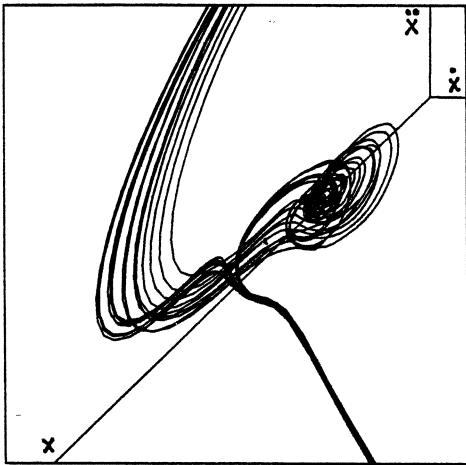
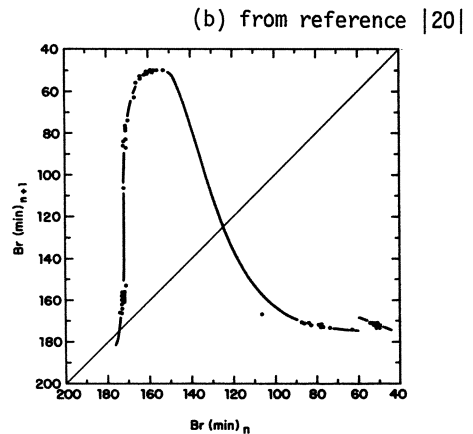
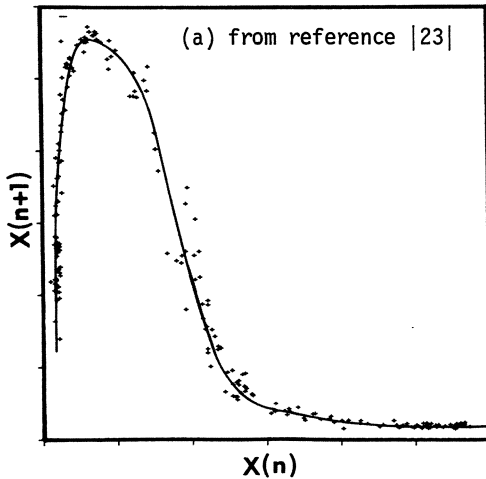


Fig.5 A X, \dot{X}, \ddot{X} phase-space portrait where the trajectories present a sensitive dependence on initial conditions. From reference [18]

Fig.6a,b. The two Poincaré maps obtained in A and C experiments looks very similar. Since the points describe a smooth curve, the chaos is probably deterministic rather than stochastic, even though this argument is far from being a proof.



gime is chaotic. It is seen that the points do not spread throughout the plane, but describe a smooth curve. Moreover one can try to calculate the Lyapunov characteristic exponent of these Poincaré maps. The values determined by A [29] and C [20] are very close to each other : respectively, 0.5 ± 0.1 and 0.62 . Such positive values mean that the phase-space trajectories diverge in one direction, as expected for an NP flow.

Other interesting results are provided by several experiments conducted in B. For instance we have found a sequence of regimes [19] in good agreement with the simulations previously carried out by TOMITA and TSUDA [41] on a model of the BZ reaction, with an analogue computer. Even more exciting is the fact that we discovered an IN regime fairly well described [21] by the Pomeau-Maneville theory of intermittency. I can even say that, up to now, this result is the most successful experimental check of this theory. Another observation worthy of mention is displayed in Fig.7. Here, from time to time, the Ce^{4+} concentration exhibits a damped oscillation immediately followed by an amplified one. This quite unusual behaviour suggests the very existence of an unstable fixed point in a (at least) fourth-order system. More recently we have also observed a new kind of dynamic state [31], characterized by a structured Fourier spectrum (see the figure of page 277): depending on the frequency resolution, this spectrum exhibits three levels of well-ordered peaks. It looks like a russian "matriochka" : i.e. peaks, within peaks, within peaks.

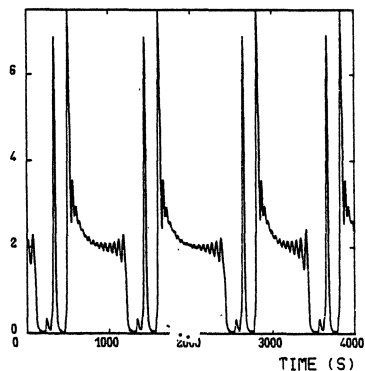


Fig.7 The time dependence of the Ce^{4+} concentration sometimes exhibits a damped oscillation immediately followed by an amplified one. This behaviour might be linked to an unstable fixed point in a fourth-order system. From reference [19].

I do not want to end this overview without reminding that computer simulations have, of course, been carried out on this problem. Very often, but not always, they lie on more or less modified version of the Oregonator [27,41-43]. A discussion of these simulations is far beyond the scope of the present paper. Nevertheless I should like to outline two significant results. Considering some sets of three ordinary differential equations, RÖSSLER was able to show, several years ago, that chaos does occur and should be observed (see for instance [13,14]). On the other hand TURNER [43] worked out a mathematical model, which is the reversible Oregonator, extended to the fourth dimension by considering HOBr as an intermediate species, and including a flow term according to the general equation (2). This model provides us with a sequence of alternating P and NP regimes, which looks very much like the sequence of Fig.3a [27].

5 Conclusion

Amongst the real physical systems whose evolution is described by sets of non-linear differential equations, the chemical systems already show a great variety

of patterns, as we have seen. I am convinced that other dynamic behaviours will be discovered in the near future, still increasing the diversity of observable nonlinear phenomena. The high signal-to-noise ratio of the chemical experiments is certainly a very promising aspect, which opens the way to a systematic use of Poincaré maps. Theoretical work is now in progress [44-48] in order to explain some of the observations reported above. The transition to turbulence via a sequence of alternating P and NP régimes seems now to be one of the most challenging theoretical problem, since it remains today an unpredicted scenario. According to a very recent work of LOBRY and LOZI [49], it seems that a quite successful analysis might be developed in the framework of a 3 variable system such as the Oregonator, provided external noise is taken into account.

References

1. D. Ruelle, some comments on chemical oscillations, Trans. NY, Acad. Sci. 35, 66 (1973)
2. Hydrodynamic instabilities and the transition to turbulence (Ed. SWINNEY H.L., GOLLUB J.P.) Springer-Verlag, Berlin (1981)
3. R.M. Clever, F.H. Busse, Transition to time-dependent convection, J. Fluid. Mech. 65, 625 (1974)
4. J. Maurer, A. Libchaber, Local probe in a Rayleigh-Bénard experiment in liquid helium, J. Phys. Lett. 39, L 369 (1978)
5. S. Fauve, A. Libchaber, Rayleigh-Bénard experiment in a low Prandtl number fluid : mercury, in "Proceedings of the international symposium on Synergetics 1981", (Ed. HAKEN H.) Springer-Verlag, Berlin, in press
6. J.P. Gollub, S.V. Benson, Many routes to turbulent convection, J. Fluid. Mech. 100, 449 (1980)
7. P. Berge, M. Dubois, Experimental study of the velocity field in Rayleigh-Bénard convection, J. Fluid. Mech. 85, 641 (1978)
8. A. Libchaber, J. Maurer, A Rayleigh-Bénard experiment : helium in a small box, in "Non-linear phenomena at phase transitions and instabilities" NATO advanced studies Institute, in press
9. M. Giglio, S. Musazzi, U. Perini, Transition to chaotic behavior via a reproducible sequence of period-doubling bifurcations, Phys. Rev. Lett. 47, 243 (1981)
10. M. Dubois, P. Berge, Instabilités de couche limite dans un fluide en convection ; évolution vers la turbulence, J. Phys. 42, 167 (1981)
11. L.F. Olsen, H. Degn, Chaos in an enzyme reaction, Nature 267, 177 (1977)
12. R.A. Schmitz, K.R. Graziani, J.L. Hudson, Experimental evidence of chaotic states in the Belousov-Zhabotinsky reaction, J. Chem. Phys. 67, 3040 (1977)
13. O. RöSSLer, K. Wegmann, Chaos in the Zhabotinsky reaction, Nature 271, 89 (1978)

14. K. Wegmann, O. Röessler, Different kinds of chaotic oscillations in the Belousov-Zhabotinsky reaction, *Z. Naturforsch.* 33a, 1179 (1978)
15. J.L. Hudson, M. Hart, D. Marinko, An experimental study of multiple peak periodic and non-periodic oscillations in the Belousov-Zhabotinsky reaction, *J. Chem. Phys.* 71, 1601 (1979)
16. C. Vidal, J.C. Roux, A. Rossi, S. Bachelart, Etude de la transition vers la turbulence chimique dans la réaction de Belousov-Zhabotinsky, *C.R. Acad. Sci. Paris* 289 C, 73 (1979)
17. C. Vidal, J.C. Roux, S. Bachelart, A. Rossi, Experimental study of the transition to turbulence in the Belousov-Zhabotinsky reaction, *Ann. NY. Acad. Sci.* 357, 377 (1980)
18. J.C. Roux, A. Rossi, S. Bachelart, C. Vidal, Representation of a strange attractor from an experimental study of chemical turbulence, *Phys. Lett.* 77A, 391 (1980)
19. J.C. Roux, A. Rossi, S. Bachelart, C. Vidal, Experimental observation of complex dynamical behavior during a chemical reaction, *Physica* 2D, 395 (1981)
20. J.L. Hudson, J.C. Mankin, Chaos in the Belousov-Zhabotinsky reaction, *J. Chem. Phys.* 74, 6171 (1981)
21. Y. Pomeau, J.C. Roux, A. Rossi, S. Bachelart, C. Vidal, Intermittent behaviour in the Belousov-Zhabotinsky reaction, *J. Phys. Lett.* 42, L 271 (1981)
22. S. Bachelart, A. Rossi, J.C. Roux, C. Vidal, Mise en évidence expérimentale de la turbulence chimique, in "Symmetries and broken symmetries in condensed matter physics", in press
23. J.C. Roux, J.S. Turner, W.D. Mc Cormick, H.L. Swinney, Experimental observations of complex dynamics in a chemical reaction, in "Non-linear problems : present and future" (Ed. BISHOP A.R.) North-Holland, Amsterdam, in press
24. C. Vidal, Dynamic instabilities observed in the Belousov-Zhabotinsky system, in "Proceedings of the international symposium on Synergetics 1981" (Ed. H. KAKEN) Springer-Verlag, Berlin, in press
25. H.L. Swinney, J.C. Roux, G.P. King, Experimental studies of noise in a chemical reaction and in a fluid flow, in "Noise in physical systems", (Ed. MOUNTAIN R.D., SOULEN R.J., MEIJER P.H.E.) NBS, in press
26. S. Bachelart, Recherches expérimentales sur la turbulence chimique, Thèse docteur-ingénieur, Bordeaux (1981)
27. J.S. Turner, J.C. Roux, W.D. Mc Cormick, H.L. Swinney, Alternating periodic and chaotic regimes in a chemical reaction : experiment and theory, *Phys. Lett.* 85A, 9 (1981)
28. C. Vidal, S. Bachelart, A. Rossi, Bifurcations en cascade conduisant à la turbulence dans la réaction de Belousov-Zhabotinsky, *J. Phys.*, in press

29. J.L. Hudson, J.C. Mankin, J.M. McCullough, P. Lamba, Experiment on chaos in a continuous stirred reactor, this volume
30. J.C. Roux, H.L. Swinney, Topology of chaos in a chemical reaction, this volume
31. C. Vidal, A. Rossi, A dynamical regime with structured Fourier spectrum, this volume
32. R.J. Field, E. Körös, R.M. Noyes, Oscillations in chemical systems II. Thorough analysis of temporal oscillations in the bromate-cerium-malonic acid system, *J. Am. Chem. Soc.* 94, 8649 (1972)
33. R.J. Field, R.M. Noyes, Oscillations in chemical systems IV. Limit cycle behavior in a model of a real chemical reaction, *J. Chem. Phys.* 60, 1877 (1974)
34. J.J. Tyson, The Belousov-Zhabotinsky reaction, Springer-Verlag, Berlin (1976)
35. D. Ruelle, private communication
36. N.H. Packard, J.P. Crutchfield, J.D. Farmer, R.S. Shaw, Geometry from a time series, *Phys. Rev. Lett.* 45, 712 (1980)
37. D. Ruelle, F. Takens, On the nature of turbulence, *Comm. Math. Phys.* 20, 167 (1971)
38. J.P. Eckmann, Roads to turbulence in dissipative dynamical systems, preprint
39. B. Belousov, A periodic chemical reaction and its mechanism (in Russian), in "Collection of abstracts on radiation medicine 1958", Medgiz, Moscow, 145 (1959)
40. P. de Kepper, A. Rossi, A. Pacault, Etude expérimentale d'une réaction chimique périodique : diagramme d'états de la réaction de Belousov-Zhabotinsky, *C.R. Acad. Sci. Paris* 283 C, 371 (1976)
41. K. Tomita, I. Tsuda, Chaos in the Belousov-Zhabotinsky reaction in a flow system, *Phys. Lett.* 71A, 489 (1979)
42. K. Showalter, R.M. Noyes, K. Bar-Eli, A modified Oregonator model exhibiting complicated limit cycle behavior in a flow system, *J. Chem. Phys.* 69, 2514 (1978)
43. J.S. Turner, Periodic and non-periodic oscillations in the Belousov-Zhabotinsky reaction, Discussion meeting on kinetics of physico-chemical oscillations, Aachen (1979)
44. K. Tomita, I. Tsuda, Towards the interpretation of Hudson's experiment on the Belousov-Zhabotinsky reaction : chaos due to delocalization, *Progr. Theor. Phys.* 64, 1138 (1980)
45. D. Ruelle, Chemical kinetics and differentiable dynamical systems, this volume

46. G. Iooss, Bifurcations élémentaires : successions et interactions, this volume
47. Y. Pomeau, Transition vers la turbulence par intermittence, this volume
48. I. Tsuda, Self-similarity in the Belousov-Zhabotinsky reaction, Phys. Lett., 85A, 4 (1981)
49. C. Lobry, R. Lozi, Bifurcation of motifs in families of mixed two-vector fields, this volume

Transition vers la turbulence par intermittence

Y. Pomeau

L'étude des transitions vers l'instationnarité et la turbulence en mécanique des fluides a largement précédé celle des mêmes phénomènes en cinétique chimique. Aussi il ne paraît pas déraisonnable de tenter quelque rapprochement entre ces deux domaines, si éloignés en apparence dans leur manifestation expérimentale. Le principe unifiant ces deux catégories de phénomènes naturels est d'origine mathématique. En effet dans l'un et l'autre cas (mécanique des fluides et cinétique chimique) on a affaire à ce que l'on appelle des systèmes dynamiques : comme remarqué déjà par David Ruelle [1], la cinétique chimique obéit à des équations différentielles ordinaires non linéaires, qui constituent le prototype même du système dynamique. La description des mouvements d'un fluide par un tel système dynamique ne va pas tout à fait de soi : en effet l'évolution d'un fluide est, à priori, celle d'un continuum spatial qui obéit à des équations aux dérivées partielles plutôt qu'à des équations différentielles ordinaires. En fait, pour des écoulements en géométrie confinée, engendrés par exemple dans une cellule de Bénard de forme à peu près cubique, on peut réduire à l'interaction de quelques "modes" significatifs une évolution régie à priori par des équations aux dérivées partielles. L'idée d'une telle réduction a guidé Lorenz [2] lorsqu'il a construit le système d'équations différentielles bien connu qui tend à modéliser la convection de Rayleigh Bénard instationnaire.

A première vue, il pourrait sembler que c'est faire bien peu de progrès que reconnaître qu'en cinétique chimique comme en mécanique des fluides on a affaire à des systèmes dynamiques : ne s'agirait-il pas d'une notion trop générale pour être utile ? Je vais tenter de montrer maintenant qu'en fait il n'en est rien. Un des succès remarquables de cette approche "globale" des systèmes dynamiques est la mise en évidence de ce que J.P. Eckmann [3] appelle des "scénarios" de transition vers la turbulence.

Considérons un certain ensemble d'équations différentielles ordinaires couplées non linéaires autonomes qu'on écrira sous la forme schématique :

$$\frac{d\vec{x}}{dt} = \vec{f}(\vec{x}, \mu) \quad (1)$$

\vec{x} est, dans cette équation un vecteur de \mathbb{R}^d (= un tableau de d quantités réelles

qui peuvent dépendent à priori du temps), et μ ce que l'on appelle un paramètre de contrôle. Dans le cas d'une réaction chimique de Belousov-Zhabotinsky (par exemple), $\vec{x}(t)$ est simplement la liste des concentrations des espèces intervenant de façon significative dans la réaction (plus éventuellement la température, si la réaction n'est pas isotherme) et μ le taux de renouvellement des réactifs. Pour éviter l'apparition de terme de diffusion spatiale, on suppose que la réaction se fait en phase homogène, par exemple par suite d'un brassage intense.

Il y a transition vers la turbulence lorsque les solutions du système (1) passent en variant μ d'un régime de cycle limite stable ou, éventuellement d'un état stationnaire à un régime d'attracteur étrange décrivant le comportement stochastique de systèmes déterministes suivant Ruelle et Takens [4]. Les "scénarios" de transition donnent une certaine image des mécanismes possible pour ce passage du régime ordonné (cycle limite ou état stationnaire) au régime stochastique. En un sens, l'idée qu'il y a un nombre restreint de "scénarios" de transition rappelle la classification des transitions de phase thermodynamiques par les Ehrenfest. Cet effort unificateur permet d'oublier certains détails de la situation physique : le point critique liquide gaz d'un fluide présente, on le sait maintenant, une analogie parfaite avec la transition de Curie d'un ferromagnétique uniaxe. On saura donc reconnaître avec précision une certaine transition à partir de données expérimentales, même si l'on est pratiquement incapable d'analyser quantitativement le détail de tous les phénomènes mis en jeu lors de cette transition. Ainsi on analysera thermodynamiquement en détail le point critique liquide gaz d'un fluide indépendamment de la structure moléculaire à courte distance.

On saura aussi identifier un scénario de transition vers la turbulence sans comprendre pour autant tous les détails de la cinétique sous jacente. A l'heure actuelle, trois scénarios ont été recensés. Ce sont (dans un ordre plus ou moins historique) la transition par couplage faible de 3 ou 4 oscillateurs de fréquences incommensurables [4], la cascade de dédoublements de fréquence [5] et la transition par intermittence. Les dédoublements de fréquence sont considérés par Feigenbaum dans cette conférence. Je vais me limiter dans ce qui suit à une description succincte de la transition par intermittence, renvoyant aux articles originaux les lecteurs intéressés.

La phénoménologie de la transition par intermittence est particulièrement simple. En dessous d'une valeur critique μ_c du paramètre de contrôle, le système présente un cycle limite stable: pour un ensemble raisonnablement grand de conditions initiales, $\vec{x}(t)$ tend pour les temps longs positifs vers une fonction périodique si $\mu < \mu_c$. Pour μ légèrement supérieur à μ_c , $\vec{x}(t)$ présente la plupart du temps des oscillations apparemment régulières et très semblables à celles qui existe pour μ légèrement inférieur à μ_c .

Mais ces oscillations sont interrompues de temps en temps par une grande fluctuation. Cette grande fluctuation est suivie d'une relaminarisation, c'est à dire d'un retour à des oscillations apparemment régulière, interrompues plus tard par une grande fluctuation, et ainsi de suite. Cette description de base est susceptible de certaines modifications. Ainsi l'état de comportement régulier séparant deux grandes fluctuations peut être un régime stationnaire plutôt qu'oscillant [6], cet état stationnaire étant stable pour $\mu < \mu_c$. Dans tous les cas, la propriété essentielle de la transition est *l'intermittence* : lorsque μ tend vers μ_c par valeurs supérieures, l'intervalle de temps moyen séparant deux grandes fluctuations croît indéfiniment. Dans le cas le plus simple (que nous avons appelé intermittence de type I avec Paul Manneville [7]) cet écart moyen croît comme $(\mu - \mu_c)^{-1/2}$ lorsque $\mu \rightarrow \mu_c$. Dans d'autres types d'intermittence la loi de croissance de cet écart est beaucoup moins simple et échappe même encore à une analyse purement théorique.

On a observé cette transition par intermittence en convection de Rayleigh-Bénard [8] et dans la réaction chimique de Belousov-Zhabotinsky [9] en phase brassée (donc homogène). Dans ce dernier cas il a même été possible d'avoir une confirmation détaillée de la nature de cette transition en analysant à partir des données expérimentales la faible instabilité des oscillations séparant, dans le régime intermittent, deux grandes fluctuations. Cette (faible) instabilité est décrite par la théorie de Floquet pour sa partie linéaire et un terme non linéaire quadratique s'y ajoute, suivant la philosophie des formes normales de Poincaré-Birkhoff.

On perçoit bien ici tout ce qu'apporte l'idée de "scénario" de transition : la forme normale de Poincaré-Birkhoff suffit à comprendre les détails essentiels de la transition, ignorant quasiment complètement la cinétique chimique sous-jacente. Nul besoin en particulier d'introduire artificiellement des variables à priori rapide ou lente : le "ralentissement critique" n'est que l'effet d'un état de stabilité marginale. Les travaux de l'Ecole Bordelaise [10] sur la réaction de Belousov-Zhabotinsky ont amplement montré qu'on pouvait étudier valablement la cinétique de cette réaction du point de vue des systèmes dynamiques et assez indépendamment des détails d'une cinétique chimique sans doute difficilement accessibles.

Une analogie superficielle donnerait à penser que cette intermittence de transition des systèmes dynamique a quelque chose à voir avec les observations classiques d'Osborne Reynolds [11] des transitions d'un écoulement de fluide visqueux dans un tuyau cylindrique. Cette dernière situation est beaucoup plus complexe que celle des systèmes dynamiques simples, en raison en particulier de ce que l'intermittence y est spatiotemporelle plutôt que temporelle. Dans ce cas des écoulements parallèles, le phénomène fondamental est l'existence marginale (par rapport à la variation du nombre de Reynolds) de perturbations *localisées* et d'amplitude finie et se déplaçant en bloc. Là encore il paraît raisonnable et possible de s'appuyer sur la théorie des systèmes dynamiques pour aboutir à une explication

cohérente des phénomènes observés. Sans doute les phénomènes classiques de structuration spatiale observés dans la réaction oscillante de Belousov-Zhabotinsky constitueront un champ d'observation particulièrement intéressant pour la transition vers la turbulence spatio-temporelle, à comparer peut être avec les instabilités des fronts de flamme instables. Peut être aussi n'est-il pas déraisonnable d'espérer ici encore mettre en évidence une liste plus ou moins exhaustive de "scénarios" de transition.

Remerciements

Je tiens à remercier le Professeur Pacault, Sabine Bachelart, Annie Rossi, Jean-Claude Roux et Christian Vidal d'avoir permis à un théoricien de participer bien modestement aux recherches sur les réactions chimiques instationnaires.

Références

- [1] D. Ruelle, Trans. N.Y. Acad. Sci. 35, 66 (1973)
- [2] E. Lorenz, J. Atmo. Sci. 20, 130 (1963).
- [3] J.P. Eckmann, Conférence à Schloss Elmau (Bavière) Mars 1981
- [4] D. Ruelle, F. Takens, Comm. Math. Phys. 20, 167 (1971) et 23, 343 (1971).
- [5] M. Feigenbaum, cette conférence.
- [6] Y. Pomeau in *Pittman Vol. on turbulence*, D.D. Joseph et G. Iooss editeurs, à paraître.
- [7] Y. Pomeau, P. Manneville, Comm. Math. Phys. 74, 189 (1980).
- [8] P. Bergé, M. Dubois, P. Manneville, Y. Pomeau, J. Physique Lett. 41; L-341 (1980).
- [9] Y. Pomeau, J.C. Roux, A. Rossi, S. Bachelart et C. Vidal, J. Physique Lett. 42, L-271 (1981).
- [10] C. Vidal, J.C. Roux, A. Rossi et S. Bachelart, C.R. Acad. Sci. Paris C289, 73 (1979), Ann. N.Y. Acad. Sci. (1980).
J.C. Roux, A. Rossi, S. Bachelart, C. Vidal, Experimental observations of complex dynamical behavior, Physica 2D, 395 (1981)
- [11] O. Reynolds, Phil. Trans. R. Soc. 174, 935 (1883).

They are two dimensional and thus are tractable with some kind of Poincaré Bendixon theory.

Contrary to ordinary differential equations, solutions of "mixed two vector fields" do not depend continuously on initial conditions, this allows chaotic behavior, which is impossible for ordinary differential equations in the plane.

Mixed two-vector fields are just the projection on the plane of the slow dynamics of a singularly perturbed differential system in \mathbb{R}^3 , where the slow manifold is a folded surface. It works like this:

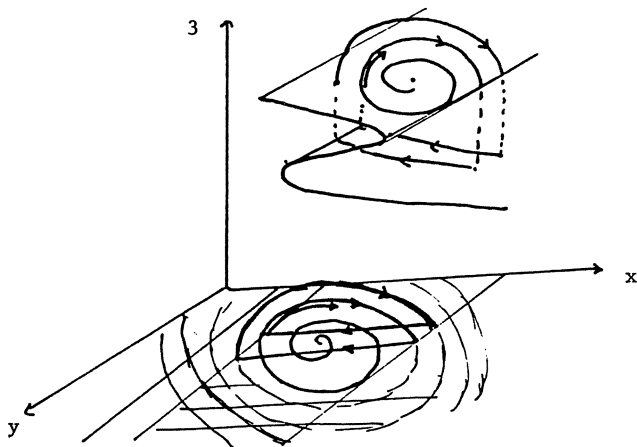


Fig.3. Fast-slow differential system in \mathbb{R}^3 with associated mixed two-vector fields

One sees on the picture that the slow manifold overlaps in the direction of the fast trajectories, and the "mixed two-vector fields" is just the projection in the plane. We emphasize here that by no mean have we proven that "mixed two-vector fields" are a correct idealization of singularly perturbed differential systems when ϵ tends to the limit 0. To our knowledge no such general results exist.

3- Abstract models for bifurcation of "motifs".

Let X be a vector field with one limit cycle,
 Let Y be a trivial vector field with parallel trajectories,
 Let D_x and D_y be half planes intersecting along a strip.

Let our bifurcation parameter be a displacement of the strip with the dynamics fixed. In the following picture one sees positions of the strip which have a limit cycle or a 3^1 "motif".

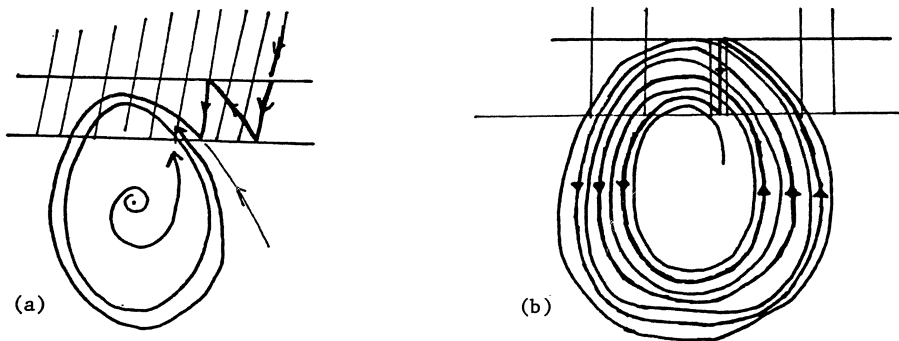


Fig.4. (a) Stable limit cycle; (b) 3^1 Motif

Below we show an example of mixing 3^1 and 2^1

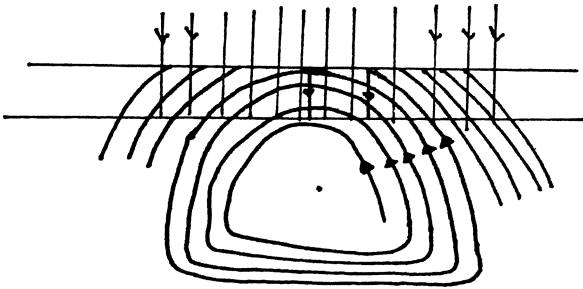


Fig.5. Mixing of 3^1 and 2^1 motifs

4. Oregonator type models: Fig. 6 is a representation of the slow manifold in a model of the Oregonator given by Tyson in [2]. We made sure of the position of the slow manifold, but we are not sure of the precise shape of the slow dynamics. Some computations will be done and will appear elsewhere.

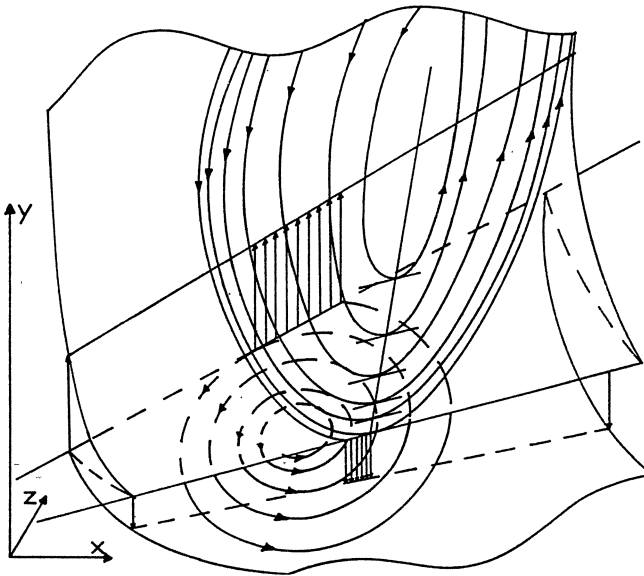


Fig.6. Dynamics of an Oregonator type system in three dimensions

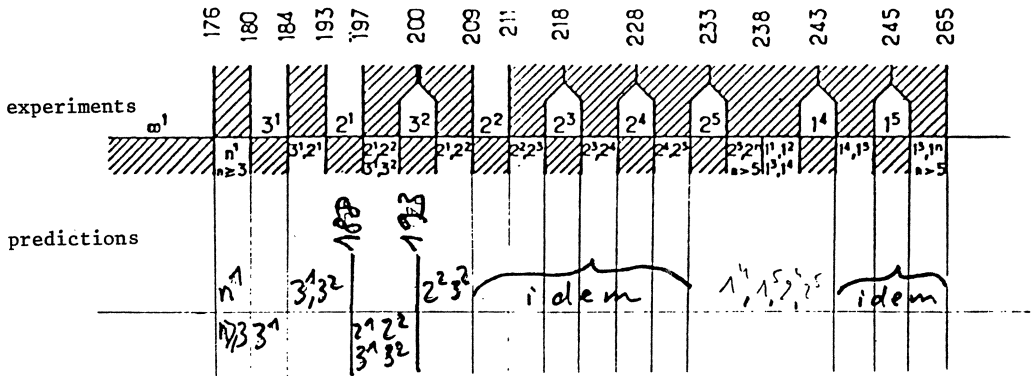


Fig.7. Comparison of experimental and predicted results

In fig. 7 one sees the comparison between experimental results and prediction from the model. One sees that the qualitative succession of "motifs" is well described in a large range of variation of the parameter. Further work and details will appear elsewhere.

5. Existence of chaotic solutions: We define a "Poincaré map" which is the first return map to some suitable part of the boundary of D_X . One sees easily that this Poincaré map is continuous in the case of a single "motif" and is discontinuous in the case of a mixing of two different "motifs". In the case of a single motif we can conclude by a standard argument the presence of a periodic regime. In the case of a mixing the conclusion is more difficult. One may have chaotic solution but it depends very much on the shape of the graph of the Poincaré map. This was proved in a recent paper by KEENER [4]. The shape of the Poincaré map depends on the geometry of the dynamics on the slow manifold. If the shape is not the right one, one has just some kind of pseudo-periodic behavior.

The shape of a "motif" is very sensitive to the displacement of the strip, this is due to the presence of a discontinuity; thus our feeling is that it is very difficult to decide whether the observed randomness of mixings is due to an "intrinsic" chaotic behaviour or to an external noise which induces a very small displacement of the strip that is amplified by the presence of the discontinuity in the dynamics. Further mathematical investigations and numerical analysis should be done.

Conclusion: The mathematical study of cascade of "bifurcations" of "motifs" of "mixed two-vector fields" is appealing for many reasons.

- Mixed two-vector fields are reasonably simple, and we hope to produce a rigorous theory of this object in the near future.
- Mixed two-vector fields are an "idealization" of singularly perturbed three-dimensional systems. It is confirmed by computer simulations and especially the beautiful stereoscopic pictures by ROSSLER. We have some hope to put this in a complete rigorous form via the tools of non-standard analysis.
- Slight modifications of the Oregonator provide systems whose idealization is able to produce observed transitions. Thus we have a mathematical model whose variables have chemical significance, with a good qualitative power of prediction.

Aknowledgements: We acknowledge A. PACAULT, S. BACHELART, A. ROSSI, J.C. ROUX and C. VIDAL for helpful discussions and for providing documents.

The first author thanks J. TYSON and J. RINZEL for helpful discussions and for providing ref. [4]

References.

- 1 O. ROSSLER, Continuous chaos - Four prototype equations, Annals of the New York Academy of Sciences p. 376-392 (1979)
- 2 J. TYSON, On the appearance of chaos in a model of the Belousov reaction. J. Math. Biology 2, 351-362, (1978).
- 3 Experiments performed at C.R.P.P. University of Bordeaux, by S. BACHELART, A. ROSSI, J.C. ROUX, and C. VIDAL. See VIDAL in this volume.
- 4 J. KEENER, Chaotic behavior in piecewise continuous difference equations, Trans. Amer. Math. Soc. 261, 589-604 (1980)

Bifurcations élémentaires - successions et interactions

Gérard Iooss

I.M.S.P., Université de Nice, Parc Valrose
F-06034 Nice

1 . INTRODUCTION

L'apparition de régimes oscillatoires périodiques par "bifurcation" d'un régime stationnaire est établie expérimentalement dans de nombreux domaines scientifiques, dont la Dynamique Chimique [8] , [2] .

Il ne semble pas que des bifurcations vers des régimes quasi-périodiques aient encore été observés dans ce domaine, bien que l'on connaisse maintenant de nombreux exemples en Mécanique des fluides notamment.

Ces bifurcations sont élémentaires dans le sens qu'elles ne nécessitent pour être comprises que les variations d'un seul paramètre du système. Or les phénomènes physiques étudiés dépendent en général de nombreux paramètres ; il est donc naturel d'étudier des situations spécifiques à l'occurrence de plusieurs paramètres (on dit "de codimension supérieure à 1"). Nous indiquons dans ce qui suit le résultat de l'interaction de deux bifurcations du type le plus simple et nous montrons qu'il est probable qu'à l'avenir des régimes quasi-périodiques se rencontrent en Dynamique Chimique.

2 . BIFURCATION DE HOPF (voir [4] pour une méthode simple de calcul).

Considérons un système régi par une famille d'équations différentielles dépendant d'un ensemble de paramètres noté $\mu \in \mathbb{R}^k$:

$$(1) \quad \frac{dX}{dt} = F(\mu, X) \quad , \quad X(t) \in \mathbb{R}^n \quad .$$

Afin de simplifier l'étude nous supposons $X(t) \in \mathbb{R}^n$, mais tout ce qui suit marche aussi bien pour les problèmes d'évolution régis par des équations aux dérivées partielles du type réaction-diffusion, et même du type Navier-Stokes. Pour l'introduction du cadre fonctionnel adapté et les résultats de régularité en temps des solutions on peut se référer à [3] .

Nous supposons que (1) admet une solution stationnaire que nous prenons comme origine de l'espace des phases : $X = 0$. Avec ce choix, nous avons

$$(2) \quad F(\mu, 0) = 0 \quad .$$

Dans la suite nous notons :

$$(3) \quad F(\mu, X) = L_{\mu} X + N_{\mu}(X)$$

où L_{μ} concentre la dépendance linéaire en X et N_{μ} la dépendance non linéaire (au moins quadratique au voisinage de 0).

La solution stationnaire $X = 0$ de (1) perd sa stabilité lorsque des valeurs propres de L_{μ} traversent l'axe des imaginaires allant vers le côté réel positif (Lyapounov). Une bifurcation de Hopf correspond au cas où une paire de valeurs propres $\sigma(\mu)$, $\bar{\sigma}(\mu)$ traverse l'axe des imaginaires pour $\mu = 0$ en $\pm i\omega_0$, les autres valeurs propres de L_{μ} restant de parties réelles négatives. Pour ce type d'étude il est suffisant de se restreindre à un seul paramètre réel μ traversant la valeur critique (0 ici).

Le résultat est alors qu'en général, dépendant du signe d'un coefficient calculé à l'aide des termes non linéaires, pour $\mu > 0$ ou pour $\mu < 0$, il existe une solution périodique $X(\mu, t)$ bifurquant à partir de $X = 0$ telle que $X(0, t) = 0$, d'amplitude $\|X(\mu, t)\| = O(\sqrt{|\mu|})$, de fréquence voisine de ω_0 (dépendant régulièrement de μ). Cette solution périodique est stable si elle bifurque pour les valeurs de μ où la solution $X = 0$ est instable (Fig. 1).

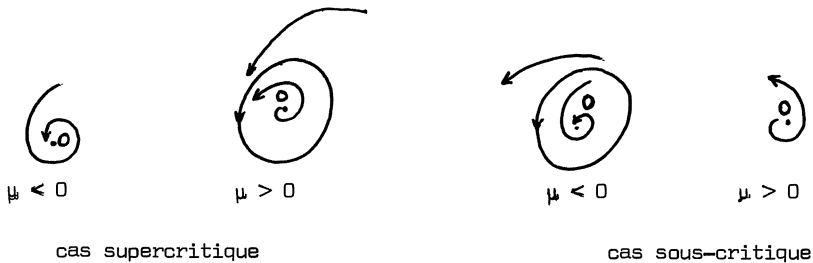


Fig. 1. Bifurcation de Hopf.

3. INTERACTION DE DEUX BIFURCATIONS DE HOPF.

3.1 - Introduction .

Considérons encore le système (1) vérifiant (2), et supposons que pour $\mu = 0$ on ait deux paires de valeurs propres de L_0 imaginaires pures : $\pm i\omega_0$, $\pm i\omega_1$, les autres valeurs propres étant de parties réelles négatives. La situation linéarisée correspond donc à deux oscillateurs indépendants.

Il est alors naturel d'étudier les situations voisines de cet état "doublement critique" de la façon suivante, à l'aide de deux paramètres : $\mu = (\mu_1, \mu_2) \in \mathbb{R}^2$ voisins de 0. On peut choisir les paramètres pour plus de commodité en posant $\text{Re } \sigma_1(\mu) = \mu_1 - \mu_2$, $\text{Re } \sigma_0(\mu) = \mu_1$, où $\sigma_0(\mu)$ et $\sigma_1(\mu)$ sont les valeurs propres de L_μ voisines de $i\omega_0$ et $i\omega_1$ lorsque μ est voisin de 0. Alors pour $\mu = (\mu_1, \mu_2) = 0$, $\sigma_0 = i\omega_0$, $\sigma_1 = i\omega_1$ et les paires $(\sigma_0(\mu), \bar{\sigma}_0(\mu))$ et $(\sigma_1(\mu), \bar{\sigma}_1(\mu))$ traversent l'axe des imaginaires respectivement lorsque μ_1 passe par 0, et μ_2 passe par μ_1 . Si $\mu_2 \neq 0$, cela entraîne une non-simultanéité des deux traversées de l'axe des imaginaires, et l'on imagine aisément qu'il sera plus facile de comprendre les phénomènes même si ces deux traversées de l'axe sont presque simultanées. On a donc un problème d'interaction entre deux oscillateurs proches de la bifurcation. Nous allons montrer comment cette interaction peut engendrer des solutions périodiques, bi-périodiques et même des solutions avec 3 fréquences fondamentales, s'enroulant sur un tore invariant de dimension 3 dans l'espace des phases.

3.2 - Le problème simplifié.

Pour comprendre les phénomènes qu'entraîne cette interaction, considérons le système différentiel suivant où z_0 et z_1 sont complexes :

$$(4) \quad \begin{cases} \frac{dz_0}{dt} = \sigma_0 z_0 + a_{30} z_0 |z_0|^2 + a_{12} z_0 |z_1|^2 \\ \frac{dz_1}{dt} = \sigma_1 z_1 + a_{21} |z_0|^2 z_1 + a_{03} z_1 |z_1|^2 \end{cases},$$

σ_0 et σ_1 sont les valeurs propres définies précédemment, fonction de $(\mu_1, \mu_2) = \mu$, et les coefficients a_{pq} sont complexes et fonctions de μ . D'où provient (4) ?

On montre [6] que tout système (1) qui vérifie l'hypothèse de l'existence de deux paires de valeurs propres simples $\pm i\omega_0$, $\pm i\omega_1$ pour $\mu = 0$, les autres valeurs propres étant de parties réelles négatives, et qui de plus vérifie $0 < \omega_0 < \omega_1$ (pour fixer les idées), et

$$(4') \quad \frac{\omega_0}{\omega_1} \text{ non rationnel, ou } \frac{\omega_0}{\omega_1} \neq \frac{1}{2}, \frac{1}{3},$$

peut se mettre, après changement de variables, sous la forme (4), modulo des termes d'ordre supérieur, au voisinage de 0. Donc, seules les 4 dimensions relatives aux vecteurs propres des 4 valeurs propres $\sigma_0, \bar{\sigma}_0, \sigma_1, \bar{\sigma}_1$ sont importantes et dans ces directions, identifiant \mathbb{R}^2 au plan complexe, les termes

non linéaires importants sont cubiques en z_0, z_1 , vérifiant de plus des propriétés de symétries. Nous parlerons plus loin de l'importance des termes négligés, et de leur influence sur les résultats déduits seulement de la forme simplifiée (4).

Posons maintenant $z_0 = r_0 e^{i\theta_0}$, $z_1 = r_1 e^{i\theta_1}$, alors l'équation

(4) devient :

$$(5) \quad \left\{ \begin{array}{l} \frac{dr_0}{dt} = \mu_1 r_0 + \alpha_{30} r_0^3 + \alpha_{12} r_0 r_1^2 \\ \frac{dr_1}{dt} = (\mu_1 - \mu_2) r_1 + \alpha_{21} r_0^2 r_1 + \alpha_{03} r_1^3 \end{array} \right.$$

$$(6) \quad \left\{ \begin{array}{l} \frac{d\theta_0}{dt} = \eta_0 + \beta_{30} r_0^2 + \beta_{12} r_1^2 \\ \frac{d\theta_1}{dt} = \eta_1 + \beta_{21} r_0^2 + \beta_{03} r_1^2 \end{array} \right.$$

où $\alpha_{jk} = \alpha_{jk} + i\beta_{jk}$, $\sigma_0 = \mu_1 + i\eta_0(\mu)$, $\sigma_1 = \mu_1 - \mu_2 + i\eta_1(\mu)$.

La discussion principale porte alors sur le système réduit (5), pour lequel nous faisons les hypothèses (génériques) :

$$(7) \quad \left\{ \begin{array}{l} \alpha_{30} \alpha_{03} \neq 0, \quad D_1 = \alpha_{21} - \alpha_{30} \neq 0, \\ D_2 = \alpha_{03} - \alpha_{12} \neq 0, \quad \Delta = \alpha_{30} \alpha_{03} - \alpha_{12} \alpha_{21} \neq 0. \end{array} \right.$$

3.3 - Bifurcations primaires.

La solution $r_0 = r_1 = 0$ correspond à la solution $X = 0$ du système (1). Sa stabilité change quand μ_1 croît en passant par 0, si $\mu_2 > 0$, ou quand μ_1 passe par μ_2 si $\mu_2 < 0$. On obtient alors deux branches "primaires" :

$$(i) \quad (8) \quad r_0^2 = -\frac{\mu_1}{\alpha_{30}}, \quad r_1 = 0$$

qui bifurque à partir de 0 en $\mu_1 = 0$ et est super (sous-) critique si $\alpha_{30} < 0$ (> 0). Cette branche correspond à une solution périodique de fréquence

$$\hat{\omega}_0 = \eta_0 - \frac{\beta_{30} \mu_1}{\alpha_{30}} ;$$

$$(ii) \quad (9) \quad r_1^2 = \frac{\mu_2 - \mu_1}{\alpha_{03}}, \quad i_0 = 0$$

qui bifurque à partir de 0 en $\mu_1 = \mu_2$ et est super (sous-) critique si $\alpha_{03} < 0 (> 0)$. Cette branche correspond à une solution périodique de fréquence

$$\hat{\omega}_1 = \eta_1 + \frac{\beta_{03}(\mu_2 - \mu_1)}{\alpha_{03}}.$$

Ces résultats pour le modèle simplifié (4) se traduisent sur le système complet (1) de façon identique à des modifications d'ordre supérieur près. A savoir que les bifurcations primaires de type Hopf ont lieu de la même façon, et que les amplitudes et fréquences sont voisines de celles indiquées ci-dessus [6] pourvu que l'hypothèse (4') soit vérifiée.

3.4 - Bifurcations secondaires.

Une bifurcation secondaire à partir de la branche (8) intervient pour

$$(10) \quad \mu_1 = \mu_1^{s_1} = -\frac{\alpha_{30}\mu_2}{D_1} \quad \text{pourvu que } \mu_2^{D_1} > 0,$$

celle-ci est super (sous-) critique si $\Delta D_1 > 0 (< 0)$.

Une autre bifurcation secondaire à partir de la branche (9) intervient pour

$$(11) \quad \mu_1 = \mu_1^{s_2} = -\frac{\alpha_{12}\mu_2}{D_2}, \quad \text{pourvu que } \mu_2^{D_2} > 0,$$

celle-ci est super (sous-) critique si $\Delta D_2 < 0$. Les branches secondaires sont données par les formules :

$$(12) \quad \left\{ \begin{array}{l} r_{0s}^2 = -\frac{D_2\mu_1 + \alpha_{12}\mu_2}{\Delta} = -(\mu_1 - \mu_1^{s_2}) \frac{D_2}{\Delta} \\ r_{1s}^2 = \frac{D_1\mu_1 + \alpha_{30}\mu_2}{\Delta} = (\mu_1 - \mu_1^{s_1}) \frac{D_1}{\Delta}, \end{array} \right.$$

et correspondant à des solutions stationnaires de (5).

Ces branches secondaires consistent en fait en tores de dimension 2, invariants par l'équation (4). Les trajectoires sur ces tores sont bi-périodiques avec les fréquences $\hat{\omega}_{0s} = \eta_0 + \beta_{30}r_{0s}^2 + \beta_{12}r_{1s}^2$ dans la direction θ_0 ,

et $\hat{\omega}_{1s} = \eta_1 + \beta_{20}r_{0s}^2 + \beta_{03}r_{1s}^2$ dans la direction θ_1 .

Une solution est quasi-périodique si $\hat{\omega}_{0s} / \hat{\omega}_{1s}$ est irrationnel sinon elle est périodique, toujours située sur le tore défini par (12).

Si $D_1 D_2 > 0$ et que μ_2 est du bon signe, la branche secondaire est en un seul morceau, allant du point $\mu_1 = \mu_1^{s_1}$ au point $\mu_1 = \mu_1^{s_2}$, ceux-ci situés sur les

branches primaires. Si $D_1 D_2 < 0$ les branches secondaires n'existent que pour des signes opposés de μ_2 .

Pour le système complet (1), ces résultats se traduisent de la façon suivante, **pourvu** que (4') soit vérifiée. L'existence des branches (12) pour (4) correspond bien encore à une bifurcation vers des tores invariants de dimension 2, mais l'on ne peut prédire si une solution sur le tore sera attirée vers une solution périodique ou non. En utilisant le spectre Fourier d'une quantité observable on peut mesurer le rapport de "2 fréquences fondamentales" et l'on a une variation continue en fonction des paramètres. Si ce rapport est rationnel pour certaines valeurs des paramètres, le mouvement est alors périodique et il y a "accrochage" des fréquences : pour des valeurs voisines des paramètres le rapport des fréquences reste constant. On voit déjà ici l'influence des termes négligés lorsqu'on n'étudie que le système simplifié (4).

Il y a pire ! Nous allons voir en effet que l'on ne peut même pas garantir l'existence des tores invariants pour le système complet (1) au voisinage d'un point de bifurcation tertiaire, ce qui fait l'objet du § suivant.

3.5 - Bifurcations tertiaires.

Si l'on considère la solution (12) de (5), on peut chercher si une bifurcation de Hopf, pour ce système de dimension 2, peut intervenir, entraînant ainsi l'existence d'une 3ème fréquence naturelle. En effet, l'opérateur linéarisé du second membre de (5) autour de la solution (12) est en fait

$$(13) \quad J_s = \begin{pmatrix} 2\alpha_{30} r_{0s}^2 & 2\alpha_{12} r_{0s} r_{1s} \\ 2\alpha_{21} r_{0s} r_{1s} & 2\alpha_{03} r_{1s}^2 \end{pmatrix},$$

de déterminant $4r_{0s}^2 r_{1s}^2 \Delta$, et trace $= 2(\alpha_{30} r_{0s}^2 + \alpha_{03} r_{1s}^2)$.

On en déduit que 2 valeurs propres complexes traversent l'axe des imaginaires à condition que

$$(14) \quad \Delta > 0, \quad \alpha_{30} \alpha_{03} < 0, \quad \mu_2 \alpha_{30} D_3 < 0,$$

$$\text{où} \quad D_3 = \alpha_{03} D_1 - \alpha_{30} D_2.$$

Dans ce cas, trace $J_s = 0$ pour

$$(15) \quad \mu_1 = \mu_1^T = - \frac{\alpha_{30} D_2}{D_3} \mu_2,$$

et le point de bifurcation sur la branche secondaire est donné par

$$(r_{0s}^T)^2 = \frac{\alpha_{12} \mu_2}{D_3}, \quad (r_{1s}^T)^2 = - \frac{\alpha_{30} \mu_2}{D_3}.$$

Mais sur le système (5), la bifurcation de Hopf est dégénérée [5], c'est-à-dire que pour $\mu_1 = \mu_1^T$ on a une infinité d'orbites périodiques. Il est donc nécessaire de considérer des termes d'ordre supérieur - i.e. d'ordre 5 - ajoutés à (4) pour lever la dégénérescence et décider de quel côté a lieu la bifurcation [5]. Pour cela on doit supposer un peu plus que (4') :

$$(16) \quad \frac{\omega_0}{\omega_1} \text{ non rationnel, ou } \frac{\omega_0}{\omega_1} \neq \frac{1}{2}, \frac{1}{3}, \frac{1}{4}, \frac{2}{3}, \frac{1}{5} .$$

Avec cette hypothèse on a bien une solution périodique qui bifurque à partir de la solution stationnaire correspondant à (12) pour le système obtenu en ajoutant à (5) les termes d'ordre 5. La fréquence de cette solution est voisine de la partie imaginaire des valeurs propres de J_5 , c'est-à-dire de $f = 2 r_{0s}^T r_{1s}^T \sqrt{\Delta}$, qui est petite pour μ voisin de 0.

La découverte du fait qu'une interaction de 2 bifurcations puisse entraîner l'apparition d'une fréquence voisine de 0 qui s'ajoute aux fréquences naturelles existantes, est due à W.F. Langford [7]. Cela se généralise à de nombreux exemples d'interactions.

Pour le système simplifié dans \mathbb{R}^4 cela correspond à l'existence d'une famille de tores invariants de dimension 3 bifurquant à partir de la famille de tores de dimension 2. Les solutions sur ces tores T^3 sont asymptotiquement quasi-périodiques avec 3 fréquences fondamentales voisines de $\hat{\omega}_{0s}$, $\hat{\omega}_{1s}$, f , (au sens de [4] chap. 10).

Pour le système complet (1) on ne peut pas décrire ce qui se passe au voisinage du point de bifurcation trouvé sur le système simplifié, mais en dehors d'une petite région de l'espace des paramètres (région qui pourrait être invisible à l'ordinateur !), on peut montrer l'existence effective de la famille de tores T^3 invariants (et des 3 fréquences asymptotiques) [6].

Pourquoi ce trou noir ? En fait, si l'on sait donner un critère précis pour la perte d'attractivité d'une solution périodique, tel n'est pas le cas pour une solution située sur un tore T^2 . Il n'y a pas de raison en général d'observer une bifurcation vers un tore T^3 [1], mais dans le cas d'interaction on impose suffisamment de conditions au système pour que ces tores T^3 existent, mais en dehors d'une petite région dans l'espace des paramètres.

On schématise à la figure 2 certains exemples où T^3 existe, en considérant un repère avec r_0 , r_1 et μ_1 , et où μ_2 est fixé.

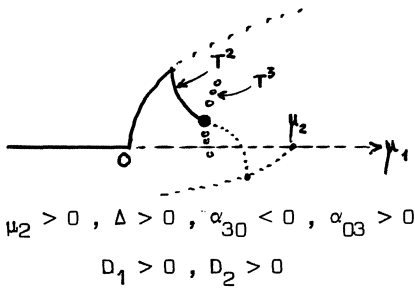
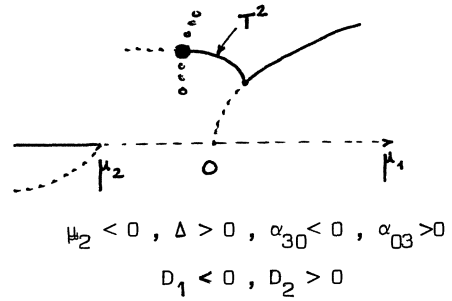
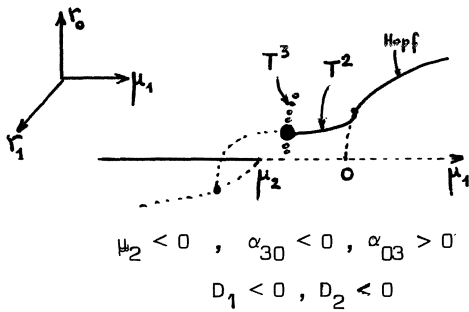


Fig. 2. Exemples avec bifurcation tertiaire. Les traits pleins (resp. pointillés) sur les branches primaires et secondaires correspondent à la stabilité (resp. à l'instabilité). La famille de tores T^3 est indiquée différemment, sa stabilité dépend d'autres coefficients. La région où l'on ne sait rien est marquée d'un gros point noir.

Remarque

En cas de présence de symétries dans le problème d'origine (par exemple une symétrie spatiale cylindrique pour un système régi par des équations aux dérivées partielles), il faut prendre garde aux bifurcations qui rompent les symétries et enrichissent encore les possibilités pour les phénomènes observés ([4], chap. 11).

[1] A. CHENCINER, G. IOOSS, Bifurcations de tores invariants, Arch. Rat. Mech. Anal., 69, 2, p. 109-198, 1979 ; 71, 4, p. 301-306, 1979.

[2] R.J. FIELD, Theoretical chemistry : Advances and Perspectives, p. 54, Ed. H. Eyring, D. Henderson, Acad. Press, New-York 1978.

[3] G. IOOSS, Sur la deuxième bifurcation d'une solution stationnaire de systèmes du type Navier-Stokes. Arch. Rat. Mech. Anal. 64, 4, p. 339-369, 1977.

[4] G. IOOSS, D.D. JOSEPH, Elementary stability and bifurcation theory. Undergraduate Texts in Mathematics, Springer-Verlag, Berlin 1980.

[5] G. IOOSS, W.F. LANGFORD, Conjectures on the routes to turbulence via bifurcations. Ann. New York Acad. Sci. 357, 489-505, 1980.

[6] G. IOOSS, W.F. LANGFORD, Interaction of two Hopf bifurcations (en préparation).

[7] W.F. LANGFORD, Periodic and steady-state mode interactions lead to tori. SIAM J. Appl. Maths. 37, p. 22-48, 1979.

[8] A. PACAULT, P. DE KEPPEL, P. HANUSSE, C. VIDAL, J. BOISSONADE, Accounts of Chemical Research, 9, 438, 1976.

Chaos and Chemistry

Otto E. Rössler

Institute for Physical and Theoretical Chemistry, University of Tübingen
D-7400 Tübingen, Fed. Rep. of Germany

1. Introduction

The thinking possibility of 'turbulent' behavior in chemically reacting systems was first seen by Ruelle and Takens [1] and Nicolis and Prigogine [2]. A few years later, when the Lorenz equation [3] was beginning to be appreciated as a concrete chaos-producing 3-variable ordinary differential equation, similarly behaving abstract reaction systems (belonging actually to a somewhat different, easier to analyze, type of equations; Rössler [4]) were soon seen and followed by experimental demonstrations; see Hudson and Mankin [5] and Pacault et al. [6] for reviews.

Chaos in simple reaction systems described by partial differential equations was (after a suggestive early experimental observation by Winfree [7] that could later be reproduced simulationally [8]) first numerically observed and analyzed by Kuramoto and Yamada [9]. More recently, degenerate center manifold bifurcation techniques are being applied to this problem (cf. [10]). A special sub-case is the existence of purely spatial ('frozen') chaotic solutions in spatially unbounded reaction-diffusion equations. Here, only 'Hamiltonian' (divergence zero) chaos is possible and, in fact, easy to obtain [11].

This leads to the problem of the existence of Hamiltonian chaos also in single ('multiple oscillator') molecules. For a review of this growing field, see Percival [12].

In the following, an attempt is made to somewhat further extend the topic of chemical chaos, in three directions. Specifically, three large systems will be considered that fall outside the usual applied mathematician's point of view (O.D.E.'s of a few degrees of freedom; P.D.E.'s). They pertain to the fields of chemical evolution, statistical mechanics, and quantum mechanics, respectively.

2. The Class of Well-stirred 'Evolutionary' Systems

At first glance, well-stirred, isothermic reaction systems of mass action type are just one more class of physically implemented nonlinear ordinary differential equations. However, there is a subtle difference that sets these systems apart: only in the case of the chemical implementation is there a complete identity between the state variables on the one hand and the supporting 'hardware' on the other. A typical example of the ordinary ('non-chemical') class would be the electronic digital computer. Here a potentially huge set of O.D.E.'s (happening to be also describable in an automata-theoretic shorthand [13]) is physically implemented, namely, as voltages across certain capacitors. This means, however, that even before any of the state variables of this 'dynamical automaton' [13] can start changing dynamically (that is, before the computer has been switched on), the whole hardware has already to sit there squarely in space.

Not so for chemically implemented 'huge computers'. Here it is possible in principle to 'buy' an equally big network (even one possessing somewhat similar equations [13]), without needing to purchase more than 5 or 10 substances - not only to 'start' the machine, but also to 'possess' it in the same sense as one owns the above

computer (after having rented it). In other words, chemistry makes 'invisible machines' possible.

The Belousov-Zhabotinsky reaction can be used to illustrate the principle. In order to make this chemical system with periodic (and even chaotic; Nagashima [14]) transients work, it suffices to pour together four substances obtained at the pharmacist's in addition to water: a bromate salt, some crystallized malonic acid, cerium sulfate, and sulfuric acid. As soon as a well-stirred mixture of these substances has been set up in a beaker, the whole system of mass-action type equations indicated by Field et al. [15] dictates what happens. This system comprises about 20 variables. (The same argument applies to the continuous-stirred-flow reactor version of the same reaction: again, only those five substances have to be supplied at a constant rate, in order to set up the whole system and let it go on indefinitely.)

In other words, a 20-variable chemical reaction system exists at the very instant that five substances have been brought together. Mathematically, there is no difference between the existence of this implementation of the Field-Körös-Noyes equations and (say) an electronic implementation of the same equations: all the variables are implemented. Physically, however, the 'existence' implied in these two alternative implementations is rather different: in the electronic case, even those variables that are presently zero are 'visible' (in the form of supporting hardware), while in the chemical case most of the implemented variables are 'invisible' at the outset (because they have zero concentration).

Of course, it would also have been possible to start the same reaction system by pouring together all of the reactants involved in the whole system (neglecting the fact that some of them are unstable when isolated). But this merely amounts to a different choice of initial conditions ('non-rarified' ones).

In the special case of the Belousov-Zhabotinsky reaction, the ratio between the number of state variables of the whole system on the one hand, and the number of state variables whose initial conditions (or influxes, respectively) have to be non-zero to start (as well as define) the whole system on the other, has been 4:1. However, this is only a conservative estimate. It could be that if the same system were let run for a much longer time than is usually allowed (for example, in a CSTR version), some additional 'late-blooming' variables would have to be taken into account too. Therefore, the general question of the minimum fraction of substances needed in order to set up a larger reaction system poses itself.

Apparently, this fraction can be rather small - for example, 10^{-1000} or even less. This is quite fortunate - computer designers would be grateful for having an analogous principle on their side. At the same time, the old philosophical problem of 'preformation' versus 'creation' takes on a new twist: invisible preformation is compatible with physical creation.

A case in point is the class of so-called evolutionary reaction systems. To define such a system (and set it going in the most inexpensive way), it suffices to provide constant influxes (or exogeneously maintained concentrations) of some ten variables. These might include water, ammonia, methane, carbonates, and some sulfates and phosphates and other salts (cf. Darwin's [16] 'warm little pond'), whereby one should not forget to provide an - on the average - constant 'concentration' of $h\nu$, that is, photons.

The situation is completely analogous to having poured together the initial reactants of the Zhabotinsky reaction and then providing for their further exogeneous supply. The reason that this time, not just 4 times five but something of the order of magnitude of 10^{1000} times ten state variables have been created lies in the capability of carbon atoms to form so-called backbones. If the free energy of the photons that were assumed as one of the reactants (which incidentally might be replaced by some more 'chemically accepted' derived substance) is not too small, a high percentage of this large set of substances can indeed be generated with appreciable finite reaction rates, supposed their precursors already exist. The same holds true for the precursors, and so forth. In other words, the whole reaction system must be taken seriously, not only mathematically but also physically, from the outset.

Instead of C-C- backbones, other backbones like B-N-B-N- are equally appropriate, just as solvents different from water, and temperatures different from those making water an appropriate solvent, are admissible. Moreover, a temperature gradient may replace the photons. (Such conditions may have been realized in a thick layer inside the planets Neptune and Uranus for millennia; see [17].)

So far it is not known how a big, 'randomly wired' chemical network of this type behaves qualitatively in the long run. (The simplifying assumption of well-stirredness may interfere with a biology-analogous type of unfolding; similarly for the stipulation of smooth concentrations - even below 10^{-23} moles per liter - implicit in any mass-action type O.D.E formulation.) Nonetheless, it appears certain that at first, at most one or two subsystems (with a few variables each) will start growing autonomously, but that after a while (when these subsystems have reached an upper quasi-steady state) the conditions for others to do the same have changed (since now twice as many 'pool substances' are available; and so forth). This amounts to a kind of 'super bifurcation' (if the word is allowed): the number of unstably growing subsystems becomes an unstably growing variable itself [18, 13].

The paradigm of chaos makes two additional suggestions possible. Firstly, the whole system (after take-off) is bound to contain chaotic subsystems over substantial segments of its further temporal evolution (if it does not even possess chaotic behavior asymptotically). This follows by induction from the fact that 3 variables of mass-action type (plus 2 exogenously maintained pools) are sufficient for chaos in isothermic well-stirred mass-action systems [19] (similarly 2 variables plus one pool are sufficient under non-isothermic conditions [20]). Secondly, the above opening up of ever new (to a first approximation uncoupled) subsystems is itself an - in a sense - 'chaotic' process.

The unstably growing subsystems that are being successively triggered into 'physical existence' show a superficial analogy to the 'eddies' that spontaneously form in succession in a turbulent P.D.E. At the same time there is also a major difference, however. While ordinary eddies are born and decay without leaving a trace, the present variety is 'rigid' enough to allow for a cumulative process to set in (in which more and more improbable channels are being opened up as a consequence of the earlier opening up of others).

This hypothesis has yet to be confirmed both numerically and analytically (see Cohen [21] for applicability of the theory of growing graphs to the present class of systems). The general idea of a 'cumulative turbulence' is at the same time interesting in its own right also, suggesting the following mathematical possibility: there might exist dynamical processes that automatically search through a universal library (with the present system forming a first candidate).

In the last century, the science fiction author Kurd Lasswitz (cited after [22]) introduced the notion of a 'universal library'. This is the set of all books of a given length that can be printed by random permutation of the about 35 letters of the alphabet (including punctuation marks and blanks). The size of a universal library made up from 500-page books is $10^2,000,000$ volumes or letters (there is no appreciable difference [22]). This number is considerably bigger than the number of chemical reactants that make up an evolutionary chemical network. Nonetheless, since every universal library contains much smaller universal libraries which faithfully specify, with the highest possible degree of abstraction and compression, the content of the whole library, even 10^{1000} possibilities do already approximate a universal library.

It is tempting to think of an evolutionary chemical network as an automatic process that scans through a universal library. If this is a valid interpretation, then this class of chemical systems has even greater theoretical interest. For by definition, a universal library contains all possible knowledge.

At this point, it is possible to point to the fact that in biology, little 'books' have evolved in the genomes of cells. A human cell, for example, contains strings of about 10^{10} nucleic acids, that is, chemical letters. This corresponds to a library of about 10,000 volumes. The finding that every advanced evolutionary system is

necessarily 'recursive' (in the sense of producing a more and more effective evolutionary system [23]) makes it probable that the information content of this particular sub-library at least has been accumulated by a highly effective search process.

Chaos is a universal library. Evolution may be its natural counterpart.

3. Time Does Not Flow

So far, we have considered a subclass of dissipative dynamical systems. These are, most generally speaking, systems of ordinary differential equations which do not fulfill the specific constraint that the divergence of the right-hand side of the whole equation is zero. Among the set of all nonlinear dynamical systems, the class of divergence-zero systems is of measure zero. Nonetheless, Hamiltonian dynamical systems (as in classical mechanics) do belong to this special subclass. An important problem since Boltzmann [24] is how to explain irreversible macroscopic behavior (in the simplest case described by dissipative differential equations) from the basis of a postulated underlying class of Hamiltonian ordinary differential equations.

In recent months, some progress has been made toward better understanding this problem of 'time's arrow', as Eddington [25] called it. Prigogine and Stengers [26] drew attention to the following fact: in chaos-generating maps of area-preserving type, the degree of 'choppedness' (how an initial volume is thinned and elongated) is increasing in both directions of time. The authors used Hopf's [27] map (the so-called baker's transformation) as an example, but the result holds true for all kinds of area-preserving chaos of the 'pure' ('not KAM', see below) type - like Sinai's [28] billiard table system. In the 'strongly mixing' system of the baker's transformation, there is one positive and one negative Lyapunov characteristic exponent. Time reversal therefore still generates one positive and one negative Lyapunov characteristic exponent. Alternatively speaking, topological entropy increases in both directions of time. (See [29] for details on these technical notions.)

A similar result was recently obtained by Hurley [30]. He showed that under the usual assumptions of statistical mechanics, indeed almost all initial conditions lead to an increase in both directions of time.

The relationship between both results (applying to systems of vastly different dimensionalities) may be nontrivial. This is because higher-dimensional nontrivial generalizations of the baker's transformation [31] do not all have the property that the numbers of positive and negative characteristic exponents are equal. In such systems, the type of chaos found can be different in both directions of time. Nonetheless, the higher the dimensionality, the more likely again is the (approximate) equality of both numbers.

What is the physical interpretation of these mathematical results? Prigogine and his school have been struggling with this question for a long time (see again [26]). If time were first going in one direction and then in the other, a co-moving observer would notice that for a while, the formerly observable increase in 'choppedness' turns around, before thereafter picking up again. Another observer, however, opening his own eyes at the moment that time starts going backward, would experience only an increase in the degree to which his own initial condition (which to him appears 'unchopped') is being spread out. This means that more than one sensible interpretation can be given to the same phenomenon.

If it is true that two observers can coexist, one of whom is observing an increase in order and the other a decrease in order, in the same system, then something is wrong with the usual interpretation of the world (presuming that such deterministic models are admissible).

The simplest solution to the problem appears to be: to abandon the notion that time is flowing altogether (cf. Minkowski [32] for an analogous, but differently motivated, proposal). In this case, the notion that time could be 'invertible' suddenly loses all meaning. There is no longer any contradiction in stating that entropy increase

in two directions simultaneously. Also, one is freed to acknowledge that indeed two different dissipative evolutions may be determined by the same divergence-zero microscopic process. To which of these two 'coexisting' dissipative worlds a macroscopic observer belongs depends solely on in which direction of time he is 'facing'.

The task to visualize the possibility of another dissipation (and perhaps evolution and intelligence) existing in the same world, facing the other way, is not easy. Nonetheless, specific experiments verifying the existence of this 'counter-current' may be devised.

From the mathematical point of view, however, there is no reason to wait for a positive outcome of such experiments. Their positive outcome is known beforehand. This is because, in mathematics, time does not flow anyhow.

Subjective time, of course, does flow. But this, as philosophers are quick to point out, has perhaps nothing to do with physics (see Husserl [33], as well as [34]).

4. A Macroscopic Illustration

While there are several levels on which chaos will be significant for an understanding of the brain (starting with the Hodgkin-Huxley equations for a single neuron, and proceeding through networks of coupled neurons), the apparently highest functional level where chaos theory can be applied is that of behavioral control ('motivation'). For one particular brain - that of the blackbird - Todt [35] showed that the next song phrase chosen by this songbird depends on the length of time that this particular strophe has not been sung. Assuming that the different phrases available to the blackbird have each their own motivation and compete for expression, Todt arrived at a model that is identical mathematically to one proposed later as an explanation for 'boiling-type turbulence': a set of (in their slow variables cross-inhibiting) relaxation oscillators of the single-threshold type [36].

If the brain can be understood as a macroscopic physico-chemical machine describable in classical space-time, it can serve as another, this time macroscopic, example by which to illustrate the likely absence of time's flowing. The following thought experiment was devised to show this.

Suppose computer science had already succeeded in building a highly intelligent artificial motivational system (for which one could moreover make plausible that it functions according to the very rules that during the course of biological evolution were incorporated into actual brains). Then it would be possible to let this artificial brain interact, not with the whole three-dimensional world that we know, but with an artificial simplified two-dimensional world only. This two-dimensional artificial world could be known and controlled completely, and the interaction between this world and the autonomous artificial brain could be recorded completely.

As a second assumption, suppose that the 'wiring' of the artificial brain was confined to two dimensions as well. This is in principle possible [37]. For example, artificial axons, that is, information-carrying wires, can be made to cross in two dimensions without 'cross-talking'; a proposed implementation involves excitable media (two-dimensional strips of such a medium) that possess junctions of a complicated shape making sure that an excitation travels only straight ahead after the junction [37]. In this way, an artificial analogue to a natural brain preserving the essential dynamics can be built in principle such that both the analogue and its environment are two-dimensional.

Now comes the crucial point: after recording the interaction of this (two-dimensional) brain with its (two-dimensional) environment, over a certain piece of time, it is possible to take all this information and build another analogue, this time three-dimensional. Mathematically, the new analogue obeys the same equations as the former system. Physically, however, the role of time as the former third dimension is now played by the third space dimension.

Thus, in principle a dynamical system of 'brain type' can be implemented in the three space-dimensions alone. If it is true that the brain 'is' a dynamical system

implemented in space-time, then this purely three-dimensional 'frozen fixture' constitutes but another such implementation.

Just as in the spatio-temporal implementation (x,y,t) the fact that one of the three dimensions was time did not show in the equations (except for the symbol used, t), so it does not this time (x,y,z) . And just as the symbol t could be meant to say: take a slide rule (preferably transparent, with a fine red hair-line running through the middle) and move it along the t -axis - in order to take into explicit account the fact that different instances in time succeed each other in a perfectly ordered manner - , so this time the same slide rule can be applied to the outside of the three-dimensional unchanging block along its z -axis, with the same words.

Of course, it could still be that physical time (or rather: the 'point of nowness') is indeed moving. But for this to become a scientifically meaningful possibility, the postulated movement would have to show up in the equations somehow. For example, one might try to add another differential equation, $\dot{t} = 1$, in order to make sure that time does change. But this in effect only means adding another independent variable t' along which time is changing. This 'super-time' would, in turn, be unchanging again, unless another variable t'' would be added, and so forth ad infinitum. Thus, it is as difficult to build a physico-mathematical theory in which time is flowing as it is to define left and right - and perhaps equally challenging.

5. Uncertainty in Classical Mechanics

Galgani [38] recently gave an interesting example of how a finite h can be derived from a purely classical context. He argued, essentially, that the non-ergodic nature of Hamiltonian chaos (with its division into two classes of trajectories: strongly chaotic ones, and those that belong to KAM tori; cf. [39]) effectively shields part of the energy contained in a classical mechanical system from interacting with the environment. This effect he took to explain the black-body radiation law with its under-representation of high frequencies, because in weakly coupled anharmonic oscillators it is also the highest frequencies that participate in the 'shielded' KAM tori.

Two points remain open in the above picture: firstly, its applicability is confined to classical mechanical systems of the 'smooth' type, that is, to the non-collision type (non-Sinai) subclass. Secondly, it is not known whether the argument remains valid in the limit of the number of coupled oscillators going to infinity, as was assumed by Galgani. This is because even linear systems in this limit become strongly mixing (see [40] for a review), and so might the KAM tori.

In the following, an alternative proposal is made based on the assumptions that (1) the class of systems is not restricted to the smooth subclass, and (2) the number of state variables is bounded from the outset. (Thus, we are back in the class of divergence-zero differential equations of finitely many variables.) It is proposed that for this class of systems, an 'uncertainty relation' holds true.

The following example may show this. Suppose that there is a 'whole system' (with a $2n$ -variable, highly nonlinear Hamiltonian H that generates strong mixing), and within it a 'subsystem' (with $2m$ state variables, $m \ll n$) that has 'wishes'. (Note that if the whole system were dissipative, there would be no problem in defining a subsystem that has wishes, that is, is an optimizer.) Specifically, assume that the subsystem wishes to catch fluctuations that occur at the boundary that it shares with the rest of the system.

Obviously, if the subsystem is to be able to realize this wish, it must be built in such a way that it somehow 'registers' fluctuations as they build up at the boundary. In the second place it must also be capable of 'responding' (by increasing the local coupling, for example). Making the last two assumptions is, however, impossible because they lead to a contradiction. For if the subsystem could succeed in attracting energy, the Liouville property (of volume of flow preservation in state space) implicit in the assumed Hamiltonian structure of the whole system would be violated. Therefore, every subsystem must be unable to register any 'equilibrium fluctuations'.

This general result can be specified. As the whole system oscillates chaotically, the mean energies of all its degrees of freedom become equal (equipartition theorem; cf. [41]) if for simplicity the potential energy terms in the Hamiltonian are assumed equal in form to the kinetic ones. Each subsystem then has a mean energy content of mH/n . However, the same subsystem's mean internal energy is always by one unit (H/n) smaller. This, too, is a consequence of the equipartition theorem [41]: each subsystem, taken as a whole, also represents just one degree of freedom to the rest of the system. A familiar illustration is a Brownian particle jiggling in a fluid. Its m internal oscillators do not possess the same mean energy as if the particles were isolated, at the same temperature, but only a rational fraction, $(m - 1/2)/m$, of this value. (Note the $1/2$ - because a Brownian particle has only kinetic energy.) Usually, this tiny difference is being ignored.

Letting m shrink makes the principle stronger, however. If $m = 1$, the internal mean energy of the subsystem becomes zero ($0/1$) - the whole mean energy of the subsystem is now 'tied up' in the interaction. If $m = 2$, the subsystem's internal mean energy becomes equal to its mean 'linking energy' (and half as big as if the subsystem existed isolated at the same 'temperature'); and so forth. This means: a subsystem can never take up arbitrary fractions of an energy offered to it by another subsystem: only the rational fractions $0, 1/2, 2/3, 3/4, \dots$ can be absorbed into its mean energy. Conversely, when acting as a source itself, a subsystem can only invest a rational fraction of its own total energy content into another subsystem ($0, 1/2, 1/3, 1/4, \dots$). Moreover, pre-existing energies of both the receptor and the donor subsystem are always 'put on the Procrustes bed' of one energy unit (H/n) as the two systems become coupled - so that their former states necessarily become 'obscured' by this amount.

Thus, the present statistical mechanical approach predicts both 'quantization' and an 'uncertainty relation' to occur in finite- n classical mechanical systems of ergodic (or mixing) type. It appears possible that an analogous reasoning led Einstein [42] in 1904 to think of applying a 'molecular theory' to a radiation field (with the well-known outcome, one year later, of kT - that is, H/n - for the mean energy of a light energy quantum in a one-dimensional black cavity [43]).

Historically, it is interesting to note that this early 'finite number of state variables view' was at variance with Max Planck's [44] original view (to whom the quantum had been a mere heuristical - even numerical - device within a continuous picture [45]). Einstein's later reluctance to continue sacrificing Maxwellian continuity (in view of the convenient Lorentz invariance of Maxwell's equations) may have contributed to the 'compromise nature' (partly continuous, partly discrete) of modern quantum mechanics (cf. [45]).

Interestingly, the fact that the second law of thermodynamics can possibly be explained by classical mechanics only under the assumption of n bounded (more precisely: H/n nonzero) was known to Boltzmann [46] already [38]. The present 'limit to observation from the inside' could also have been seen and experimentally pursued in the last century. In fact, it has been seen - but only in the allegorical context of Maxwell's demon [47]. A first concrete version of the demon is Feynman's [41, p.46-7] membrane (possessing trapdoors that can open to one side only when hit by flying particle). Here a kind of 'microscopic providence' prevents any macroscopic anisotropic diffusion from occurring - if the number of internal degrees of freedom of the membrane is finite. Feynman [41] likened his membrane to a Brownian particle. The present theory is an attempt to further 'nail down' the point where the non-observability arises.

The proposed classical mechanical derivation of quantum mechanics would, if successful, not improve the observability 'from within' of the world's Hamiltonian - in accordance with the spirit of the Copenhagen interpretation of quantum mechanics. Nevertheless, something 'symbolical' would be gained: one could set up model worlds (for example, in a computer) in which little subsystems (termed 'physicists') would be subjected to an analogous observation limit with respect to their own H - while the higher-world operator would be able to fully understand their struggling.

Thus, we are back to science fiction at last (cf. [48]). Being able to control a model world not demonstrably isomorphic, but also not demonstrably nonisomorphic, to one's own world is all-important - according to Descartes. In his booklet on the foundations of science and everything, Descartes [49] insisted on a minimum degree of consistency required from any world into which one has been thrown against one's will, if the verdict of unfairness (Descartes said: a bad joke) is to be refutable. In the 17th century, the boost in responsibility to be gained from a scientifically consistent world helped to create modern science. Chaos theory might reinstate that optimism.

7. Summary

The paradigm of chaos suggests a second look at three more than 100 years old theoretical chemical problems: the qualitative behavior of well-stirred evolutionary chemical soups; the reversibility-irreversibility problem of statistical mechanics; and the nature of the measurement process in classical mechanics. Three new notions are suggested (invisible machines; counter-current dissipation; classical uncertainty).

Acknowledgments

I thank John Kozak, Joe Ford, Rob Shaw, Tim Poston, and Ulrich Wais for discussions. Part of the results were also presented at 'Chaos Day' International Conference, Guelph University, Ontario, March 1981. A visiting professorship by the Department of Mathematics, University of Guelph, is gratefully acknowledged. I especially thank Bill Smith and Pal Fischer for many stimulating discussions.

References

- 1 D. Ruelle and F. Takens, *Commun. Math. Phys.* 20, 167 (1971)
- 2 G. Nicolis and I. Prigogine, *Proc. Nat. Acad. Sci. (USA)* 68, 2102 (1971)
- 3 E.N. Lorenz, *J. Atmos. Sci.* 20, 130 (1963)
- 4 O.E. RöSSLer, *Z. Naturforsch. Teil A* 31, 259 (1976)
- 5 J.L. Hudson and J.C. Mankin, *J. Chem. Phys.* 74, 6171 (1981)
- 6 A. Pacault and C. Vidal, *These Proceedings*
- 7 A.T. Winfree, *Science* 181, 937 (1973)
- 8 O.E. RöSSLer and C. Kahlert, *Z. Naturforsch. Teil A* 34, 565 (1979)
- 9 Y. Kuramoto and T. Yamada, *Progr. Theor. Phys.* 55, 679 (1976)
- 10 J. Guckenheimer, *On a codimension two bifurcation* (preprint 1979)
- 11 O.E. RöSSLer and H. Thomas, *in preparation*
- 12 I.C. Percival, *Advan. Chem. Phys.* 36, 1 (1977)
- 13 O.E. RöSSLer, *Springer Lect. Notes Biomath.* 4, 399 (1974)
- 14 H. Nagashima, *J. Phys. Soc. Japan* 49, 2427 (1980)
- 15 R.J. Field, E. Körös, and R.M. Noyes, *J. Amer. Chem. Soc.* 94, 8649 (1972)
- 16 C. Darwin, in: *Life and Letters of Charles Darwin*, F. Darwin Ed., vol. 3, 202 (Murray, London 1887)
- 17 M. Ross, Berkeley (quoted in *Time Magazine*, 24 Aug. 1981, p. 55)
- 18 O.E. RöSSLer, *Z. Naturforsch. Teil B* 26, 741 (1971)
- 19 K.D. Willamowski and O.E. RöSSLer, *Z. Naturforsch. Teil A* 35, 317 (1980)
- 20 C. Kahlert, O.E. RöSSLer and A. Varma, in: *Proc. Heidelberg Workshop Modelling Chemical Reaction Systems 1980* (Springer Series of Chemical Physics 1981)
- 21 J.E. Cohen, in: *Proc. Science in the Service of Life*, Vienna 1979, M. Marois Ed.
- 22 H. Flechtner, *Fundamental Notions of Cybernetics* (in German) (Wissenschaftliche Verlagsgesellschaft, Stuttgart 1968)

- 23 O.E. RöSSLer, *BioSystems* 11, 193 (1979)
- 24 L. Boltzmann, *Sitz.-Ber. Akad. Wiss. Wien II* 66, 275 (1872)
- 25 A.S. Eddington, *The Nature of the Physical World* (Cambridge University Press, Cambridge 1929)
- 26 I. Prigogine and I. Stengers, *Dialogue with Nature* (in German)(Piper, München 1981)
- 27 E. Hopf, *Ergodic Theory* (in German) p.42 (Springer-Verlag, Berlin 1937)
- 28 Ya.G. Sinai, *Sov. Math. Dokl.* 4, 1818 (1963)
- 29 J.P. Crutchfield and N.H. Packard, *Symbolic dynamics of one dimensional maps* (preprint 1981)
- 30 J. Hurley, *Phys. Rev. A* 23, 268 (1980)
- 31 O.E. RöSSLer, in: *New Approaches to Nonlinear Problems in Dynamics*, P. Holmes Ed., 477 (SIAM, Philadelphia 1980)
- 32 H. Minkowski, *Space and Time* (in German)(Teubner, Leipzig 1909)
- 33 E. Husserl, *On the Phenomenology of the Inner Consciousness of Time* (in German), *Collected Works = Husserliana*, vol. 10 (M. Nijhoff, The Hague 1966)
- 34 K. Vonnegut, *Slaughterhouse Five* (Dell, New York 1968)
- 35 D.J. Todt, in: *Kybernetik* 68, H. Marco and G. Farber Eds., 465 (Oldenbourg, Munich 1969)
- 36 O.E. RöSSLer, in: *Dynamics of Synergetic Systems*, H. Haken Ed., 147 (Springer-Verlag, Heidelberg 1980)
- 37 A.K. Dewdney, *J. Recreational Math.* 12, 16 (1979)
- 38 L. Galgani, *Statistical mechanics of weakly coupled oscillators presenting stochastic thresholds* (preprint 1981)
- 39 R. Abraham and J.E. Marsden, *Foundations of Mechanics*, 2nd ed. (Freeman, San Francisco 1978)
- 40 J.L. Van Hemmen, *Springer Lect. Notes Phys.* 93, 232 (1979)
- 41 R.P. Feynman, R.B. Leighton, and M. Sands, *The Feynman Lectures on Physics*, vol. 1 (Addison-Wesley, Reading, Mass. 1965)
- 42 A. Einstein, *Ann. d. Phys. Ser. 4*, 14, 354 (1904)
- 43 A. Einstein, *Ann. d. Phys. Ser. 4*, 17, 132 (1905)
- 44 M. Planck, *Verh. d. D. Phys. Ges.* 2, 237 (1900)
- 45 T.S. Kuhn, *Black-body Theory and the Quantum Discontinuity 1894-1912* (Oxford University Press, New York 1978)
- 46 L. Boltzmann, *Nature* 51, 413 (1895)
- 47 J.C. Maxwell, *Theory of Heat*, p. 308 (1871)
- 48 D.F. Galouye, *Simulachron-Two* (Gregg, London 1964)
- 49 R. Descartes, *Meditations on the First Philosophy* (in Latin) (Soly, Paris 1641)

Evolution of Chaos and Power Spectra in One-Dimensional Maps

Hazime Mori

Department of Physics, Kyushu University 33
Fukuoka 812, Japan

1. Introduction

Low-dimensional maps have turned out to be useful for discovering and understanding new properties of dynamical systems. Outstanding examples are the Bernoulli shifts [1] and the β transformations [2] in ergodic theory and the Lorenz map [3] and the quadratic model for the onset of fluid turbulence [4]. In fact these discrete processes have led us not only to a deeper understanding of chaotic orbits in terms of the topological entropy and the Lyapunov exponent, but also to the discovery of a band-splitting transition [5] and a dynamic scaling law near a chaotic transition point [4,6].

The structure of chaos can be described by the power spectrum, i.e., the Fourier-Laplace transform of the time-correlation function of nonperiodic orbits [7]. In this talk, we shall discuss how chaos evolves and the power spectrum changes as the excitation parameter is increased, taking two one-dimensional maps which display the transition from non-chaotic to chaotic states. In particular we shall be interested in an ordered motion in chaos which is represented by a sharp peak of the power spectrum.

Chaos is exhibited by nonperiodic orbits, but its structure can be characterized by periodic orbits which exist densely among nonperiodic orbits. We shall take this point of view and make use of Sharkovsky's ordering of periodic orbits for a continuous map [8] and Takahashi's ordering for the β transformations [2]. This work was performed in collaboration with T. Yoshida, H. Okamoto, H. Shigematsu and T. Ose.

2. Power spectrum $P(\omega)$

For many chaotic systems, an essential feature of the long-time behavior can be described by a one-dimensional discrete process $\{x_n\}$, ($n=1,2,\dots$) which is generated by a nonlinear transformation $f(x)$;

$$x_{n+1} = f(x_n) = f^n(x_1), \quad (2.1)$$

where f^n denotes the n -th iterate of f . If the slope $|f'(x)|$ is larger than unity in an attractor Ω except at finite number of points, then 1) there exist periodic orbits densely everywhere in Ω and they are all unstable, 2) $f(x)$ is ergodic in Ω ; namely, for almost all initial values x_1 , the orbit $f^n(x_1)$ is a nonperiodic orbit and the long-time average is equal to the space average with a probability density $\rho(x)$;

$$\langle G \rangle \equiv \lim_{N \rightarrow \infty} \frac{1}{N} \sum_{n=1}^N G(x_n) = \int_{\Omega} dx \rho(x) G(x). \quad (2.2)$$

The slope $|f'(x)| > 1$ ensures the stretching and folding of intervals in Ω which leads to the ergodicity. Two interesting models satisfying this condition are the β transformation

$$f(x) = \begin{cases} 2hx, & (0 \leq x \leq 1/2) \\ 2hx - h, & (1/2 < x \leq 1) \end{cases} \quad (2.3)$$

and the tent transformation

$$f(x) = \begin{cases} 2hx & (0 \leq x \leq 1/2) \\ -2hx + 2h & (1/2 < x \leq 1) \end{cases} \quad (2.4)$$

where $1 \geq h > 0$. The β transformation is a generalization of the projection of the Baker's transformation onto the stretching axis, and the tent transformation is a simplification of the Lorenz map and the quadratic model. Both have the slope $|f'(x)| = 2h > 1$ if $h > 1/2$. If $h < 1/2$, then any orbit is attracted by the fixed point $x=0$. Thus the two models are chaotic if $h > 1/2$ and non-chaotic if $h < 1/2$. The power spectrum is given by

$$P(\omega) = \sum_{n=0}^{\infty} C_n e^{-i\omega n} + \text{c.c.}, \quad (2.5)$$

where C_n is the time-correlation function of orbits

$$C_n \equiv \int_{\Omega} dx \rho(x) f^n(x) \delta x, \quad (\delta x \equiv x - \langle x \rangle) \quad (2.6)$$

and c.c. denotes the complex conjugate of the first part. C_n can be written as

$$C_n = \int_{\Omega} dx x H^n[\rho(x) \delta x] \quad (2.7)$$

in terms of the Frobenius-Perron operator H [7]. Let $\psi_{\ell}(x)$ be an eigenfunction of H ,

$$H \psi_{\ell}(x) = v_{\ell} \psi_{\ell}(x), \quad \ell = 0, 1, 2, \dots, \quad (2.8)$$

with an eigenvalue v_{ℓ} . The probability density $\rho(x)$ is the eigenfunction with eigenvalue unity; $H \rho(x) = \rho(x)$. ($v_0 = 1$). Expanding $\rho(x) \delta x$ in terms of $\{\psi_{\ell}(x)\}$, we obtain

$$C_n = \sum_{\ell=1}^{\infty} A_{\ell} v_{\ell}^n \quad (2.9)$$

which is inserted into (2.5) to give

$$P(\omega) = \sum_{\ell=1}^{\infty} A_{\ell} \frac{1}{1 - v_{\ell} e^{-i\omega}} + \text{c.c.} \quad (2.10)$$

Therefore, the power spectrum has a sharp peak at $\omega = \omega_{\ell}$ if $\gamma_{\ell} \ll 1$, where

$$v_{\ell} = |v_{\ell}| e^{i\omega_{\ell}} = e^{-\gamma_{\ell} + i\omega_{\ell}}. \quad (2.11)$$

3. β transformation ($\beta \equiv 2h$) [9]

In this section we shall discuss $P(\omega)$ of the β transformation whose mapping function is given by (2.3). Let $\{p_n\}$ ($n=1, 2, \dots$) be a periodic orbit of period N ($N=2, 3, \dots$);

$$P_{N+i} = f^N(p_i) = p_i, \quad i = 1, 2, \dots, N. \quad (3.1)$$

A periodic orbit of period N exists if and only if $\beta \equiv 2h \geq \beta_N$, where

$$\beta_N = 1 + \beta_N^{-N+1}, \quad \beta_N > \beta_{N+1} > \beta_{\infty} = 1. \quad (3.2)$$

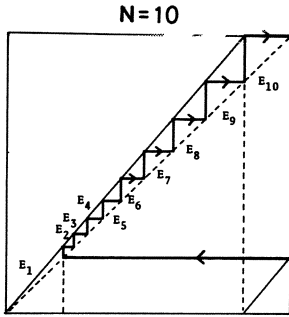


Fig.1 $f(x)$ of (2.3) vs. x in the attractor at $\beta = \beta_{10} \doteq 1.198$,

where the intervals flow as $E_1 \rightarrow E_1$, $E_2; E_i \rightarrow E_{i+1}$ ($i=2,3, \dots, N-1$); $E_N \rightarrow E_1$.

the mechanism of the degradation of chaos or, inversely, the evolution of chaos in terms of periodic orbits. Now let us calculate $P(\omega)$ at $\beta = \beta_N$. Let E_i be the subinterval (p_{i-1}, p_i) with $p_0 \equiv 0$, as in Fig.1, and $E_i(x)$ be its characteristic function (1 if $x \in E_i$, 0 otherwise). Then the flow of intervals leads to

$$H \begin{bmatrix} E_1(x) \\ E_2(x) \\ \vdots \\ E_N(x) \end{bmatrix} = \frac{1}{\beta} \begin{bmatrix} 1 & 1 & & & \\ & 0 & 1 & & \\ & & \ddots & \ddots & \\ & & & \ddots & 1 \\ 1 & 0 & \dots & \dots & 0 \end{bmatrix} \begin{bmatrix} E_1(x) \\ E_2(x) \\ \vdots \\ E_N(x) \end{bmatrix} \quad (3.5)$$

The eigenvalues of the structure matrix are given by

$$\det [S \mathbf{1} - M] = S^N - S^{N-1} - 1 = 0. \quad (3.6)$$

This algebraic equation has N roots, S_0, S_1, \dots, S_{N-1} , satisfying $S_{N-\ell} = S_\ell^*$, which lead to eigenvalues of H , $\nu_\ell = S_\ell / \beta$. Only one positive root $S_0 = \beta$ corresponds to $\nu_0 = 1$ and leads to the probability density

$$\rho(x) = a_{01} \sum_{i=1}^N \beta^{-i+1} E_i(x), \quad a_{01} \equiv \beta^N / (N(\beta-1) + 1). \quad (3.7)$$

Other $(N-1)$ roots, satisfying $|S_\ell| < \beta$, determine $P(\omega)$ as

$$P(\omega) = \sum_{\ell=1}^{N-1} \frac{A_\ell}{1 - |\nu_\ell| e^{i(\omega_\ell - \omega)}} + \frac{B}{1 - \frac{1}{\beta} e^{-i\omega}} + \text{c.c.} \quad (3.8)$$

$$A_\ell = \frac{S_\ell}{N\beta(\beta-1) - 1} \frac{1 + N(\beta-1)}{1 + N(S_\ell - 1)} \frac{\beta^2 - 1}{\beta^2 - S_\ell}, \quad B = 1 - \sum_{\ell=1}^{N-1} A_\ell, \quad (3.9)$$

Examples of β_N are

$$\beta_2 = (1 + \sqrt{5})/2 \doteq 1.618, \quad \beta_3 \doteq 1.466, \quad (3.3)$$

$$\beta_{25} \doteq 1.100, \quad \beta_{100} \doteq 1.034.$$

The minimal periodic orbit is the rising periodic orbit which has only one point on the right branch ($1/2 < x \leq 1$). At $\beta = \beta_N$ the rising periodic orbit of period N lies on the top, as in Fig.1. It may easily be understood that Takahashi's ordering

$$2 \vdash 3 \vdash 4 \vdash 5 \vdash \dots \vdash N \vdash \dots \vdash 1 \quad (3.4)$$

holds [2], where $j \vdash k$ means that, if a periodic orbit of period j exists, then a periodic orbit of period k also exists. Therefore, if $\beta \geq \beta_2$, then periodic orbits of all periods exist. As $\beta \rightarrow \beta_\infty = 1$, however, periodic orbits disappear successively in Takahashi's sequence, and all periodic orbits disappear at the transition point $\beta = 1$. This gives

where $P(\omega)$ has been normalized so that $\int_{-\pi}^{\pi} d\omega P(\omega) = 1$, $\nu = 1/\beta$ in the second term of (3.8) is an eigenvalue of H characteristic of the time-correlation function (2.7). Thus $P(\omega)$ is completely determined by S_ℓ .

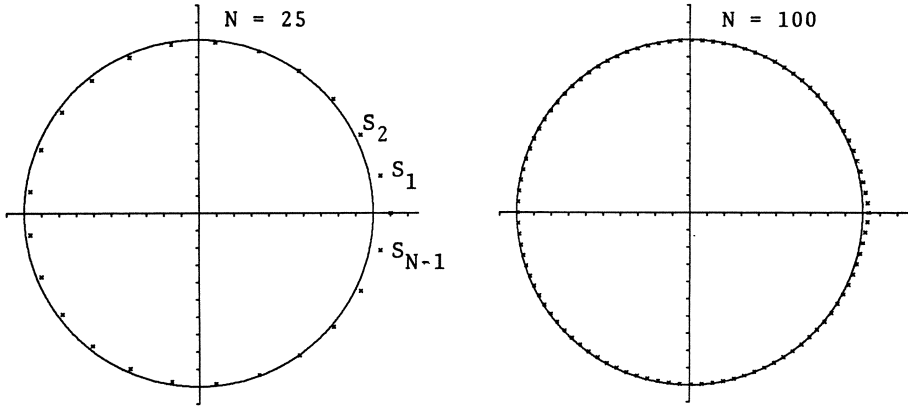


Fig.2 N roots of (3.6) with $N=25$ and 100 in the complex plane, where the circle is the unit circle.

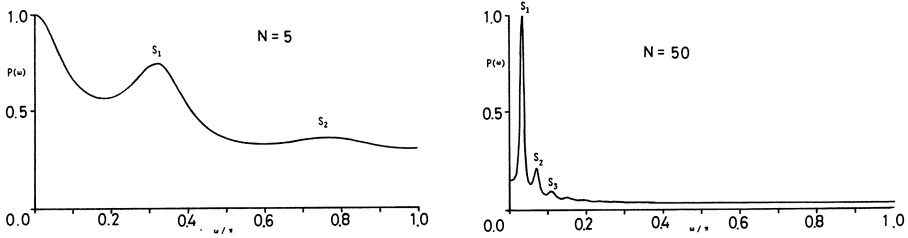


Fig.3 $P(\omega)$ vs. ω/π at $\beta = \beta_N$. ($N=5,50$), where the height of the highest peak is normalized to be unity. The peak at $\omega=0$ arises from $\nu=1/\beta$, but its height rapidly decreases as $N \rightarrow \infty$. The ℓ -th peak comes from $\nu_\ell = S_\ell/\beta$ ($\ell=1,2,\dots,N-1$), and the first peak S_1 is rapidly enhanced as $N \rightarrow \infty$ (i.e., $\beta \rightarrow 1$).

Fig. 2 shows S_ℓ of $N=25$ & 100 in the complex plane. S_ℓ 's lie on an ellipse. This ellipse approaches the unit circle as $N \rightarrow \infty$ (i.e., $\beta \rightarrow 1$). If $|\omega_\ell| < \pi/3$, then $|S_\ell| > 1$. The nearest neighbors of the positive root, S_1 and $S_{N-1} = S_1^*$, have the largest magnitude among $\ell \neq 0$ and hence are the slowest eigenmodes which determine the main feature of $P(\omega)$ as $N \rightarrow \infty$. This is illustrated in Fig.3. Thus, for large N , the nearest neighbor S_1 dominates and leads to

$$P(\omega) \approx \frac{A_1}{1 - e^{-\gamma_1 + i(\omega_1 - \omega)}} + \text{c.c.} + (\omega \rightarrow -\omega), \quad (3.10)$$

where $(\omega \rightarrow -\omega)$ denotes those obtained by changing ω to $-\omega$ in the first two terms. This leads to

$$C_n \approx e^{-\gamma_1 n} \cos(\omega_1 n). \quad (3.11)$$

A dynamic scaling law holds as shown in Fig.4:

$\omega_1 \sim N^{-\theta_f}$, $\gamma_1 \sim N^{-\theta_d}$. We have $\theta_f \approx 0.98$, $\theta_d \approx 1.22$ for $200 < N < 500$. Since (3.2) leads to $1/N \rightarrow (\beta-1)/|\ln(\beta-1)|$ as $N \rightarrow \infty$, we have

$$\omega_1, \gamma_1 \sim \left| \frac{\beta-1}{\ln(\beta-1)} \right|^\theta \text{ as } \beta \rightarrow 1. \quad (3.12)$$

This scaling law implies that

A. Least-period hypothesis: $P(\omega)$ and C_n are determined by the neighborhood of the minimal periodic orbit of the least period N as $N \rightarrow \infty$.

B. Similarity hypothesis: The neighborhood becomes similar as $N \rightarrow \infty$. These ensure that (3.10) and (3.11) with (3.12) are valid even when the vertex is a nonperiodic point. The details will be reported elsewhere [9].

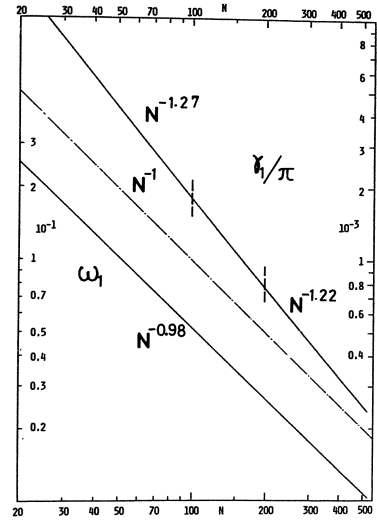


Fig.4 ω_1 and γ_1 vs. N in the logarithmic scale, where $\theta_f \approx 0.98$ for $25 < N < 500$, whereas $\theta_d \approx 1.27$ for $25 < N < 100$ and $\theta_d \approx 1.22$ for $200 < N < 500$.

4. Tent transformation ($\alpha \equiv 2h$) [10,11]

The mapping function is given by (2.4), for which Sharkovsky's ordering holds [8]:

$$\begin{aligned} & 3 \mid 5 \mid 7 \mid \dots \mid 2 \times 3 \mid 2 \times 5 \mid 2 \times 7 \mid \dots \\ & \dots \mid 2^n \times 3 \mid 2^n \times 5 \mid 2^n \times 7 \mid \dots \\ & \dots \mid 2^n \mid \dots \mid 8 \mid 4 \mid 2 \mid 1 \end{aligned} \quad (4.1)$$

where the first two lines consist of the ascending sequences of $2^n \times N$, $N=2m+1$, ($m=1,2, \dots$) with $n=0,1,2, \dots$, and the last line is the descending powers of 2. A periodic orbit of odd period N exists if and only if $\alpha \equiv 2h \geq \alpha_N$, [12], where

$$\alpha_N^N - 2\alpha_N^{N-2} - 1 = 0, \quad \alpha_N > \alpha_{N+2} > \alpha_\infty = \sqrt{2}. \quad (4.2)$$

Therefore, all periods exist if $\alpha \geq \alpha_3 = (1+\sqrt{5})/2 \doteq 1.618$. As $\alpha \rightarrow \alpha_\infty = \sqrt{2}$, however, odd periods disappear successively in Sharkovsky's sequence and all odd periods disappear at $\alpha = \sqrt{2}$, where the attractor splits into two bands. This is the mechanism of the band-splitting transition. Below $\alpha = \sqrt{2}$, each of the two bands repeats the above process in the map $f^2(x)$ with slope α^2 and splits into two bands at $\alpha^2 = \sqrt{2}$. Thus it turns out that period $2^n \times N$ disappears below

$$\alpha = \alpha_{n:N} \equiv (\alpha_N)^{1/M}, \quad M \equiv 2^n \quad (4.3)$$

and the attractor splits into $2M$ bands at $\alpha = \alpha_{n:\infty} = 2^{1/2M}$. All periods, except 2^n , disappear at $\alpha = \alpha_{\infty:\infty} = 1$ where chaos disappears.

Now let us calculate $P(\omega)$ at $\alpha = \alpha_N$, where the vertex is the rotating periodic orbit of odd period N like Fig.5. Then the flow of intervals leads to

$$H \begin{bmatrix} E_1(x) \\ \vdots \\ E_m(x) \\ E_{m+1} \\ \vdots \\ E_{2m} \end{bmatrix} = \frac{1}{\alpha} \begin{bmatrix} | & 1 & \dots & 1 \\ & & & 1 \\ & 0 & & \\ \hline & & 0 & 1 \\ & & & \\ & 1 & & \\ \vdots & & & \\ 1 & & & 0 \end{bmatrix} \begin{bmatrix} E_1(x) \\ \vdots \\ E_m(x) \\ E_{m+1} \\ \vdots \\ E_{2m} \end{bmatrix} \quad (4.4)$$

The eigenvalues of the structure matrix are given by

$$S^{2m+1} - 2S^{2m-1} - 1 = 0 \quad (S \neq -1). \quad (4.5)$$

This leads to $2m$ roots, $S_0, S_1, \dots, S_{2m-1}$ which are illustrated in Fig.6. The positive root $S_0 = \alpha$ and the negative root S_1 change as $S_0 \rightarrow \sqrt{2}$, $S_1 \rightarrow -\sqrt{2}$ as $m \rightarrow \infty$, whereas the other roots remain inside the unit circle $|S_\ell| < 1$. Hence S_1 is the slowest eigenmode which has the largest eigenvalue. Equation (2.9) takes the form [10]

$$C_n = \sum_{\ell=1}^{2m-1} A_\ell \left[\frac{S_\ell}{\alpha} \right]^n + \sum_{\ell=1}^{2m} B_\ell \left[\frac{t_\ell}{\alpha^2} \right]^n, \quad (4.6)$$

where $t_\ell = \exp[2\pi i \ell / (2m+1)]$. Therefore, for $n \gg 1$, the S_1/α term dominates, leading to

$$C_n \approx \frac{7+4\sqrt{2}}{17} (-1)^n e^{-\gamma_1 n} \quad (4.7)$$

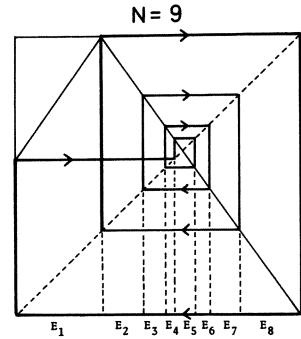


Fig.5 $f(x)$ of (2.4) vs. x in the attractor at $\alpha = \alpha_9 = 1.441$, where the intervals flow as $E_1 \rightarrow E_{m+1}, E_{m+2}, \dots, E_{2m}$; $E_i \rightarrow E_{2m+2-i}$ ($i=2,3,\dots,m$); $E_{m+1} \rightarrow E_{m+1}, E_m; E_{m+i} \rightarrow E_{m+1-i}$.

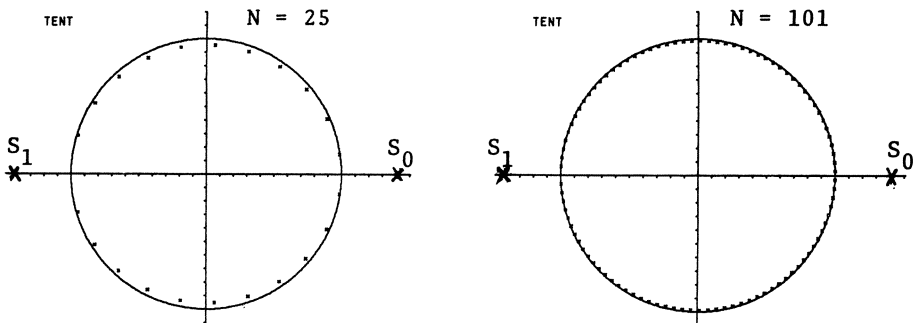


Fig.6 $2m$ roots of (4.5) with $N=2m+1=25$ and 101 in the complex plane.

with $\gamma_1 = -\ln|S_1/\alpha| \approx \sqrt{2}(\alpha - \sqrt{2})$ near $\alpha = \sqrt{2}$. This is the critical mode which agrees with the cycling mode between two bands below $\alpha = \sqrt{2}$. Thus the slowest eigenmode S_1

produces a sharp peak of $P(\omega)$ at $\omega=\pi$. It also turns out that, as $\alpha \rightarrow 1$, a sharp peak centered at $\omega=\pi/M$ with width γ_1/M appears near $\alpha=2^{1/2M}$ ($M=2^n$, $n=0,1,2,\dots$) successively so that $P(\omega)$ has $(n+1)$ sharp lines at $\omega=\pi/2^k$, $k=0,1,\dots,n$. It seems that, even when the vertex is a nonperiodic point, there exists a negative eigenvalue ν_1 , isolated from the others, and the above is still valid. The details will be reported elsewhere [10,11].

5. Short summary

- 1) Chaos evolves by the successive excitation of a sequence of periodic orbits; e.g., Takahashi's sequence for the β transformation and Sharkovsky's sequence for the tent transformation.
- 2) This evolution of chaos can be described by $P(\omega)$ whose sharp peak represents an ordered motion in chaos.
- 3) A dynamic similarity law holds for $P(\omega)$ & C_n near a critical point. Its mechanism is that, in the β transformation, the neighborhood of the minimal periodic orbit of the least period dominates near $\beta=1$, while, in the tent transformation, the critical mode of the band splitting dominates near $\alpha=\sqrt{2}$. These differ from Feigenbaum's scaling [4] which results from the similarity of map directly. In the tent transformation, Feigenbaum's type scaling [6] holds near $\alpha=1$ with $\delta=2$.

References

- 1) D.S. Ornstein, in Statistical mechanics, ed. S.A. Rice, K.F. Freed and J.C. Light (Univ. Chicago Press, 1972), 13-22.
- 2) Y. Takahashi, Chaos of Interval Dynamical Systems and Periodic Points, (Seminar Report of Math. Dept., Tokyo Metropolitan Univ., 1980), 1-137 (in Japanese).
- 3) E.N. Lorenz, J. Atoms. Sci. 20 (1963), 130.
- 4) M.J. Feigenbaum, J. Stat. Phys. 19 (1978), 25; Phys. Letters 74A (1979), 375.
- 5) S. Grossmann and S. Thomae. Z. Naturforsch. 32a (1977), 1353.
- 6) B.A. Huberman and J. Rudnick, Phys. Rev. Lett. 45 (1980), 154.
J.P. Crutchfield and B.A. Huberman, Phys. Lett. 77A (1980), 407.
S.-J. Chang and J. Wright, Phys. Rev. A23 (1981), 1419.
- 7) H. Mori, B.-C. So and T. Ose, Prog. Theor. Phys. 66 (1981), No.4.
- 8) P. Stefan, Commun. math. Phys. 54 (1977), 237.
- 9) H. Mori, T. Ose and H. Okamoto, Prog. Theor. Phys. (to be submitted).
- 10) H. Shigematsu, H. Mori and T. Yoshida, Prog. Theor. Phys. (to be submitted).
- 11) T. Yoshida, H. Mori and H. Shigematsu, Prog. Theor. Phys. (to be submitted).
- 12) S. Ito, S. Tanaka and H. Nakada, Tokyo J. Math. 2 (1979), 221.

Tests of the Period-Doubling Route to Chaos

Mitchell J. Feigenbaum

Los Alamos National Laboratory, Theoretical Division
Los Alamos, NM 87545, USA

Abstract

The period-doubling route to chaotic behavior has characteristic spectral and temporal properties which are here outlined.

When a system makes a transition to chaotic behavior by what is now termed period-doubling, there are well-determined universally true properties that are encountered. That is, there are definite temporal relations and equivalent spectral relations that can easily be put to experimental test.

Simply put, as a control parameter is varied, any dynamical variable demonstrates a systematic doubling of its period prior to the aperiodic limit signalling the onset of chaos. This doubling occurs at particular parameter values which converge to the value at the transition point geometrically at the universal rate $\delta = 4.6692..$ This is the most elementary test of the theory of this kind of transition. Unfortunately, it is a delicate test requiring a resolution that at the level of present experiments usually forbids a determination beyond order of magnitude.

However, since the period doublings accumulate so quickly, gross features remain nearly constant, while the new temporal features characterizing the newly doubled period contain a small fraction of the energy. Moreover, as period-doubling is periodic in terms of logarithmic deviations from the transition point, each new modification is a constant fraction of its predecessor. This entails very definite consequences, whether viewed temporally or through a Fourier transform, which we explore in this note.

The basic theoretical quantification of this notion is that the deviations from the old periodicity that determine the new and doubled period systematically (and universally) scale from one doubling to the next. Formally, write

$$d_n(t) = \frac{x_n(t) - x_n(t+T_{n-1})}{2} \quad (1)$$

where $x_n(t)$ is any coordinate when the parameter is such that the n -th period doubling has occurred, for which the period is

$$T_n = 2 \cdot T_{n-1} \quad (2)$$

(Actually, as the parameter varies T_n is only approximately constant. However, since the parameter values accumulate, (2) is asymptotically correct.) Equation (1) defines d_n to be non-zero if the period of x_n is really T_n and not T_{n-1} , and so is the deviation in the trajectory associated with the doubled period. The theoretical result (which is published elsewhere[1]) is that for large n ,

$$d_{n+1}(t) \sim \sigma(t/T_{n+1})d_n(t) \quad . \quad (3)$$

where $\sigma(x)$ is a universal function a priori computable (the same function for each coordinate of the system), depending upon the level of period-doubling (n), only through a scaling of its argument. Observe that according to (1)

$$d_{n+1}(t+T_n) = -d_{n+1}(t)$$

so that σ has the symmetry

$$\begin{aligned} \sigma(x+1/2) &= -\sigma(x) \\ \sigma(x+1) &= \sigma(x) \quad . \end{aligned} \quad (4)$$

Equation (3) is a very strong prediction : acquire the temporal data $x_n(t)$ and compute from it the half-period deviation function of (1) ; similarly obtain d_{n+1} and divide it by d_n ; then for each n on an appropriately scaled plot, the same function $\sigma(x)$ should be observed. This is already a strong scaling result. However, there is an even stronger feature being tested : namely that $\sigma(x)$ is a known, available function with the approximate value

$$\sigma(x) = \begin{cases} \alpha^{-2} = 1/6.25\dots & 0 < x < 25 \\ \alpha^{-1} = 1/2.5029\dots & 25 < x < 5 \quad . \end{cases} \quad (5)$$

All spectral tests for period-doubling universality are tests of (3), while at present, the results following from the approximation (5) are as precise as experiment can hope to resolve.

There are, however, difficulties in employing (3) as an experimental test which follow from the requirement of making two sets of measurements at different parameter values. The simpler problem is the phasing of the two time bases : to use (3) the time origins must be the same. This is most easily handled by varying a delay, in say $d_n(t)$, until its zero crossings are most nearly coincident with those of $d_{n+1}(t)$. (There are indeed many nearly coincident crossings. Also, the time scale of $d_n(t)$ might require some adjustment so that d_{n+1} has precisely twice the period of d_n .) More seriously, the parameter values must be chosen so that the limit cycles of x_n and x_{n+1} have identical stability. This requires, for example, some convergence data which might be hard to come by unless successive parameter values

at the bifurcation points (when the period doubles) are used. If these difficulties are attended to, however, (3) and (5) then serve as a simple and very direct measurement of the universality theory. (These same difficulties afflict the Fourier measurements, except that phasing is obviously unimportant if only amplitude spectra are determined).

In fact, the universal function σ is different for different stabilities (e.g. at superstable values as opposed to bifurcation values of the parameter.) However, the differences show up only in the corrections to the approximation (5). Indeed there are other functions σ agreeing to the level of (5) which determine deviation signals, $d(t)$, pertaining to the same parameter value (typically to be used at the transition value) which then bypasses the above difficulties. We shall explore these tests after determining Fourier properties which shall motivate them.

Corresponding to the deviation signal, the fundamental frequency of x_n is $1/T_n = \frac{1}{2}(1/T_{n-1})$, that is, a half subharmonic of the previous fundamental. Had $d_n(t)$ vanished, there would have been no components at the odd multiples of the new fundamental. The even multiples represent the components at the previous fundamental; since the parameter change becomes increasingly small, these components cannot suffer significant changes. Accordingly, the basic result of the doubled period is the set of spectral lines at the odd multiples of the new subharmonic fundamental. These are determined not by all of $x_n(t)$, but only by its "subharmonic part" $d_n(t)$. Since these scale (by σ), it is then clear that these successive additions to the spectrum geometrically decrease in a universal way, as determined by the Fourier analysis of σ . Let us now make these observations quantitative.

By definition,

$$\hat{x}_{(n)}(p) = \frac{1}{T_n} \int_0^{T_n} dt x_n(t) e^{2\pi i p t / T_n} \quad (5)$$

with inverse,

$$x_n(t) = \sum_p \hat{x}_{(n)}(p) e^{-2\pi i p t / T_n} \quad (6)$$

Manipulating (5),

$$\hat{x}_{(n)}(2p+1) = \frac{1}{T_{n-1}} \int_0^{T_{n-1}} dt \left[\frac{x_n(t) - x_n(t+T_{n-1})}{2} \right] e^{2\pi i \frac{(2p+1)t}{T_n}} \quad (7)$$

or

$$\hat{x}_{(n)}(2p+1) = \frac{1}{T_{n-1}} \int_0^{T_{n-1}} dt d_n(t) e^{2\pi i \frac{2p+1}{T_n} t} \quad (8)$$

with inverse

$$d_n(t) = \sum_t \hat{x}_{(n)}(2p+1) e^{-2\pi i \frac{2p+1}{T_n} t} \quad (9)$$

Thus, the spectral components at odd multiples of the subharmonic fundamental are determined solely by the deviation signal $d_n(t)$.

Since all the new subharmonic components arise from the same time signal, they can be smoothly connected as an ensemble by interpolating them. The natural interpolation that reflects their common source is, then, the analytic continuation provided by (8) :

$$\hat{x}_n(\omega) = \frac{1}{T_{n-1}} \int_0^{T_{n-1}} dt d_n(t) e^{2\pi i \omega t} \quad (10)$$

with

$$\hat{x}_n\left(\frac{2p+1}{T_n}\right) = \hat{x}_{(n)}(2p+1) \quad .$$

Utilizing (9), this interpolation is

$$\hat{x}_n(\omega) = \sum_p \hat{x}_{(n)}(2p+1) \frac{1}{T_{n-1}} \int_0^{T_{n-1}} dt e^{-2\pi i (2p+1 - \omega T_n) t / T_n} \quad (11)$$

or

$$\hat{x}_n(\omega) = (1 + e^{\pi i \omega T_n}) \frac{1}{\pi i} \sum_p \frac{\hat{x}_{(n)}(2p+1)}{2p+1 - \omega T_n} \quad . \quad (12)$$

We now ask how $\hat{x}_{n+1}(\omega)$ is related to $\hat{x}_n(\omega)$. By definition

$$\hat{x}_{n+1}(\omega) = \frac{1}{T_n} \int_0^{T_n} dt d_{n+1}(t) e^{2\pi i \omega t} \quad .$$

Employing the scaling formula for large n , we have

$$\begin{aligned} \hat{x}_{n+1}(\omega) &\sim \frac{1}{T_n} \int_0^{T_n} dt \sigma\left(\frac{t}{2T_n}\right) d_n(t) e^{2\pi i \omega t} \\ &= \sum_p \hat{x}_{(n)}(2p+1) \frac{1}{T_n} \int_0^{T_n} dt \sigma\left(\frac{t}{2T_n}\right) e^{-2\pi i (2p+1 - \omega T_n) \frac{t}{T_n}} \\ &= \sum_p \hat{x}_{(n)}(2p+1) \frac{1}{2T_{n-1}} \int_0^{T_{n-1}} dt \left[\sigma\left(\frac{t}{2T_n}\right) - e^{\pi i \omega T_n} \sigma\left(\frac{t}{2T_n} + \frac{1}{4}\right) \right] e^{-2\pi i (2p+1 - \omega T_n) t / T_n} . \end{aligned}$$

If we now use the approximation of (5), then

$$\hat{x}_{n+1}(\omega) \approx \frac{1}{2\alpha} \left(\frac{1}{\alpha} - e^{\pi i \omega T_n} \right) \sum_p \hat{x}_{(n)}(2p+1) \frac{1}{T_{n-1}} \int_0^{T_{n-1}} dt e^{-2\pi i (2p+1 - \omega T_n) t / T_n}$$

or

$$\hat{x}_{n+1}(\omega) \approx \frac{1}{2\alpha} \left(\frac{1}{\alpha} - e^{\pi i \omega T_n} \right) \hat{x}_n(\omega) \quad (13)$$

by use of the interpolation formula (11).

Equation (13) is the basic result of this paper regarding Fourier analysis, and is rich in content [2]. The first conclusion to be drawn is that rather than scaling uniformly, different parts of the spectrum scale very differently. Thus

1. At $\omega = \frac{2p+1}{T_{n+1}}$, the actual new spectral components characterizing the $n+1$ -st level of period doubling are

$$\hat{x}_{(n+1)}(2p+1) \approx \frac{1}{2\alpha} \left(\frac{1}{\alpha} - (-1)^p i \right) \hat{x}_n \left(\frac{2p+1}{T_{n+1}} \right)$$

or

$$|\hat{x}_{(n+1)}(2p+1)| \approx \frac{1}{2} \sqrt{\frac{1}{\alpha^2} + \frac{1}{\alpha^2}} |\hat{x}_n \left(\frac{2p+1}{T_{n+1}} \right)| \quad (14)$$

That is, the new spectral components are obtained by scaling the previous interpolation at these new positions by a factor of

$$\frac{1}{2} \sqrt{\frac{1}{\alpha^2} + \frac{1}{\alpha^2}} \approx \frac{1}{4.6}$$

or dropped logarithmically by

$$10 \log_{10} 4.6 \approx 6.6$$

(The approximation (14) is the same as that for the scaling of successive RMS averages of spectral lines as obtained by Nauenberg [3].)

2. At $\omega = \frac{2p+1}{T_n}$, that is at those frequencies of the n -th level, one finds the $n+1$ interpolation scaled by

$$\hat{x}_{n+1} \left(\frac{2p+1}{T_n} \right) \approx \frac{1}{2\alpha} \left(\frac{1}{\alpha} + 1 \right) \hat{x}_{(n)}(2p+1) \quad (15)$$

That is, in the next generation of doubling, the interpolation scales by the anomalously small amount of

$$\frac{1}{2\alpha} \left(\frac{1}{\alpha} + 1 \right) \approx \frac{1}{3.6}$$

or

$$10 \log_{10} 3.6 \approx 5.5 \text{ db}$$

at those frequencies that had just previously come into existence.

3. At $\omega = \frac{2p}{T_n}$ one has

$$\hat{x}_{n+1} \left(\frac{2p}{T_n} \right) \approx \frac{1}{2\alpha} \left(\frac{1}{\alpha} - 1 \right) \hat{x}_n \left(\frac{2p}{T_n} \right) \quad (16)$$

where

$$\frac{1}{2\alpha} \left(\frac{1}{\alpha} - 1 \right) \approx - \frac{1}{8.3}$$

or

$$10 \log_{10} 8.3 \approx 9.2 \text{ db} \quad .$$

Thus, in the second and all following generations after a spectral line has appeared, the successive interpolations drop anomalously quickly. (The approximation (16) is easily seen to be the same approximation of Grossman [4] for the "leading" edge of the spectrum).

4. As a consequence of 2. and 3., if the n-th interpolation is raised by x_n for any $5.5 \text{ db} < x < 9.2 \text{ db}$, these spectra will all have regions of overlap. In particular, the original spectral prediction [1] of $x = 8.2 \text{ db}$ is included in this range. The present formula (13) is the full realization of the ideas of that previous paper.

5. Since different parts of the spectrum have different geometric scalings, a geometric mean of the n-th level spectral lines is a more significant average than the mean of the squares. Given (13), we can then compute the scaling of the geometric mean, or logarithmically, the average of log-amplitudes :

$$\hat{X}_n \equiv \frac{1}{2^{n-1}} \sum_{p=0}^{2^{n-1}-1} \ln |\hat{x}_{(n)}(2p+1)| \approx \int_0^1 d\omega \ln |\hat{x}_n(\omega)| \quad .$$

Then,

$$\hat{X}_{n+1} - \hat{X}_n \approx \int_0^1 d\omega \ln \left| \frac{\hat{x}_{n+1}(\omega)}{\hat{x}_n(\omega)} \right| \approx -\ln(2\alpha) + \int_0^1 d\omega \ln \left| \frac{1}{\alpha} - e^{\pi i 2^n \omega} \right| \quad .$$

However, the integral on the right identically vanishes for $|\alpha| > 1$. Thus,

$$\hat{X}_{n+1} - \hat{X}_n \approx -\ln(2\alpha) \quad (17)$$

or the mean log amplitudes drop by

$$10 \log_{10}(2\alpha) \approx 10 \log_{10} 5.0 = 7.0 \text{ db} \quad . \quad (18)$$

(This result is unchanged if the averaging is performed over all the n-th level spectral lines up to any multiple of the original fundamental, rather than just the subharmonic part.)

(17) is a new result, and this approximate value has been numerically verified to be correct to the precision of (18).

At this point we want to extend these results to spectral properties at a fixed parameter value, rather than at successive period-doubling values. As previously demonstrated, as the parameter increases, the n-th level lines slightly increase until they saturate after several further period doublings. This increase is uniform for each level of introduced spectral lines from which it follows that properties 1.-5.

are equally valid within a spectrum at fixed λ for all intermediate values of n (i.e. after several period doublings have occurred, but not for the lowest lying interpolations which have not yet saturated.) Taking the fundamental period to be 1, $\omega = 1$ is the original fundamental, and the n -th level of spectral lines are located at the frequencies

$$\omega = \frac{2p+1}{2^n} \quad (19)$$

Now, all the spectral properties are consequences of (13) which itself is a consequence of (3). Working backwards, if we define, at a fixed parameter value λ_n , $d_{n,m}(t)$ as that part of $x_n(t)$ constructed purely from the m -th level spectral lines, then (3) must again hold for a new scaling function σ which has the same approximate value as (5). That is,

$$d_{n,m+1}(t) \sim \tilde{\sigma}(t/T_{m+1}) d_{n,m}(t) \quad (20)$$

where (20) is valid for all m such that $1 \ll m \ll n$ and $\tilde{\sigma}$ has the approximate value (5). Once $d_{n,m}(t)$ is specified, (20) is now a direct time-domain test of the theory. It is probably the best test to perform since just one time series is required, and there are no phasing problems. All that remains to be specified is $d_{n,m}(t)$:

$$d_{n,m}(t) = \frac{1}{2^{n-m+1}} \sum_{r=0}^{2^{n-m+1}-1} (-1)^r x_n(t+rT_{m-1}) \quad (21)$$

where

$$x_n(t) = \sum_{m=1}^n d_{n,m}(t) + \frac{1}{2^n} \sum_{r=0}^{2^n-1} x_n(t+rT_0) \quad (22)$$

so that $d_{n,m}$ is just that part of x_n which determines its m -th level spectrum.

For numerical experiments (20) is very readily verified; the theory leading to (20) will be published elsewhere. (20) can be iterated so that (20) and (22) approximately determines $x_n(t)$ from that part of it with period $2T_0$. This is a general structure arising from an underlying Cantor set, so that this type of data processing might be more generally applicable to dynamical systems with a strange attractor present. The analogue to (13) is

$$\hat{x}_{n,m+1}(\omega) \simeq \frac{1}{2\alpha} \left(\frac{1}{\alpha} - e^{-\pi i \omega T_m} \right) \hat{x}_{n,m}(\omega)$$

so that the log-amplitude spectrum is built out of sums of determined periodic functions of successively doubled periods.

Acknowledgements

I would like to thank the IHES and the Stiftung Volkswagenwerk for the hospitality and support that facilitated the production of this paper.

R E F E R E N C E S

1. M.J. Feigenbaum, Phys. Lett. 74A, 375 (1979), Comm. Math. Phys. 77, 65 (1980).
2. This formula first appeared as the scaling for the broadband part of a noisy spectrum in A. Wolf, J. Swift. University of Texas at Austin preprint "Universal Power Spectra for the Reverse Bifurcation Sequence" (1981).
3. M. Nauenberg, J. Rudnick, Universality and the power spectrum at the onset of chaos. Preprint UCSC (1981).
4. S. Grossman, S. Thomae. University of Marburg, preprint (1981).

Part III

Stochastic Analysis

Thermal Fluctuations in Nonlinear Chemical Systems

G. Nicolis, F. Baras and M. Malek Mansour

Faculté des Sciences de l'Université Libre de Bruxelles
Campus Plaine, C.P. 226
1050 Bruxelles, Belgium

1. Introduction.

The study of fluctuations is an integral part of the analysis of nonlinear phenomena in far from equilibrium conditions [1-3]. In this respect, systems undergoing chemical reactions and transport phenomena have been among the most privileged examples on which new ideas and new techniques have been tested. So far however, practically all the results obtained are limited to the behavior of the composition variables. It is the purpose of the present communication to outline an extension of the theory of fluctuations which includes energy and temperature fluctuations as well.

Our motivation for undertaking this extension is manifold. Chemical reactions reflect the behavior of those molecules whose translational energy exceeds some threshold value. The statistical distribution of these molecules depends on the instantaneous ambient temperature. It follows that fluctuations of the reagent's temperature will be immediately sensed by the reacting molecules. Energy fluctuations are also frequently invoked in discussions of the molecular basis of enzyme activity [4]. On a more macroscopic scale, such common phenomena as energy transfer between a system and its environment, exothermic reactions, combustion, explosions, or flames, involve in one way or the other the internal energy or the temperature as a key variable. The stochastic analysis of these systems, which are known to exhibit a rich variety of bifurcation and other transition phenomena, must therefore take into account the thermodynamic fluctuations of these variables.

2. Some typical problems involving temperature variations.

In the following we consider, in the order of increasing complexity, a number of typical situations involving internal energy or temperature fluctuations. In each case, we assume that the reacting mixture is a dilute gas, and therefore do not consider explicitly the effect of intermolecular interactions. It is known [5] that this provides a realistic description of an important class of combustion processes known as rarefied flames. In the present Section we merely compile these various examples and briefly recall their macroscopic behavior, postponing the analysis of fluctuations for later on.

(i) Energy transfer between system and external reservoirs.

The simplest case involves the transport of energy between two vessels. Within the framework of our assumptions this will proceed solely through the transfer of particles. We are thus led to a Knudsen flow model. Assuming that the two (well-mixed) phases com-

municate by an opening whose diameter σ is small compared to the mean free path and that at each moment the velocity distribution remains Maxwellian, we obtain the following expressions for the total flow of particles and internal energy per unit time in a direction perpendicular to the opening (see e.g. [6]) :

$$\begin{aligned} \frac{d\bar{n}}{dt} &= \sigma \left(\frac{1}{2\pi m} \right)^{1/2} \frac{1}{V} \left[-\bar{n} (k_B \bar{T})^{3/2} + n_1 (k_B T_1)^{3/2} \right] \\ \frac{d\bar{e}}{dt} &= 2\sigma \left(\frac{1}{2\pi m} \right)^{1/2} \frac{1}{V} \left[-\bar{n} (k_B \bar{T})^{5/2} + n_1 (k_B T_1)^{5/2} \right] \end{aligned} \quad (2.1)$$

Here \bar{n} , \bar{e} and \bar{T} denote, respectively, the particle density, energy density and temperature of the system, m the molecular mass, k_B the Boltzmann constant, and V the volume of the system. The subscript 1 refers to the reservoir variables. Strictly speaking, a system described by eqs.(2.1) will sooner or later come to equilibrium with the reservoir : $\bar{n} = \bar{n}_1$, $\bar{T} = \bar{T}_1$. On the other hand, eqs.(2.1) are readily extended to the case of a system interacting with several reservoirs. Such a situation allows for the existence of nonequilibrium steady states. In the simplest case of two reservoirs maintained at fixed temperatures T_1 , T_2 and densities n_1 , n_2 , one obtains the following steady-state values \bar{T}_s , \bar{n}_s for the system :

$$\begin{aligned} \bar{T}_s &= \frac{n_1 T_1^{3/2} + n_2 T_2^{3/2}}{n_1 T_1^{1/2} + n_2 T_2^{1/2}} \\ \bar{n}_s &= \frac{n_1 T_1^{1/2} + n_2 T_2^{1/2}}{2 \bar{T}_s^{1/2}} \end{aligned} \quad (2.2)$$

(ii) Adiabatic explosion.

In (i) we considered transport phenomena in the absence of chemical reactions. We now consider the other extreme case, in which a single exothermic irreversible reaction proceeds in an isolated system. Let r_v be the heat of the reaction at constant volume, $k(\bar{T})$ the (temperature-dependent) rate constant, c_v the specific heat at constant volume. One then has :

$$\begin{aligned} X &\xrightarrow{k(\bar{T})} A \\ \frac{d\bar{x}}{dt} &= -k(\bar{T}) \bar{x} \\ c_v \frac{d\bar{T}}{dt} &= -r_v \frac{d\bar{x}}{dt} = r_v k(\bar{T}) \bar{x} \end{aligned} \quad (2.3)$$

where \bar{x} is an intensive variable descriptive of the chemical composition. It is immediately seen that eqs.(2.3) give rise to the conservation condition

$$c_v T_{\max} = c_v T_0 + r_v x_0 = c_v \bar{T} + r_v \bar{x} = K \quad (2.4)$$

where (T_0, x_0) are the initial values of (\bar{T}, \bar{x}) and $(T_{\max}, \bar{x} = 0)$ are the final ones (after the reaction has been completed). Thanks to (2.4), eqs.(2.3) take the alternative simple form

$$\frac{d\bar{T}}{dt} = k(\bar{T}) (T_{\max} - \bar{T}) \quad (2.5)$$

The solution of eq.(2.5) is depicted in Fig.1, for a temperature dependence of $k(\bar{T})$ given by the Arrhenius law, $k(\bar{T}) = k_0 \exp(-E_0/k_B\bar{T})$. It is seen [5] that the reaction rate abruptly reaches its maximum value at a temperature near the maximum one. The time corresponding to this value can be referred to as the "explosion time".

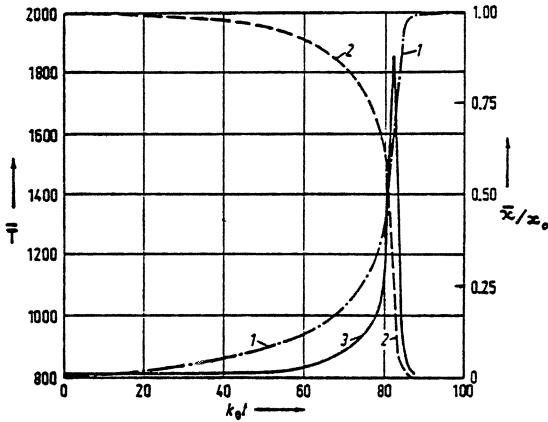


Fig.1. Variation in temperature (1, left-hand ordinate), relative concentration x/x_0 (2, right-hand ordinate) and reaction rate (3, arbitrary units) as a function of $k_0 t$ for an adiabatic reaction.

(iii) Exothermic reaction in an open system.

We finally discuss the more realistic case in which, in addition to the exothermic reaction considered in (ii), the system is exchanging energy with its environment by the mechanism considered in (i). We take for simplicity a single external reservoir. From eqs.(2.1) and (2.3) we obtain :

$$\frac{d}{dt} \bar{x} = -k(\bar{T}) \bar{x} + \mathcal{K} (x_1 T_1^{1/2} - \bar{x} \bar{T}^{1/2}) \tag{2.6}$$

$$\frac{d}{dt} \bar{e} = r_v k(\bar{T}) \bar{x} + 2 \mathcal{K} k_B (x_1 T_1^{3/2} - \bar{x} \bar{T}^{3/2})$$

where we set

$$\mathcal{K} = \sigma \left(\frac{k_B}{2\pi m} \right)^{1/2} \tag{2.6a}$$

$$\text{and } k(\bar{T}) = k_0 \exp(-E_0/k_B\bar{T}). \tag{2.6b}$$

The competition between local energy release from the reaction and transport now allows the system to reach nonequilibrium steady states, even though it interacts with a single reservoir. It is convenient to analyze the properties of these states by fixing the values of $\rho = 2k_B/r_v$, and $g = E_0/k_B$, and by using T_1 and \mathcal{K} as control parameters. Fig.2. describes a typical result. In the range $T_1^{(*)} < T_1 < T_1^{(*)}$ and for a sufficiently small value of \mathcal{K} , the system exhibits multiple stable steady states and hysteresis. The temperatures at the limit points $T_1^{(*)}$ and $T_1^{(*)}$, which can be appropriately referred to as

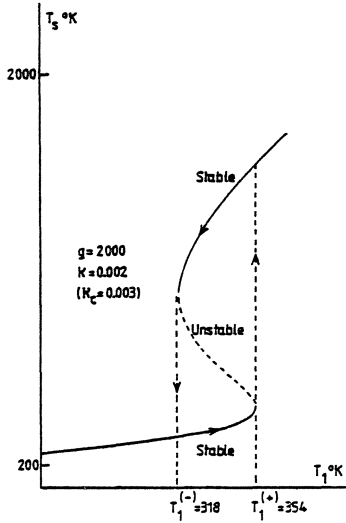


Fig.2. Multiple steady states and hysteresis for the system described by eqs. (2.6)

extinction and ignition points, are given by

$$\bar{T}_{\pm} = \frac{1}{6} \left[T_1 + 2q \pm \sqrt{(T_1 + 2q)^2 - 24T_1q} \right]. \quad (2.7)$$

When these two values coalesce, the system presents a bifurcation point. One easily finds the following critical values of the variables and the control parameters :

$$\begin{aligned} \bar{T}_c &= \frac{2q}{3} (3 - \sqrt{6}) \\ T_{1c} &= 2q (5 - 2\sqrt{6}) \\ K_c &= \frac{k(\bar{T}_c)(1 + gT_{1c})}{g\bar{T}_c^{1/2}(\bar{T}_c - T_{1c})}. \end{aligned} \quad (2.8)$$

For $K < K_c$ the system presents multiple steady states and hysteresis. Actually, the results shown in Fig.2 correspond to a value of K relatively close to the critical one. For $K \ll K_c$ one obtains a still larger variety of temperature-induced transitions, which are beyond the scope of the present communication.

3. Construction of the transition probabilities.

To study the fluctuations associated with eqs.(2.1), (2.5) and (2.6), we need to write down the master equation for the appropriate probability ensemble. The explicit form of this equation depends on the transition probabilities per unit time corresponding to the various steps involved in the phenomenon. This is easily determined for the chemical reactions [1], but is much less obvious for transitions affecting the temperature or the internal energy. We therefore resort to the following thermodynamic argument. The transition rates depend on the microscopic mechanisms which are at the basis of a transition, and for this reason they do

not involve explicitly the nonequilibrium constraints. Moreover, at equilibrium, they must satisfy the property of detailed balance separately for each individual chemical reaction and for each individual transport process. Now at thermodynamic equilibrium the probability of fluctuations is given by the familiar Einstein relation [8]. We may therefore utilize all these properties to obtain information on the structure of the transition probabilities.

Let us first examine from this point of view a typical energy transport process of the kind described in Section 2, part (i). The basic quantity to be determined here is the transition rate $W(E+\epsilon, N+1, E_1-\epsilon, N_1-1 | E, N, E_1, N_1)$ where E and N are, respectively, the total energy and number of particles of the system and ϵ the amount of energy carried per particle.

The detailed balance condition reads :

$$\frac{W(E+\epsilon, N+1, E_1-\epsilon, N_1-1 | E, N, E_1, N_1)}{W(E, N, E_1, N_1 | E+\epsilon, N+1, E_1-\epsilon, N_1-1)} = \frac{P_{eq}(E, N, E_1, N_1)}{P_{eq}(E+\epsilon, N+1, E_1-\epsilon, N_1-1)} \quad (3.1a)$$

with [8]

$$P_{eq} \sim \exp \frac{1}{k_B} S_{total} \sim \exp \frac{1}{k_B} [S(E, N) + S_1(E, N)] \quad (3.1b)$$

S , S_1 being respectively the entropy of the system and of the reservoir. The most symmetric relation which one can derive for the W 's themselves and which is compatible with (3.1a) is :

$$W(E+\epsilon, N+1 | E, N) d\epsilon = \sigma \varphi(\epsilon) d\epsilon \exp \frac{1}{k_B} [S(E, N) - S(E+\epsilon, N+1)] \quad (3.2)$$

where the presence of the cross-section σ of the opening between the two vessels ensures extensivity. A similar expression is expected for W_1 . The function $\varphi(\epsilon) d\epsilon$ stands for the velocity dependence of the flow of particles per unit surface in a direction \underline{n} perpendicular to the opening :

$$\varphi(\epsilon) d\epsilon = \int_{\text{angles}} |\underline{v} \cdot \underline{n}| d\underline{v} = \frac{4\pi}{m^2} \epsilon d\epsilon .$$

Expanding the right hand side of (3.2) around the state $(E+\epsilon, N+1)$ and introducing the well-known thermodynamic relations for the derivatives of entropy we obtain :

$$W(E+\epsilon, N+1 | E, N) d\epsilon = \frac{4\pi\sigma}{m^2} \epsilon d\epsilon \left(\frac{m}{2\pi k_B T}\right)^{3/2} \frac{N+1}{V} \cdot \exp \left[- \frac{\epsilon}{k_B T} + o(V^{-1}) \right] . \quad (3.3a)$$

In eq.(3.3a) it is understood that T is a function of the instantaneous state of the system as expressed by the stochastic variables

E, N :

$$\frac{\partial}{\partial E} S(E, N) \Big|_{E+\epsilon, N+1} = \frac{1}{T(E+\epsilon, N+1)} . \quad (3.3b)$$

We hereafter call this quantity the fluctuating temperature. Remarkably, eq.(3.3a) displays the Maxwell-Boltzmann distribution with fluctuating particle density and temperature.

The final step in the construction of the transition probabilities is to derive an expression for a typical exothermic chemical reaction. Consider the processes



of which the forward one is assumed to be exothermic. Let $W(X+1, A-1 | X, A)$ be the corresponding transition rate. Because of energy conservation (cf.eq.(2.4)), X and A completely characterize the process. Working out the detailed balance condition along the same lines as before, we arrive at

$$W(X+1, A-1 | X, A) \equiv W(X+1 | X) = (X+1) \exp \left[-E_0 / k_B T \right] . \quad (3.5)$$

Again, it is understood that T is a fluctuating temperature, $T=T(X+1)$. The "activation energy" E_0 arises through the difference between the standard chemical potential of X , μ_x^* , and that of the activated complex, μ_x^\ddagger . We recognize the familiar Arrhenius factor, with the important additional feature that temperature is to be interpreted as a stochastic variable.

4. Fluctuation-dissipation theorem in the transport regime.

Using Eqs.(3.3a) and (3.3b) one can write down the master equation corresponding to either of the three situations described in Section 3. We first analyze the properties of this equation in the simplest case of transport between a well-mixed system and two external reservoirs, in the absence of chemical reactions. As the corresponding evolution equations, essentially of the same form as (2.1), have a single asymptotically stable steady state solution, it is legitimate to convert in the thermodynamic limit $V \rightarrow \infty$, the master equation for the extensive variables (N, E) to a Fokker-Planck equation [9] for the corresponding intensive variables $n = N/V$, $e = E/V$. As well known, the latter is equivalent to a pair of stochastic differential equations for the random processes $n(t)$, $e(t)$. For the problem considered in the present Section we obtain the following explicit form valid in the vicinity of the unique stable steady state :

$$\begin{aligned} \frac{d}{dt} n &= \chi \left(n_1 T_1^{1/2} + n_2 T_2^{1/2} - 2n T(n, e) \right) + F_n(t) \\ \frac{d}{dt} e &= 2 \chi k_B \left(n_1 T_1^{3/2} + n_2 T_2^{3/2} - 2n T(n, e) \right) + F_e(t) . \end{aligned} \quad (4.1)$$

The correlation matrix of the random forces F_n , F_e is :

$$\begin{bmatrix} \langle F_n(t) F_n(t') \rangle & \langle F_n(t) F_e(t') \rangle \\ \langle F_e(t) F_n(t') \rangle & \langle F_e(t) F_e(t') \rangle \end{bmatrix} = 4 \lambda \bar{T}_s^{1/2} \bar{n}_s \delta(t-t') \\ = \frac{1}{V} \begin{bmatrix} 1 & 2k_B \bar{T}_s \\ 2k_B \bar{T}_s & 6k_B^2 \bar{T}_s^2 \left(1 - \frac{(\bar{T}_s - T_1)(\bar{T}_s - T_2)}{\lambda \bar{T}_s^2} \right) \end{bmatrix} \quad (4.2)$$

where (\bar{T}_s, \bar{n}_s) is given by (2.2). Eqs. (4.2) provide a generalized fluctuation-dissipation theorem, valid for arbitrary deviations from the equilibrium state $\bar{T}_s = T_1 = T_2$. It is noteworthy that the terms reflecting the deviation from the classical fluctuation-dissipation theorem are quadratic with respect to the deviation from equilibrium (essentially the thermal gradient across the system).

Having relations (4.1) and (4.2) it is an easy matter to evaluate the static as well as the time-dependent properties of the response. It is most convenient to switch from (n, e) to (n, T) . One then obtains the following expressions for the second moments of the fluctuations :

$$\begin{aligned} \langle \delta n^2 \rangle &= \frac{1}{V} n_s \left[1 - \frac{(\bar{T}_s - T_1)(\bar{T}_s - T_2)}{10 \bar{T}_s^2} \right] \\ \langle \delta n \delta T \rangle &= \frac{1}{V} \frac{(\bar{T}_s - T_1)(\bar{T}_s - T_2)}{5 \bar{T}_s^2} \\ \langle \delta T^2 \rangle &= \frac{1}{V} \frac{k_B \bar{T}_s^2}{c_v} \left[1 - \frac{7(\bar{T}_s - T_1)(\bar{T}_s - T_2)}{5 \bar{T}_s^2} \right] \end{aligned} \quad (4.3)$$

where the specific heat per unit volume is given by $c_v = 3\bar{n}_s k_B/2$. At equilibrium, $\bar{T}_s = T_1 = T_2$ and eqs. (4.3) reduce to the well-known expressions derived from Einstein's formula [8]. A surprising feature is that the equilibrium-like expressions remain valid even in the linear range of irreversible processes (the range of the theorem of minimum entropy production [10]), provided that the equilibrium values of n and T are replaced by the values descriptive of the nonequilibrium steady state. This is to be contrasted with the case of chemical reactions in isothermal systems, where the equilibrium-like expressions are affected by corrections which are linear in the deviation from equilibrium (ref. [3], lecture by G. Nicolis).

By switching from (4.1) to equations for (n, T) or more precisely to equations for $\delta n = n - \bar{n}_s$, $\delta T = T - \bar{T}_s$, linearized around the steady state (\bar{T}_s, \bar{n}_s) , one can also compute straightforwardly the time correlation of the mass and heat fluxes j_n and j_T respectively. As a matter of fact, since in our system the only irreversible processes going on are transport processes, j_n and

j are simply linear combinations of the random forces F_n and F_e . We thus obtain, for instance,

$$\langle \delta j_T(t) \delta j_T(t') \rangle = \frac{g}{2} \chi \bar{T}_s^{1/2} 2 k_B \bar{T}_s^2 \cdot \frac{1}{V} \left[1 - \frac{4(\bar{T}_s - T_1)(\bar{T}_s - T_2)}{3\bar{T}_s^2} \right] \delta(t-t') \quad (4.4)$$

Noting that $g\chi\bar{T}_s^{1/2}/2$ is simply the coefficient of the part of eq. (4.1) which is linearized in δT , we recognize in the prebracket factor of (4.4) the Landau-Lifshitz result [11]. In addition, eq. (4.4) provides a generalization of the classical theory to fluctuations around far-from-equilibrium states. As before, the correction is quadratic in the thermal constraint. Similar results are obtained for $\langle \delta j_n(t) \delta j_n(t') \rangle$ and $\langle \delta j_n(t) \delta j_T(t') \rangle$.

5. Fluctuations in the presence of exothermic reactions.

We next consider the situation described in Section 2, part (iii). In the presence of fluctuations, a master equation can be derived using the transition rates evaluated in Section 3. In the regime of a unique stable steady-state solution of (2.6), one can reduce this equation to a Fokker-Planck equation as explained already in the preceding Section. The corresponding stochastic differential equations have the form;

$$\begin{aligned} \frac{d}{dt} x &= -k[T(e,x)] x + \chi \left(x_1 T_1^{1/2} - x T(e,x)^{1/2} \right) + F_x(t) \\ &\equiv f \left[x, T(e,x) \right] + F_x(t) \\ \frac{d}{dt} e &= r_v k[T(e,x)] x + 2\chi k_B \left(x_1 T_1^{3/2} - x T(e,x)^{3/2} \right) + F_e(t) \\ &\equiv h \left[x, T(e,x) \right] + F_e(t) \end{aligned} \quad (5.1)$$

where the correlation matrix $\{Q_{ij}\}$ of the random forces F_x and F_e is given by

$$\begin{aligned} V Q_{xx} &= \bar{x}_s k(\bar{T}_s) + \chi \left(x_1 T_1^{1/2} + \bar{x}_s \bar{T}_s^{1/2} \right) = 2\bar{x}_s \left[k(\bar{T}_s) + \chi \bar{T}_s^{1/2} \right] \\ V Q_{xe} &= r_v \bar{x}_s k(\bar{T}_s) + 2\chi k_B \left(x_1 T_1^{3/2} + \bar{x}_s \bar{T}_s^{3/2} \right) = 2\bar{x}_s \left[r_v k(\bar{T}_s) + 2\chi k_B \bar{T}_s^{3/2} \right] \\ V Q_{ee} &= r_v^2 \bar{x}_s k(\bar{T}_s) + 6\chi k_B^2 \left(x_1 T_1^{5/2} + \bar{x}_s \bar{T}_s^{5/2} \right) \end{aligned} \quad (5.2)$$

In the absence of transport ($\chi = 0$) we find the limiting case discussed in Section 2, part (ii). As the mass and energy balances are then related, the system is described by a single random variable. Choosing the latter to be the temperature T , we can write the following Fokker-Planck equation with nonlinear friction and diffu-

sion coefficients :

$$\frac{\partial}{\partial t} P(T, t) = - \frac{\partial}{\partial T} [T_{\max} - T] k(T) P + \frac{r_v}{c_v} \frac{1}{V} \frac{\partial^2}{\partial T^2} [T_{\max} - T] k(T) P \quad (5.3)$$

$$T_0 \leq T \leq T_{\max}$$

where we use the notation of eqs.(2.3) to (2.5). One can show that T_0 and T_{\max} are, respectively, regular and exit boundaries [12]. Using reflecting and absorbing boundary conditions at T_0 and T_{\max} , one can then compute first passage times and related quantities. In particular, the mean first passage time M_1 to state T_2 , starting from some state T_1 , is :

$$\frac{1}{V} \frac{r_v}{2c_v} M_1(T_2 | T_1) = \int_{T_1}^{T_2} d\eta \ e^{-2\eta} \frac{v_{c_v}}{r_v} \int_{T_0}^{\eta} d\xi \frac{e^{2\xi} \frac{v_{c_v}}{r_v}}{(T_{\max} - \xi) k_0 e^{-E_0/\xi k_0}} \quad (5.4)$$

A close look at eq.(5.4) shows that at zeroth order in V^{-1} , M_1 reduces to the deterministic expression. On the other hand, the first-order correction in V^{-1} is positive for $T_2 < T_{\text{expl}}$ and negative for $T_2 > T_{\text{expl}}$, where the explosion temperature T_{expl} is defined in Fig.1. Thus, fluctuations have a "stabilizing" effect by slowing down the evolution prior to explosion.

We now come back to the full chemical-transport problem, eqs. (5.1) and (5.2). We are interested in the behavior of fluctuations close to, but before, the bifurcation point leading to multiple steady states (cf. Fig.2). This type of problem has been discussed extensively in the case of isothermal chemical reactions [1], [9] and most of this discussion can be transposed straightforwardly to the present case. One finds that the solution of eq.(5.1) is a propagating bivariate Gaussian density distribution. At the steady state near the bifurcation point the variances of the fluctuations computed with this distribution show the, by now familiar, critical divergence. For instance, the variance of the temperature fluctuations turns out to be :

$$\langle \delta T^2 \rangle = \frac{Q_{xx}^2}{V \ 18 \ f_e^2 \ k_B^2 \ \bar{x}_s \ 4 \ \lambda_1 \lambda_2 (\lambda_1 + \lambda_2)} \quad (5.5)$$

$$\cdot \left[-h_e^2 Q_{xx} + 2f_e h_e Q_{xe} - f_e^2 Q_{ee} \right] .$$

Here f_e, h_e are derivatives of the rate functions f and h (cf. eq. (5.1)) with respect to the internal energy e , and λ_1, λ_2 are the eigenvalues of the linearized stability operator. As one approaches the bifurcation point, one of the λ 's approaches zero, according to some power of the distance from this point. Thus $\langle \delta T^2 \rangle$ diverges. Similar conclusions hold for the other moments. Finally, at the bifurcation point itself the probability distribution becomes the exponential of a quartic function in x, e and the fluctuations cease to be extensive. Again, this is in accord with the be-

havior found in isothermal chemical systems [9] .

6. Discussion.

In this paper we outlined a mean-field theory of temperature and internal energy fluctuations in nonequilibrium systems. We have reproduced the familiar equilibrium and near equilibrium expressions [8] , [11] and, in addition, we have obtained a number of new results in the nonlinear range of irreversible processes.

Several extensions of this work can be envisaged. It would be essential to work out a theory of spatially inhomogeneous fluctuations going beyond the mean-field result. Of equal importance would be the extension of the results of Sec.5, especially eq. (5.5), to the region of multiple coexisting steady states. Indeed, in most problems involving exothermic reactions, like for instance combustion, the situation depicted in Fig.2 is much more typical than bifurcation. Such questions as what happens to fluctuations near the ignition or extinction points, or whether there is a Maxwell construction defining the true transition between extinction and ignition regimes, would find an answer within the framework of such an augmented theory. The model of Knudsen flow adopted throughout our work might also prove to be unnecessarily restrictive. In any case, the connection between eqs.(2.1) or (2.6) and the more familiar transfer laws like Newton's cooling law [13] should be elucidated.

On the experimental side, we believe that nonequilibrium effects on temperature fluctuations may prove to be more accessible to observation than composition fluctuations in isothermal systems. Indeed, the mechanism of exothermic reactions giving rise to nonequilibrium transitions is often simpler and better understood than the mechanism of reactions leading to chemical dissipative structures [13] . In addition, the variations of the different quantities involved are more pronounced. Finally, the fact that the system frequently operates at temperatures of the order of 1,000°K, should enhance the level of thermal noise.

References.

1. G. Nicolis and I. Prigogine, "Self-Organization in Nonequilibrium Systems" (Wiley, New York, (1977)).
2. "Order and Fluctuations in Equilibrium and Nonequilibrium Statistical Mechanics", G. Nicolis, G. Dewel and J.W. Turner eds. (Wiley, New York (1981)).
3. "Stochastic Nonlinear Systems", L. Arnold and R. Lefever eds. (Springer, Berlin (1980)).
4. See, for instance, G.R. Welch, B. Somogyi and S. Damjanovich, "The Role of Protein Fluctuations in Enzyme Action : A Review" preprint, Univ. of New Orleans.
5. N.V. Kondratiev and E.E. Nikitin, "Gas-Phase Reactions" (Springer, Berlin (1981)).
6. See, for instance, E.H. Kennard, "Kinetic Theory of Gases" (McGraw Hill, New York (1938)).
7. G.R. Gavallas, "Nonlinear Differential Equations of Chemically Reacting Systems" (Springer, Berlin (1968)).
8. L.D. Landau and E.M. Lifschitz, "Statistical Physics" (Pergamon Press, Oxford (1959)).

9. M. Malek Mansour, C. Vanden Broeck, G. Nicolis and J.W. Turner, *Annals of Physics* 131, 283 (1981).
10. I. Prigogine and G. Meyer, *Bull. Cl. Sci. Acad. Roy. Belg.* 41, 22 (1955).
11. L.D. Landau and E.M. Lifschitz, "Fluid Mechanics" (Pergamon Press, Oxford (1959)).
12. N.S. Goel and N. Richter-Dyn, "Stochastic Models in Biology", (Academic Press, New York, (1974)).
13. C.L. Creel and J. Ross, *J. Chem. Phys.* 65, 3779 (1976).

Fluctuations in Non-Equilibrium Phase Transitions: Critical Behavior

P. Hanusse

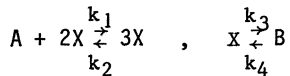
Centre de Recherche Paul Pascal (C.N.R.S.), Domaine Universitaire
F-33405 Talence Cédex, France

It is now well recognized that there exists a formal analogy between bifurcations in non-equilibrium dynamical systems and equilibrium phase transitions, hence the term non-equilibrium phase transitions now commonly used [1]. The equivalent of a first-order phase transition can be seen in model systems [2] as well as in experiments, for instance in chemical systems [3] when bistability is observed: two stable stationary states coexist for the same value of a bifurcation parameter. A second-order transition can be defined in the same situations when, by changing some control parameter or constraint, this bistability vanishes at a *critical point* as shown in an example later. Also a supercritical Hopf bifurcation can be considered as another example where the amplitude of the limit cycle is taken as an order parameter. This analogy is described only within the framework of a purely deterministic approach. Now, all that we know about equilibrium phase transitions tells us that fluctuations in the state of the system play a very important role, to such an extent that a phase transition can be viewed essentially as a fluctuation phenomenon. A similar feature is suggested by the evolution equations of a dynamical system near a bifurcation point where an eigenvalue of the linear stability matrix goes to zero. In other words, some relaxation time goes to infinity. However, whereas for equilibrium phase transitions the very definition of the system includes a microscopic level having particular properties resulting from equilibrium requirements from which we can in principle deduct some description of fluctuations, on the contrary for a dynamical system evolving near a bifurcation point, we have no such possibility. Usually these evolution equations result from a phenomenological description of a physical system that is not derived from first principles or, more specifically, from a microscopic or molecular level which is, in the end, the only source of stochasticity. Here we do not consider the deterministic stochasticity of strange attractors, but, for example, a chemical system near a bifurcation point. Clearly in this case the molecular level is indeed a source of fluctuations that will determine the behavior near a bifurcation point. But obviously mass-action kinetic equations for a chemical system are essentially phenomenological ones. Of course, one can argue that this kind of equations results from reasonable statistical views, assumptions and so forth. But how good is this near a bifurcation point? In fact we have no guaranty that the macroscopic equations that we would derive from microscopic level in some statistical limit for a non-equilibrium system would have the same properties near a bifurcation point as the phenomenological equations that we usually postulate. Similarly the behavior of fluctuations predicted by such a theory might well be different from that given by phenomenological approaches like stochastic differential equations obtained by adding a random force to the deterministic rate equation or like birth and death stochastic dynamics leading to a master equation. It is not clear yet that the result does not depend on the various approaches or assumptions used, like the expression of the random force in one case, or that of the transition rates in other case, not to speak about the approximations that we are forced to use to obtain explicit solutions. We think that this is still an open question and that the results obtained in the study of equilibrium phase transitions and the techniques used there cannot be applied straightforwardly to non-equilibrium situations. To some authors it is even doubtful that a *real* phase transition can occur in a non-equilibrium system

[4]. For this reason we think that being able to solve a model system as exactly and explicitly as possible is highly desirable. This is what we are aiming at by studying the critical behavior of the Schlögl model [2] using the birth and death formalism and a Monte-Carlo technique to calculate the spatial correlation function. So, leaving aside the question of the relevance of the approach used here, at least we should be able to know what such a description of fluctuations predicts without a priori postulating the existence of a critical phenomenon. In other words we would like to go beyond a study of the scaling properties or asymptotic behavior which does not in fact *solve* the model.

Obtaining a definite answer to the questions above, even for an apparently simple model is not so easy. The multivariate master equation that result in the approach that we have chosen cannot be solved exactly and no systematic scheme of approximations is available up to now. The same thing is true when using other possible approaches. This is why we have started Monte-Carlo calculations some time ago. Details on the simulation technique [5] and preliminary results on one dimension [6] can be found elsewhere.

We consider the following model system [2],



where A and B are held at fixed concentration and X is the free species that we allow to diffuse in space. We adopt the usual representation of space by a lattice of cells between which a linear diffusion process moves particles. Using a now standard change of variable [7] $k_1 = 3/A$, $k_2 = 1/A$, $k_3 = 3 + \delta$, $k_4 = 1$, $B = A(1 + \delta')$, $x = X/A$, defining δ and δ' as new bifurcation parameters, we obtain the following deterministic homogeneous equation

$$\frac{dx}{dt} = (x - 1)^3 + \delta x - \delta',$$

It admits a triple point at $\delta = \delta' = 0$ which corresponds to the *critical point* in the equivalent equilibrium phase transition picture. If we go along the line $\delta = \delta'$ the system has one stationary state at $x = 1$ for $\delta > 0$ and three of these states, at $x = 1$, $x = 1 \pm \sqrt{-\delta}$ for $\delta < 0$. Here again we should point out that this is a deterministic definition of the critical point. The critical point of the stochastic description may not be located at $\delta = \delta' = 0$. Other phenomenological definitions might be used as, for example, the triple point of $\lambda(X) - \mu(X)$ where λ and μ are the birth and death rates defined by

$$\lambda(X) = k_1 A X(X - 1) + k_4 B$$

$$\mu(X) = k_2 X(X - 1)(X - 2) + k_3 X$$

which are the ones that we use in our simulations. The rate of the diffusion process between two neighbouring cells is taken equal to $DX/2d$, where d is the dimensionality, and D a stochastic diffusion constant. For the birth and death approach to be valid we must consider a situation in which at cell level the rate of the diffusion process is somewhat larger or at least of the order of the rate of chemical reactions. This ensures that our description is local enough to satisfy the local equilibrium condition that requires that reactive collisions are dominated by elastic collisions. On the other hand our treatment should not be too local to preserve the Markovian character of the dynamics.

As mentioned above the resulting multivariate master equation for this reaction-diffusion model cannot be solved exactly. No need to say that an inverse system size expansion [8] or moments hierarchy truncation fails near the critical point. The best approximate treatment available so far is due to MALEK-MANSOUR and HOUARD [9] (MH thereafter). From the multivariate master equation they derive a nonlinear

reduced master equation for one cell involving the mean particle number $\langle X \rangle$ and the conditional mean $\langle X \rangle_c(X)$, i.e. the mean particle number in one cell knowing the number of particles X in the nearest-neighbor cell. Next they use the following ansatz

$$\langle X \rangle_c(X) = \langle X \rangle + g \delta X \quad ; \quad \delta X = X - \langle X \rangle$$

where g is the nearest-neighbor correlation coefficient defined by $g = \langle \delta X_r \delta X_{r+1} \rangle / \langle \delta X^2 \rangle$. It expresses a linear interpolation between two limiting cases, namely, $g = 0$ (there is no correlation between adjacent cells and a mean field value $\langle X \rangle_c = \langle X \rangle$ is valid) and $g = 1$ (there is complete correlation, then $\langle X \rangle_c = X$). The expression of the spatial correlation function can be obtained analytically and an iterative numerical procedure can be used to evaluate it self-consistently. Let us skip immediately to the main result. (i) It agrees fairly well with simulation estimates, (ii) it does not predict any critical behavior in one, two or three dimensions. However, it is clear that this approach is unfortunately not systematic and by no way exact. It is the purpose of simulations to show how good is the MH scheme quantitatively as well as qualitatively. We have performed extensive calculations in one and two dimensions. Detailed results will be found elsewhere [10]. We shall only give here a few typical results supporting the main conclusions.

The main quantity of interest is the static spatial correlation function $C(\ell) = \langle \delta X_r \delta X_{r+\ell} \rangle$ which contains the essential features of the stationary fluctuating behavior. The integral of this function over space is simply related to the variance of the total number of particles in the system, or global variance, by $I = \langle \delta X^2 \rangle / V$ where V is the volume of the system. If this integral converges, then the global variance is extensive, which indicates a *normal* behavior. If not, there is critical behavior. The system size that we can consider in simulations is of course always finite. Therefore we have performed simulations at fixed systems size as a function of δ and δ' , and at $\delta = \delta' = 0$ as a function of system size defined by n , the number of cells in the system. Table I gives a few results in one dimension. First we remark that far from the critical point the MH prediction and simulation results agree perfectly well (Table 1(a)). This was expected and may be considered as a test for the simulation procedure. The discrepancy is largest when the local variance is large, i.e. at the critical point or when the system is small (Table 1(a) and (c)). In that case the MH prediction is lower than the simulation result. This general. The MH approximation predicts always smaller fluctuations and

Table 1 Spatial correlation function as a function of space r in one dimension. $A = 20, D = 20$. (a) $\delta = \delta' = 1, n = 21$; (b) $\delta = \delta' = 0, n = 10$; (c) $\delta = \delta' = 0, n = 41$. Simulation (S), MALEK-MANSOUR-HOUARD prediction (MH), curve fitting of simulation results by MH function (F). 90% confidence interval of the order of 0.3.

	r	0	1	2	3	4	5	6	7
(a)	S	31.92	8.59	6.19	4.50	3.34	2.21	1.69	1.10
	MH	31.82	8.54	6.15	4.44	3.21	2.34	1.72	1.30
(b)	S	55.47	34.14	31.66	29.88	29.02	28.61		
	MH	51.22	29.35	26.96	25.31	24.33	24.00		
	F	55.63	33.90	31.58	29.96	29.01	28.69		
(c)	S	46.49	24.17	21.38	18.80	16.59	14.57	13.03	11.32
	MH	44.44	22.09	19.13	16.58	14.38	12.48	10.84	9.42

weaker correlation. An interesting result is shown in Table 1(b), line F. These values are obtained by fitting the simulation results with the MH function. It shows that the shape of the MH function is much better than the values that it predicts. This also is general and should be kept in mind if one wishes to improve the MH scheme. Nevertheless a finer analysis reveals that long-range correlation is systematically underestimated.

Table 2 Diagonal spatial correlation function as a function of space r in two dimensions, i.e. $C(\ell_1, \ell_2)$ with $\ell_1 = \ell_2 = r$. $A = 20$, $D = 20$, (a) $\delta = \delta' = 0$, $n = 10 \times 10$; (b) $\delta = \delta' = 0$, $n = 30^2 \times 30$.

	r	0	1	2	3	4	5	6	7
(a)	S	33.32	9.42	8.05	7.40	7.88	7.29		
	MH	32.62	8.58	7.24	6.65	6.39	6.32		
	F	33.31	9.38	8.06	7.47	7.21	7.14		
(b)	S	29.25	4.90	3.36	2.53	2.01	1.59	1.27	1.15
	MH	28.94	4.69	3.18	2.35	1.82	1.45	1.19	1.00

All these general observations are also valid in two-dimensional systems as it appears in Table 2. Quantitatively the results seem even better. This is related to a smaller value of the nearest-neighbor correlation. So, the statement that MH ansatz is better, the smaller g is, seems to be generally valid whatever is causing such a low value: the distance from the critical point, the system size in connection with periodic boundary conditions or the dimensionality. However there are indications that the behavior might be qualitatively different in one and two dimensional systems. In one dimension if one considers larger and larger systems, the global variance saturates at a larger value than predicted by MH, which means that although quantitatively slightly different, the qualitative behavior predicted by MH is correct. In two dimensions even for systems with $n = 1\ 600$ cells, saturation does not seem to be achieved. Clearly it is difficult to conclude definitely in this kind of computations. Simulations on bigger systems are under progress. These are heavy calculations and because the correlation time tends to increase with system size - again an indication of critical behavior - one has to wait long enough between sampling times to avoid having biased long-range correlation values. So it is not yet certain that we shall be able to conclude by direct simulation. Much more interesting is the possibility given by such calculations to check directly the various assumptions or approximations that one would like to use in analytical treatments. For instance we have measured the conditional mean $\langle X \rangle_c$ which is the essential ingredient of MH scheme. We can clearly see where and why it fails. We hope that it will be soon possible to use this information to build a better approximation scheme, hopefully a more systematic one, and then to answer our initial question: does such a model using such a description exhibits a critical behavior?

This work has been done with A. Blanché.

References

- ¹G. Nicolis and I. Prigogine, Self organisation in non-equilibrium systems, Wiley, N.Y. (1977), H. Haken, Synergetics, An Introduction, Springer, Berlin (1977)
- ²F. Schlögl, Z. Phys., 253, 147 (1972)
- ³A. Pacault, P. Hanusse, P. de Kepper, C. Vidal and J. Boissonade, Acc. Chem. Res. 9, 438 (1976)
- ⁴D.L. Stein, J. Chem. Phys., 72, 2869 (1980)

- ⁵P. Hanusse and A. Blanché, *J. Chem. Phys.*, 74, 6148 (1981)
- ⁶P. Hanusse and A. Blanché, *Lectures notes in Physics* vol. 132, pp 337-344, Springer, Berlin (1980). P. Hanusse, *Proceedings of the meeting "Méthodes numériques pour l'étude des phénomènes critiques" Carry le Rouet, 1980*, to appear in Springer series.
- ⁷G. Nicolis, R. Lefever, *Phys. Letters* 64A, 19-21 (1977)
- ⁸N.J. Van Kampen, *Adv. Chem. Phys.* vol. 34, 247 (1976)
- ⁹M. Malek-Mansour and J. Houard, *Phys. Letters* 70A, 366 (1979)
- ¹⁰P. Hanusse and A. Blanché, to be published, and A. Blanché, *Thesis, University of Bordeaux* (1981).

Critical Exponents of a Pure Noise Induced Transition, Nonlinear Noise and Its Effect on an Electrohydrodynamic Transition in Nematics

Rène Lefever

Chimie Physique II, Université Libre de Bruxelles C.P.231
B-1050 Bruxelles, Belgium

and

Werner Horsthemke

Physics Department and Institute for Fusion Studies, University of Texas
Austin, TX 78712, USA

1. Introduction

The surrounding of natural systems is rarely constant. Often indeed, biological populations, climatic systems, metabolic systems and other natural systems experience external driving forces whose precise temporal evolution is unpredictable because it involves a significant amount of stochasticity. The characteristic property of this external noise is that generally it is independent of the internal fluctuations which systems with many degrees of freedom exhibit spontaneously. The latter fluctuations scale with the inverse of the system size and become negligible once the limit of a large system has been taken. This is not the case with external noise: even in this limit, it still shows up in the form of fluctuating parameters.

It is only recently that the full importance of these parametric fluctuations in physical, chemical and biological systems has been appreciated (for recent surveys see [1-3]). In general the influence of these fluctuations does not average out even in the limit of an extremely rapid and incoherent noise like white noise. In consequence of this fact it has come somewhat as a shock that external noise shifts deterministic transition points and furthermore induces new transitions which are missing in the usual bifurcation diagrams. This fascinating class of behaviors has become a subject of systematic investigations. Experimental studies in the laboratory, where external noise can be generated at will in a controlled fashion, have been undertaken for a rich variety of photochemical [4,5], electrical [6], and hydrodynamical systems [7,8]. The results reported in this paper concern the theoretical side of these phenomena. We first discuss the fundamental unity which exists between some pure noise induced transitions and the usual equilibrium and nonequilibrium phase transitions taking place under constant environmental conditions. Second, we consider the problems raised by the modelling of nonlinear fluctuating parameters. We show how these situations can be handled using the wide band perturbation method which we presented elsewhere [9]. We apply these results to the analysis of the influence of external white noise on an electrohydrodynamical instability in nematic liquid crystals. This problem was recently studied experimentally by Kai et al. [7].

2. Modelling of nonequilibrium systems subjected to external noise

The modelling of the influence of external noise involves two steps. First, one establishes a phenomenological equation describing the system without noise. Second, some appropriate parameter of this equation is considered to undergo fluctuations with prescribed statistics. In simplest cases, the deterministic equation is a first order differential equation in time

$$\dot{x} = f(x, \lambda) . \tag{1}$$

Two possibilities then arise. If the fluctuating parameter λ_t enters linearly in the deterministic equation, i.e. (1) is of the form

$$\dot{x} = h(x) + \lambda_t g(x), \quad (2)$$

and if there is no systematic evolution of the environment, i.e.

$$\lambda_t = \lambda + \zeta_t \quad \text{with } \lambda = \text{constant and } E\{\zeta_t\} = 0, \quad (3)$$

then the equation describing the evolution of the system is

$$\dot{x} = h(x) + \lambda g(x) + \zeta_t g(x). \quad (4)$$

The second possibility is that the parameter undergoing fluctuations enters nonlinearly in the equation. For instance, one has

$$\dot{x} = h(x) + \mu(\lambda)g(x), \quad (5)$$

where $\mu(\lambda)$ is some power or some transcendental function of λ . If λ_t is again given by (3), the evolution equation for x now reads

$$\dot{x} = h(x) + \mu(\lambda + \zeta_t)g(x). \quad (6)$$

To proceed further with either (4) or (6), the structure of the noise ζ_t must be specified. This introduces two additional parameters into the description, namely the variance of the external noise σ^2 which measures the intensity of the noise and its correlation time τ_{cor} which measures the rapidity with which ζ_t fluctuates. In laboratory experiments, the choice of the noise is arbitrary and the number of possibilities is a priori infinite. This means that some noise induced phenomena may be specific of particularities in the structure of the noise chosen. There exist however transitions which seem fairly general, in the sense that they are generally recovered within a certain limit even for very different noises. In the following we refer to transitions of this type and for simplicity we deal with the broad class of situations where the fluctuations of the external parameter are given by an Ornstein-Uhlenbeck noise (O-U noise) (reasons for this choice are given in [1]). Accordingly, ζ_t obeys the stochastic differential equation (SDE)

$$d\zeta_t = -\gamma\zeta_t dt + \sigma dW_t \quad \text{with } \tau_{\text{cor}} = \gamma^{-1}. \quad (7)$$

W_t is the Brownian motion process. The O-U noise has an exponentially decreasing correlation function, a form which is widely found in applications, and a power spectrum $S(\nu)$ which is a Lorentzian. In the limit $\gamma \rightarrow \infty$, $\sigma \rightarrow \infty$ such that $\sigma^2/\gamma^2 = \bar{\sigma}^2 = \text{constant}$, one has $S(\nu) \rightarrow \bar{\sigma}^2/2\pi$ for all values of the frequency ν , i.e. the white noise limit. This is the appropriate limit for the study of the frequently encountered situations where $\tau_{\text{cor}} \ll \tau_{\text{macro}}$, τ_{macro} being a measure of the time scale on which (1) evolves. The advantage is then that when λ_t appears linearly in (1), the latter equation is in a fluctuating environment replaced by the SDE

$$dx_t = [h(x_t) + \lambda g(x_t)]dt + \sigma g(x_t)dW_t, \quad (8)$$

x_t , as is well known, is a diffusion process and its transition probability density $p(x,t)$ is the solution of a Fokker-Planck equation (FPE).

In the following we now introduce the phenomenon of pure noise induced transition and focus on some of its essential properties within the framework of the white noise limit and for a linear fluctuating external parameter; later on we will consider the case that the fluctuating parameter is nonlinear.

3. Similarity of noise induced transitions with classical and nonequilibrium phase transitions

The first point which we want to make can easily be established in the white noise limit: among the various kinds of noise induced transitions encountered on varying the parameters describing some external noise, there may appear transitions which are not found in a constant environment but which are nevertheless closely connected with the classical equilibrium or nonequilibrium phase transitions.

To see this we will mainly be interested in the stationary behavior of systems subjected to external noise and focus on the stationary solution of the FPE. A noise induced transition occurs for that value of the noise strength where the stationary probability density $p_s(x)$ undergoes a qualitative change. We will however not retain the complete information contained in $p_s(x)$, but will consider only its extrema x_m which are sufficient indicators for such a change. There are three main reasons for this procedure: (i) the number and location of the extrema are the most distinguishing feature of $p_s(x)$ and contain essential information on the stationary behavior of the system; (ii) the extrema are so to speak the continuation of the deterministic steady states. Indeed for $\sigma^2 \rightarrow 0$, $x_m \rightarrow x_s$, the zeroes of the rhs of (1); (iii) $p_s(x)$ is a measure for that part of time that an arbitrary sample path spends in an infinitesimal vicinity of x . This motivates the identification of the extrema, which are preferentially seen in an experiment, with the macroscopic steady states: the maxima, where the process spends relatively much time, as the stable states and the minima which the process leaves quickly as unstable ones. We do not imply however that the maxima dominate the probability density. Since external noise is of order V , the peaks are broadened and the system switches more or less rapidly from one maxima to the other. Nevertheless, the peaks correspond to privileged regions in phase space as recalled above and can thus be likened to macroscopic phases. This interpretation is furthermore supported by the behavior of systems for additive noise.

We now consider the following system

$$\dot{x} = \frac{1}{2} - x + \lambda x(1 - x) \quad (9)$$

which finds realisations in population genetics and chemistry [2,10]. λ is the parameter which fluctuates. Obviously x is restricted to the interval $[0,1]$ for values of $\lambda \in (-\infty, +\infty)$. Furthermore x_s is a single valued function of λ over the entire range of λ ; it is an absolute attractor, i.e. an asymptotically globally stable state. Since λ is a linear parameter in (9), the effect of its fluctuations can immediately be obtained in the white noise limit from the stationary solution of the FPE. For $\lambda = 0$, the extrema of $p_s(x)$ are [10]:

$$x_{m\pm} = 1/2 \text{ and } x_{m\pm} = \frac{1}{2} [1 \pm (1 - \frac{4}{\sigma^2})^{1/2}] \quad (10)$$

Accordingly, for $\sigma^2 < 4$ $p_s(x)$ has a unique extremum which is a maximum corresponding to the deterministic steady state. At $\sigma^2 = 4$, x_{m1} is a triple root; for $\sigma^2 > 4$, x_{m1} is a minimum. The peak corresponding to a stable steady state under deterministic conditions has split into two peaks having maxima at $x_{m\pm}$. This shows that as to the extrema of $p_s(x)$, in the (λ, σ^2) -half plane we have a critical point at $(0,4)$. This critical point necessarily occurs for a finite value of σ . Clearly, this noise induced transition has no deterministic equivalent for $\sigma^2 \rightarrow 0$. For colored noise, σ^2 undergoes a shift due to the influence of the noise correlations; however whatever the value of the latter it remains finite. [9,10-12].

To establish the close ties of the noise induced transitions just described and the usual phase transitions, we now consider their critical exponents. Since the system is spatially homogeneous, we expect mean field results, and we will see that indeed the pure noise induced transition displayed by (9) is governed by classical critical exponents. In this sense one really is justified to speak of a phase transition.

As we explained, the order parameter for noise induced transitions is the position of the extrema of $p_c(x)$. To be precise, we chose $m = |x_m - x_s|$ and compare the behavior of model (9) near its noise induced critical point with the classical paramagnetic to ferromagnetic transition. The role of the temperature T is played here by the intensity σ^2 of the noise; the analog of the applied external field h is the parameter describing the average state of the environment, i.e. λ . To determine the critical exponent β (order parameter m as a function of σ^2 for λ vanishingly small), we have to find the behavior of m near σ_C^2 . One obtains

$$m = \frac{1}{2} \left(1 - \frac{4}{\sigma^2}\right)^{1/2} \approx (\sigma^2 - \sigma_C^2)^{1/2} \text{ for } \sigma^2 \downarrow \sigma_C^2. \text{ Hence } \beta = \frac{1}{2}. \quad (11)$$

To determine the critical exponent δ (order parameter m as a function of λ at $\sigma^2 = \sigma_C^2$), we write the equation for the extrema in term of m and specify that $\sigma^2 = \sigma_C^2$. This yields

$$m^3 + \frac{\lambda}{4} m^2 - \frac{\lambda}{16} = 0 \text{ from which we deduce that } m \approx (\lambda)^{1/3} \text{ showing } \quad (12)$$

that the critical exponent δ also takes on the classical value 3. To determine the exponent γ , we have to calculate the behavior of the susceptibility

$$\chi = \left(\frac{\partial m}{\partial \lambda}\right) \text{ as a function of } \sigma^2 \text{ for } \lambda = 0. \text{ This yields that } \chi \approx (\sigma^2 - \sigma_C^2)^{-1}.$$

Hence $\gamma = 1$, and all the critical exponents of the pure noise induced transition are given by the classical values. This shows that equilibrium phase transitions, nonequilibrium phase transitions and noise induced phase transitions are indeed close kin. There is a deep unity in the fundamental phenomenon, namely to be a phase transition, and except for the qualifiers no further distinction is warranted.

4. Nonlinear noise induced transition in nematic liquid crystals

The case of systems described by an evolution equation of the form (6) in which the fluctuating parameter appears nonlinearly is of general interest and furthermore occurs frequently in applications: typical examples are the biphotonic photochemical systems studied by Mischeu et al. [5,14] under the influence of a fluctuating light intensity and the nematic systems in which Kai et al. [7] studied the onset of Williams domain and of turbulence under the influence of a fluctuating electrical field. Recently San Miguel and Sancho provided a treatment for such situations using their functional method to derive an approximate FPE for the probability density when the noise approaches the white noise limit [15]. Here we will consider the same problem but proceed in a completely different manner. We report indeed the way in which a systematic and practical approach to this problem can be based on the wide band perturbation expansion [9,13].

To situate the problem concretely, let us first have a look on the experiment of Kai et al. Nematic molecules are little rods which when distributed in a layer tend to align all parallel to a privileged direction. When this layer is stressed by an electric field, at a certain intensity of the field, a roll structure appears: the so-called Williams domains. Increasing further the stress leads to a turbulent or

chaotic regime. When the applied voltage fluctuates, the average external field which must be imposed to trigger either one of these transitions increases with the intensity of the noise. Below, we will only consider the first transition to the Williams domains. The electrohydrodynamic description of transition phenomena in nematics is rather complicated. Kai et al. argue that the following equation for the director angle with respect to the privileged direction gives a good description of the situation:

$$\dot{\theta} = \frac{1}{2}(V^2 - V_c^2)\theta - \frac{1}{3}V^2\theta^3. \quad (13)$$

V is the applied field; V_c is the critical voltage at which the first transition occurs under deterministic conditions. Obviously the fluctuating parameter V appears in a nonlinear manner. The evolution equation is of the form (6). It is meaningless to pass to the white noise idealisation by simply letting $\lambda_t = \lambda + \sigma\xi_t$ where ξ_t is white noise. Plugging white noise in (6) does not make sense. It is impossible to give a well-defined meaning to nonlinear operations on the white noise ξ_t . Independently, however, of this mathematical impossibility, it remains of course true that the environment in the Kai's experiment varies on a much faster time scale than the system. In other words, ζ_t is a process with a short correlation time. It is thus natural to look for a possibility to define an appropriate white noise limit to the SDE. The obvious short cut is to write $\mu(\lambda) + \zeta_t$ instead of $\mu(\lambda + \zeta_t)$ and then pass to the white noise idealisation by setting $\zeta_t = \sigma\xi_t$. This approach which ends up with the Stratonovic SDE

$$dx_t = [h(x_t) + \mu(\lambda)g(x_t)]dt + \sigma g(x_t)dW_t, \quad (14)$$

has been employed by Schenzle and Brand [16]. The fact is that it yields results which are seemingly in qualitative agreement with the experiment. This result however is far from solving the problem for the following reasons. The procedure is not legitimate. If the potential fluctuations are, for instance, Gaussian distributed, then $\mu(\lambda_t)$ is a nongaussian process. To replace $\mu(\lambda_t)$ by $\mu(\lambda) + \sigma\xi_t$ is an arbitrary procedure which completely neglects the physics specific to the problem at hand. There is no solid connection between the results obtained in this way and the physical reality they purport to describe. In fact such results may even be misleading was also pointed out by San Miguel and Sancho [15].

Following up with our above discussion, we will again consider that ζ_t is an 0-U process and explore the behavior of a system subjected to a rapid external noise using the band width perturbation expansion. Defining the external noise process η_t by

$$\eta_t = \mu(\lambda + \zeta_t) - m(\lambda, \sigma^2) \text{ with } m(\lambda, \sigma^2) = E\{\mu(\lambda + \zeta_t)\}, \quad (15)$$

(6) can be written as

$$dx_t = [h(x_t) + m(\lambda, \sigma^2)g(x_t)]dt + g(x_t)\eta_t dt. \quad (16)$$

Speeding up the 0-U process, i.e. putting $\eta_t^\epsilon = \eta_t/\epsilon^2 = \mu(\lambda + \zeta_t/\epsilon^2) - m(\lambda, \sigma^2)$, to take account of the fact that we are particularly interested in the white noise limit where the band width ϵ goes to zero, (16) and (7) read

$$dx_t^\epsilon = [h(x_t^\epsilon) + m(\lambda, \sigma^2)g(x_t^\epsilon)]dt + \frac{1}{\epsilon}g(x_t^\epsilon)\eta_t^\epsilon dt \quad (17)$$

$$d\zeta_t = -\epsilon^{-2}\zeta_t dt + \epsilon^{-1}\sigma dW_t. \quad (18)$$

The diffusion pair process (x_t^ϵ, ζ_t) is associated to a FPE which can be

handled in exactly the same manner as in the linear case [9] but where now (in the notation of that paper):

$$F_1 = \partial_z z + \frac{\sigma^2}{2} \partial_{zz}; \quad F_2 = -[\mu(\lambda+z) - m(\lambda, \sigma^2)] \partial_x g(x); \quad F_3 = -\partial_x f(x) - \partial_t.$$

This permits one to evaluate the probability density of x in a straightforward systematic way. To the lowest order in the case where $\mu(\mu) = \lambda^2$, it is found after some lengthy but simple calculations that the critical point of (13) is shifted by the noise to the value

$$V_c^{2'} = V_c^2 / (1 - \sigma^2) - \frac{\sigma^2}{4} (2 - \sigma^2) / (1 - \sigma^2) \quad \text{or} \quad V_c^{2'} = V_c^2 + (V_c^2 - \frac{1}{2}) \sigma^2 \quad \text{for}$$

$\sigma^2 \rightarrow 0$. Accordingly, it increases with σ provided that $V_c^2 < 1/2$, which is the case experimentally. Because of the divergence at $\sigma^2 = 1$, the description becomes bad when the strength of the noise increases. In that case the results seem to suggest that the deterministic starting point (13) needs to be improved.

Finally let us remark that a theoretical treatment of the second transition towards a turbulent regime is at present intractable. It is, however, particularly interesting to remark that at variance with the results reported for other hydrodynamical systems [17,18], the effect of the noise observed experimentally here is an inhibition of the transition towards the chaotic regime.

References

1. W. Horsthemke, "Noise Induced Transitions", in Stochastic Non-linear Systems, ed. by L. Arnold, R. Lefever (Springer, Berlin, Heidelberg, New York 1981)
2. R. Lefever, "Noise Induced Transitions in Biological Systems", in Stochastic Nonlinear Systems, ed. by L. Arnold, R. Lefever (Springer, Berlin, Heidelberg, New York 1981)
3. M. San Miguel and J. M. Sancho, in Stochastic Nonlinear Systems in Physics, Chemistry and Biology, Synergetic Series, Springer Verlag (1981).
4. P. de Kepper, W. Horsthemke, C. R. Acad. Sci. Paris C287, 251 (1978)
5. J. C. Micheau, W. Horsthemke, R. Lefever, this volume.
6. S. Kabashima, S. Kogure, T. Kawakubo, T. Okada, J. Appl. Phys. 50, 6296 (1979).
7. S. Kai, T. Kai, M. Takata, K. Hirakawa, J. Phys. Soc. Jpn 47, 1379 (1979).
8. J. P. Gollub, J. F. Steinman, Phys. Rev. Lett. 45, 551 (1980).
9. W. Horsthemke, R. Lefever, Z. Physik B40, 241 (1980).
10. L. Arnold, W. Horsthemke, R. Lefever, Z. Physik B29, 367 (1978).
11. J. M. Sancho, M. San Miguel, Z. Physik B36, 357 (1980).
12. K. Kitahara, W. Horsthemke, R. Lefever, Y. Inaba, Prog. Theor. Phys. 64, 1233 (1980).
13. G. Blankenship, G. C. Papanicolaou, SIAM J. Appl. Math. 34, 437 (1978).
14. J. C. Micheau, S. Boué, E. Vanderdonckt, J. Chem. Soc. Farad. Trans (to appear).
15. M. San Miguel, J. M. Sancho, Z. Physik B (to appear).
16. H. Brand, A. Schenzle, J. Phys. Soc. Jpn. 48, 1382 (1980).
17. J. Crutchfield, M. Nauenberg, J. Rudnick, Phys. Rev. Lett. 46, 933 (1981).
18. A. Zippelius, M. Lücke, J. Stat. Phys. 24, 345 (1981).

Part IV

Critical Phenomena

Critical Slowing down of Chemical Reactions Near Thermodynamic Critical Points

Itamar Procaccia

Department of Chemical Physics
Weizmann Institute of Science
Rehovot 76100, Israel

1. Introduction

In this contribution I review our recent theoretical work concerning dynamical critical phenomena in chemically reactive fluid mixtures [1-3]. Of prime interest to us is the possible existence of a universal slowing down of chemical reactions near thermodynamic critical points; however, the influence of the occurrence of a slowed down chemical reaction on the critical behavior of transport processes (diffusion, viscosity etc.) is also interesting. In particular, the critical behavior of the complex sound attenuation coefficient seems to offer a good probe for some of our novel predictions.

Regarding the slowing down of chemical reactions near critical points, the following rules of thumb have been proposed [2]: in an n-component reactive fluid mixture, when all the components participate in the chemical reaction, the reaction rate is expected to vanish like $[(T-T_C)/T_C]^{\gamma}$, the critical exponent $\gamma \approx 1.25$, T is the temperature and T_C its critical value; when one component is non-reactive, and n-1 components react, the rate depends on T like $[(T-T_C)/T_C]^{\alpha}$, where α is another critical exponent, $\alpha \approx 0.12$; when two or more components do not react, we expect the rate to be insensitive to the approach to the critical point. The above predictions hold irrespective of the nature of the chemical constituents. In section II I summarize the theory that leads to these predictions. The (scant) experiments that exist so far are in accord with these "rules" [1].

Concerning the effects on the critical behavior of transport processes, we have studied in detail only reactive binary mixtures. Here we found that the (weak) divergence of η (the shear viscosity), which occurs in the non-reactive case, is removed, and the viscosity is finite. The diffusion constant D has a novel temperature and wave vector dependence. The complex bound attenuation coefficient, $\hat{\alpha}_q(\omega)$, has a divergent contribution, whose critical exponents are determined by the chemical rather than the diffusional pathway for composition relaxation. The mode coupling theory used in this context is summarized in sections III and IV. Section V is a short discussion.

2. "Conventional" Theory and Mode-Coupling Considerations

Consider an n-component reactive fluid and a linear theory of chemical reaction rates; for small deviations from chemical equilibrium the rate of reaction is proportional to the affinity [4]:

$$\text{rate} = LA \quad (1)$$

The affinity

$$A \equiv - \sum_{i=1}^n \nu_i \mu_i$$

where ν_i are the stoichiometric coefficients and μ_i the chemical potentials of the

various species. The coefficient L contains microscopic information about rate constants, etc. Since the affinity vanishes at equilibrium, we expand A at constant temperature and pressure:

$$\text{rate} = L \left(\frac{\partial A}{\partial \zeta} \right)_{P,T} (\zeta - \zeta_{\text{eq}}) \quad (2)$$

where ζ is the "progress variable", conveniently chosen through the relation $\nu_i d\zeta = dN_i$, where N_i is the number of molecules of species i .

The crux of the argument is the fact that the derivative $(\partial A / \partial \zeta)_{P,T}$ vanishes at the critical point. To see this, write the Gibbs free energy as:

$$dG = Vdp - SdT + \sum_{i=1}^n \mu_i dN_i \quad (3)$$

In a closed system in which all components participate in the reaction, $dN_i = \nu_i d\zeta$ and thus:

$$dG = Vdp - SdT - Ad\zeta \quad (4)$$

The condition for a stable equilibrium is:

$$\left(\frac{\partial G}{\partial \zeta} \right)_{P,T} = -A = 0 \quad (5)$$

and

$$\left(\frac{\partial^2 G}{\partial \zeta^2} \right)_{P,T} = - \left(\frac{\partial A}{\partial \zeta} \right)_{P,T} > 0 \quad (6)$$

At the critical point, which lies at the boundary of stability [2,4],

$$\left(\frac{\partial A}{\partial \zeta} \right)_{P,T} = \left(\frac{\partial^2 A}{\partial \zeta^2} \right)_{P,T} = 0 \quad (7)$$

Since equilibrium requires $A=0$ (c.f. Eq. (5)) ζ_{eq} is a function of P,T . As a consequence, such a system has an isolated critical point, and the behavior near this critical point is isomorphous to that of a pure fluid near its liquid-gas critical point [2,5]. Consequently, the derivative $(\partial A / \partial \zeta)_{P,T}$ vanishes like

$$\left(\frac{T-T_c}{T_c} \right)^\gamma, \quad \gamma \sim 1.25$$

This stability argument leads to the prediction of the slowing down of the chemical reaction.

In the case in which $n-1$ components react, the argument is the same except that now the rate is proportional to $(\partial A / \partial \zeta)_{P,T, N_0}$ where N_0 is the number of non-reactive particles. Being a thermodynamic derivative computed with one extensive quantity held fixed, this quantity has a weaker singularity and is expected [5] to vanish like $[(T-T_c)/T_c]^\alpha$. If more than one component is non-reactive, the rate is proportional to $(\partial A / \partial \zeta)_{P,T, N_1, N_2, \dots}$ where all the numbers of non-reactive components are held fixed. Such a thermodynamic derivative is non-singular at T_c [5].

To complete the argument we have to worry about the critical behavior of the quantity L in Eq. (2). Clearly, the slowing down might disappear if L diverges near T_c . We have studied this question by using mode coupling theory. It can be shown that the quantity L is related to a correlation function of the form

$$L = \lim_{k \rightarrow 0} \int_0^\infty dt \langle \Gamma_k(t) \Gamma_{-k} \rangle \quad (8)$$

where Γ_k is a microscopically defined quantity whose exact form is immaterial for the argument. The important thing is its symmetry property: Γ_k is odd under time

reversal but even under parity. Consequently, it cannot couple, in the sense of correlation functions, to any of the slow (conserved) variables or to any multi-linear combination of them [6]. As a result L has no mode coupling renormalization (to all orders). The only possible renormalization arises from dissipative non-linearities, and these change the dynamical critical exponents only to the order of the critical exponent η , where $\eta \sim 0.02$ [1,7]. Thus we conclude that the critical slowing down of the chemical reaction is determined by the behavior of $(\partial A / \partial \zeta)$, leading to the above-mentioned rules of thumb.

3. Transport Coefficients: Shear Viscosity and Diffusion Constant

The existence of a chemical reaction, and its slowing down, has interesting implications on the critical behavior of the shear viscosity, η , and the diffusion constants, D. We have studied this problem in detail for reactive binary mixtures. In this context one can think about a dissociation-recombination reaction or an isomerization in a binary mixture near, say, the liquid-gas critical point. In non-reactive binary mixtures the shear viscosity and the quantity α , (defined by

$$D \equiv \alpha \frac{\partial \mu}{\partial c}$$

where

$$\mu = \frac{\mu_1}{m_1} - \frac{\mu_2}{2} \quad ,$$

m_1 and m_2 the molecular masses of the species) both diverge at T_c [8]. It has been shown that $\alpha \eta \sim \xi$ where ξ is the correlation length. Most of the divergence is attributed to α , whereas η has a weak divergence, calculated to be logarithmic within the mode-coupling theory. In the reactive case we have shown that D and η are renormalized by the mode coupling non-linearities as follows:

$$D(\vec{q}) = D^0(\vec{q}) + \frac{k_B T}{(2\pi)^2 \rho} \int_0^\infty dk k^2 \int_0^\pi d\theta \sin^3 \theta \frac{\chi_{\vec{q}-\vec{k}}}{\chi_{\vec{k}}} \frac{1}{k^2 \eta(\vec{k}) + (\vec{k}-\vec{q})^2 D(\vec{k}-\vec{q}) + L \chi_{\vec{k}-\vec{q}}^{-1}} \quad (9)$$

$$\eta(\vec{q}) = \eta^0(\vec{q}) + \frac{k_B T}{(4\pi)^2 q^2 \rho_0} \int_0^\infty dk k^4 \int_0^\pi d\theta \sin^3 \theta \frac{1}{\chi_{\vec{k}} \chi_{\vec{q}-\vec{k}}} \left(\frac{1}{\chi_{\vec{k}}} - \frac{1}{\chi_{\vec{k}-\vec{q}}} \right)^2 \frac{1}{k^2 D(\vec{k}) + (\vec{q}-\vec{k})^2 D(\vec{q}-\vec{k}) + L \chi_{\vec{k}}^{-1} + L \chi_{\vec{q}-\vec{k}}^{-1}} \quad (10)$$

In these equations $D^0(\vec{q})$ and $\eta^0(\vec{q})$ are the "bare" values of the respective quantities, $\chi_{\vec{k}}$ is the correlation function $\langle \zeta_{\vec{k}} \zeta_{-\vec{k}} \rangle$ and ρ the density. Notice the contribution of the chemical reaction, appearing as $L \chi_{\vec{k}}^{-1}$ in the denominators of the integrands in Eqs. (9), (10).

The details of the calculation of the quantities $D(\vec{q})$ and $\eta(\vec{q})$ are given in ref. 2. In calculating these two quantities we have used the Ornstein-Zernike form for the susceptibility $\chi_{\vec{k}} \sim [k^2 + \xi^{-2}]^{-1}$. This approximation is acceptable for the evaluation of D and η , but it should be changed in favor of a scaling form in the calculation of $\hat{\alpha}_{\vec{q}}(\omega)$, as is shown below. The final results for D and η are as follows:

a) Denoting $D(\vec{q}) - D^0(\vec{q})$ by ΔD we get

$$\Delta D = \frac{k_B T \kappa}{6\pi \eta x^2 \rho} \left[K(x) - \beta \frac{x^3}{y} K(y) \right] \quad (11)$$

where $\kappa \equiv \xi^{-1}$, $x \equiv k \xi$, $\beta \equiv \frac{v}{1+v}$, $v \equiv L/\eta$ and $y = [v/(1+v+x)]^{1/2}$. The function K(x) is:

$$K(x) = \frac{3}{4} [(1+x^2) + (x^3 - x^{-1}) \tan^{-1} x] \quad (12)$$

One can see that if η diverges, then $v \rightarrow 0$ and respectively $\beta \rightarrow 0$ and then one gets the

usual result for ΔD in a system without a chemical reaction [8]. However, we find:

b) The quantity η remains finite near the critical point. We found that the most dangerous contribution to $\Delta\eta$ is an integral of the form

$$\Delta\eta \sim \int_{\kappa}^{\kappa_c} \frac{dk k^2}{k^3 + Lk^2} . \quad (13)$$

The lower limit of the integral vanishes at T_c . When there is no reaction (i.e. $L=0$) this integral diverges logarithmically and $\Delta\eta \sim \ln \xi$. However, when $L \neq 0$, the integral is protected and does not diverge. As was mentioned before, L has no mode coupling corrections. Thus η is finite at T_c . The implication of this result is that Eq. (11) can be interpreted now as a closed equation for ΔD rather than for the product $\Delta D \eta$ as is the case in non-reactive binary mixtures [8]. Consequently we can state that α diverges like ξ .

The inclusion of dissipative non-linearities via a renormalization group calculation might modify these conclusions slightly (to the order of the critical index $\eta \sim 0.02$) but is not expected to change the nature of the results [7].

4. Sound Attenuation and Dispersion

Sound attenuation is an attractive experimental probe of dynamical critical behavior since it offers a direct measurement of relaxation time scales with a minimal perturbation of the equilibrium state. In the present context of a reactive binary mixture, both the chemical and diffusional pathways for composition relaxation contribute to sound attenuation. It is important to analyze the competition between these two pathways to find which of them governs the critical divergencies in the complex sound attenuation coefficients, $\hat{\alpha}_q(\omega)$. This quantity is related to the measurable sound attenuation coefficient $\alpha(\omega)$ and the change in sound velocity $\Delta C(\omega) = C(\omega) - C(0)$ through the relations

$$\alpha(\omega) = \text{Re } \hat{\alpha}(\omega)$$

$$\frac{\Delta C(\omega)}{C} = \frac{C}{2\omega} \text{Im } \hat{\alpha}(\omega) .$$

The mode-coupling expression for $\hat{\alpha}_q(\omega)$ was derived by Kawasaki [8], and in the present case it assumes the form [3]

$$\hat{\alpha}_q(\omega) = \frac{\omega^2}{2C^3} \frac{k_B T^3}{\rho^3 C_{v,\zeta}} \left(\frac{\partial P}{\partial T} \right)_{v,\zeta}^2 \frac{1}{(2\pi)^3} \int d\vec{k} \left(\frac{\partial \ln \chi_{\vec{k}}}{\partial T} \right)_{\rho,\zeta}^2 \frac{1}{2k^2 D(\vec{k}) + 2L \chi_{\vec{k}}^{-1} - i\omega} . \quad (14)$$

Here $C_{v,\zeta}$ is the specific heat at constant volume and concentration and P the pressure. Since this expression involves a temperature derivative of $\chi_{\vec{k}}$ it is important to use a scaling form for $\chi_{\vec{k}}$, rather than the Ornstein-Zernike expression:

$$\chi_{\vec{k}} = k^{-2+\eta} f(k\xi) . \quad (15)$$

We have found that close to the critical point, $\hat{\alpha}_q(\omega)$ is governed by the chemical process rather than the diffusional one and assumes the form

$$\hat{\alpha}_q(\omega) = \frac{\omega^2}{2C^3} \frac{k_B T}{\rho^3 C_{v,\zeta}^2} \left(\frac{\partial P}{\partial T} \right)_{v,\zeta}^2 \left(\frac{1}{2\pi} \right)^2 \left[\frac{\tau}{\xi^3} \left(\frac{\partial \ln \xi}{\partial T} \right)^2 \right] I\left(\frac{\omega\tau}{2}\right) \quad (16)$$

where

$$I(X) = \int_0^\infty y^4 dy \left(\frac{\partial \ln f(y)}{\partial y} \right)^2 \frac{1}{y^2 - f^{-1}(y) - iX} \quad (17)$$

and where $\tau^{-1} = L\xi^{-2+\eta}$ is the chemical time scale.

The reason why chemistry wins over diffusion can be summed up as follows: A sound wave will create local non-equilibrium conditions in a liquid which will relax back to equilibrium by the fastest available process. In the non-reactive case the only available pathway is diffusion and as diffusion processes show critical slowing down with a time scale $\tau_D \sim (Dk^2)^{-1} \sim \xi^3 \sim (T-T_C)^{-3\nu}$, the sound attenuation will show critical behavior given by this time scale $\hat{\alpha}(\omega)/\omega^2 = \tau_D B(\tau) I(\omega \tau_D)$. On the other hand, if relaxation can also take place via a chemical reaction, this situation may change. We can distinguish three cases: (1) the chemical reaction is on a slower time scale than the diffusion, (2) the chemical reaction is on a faster time scale but has no critical behavior, (3) the chemical reaction is on a faster time scale but also shows critical slowing down. Clearly for case (1) diffusion will still be the fastest process and will win over chemistry, giving the same exponents as for the non-reactive case (which is after all only the extreme limit of case (1)). For case (2) chemistry will win but as the chemistry shows no critical behavior neither will the sound attenuation. Finally there is case (3) of sound attenuation in critically slowed down chemically reactive mixtures which relax on a time scale $\tau_C \sim \xi^{2-\gamma} \sim (T-T_C)^{-\gamma}$. As $\gamma < 3\nu$ the chemistry is faster and will win over diffusion, and we thus expect the sound attenuation to obey $\hat{\alpha}(\omega)/\omega^2 = \tau_C B(\tau) I(\omega \tau_C)$.

One caveat must be made to the above analysis. The diffusion constant $D(k)$ is wave vector dependent, and very high frequency sound waves will relax by high wave vector diffusion processes on a time scale $\tau_D^{-1} \sim D(k)k^2 \sim k^3$. This will finally occur on a faster time scale than the chemistry and cross-over will occur back to diffusion controlled sound attenuation. Some possible experiments that utilize these effects were suggested in ref. 3.

5. Discussion

The phenomenon of slowing down of chemical reactions near critical points has been observed experimentally by Krichevskii and coworkers. They looked at dissociation-recombination reactions in pure binary mixtures [9] ($\text{Cl}_2 \rightleftharpoons 2\text{Cl}$) and in ternary mixtures [10] ($\text{CO}_2/\text{I}_2 \rightleftharpoons 2\text{I}$) near the liquid-gas critical points. These examples indeed should show slowing down according to our rules of thumb. Other experiments dealt either with complicated reaction schemes or with more than one non-reactive component [1] and thus, as expected, did not show any universal behavior. It should be stressed that the phenomenon of slowing down in chemistry is independent of the slowing down in diffusion. It is the thermodynamic driving force for reaction ($\partial A/\partial \xi$), which vanishes at T_C . The diffusion of individual particles is insensitive to the approach to T_C and slowing down of diffusion cannot account for slowing microscopic collision rates [1]. In addition, it is important to realize that individual rate constants (like the ones for the forward or backward reaction) are not singular at T_C . It is only the observed rate, which is the net difference between forward and backward reactions, which slows down near T_C .

Additional experiments are needed to test our theory.

Acknowledgements

The collaboration of Professor M. Gitterman and Dr. H.G.E. Hentschel is gratefully acknowledged. This work has been supported in part by the Israel Academy of Sciences and Humanities - Basic Research Foundation.

References

1. I. Procaccia and M. Gitterman, Phys.Rev.Lett. **46**, 1163 (1981).
2. I. Procaccia and M. Gitterman, Phys.Rev.A, in press.
3. H.G.E. Hentschel and I. Procaccia, J.Chem.Phys., submitted.
4. I. Prigogine and R. Defay, Chemical Thermodynamics (Longmans Green, London 1954).
5. R.B. Griffiths and J.C. Wheeler, Phys.Rev.A**2**, 1047 (1970).
6. T. Keys and I. Oppenheim, Phys.Rev.A**7**, 1389 (1973).

7. B.I. Halperin, P.C. Hohenberg and S.K. Ma, *Phys.Rev.*B10, 139 (1974).
8. K. Kawasaki, in Phase Transitions and Critical Phenomena eds. C. Domb and M.S. Green, Vol. 5A (Academic, London 1976).
9. I.R. Krichevskii, Yu.V. Tsekhanskaya and Z.A. Polyakova, *Russian J.Phys.Chem.* 40, 715 (1966).
10. I.R. Krichevskii and Yu.V. Tsekhanskaya, *Inzh.-Fiz.Zhur.* 5, no. 12, 104 (1962) (in Russian).

Metastability and Nucleation in Chemical Systems with Multiple Steady States

J. Boissonade

Centre de Recherche Paul Pascal (C.N.R.S.)
Domaine Universitaire - 33405 Talence Cédex (France)

1. Introduction

In 1971 Prigogine and Nicolis [1] suggested that the transitions between non-equilibrium chemical steady states are induced from local fluctuations by a nucleation process and exhibit metastability phenomena. In this frame, the chemical bistability appears as a close analog to the Van der Waals isotherm problem of the first-order equilibrium transitions [2]. The two deterministic steady states can only coexist, when fluctuations are included, for a single set of the constraints (*coexistence point*). Elsewhere, the *metastable state*, say E_m , converts into the *stable state*, say E_s , as soon as a spontaneous fluctuation into state E_s is large enough to spread to the whole system. The existence of a critical size for this fluctuation is related to the competition between the bulk nonlinear reactive processes and the diffusion processes which break and dilute the fluctuation, but are localized only to the surface between E_m and E_s . So the last dominate only for small fluctuations. When this critical size is large, near the coexistence point, or for fast diffusion, the life time τ of E_m is long and E_m appears as stable. When this size is small, far away from the coexistence point on the metastable branch, or for slow diffusion, τ is small, the transition occurs at once and E_m appears to be unstable.

These ideas are corroborated by analytical [3, 4, 5] and numerical [6, 7] solutions of various master equations in the frame of the stochastic theory, but in regard to numerous technical difficulties, no reliable real experiment has been achieved. A substitute can be partially found in a numerical experiment of the *molecular dynamics* (M.D.) type : the dynamics of the system are then deduced in a fully deterministic way from the laws of mechanics and elementary reactive processes, both described at a microscopic level. Several works, devoted to such techniques in the field of nonequilibrium systems (not focused on the nucleation problem), have been published [8-11], but they use global nonequilibrium conditions or additional local cooperative rules. Recently, we have developed a powerful MD method in order to deal with the reaction process and the nonequilibrium conditions commonly used in the theoretical models [12, 13]. The technique is fully described elsewhere [14]. As we limit ourselves to the results obtained in the nucleation field, we shall only summarize the essential features.

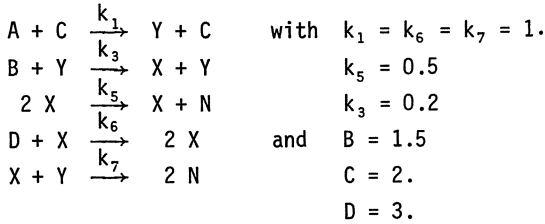
- The system, in mechanical equilibrium, is a two-dimensional assembly of 4 500 hard disks, interacting through a hard-core potential and labeled according to the considered species in a square box with periodic boundary conditions.

- The reactions are all bimolecular (first and second order kinetics) and occur during the elastic collisions (null global energy balance). The kinetic constants are adjusted by means of symmetric activation energy.

- The concentration of the constrained species are kept constant and homogeneous in the whole system, in accordance with the classical theoretical description. The diffusion processes are, of course, automatically included in the microscopic dynamics.

2. The numerical experiments

We shall study the following model : [15]



A, B, C, D are the constrained species (constant and homogeneous concentrations), X, Y the intermediate ones and N a neutral species not involved in the kinetics.

With these values the system exhibits two stable steady states, E_1 (X low, Y high) and E_2 (X high, Y low) for $1.61 < A < 2.51$.

By dividing the system into 100 boxes (10×10), the local concentrations of the intermediate species X and Y are followed and their maps are drawn as functions of time.

The stability picture predicted by the theory is shown on Fig.1a, but in our simulation, as well as in a real experiment, we must take into account the ratio of the life time of the metastable states to the experimental times. Far from the coexistence point A_0 , it is generally so small that the transition occurs almost at once and the system appears as unstable, but near A_0 it can be so long that the transition never occurs during the experiment and the systems appears to be effectively stable. Observable finite life time (of the order of the experimental times) will be restricted to a narrow range of the constraint values around "thick" transition points, A'_1 and A'_2 . The expected picture is given on Fig.1b where the shadowed

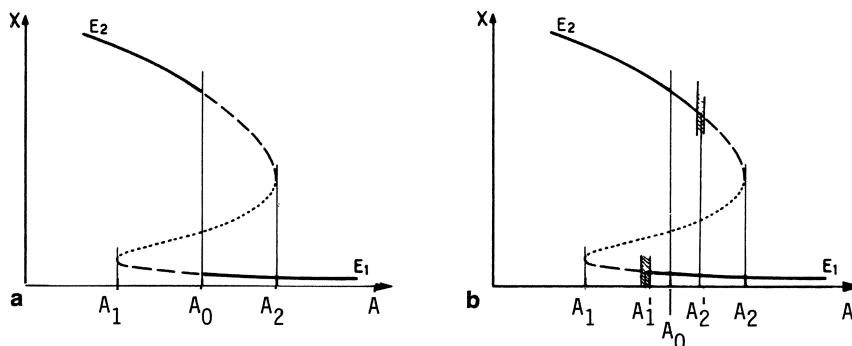


Fig.1.a,b. (—) stable; (---) metastable; (.....) unstable

regions are for the observable finite life times. The hysteresis range is reduced in comparison of the deterministic predictions. The effective stability of our system, initialized into state E_1 or E_2 , was tested for a discrete set of the concentration of A, covering the whole deterministic bistability range, and for two values of the radius R of the particles, corresponding to two different ratios of the reactive processes to the diffusive process. The limits of stability A'_1 and A'_2 were determined in the two cases.

3. Results

In Fig.2 are represented the results of the stability studies for the two diffusion levels. The hysteresis range is reduced in accordance with the theory and some of the deterministic stable steady states are unstable.

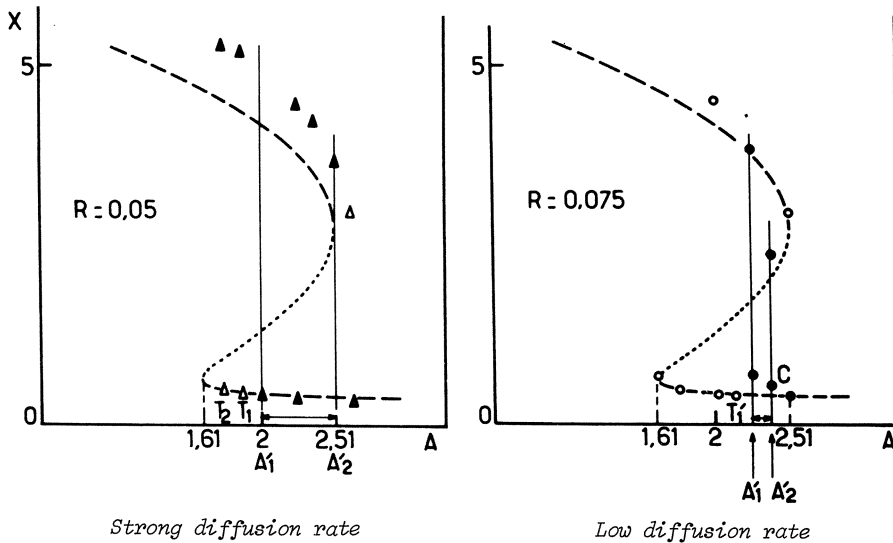


Fig.2 Computed stability plot
 ----- deterministic stable states
 deterministic unstable state
 ● ▲ stable state
 ○ △ unstable states

Finite life times are expected for the state E_1 in the vicinity of A'_1 . Consider, for example, X as a function of t for the transition T_1 (Fig.3): one can see that the system stays for a long time (the typical duration of our experiments is 900 time units except if a transition occurs) before the transition begins. Also, a life time of 350 time units was observed for T'_1 in the low diffusion case.

The temporal evolution of the concentrations maps of X and Y is shown in Fig.4a for the transition T_1 . They are represented only by their low level (symbol ●: E_1 for X, E_2 for Y) or their high level (symbol *: E_2 for X, E_1 for Y). A nucleus of the stable state E_2 forms in the metastable state E_2 and spreads gradually to the whole system. A still more striking evidence for a nucleation mechanism is shown on Fig.4b for the transition T_2 .

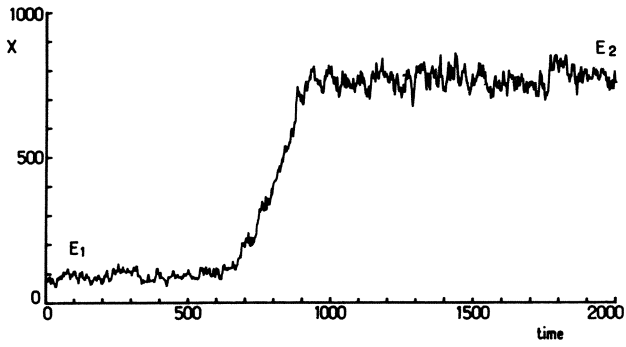


Fig.3

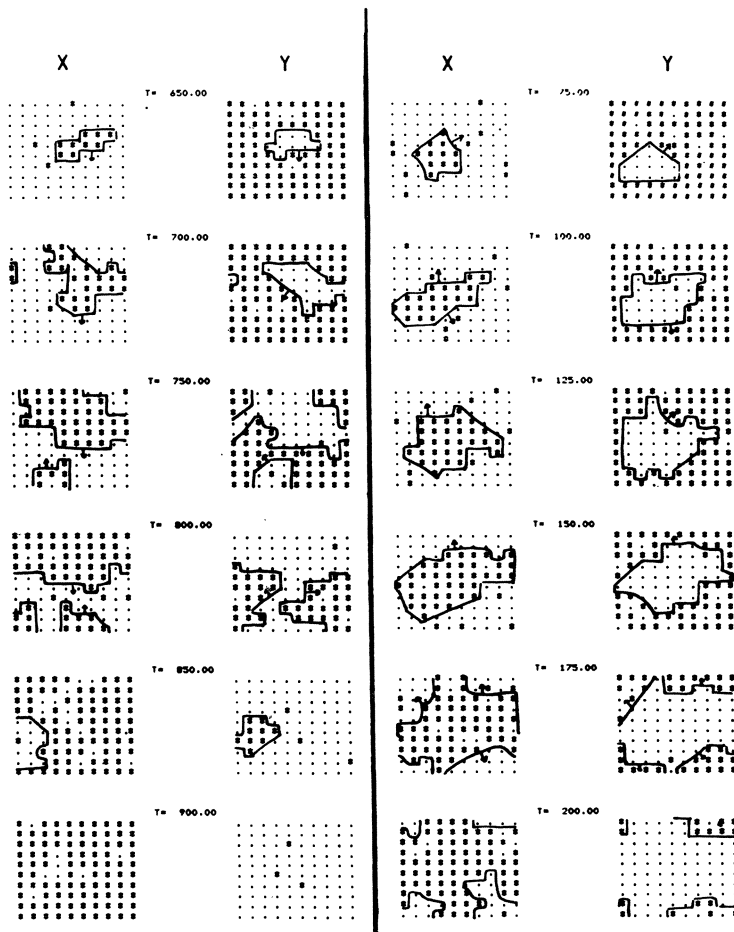


Fig.4a
Transition T_1

Fig.4b
Transition T'_1

Coming back to Fig.2, we observe that the hysteresis (or bistability range) is $\Delta A = 0.125$ for low diffusion rates and $\Delta A = 0.50$ for large diffusion rates. This last result is in accordance with the theory, since, as mentioned in the introduction, increasing diffusion increases the critical size of the nuclei.

4. Conclusions

Our molecular dynamics simulations support the nucleation theory of transitions in non-equilibrium chemical systems. They give evidence for :

- metastable states
- formation and growth of nuclei during the transition
- stabilization by diffusion.

More details about the computations will be given in a forthcoming paper [16].

5. References

1. I. Prigogine and G. Nicolis : Proc. 3rd Int. Conf. "From Theoretical Physics to Biology" ed. by M. Marois (Karger, Basel 1973) p.89
2. E.A. Guggenheim : Thermodynamics, North Holland (1965)
3. A. Nitzan, P. Ortoleva and J. Ross : Faraday Symp. Chem. Soc., 9, 241 (1975)
4. I. Prigogine, R. Lefever, J.S. Turner and J.W. Turner : Phys. Lett. 51A, 317 (1975)
5. C.Y. Mou : J. Chem. Phys. 68, 1385 (1978)
6. P. Hanusse: "Stochastic Simulation of Chemical Systems Out of Equilibrium", in Synergetics, Far from Equilibrium, ed. by A. Pacault, C. Vidal (Springer, Berlin, Heidelberg, New York 1979)
7. P. Hanusse and Blanché : This conference
8. J. Portnow : Phys. Lett. 51A, 370 (1975)
9. P. Ortoleva and S. Yip : J. Chem. Phys. 65, 2045 (1976)
10. J.S. Turner : J. Phys. Chem. 81, 2379 (1977)
11. J. Boissonade and W. Horsthemke : Phys. Lett. 68A, 283 (1978)
12. J. Boissonade : Phys. Lett. A285 (1979)
13. J. Boissonade : Thesis (1980)
14. J. Boissonade : " A Molecular Dynamics Technique to Study Fluctuations in Non-Equilibrium Chemical Systems", in Modelling of Chemical Reaction Systems, ed. by K.H. Ebert, P. Deuflhard, W. Jäger, Springer Series in Chemical Physics, Vol.18 (Springer, Berlin, Heidelberg, New York 1981)
15. C. Vidal, C.R. Acad. Sc. Paris, C 274, 1713 (1972)
16. J. Boissonade, Submitted to Physica A

Part V

Coupling of Oscillators

terferential filter selects the monochromatic light at 460 nm which irradiates the reactor (this wavelength corresponds to the maximum absorption of iodine which the reaction produces in high quantity). A diaphragm allows us to adjust the quantity of light. By means of a set of lens, the beam is focused at two points : at the center of the reactor and on a shutter which is driven by an electronic clock : the opening and closing times (i.e. illumination and extinction) obtained range from 1/10 sec to 1000 sec. (the period P_{ch} of the chemical oscillation is always of the order of a minute).

Two values are simultaneously recorded :

- The chemical potential E of the reaction mixture, the evolution of which is exactly parallel to that of the chemical reaction.

- The flux L of a derived beam from the main beam (in all our experiments, we have verified that L is always proportional to the flux \mathcal{L} that effectively irradiates the reactor).

Square pulses of light are applied either isolated or in a periodic fashion.

The periodic pulses are conveniently described in terms of size and duration by two parameters : (Fig.2)

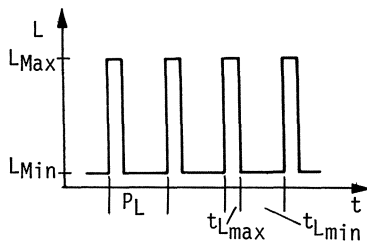


Fig.2 The square light pulses

- the photoperiod P_L = sum of the durations of illumination and extinction.

$$P_L = t_{LMax} + t_{LMin}$$

- the magnitude ΔL of each perturbation.

$$\Delta L = L_{Max} - L_{Min}$$

Notice that the interaction between the two oscillators is univocal. So, we are not dealing with coupled oscillators but only with a *chemical oscillation forced* by the periodic illumination.

We present the experimental results on the effect of light perturbations on two types of states of the chemical system :

- 1 : oscillating states
- 2 : non-oscillating states

1. Effects of light on oscillating states :

Two types of oscillations of the B.R. reaction have been studied : quasi-harmonic and relaxation oscillations.

A) Effects of a single perturbation

Let the period of the oscillation be τ and the phase be ϕ . The effect of a single perturbation $|8|$ can be described as follows (Fig.3) :

Considerer two identical stable oscillators which are originally in phase. If a perturbation is applied to one of them, its period returns to τ after some time, but it is no longer in phase with the unperturbed oscillator : the *phase-shift* $\Delta\phi$ can be measured as in Fig.3.

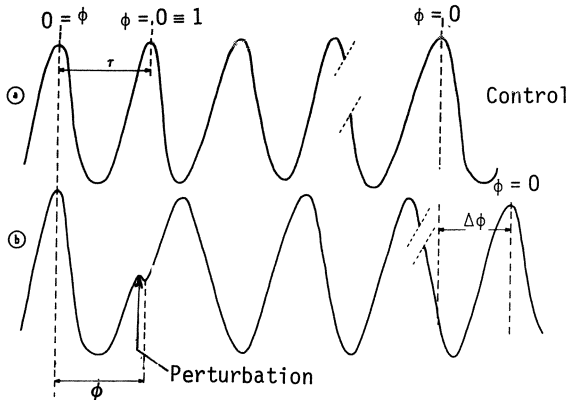


Fig.3 Determination of the phase-shift $\Delta\phi$

- The value of $\Delta\phi$ depends on the phase ϕ of application of the perturbation :
 $\Delta\phi = f(\phi)$

f is called the response curve.

These curves have different aspects, depending on the type of the perturbed oscillation :

- The phase-shift measured for the quasi-harmonic oscillation (Fig.4) progressively increases and decreases as ϕ goes along the oscillation.

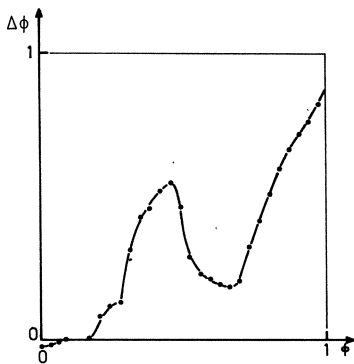


Fig.4 Response curve for the quasi-harmonic oscillation

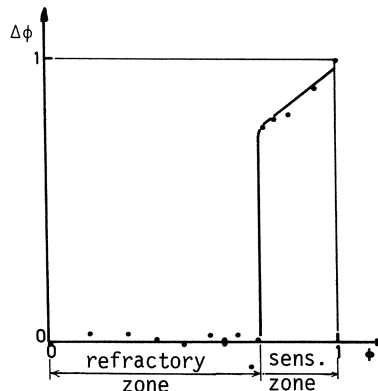


Fig.5 Response curve for the relaxation oscillation

- The response curve for relaxation oscillation looks different (Fig.5) : it appears as a refractory zone where $\Delta\phi$ is always zero : whatever the phase ϕ in this zone where one applies the perturbation, it has no effect. At the border of this zone, $\Delta\phi$ sharply increases, then continues to increase progressively. This is the sensitive zone. This sudden jump of $\Delta\phi$ is related to an underlying excitability property.

B) Effects of periodic perturbations

Periodic light pulses also have different effects on the two types of oscillations :

a) On quasi-harmonic oscillations

Periodic light pulses have no effect on these oscillations, except in very special conditions :

then, phenomena analogous to *beating* can be observed sometimes.



Fig.6 Effect of periodic light pulses on quasi-harmonic oscillation : *beating*

b) On relaxation oscillations

Periodic light pulses always synchronize these oscillations. Two modes of synchronization have been observed .

- Mode A defined by

$$P_{ch} = n P_L , \quad n \text{ integer.}$$

The chemical period is always an integer multiple of the photoperiod. When P_L is growing, n takes the successive integer values $n = \dots 5, 4, 3, 2, 1$.

- Mode B defined by

$$P_{ch} = n P_L \quad \text{and} \quad \bar{P}_{ch} = \frac{Y}{X} P_L , \quad n, x, y, \text{ integer.}$$

In this case, depending on the P_L values, P_{ch} can be either an integer multiple or a fractional multiple of P_L .

1) Figure 7 illustrates the mode A for $n = 2$ and $n = 1$ (in the corresponding experiment, $\Delta L = 8$) .

In the simplest case, we have $n = 1$. This is the fundamental forced oscillation. One chemical oscillation is achieved exactly during one photoperiod.

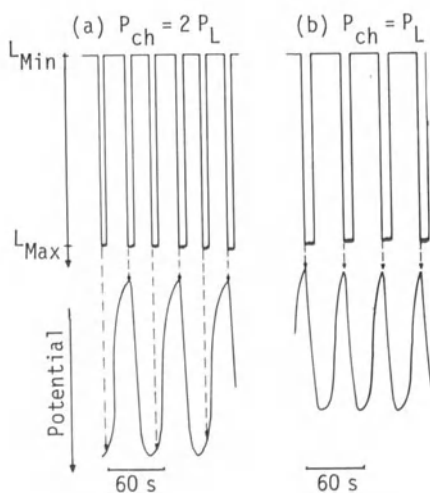


Fig.7 Synchronization Mode A

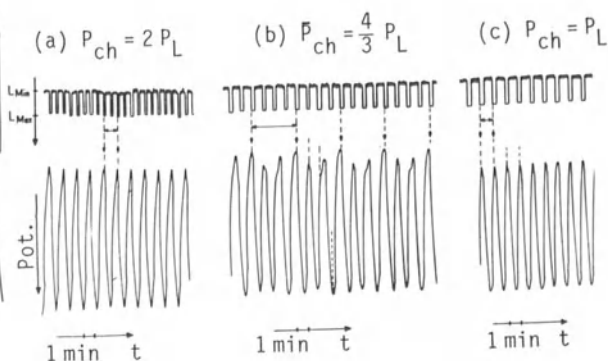


Fig.8 Synchronization Mode B

Two events occur simultaneously : sudden jump of L from L_{Min} to L_{Max} and reversal of the sense of evolution of the chemical potential. This usually results in a decrease in amplitude and period of the oscillation. The successive perturbations are applied at the same phase of the successive oscillations. This phase, of course, belongs to the sensitive zone.

When $n = 2$ (this is the first sub-harmonic forced oscillation), then every other perturbation occurs in the sensitive zone of the oscillation : it is effective. The second one occurs in the refractory zone : it is uneffective.

2) Figure 8 illustrates the mode B (same experimental conditions as in Fig.7, except $\Delta L = 1$).

On the left side, one has $n = 1$, and on the right one, one has $n = 2$.

In between, one observes repetitive patterns composed of a number of oscillations x during y photoperiods (in the Fig.8b, $x = 3$, $y = 4$). The x oscillations have different amplitudes and periods because the y successive perturbations are applied at different phases of the x oscillations. Then, one defines a mean-chemical period \bar{P}_{Ch} :

$$\bar{P}_{Ch} = \frac{Y}{X} P_L \cdot$$

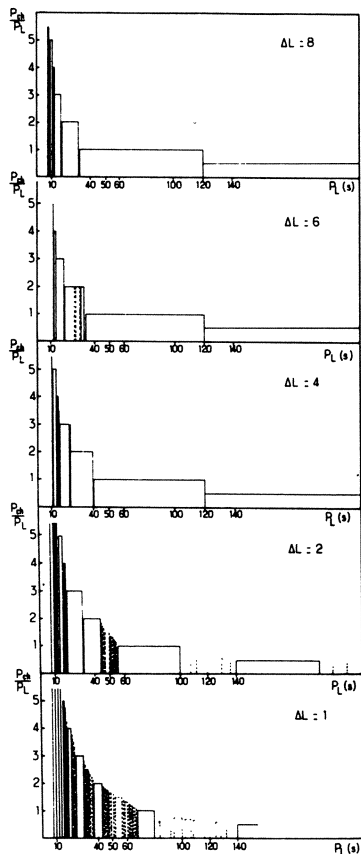


Fig.9 Diagrams P_{Ch}/P_L vs P_L obtained for five different values of ΔL .

3) In Fig.9 the ratio P_{ch}/P_L (i.e. n or Y/x) is given as function of P_L . These kind of diagram presents the domain of existence of the various sub-harmonics: We report here five experiments for five different values of ΔL :

- When the perturbations magnitude is large ($\Delta L = 8$ or 6), $\frac{P_{ch}}{P_L}$ take only integer values.

- When the perturbations magnitude is small ($\Delta L = 2$ or 1), $\frac{P_{ch}}{P_L}$ can take integer or fractional values. The smaller ΔL , the more numerous the fractional values are (see Fig.9 for $\Delta L = 1$).

2. Effects of light on non-oscillating states

A) On an excitable stationary state

- When an excitable stationary state receives a *single perturbation* (Fig.10) an excitability peak appears, provided the perturbation magnitude is large enough (example in Fig.10 for L jumping from $L = 4$ to $L = 0$) : instead of returning directly back to the stationary state, the system first undergoes a huge deviation. This excitability peak looks exactly like a single relaxation oscillation.

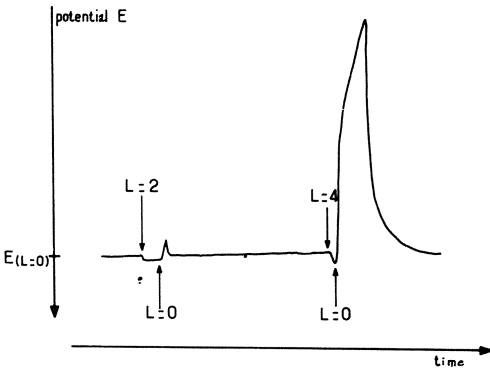


Fig.10 Effect of a single perturbation on an excitable stationary state

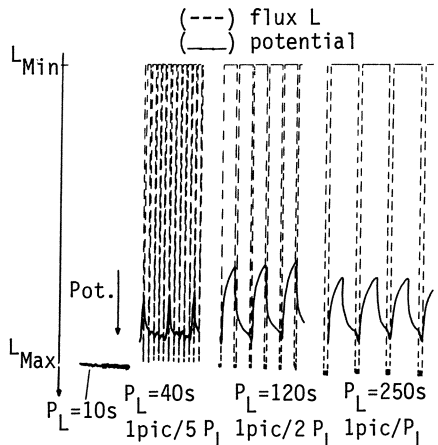


Fig.11 Effect of periodic light pulses on an excitable stationary state

- Periodic light pulses (provided P_L is long enough with respect to the response time of the system) induce a series of excitability peaks. Of course, these peaks are synchronized with the light pulses which generate them. So, we can see in Fig.11 :

- no response for $P_L = 10$ sec ;
- 1 peak / $5 P_L$ for $P_L = 40$ sec ;
- 1 peak / $2 P_L$ for $P_L = 120$ sec ;
- 1 peak / P_L for $P_L = 250$ sec.

Although not shown here, modes A and B have been observed also in this case.

B) On a bistable system

a) In continuous illumination

Under continuous illumination, a bistability can appear in the B.R. reaction : as in Fig.12, two different potential levels (corresponding to states I and II) are possible, depending on the light flux L . Variations of L induce transi-

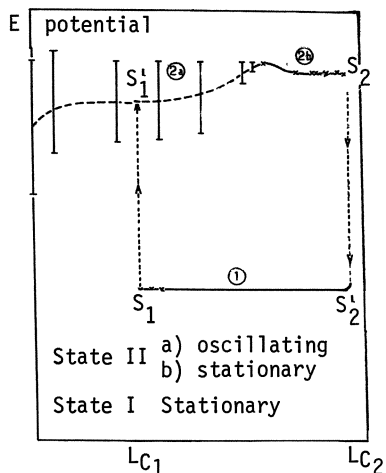


Fig.12 Bistability appeared under continuous illumination

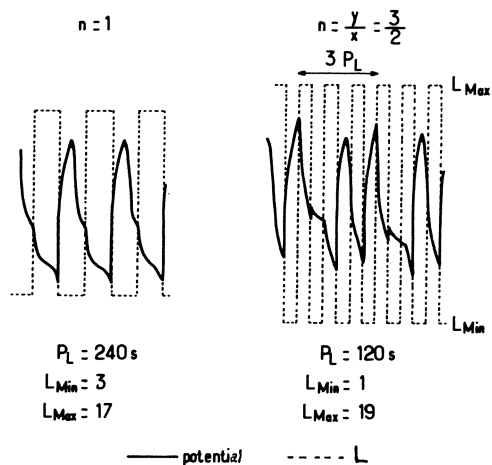


Fig.13 Synchronization of induced oscillations by periodic light pulses

tions with hysteresis between these two states. The transitions take place for two critical values L_{C_1} and L_{C_2} ; ΔL_C is defined as $\Delta L_C = L_{C_2} - L_{C_1}$.

b) Periodic light pulses

When such a system receives periodic light pulses, it is easy to understand that (provided the perturbation magnitude is $\Delta L \geq \Delta L_C$), each change in illumination level ($L_{Max} \neq L_{Min}$) can induce a transition from one state to the other ($I \neq II$). Then, the system runs around the hysteresis cycle. These are induced relaxation oscillations (this requires that the time interval between two successive illumination jumps is compatible with the transition times).

This has been observed (Fig.13) for large enough ΔL and long P_L . Of course, induced oscillations synchronize with periodic light perturbations. Both modes A and B exist also in this case.

Conclusion

The aptitude for synchronization appears as an exclusive property of relaxation oscillators which are characterized by excitability.

1. Vanden Driesche T., "Circadian rhythms and Molecular Biology" - Biosystems 6; 188, 1975
2. Brulfert J., Guerrier D., Queiroz O., Planta 125, 33, 1975
3. Briggs T.S., Rauscher W.C., J. Chem. Educ. 50, 7, 1973
4. Pacault A., De Kepper P., Hanusse P. Rossi A., C.R. Acad. Sci. Paris, C 281 215, 1975
5. De Kepper P., C.R. Acad. Sci. C 283, 25, 1976
6. De Kepper P. Thesis Bordeaux 1978
7. Dulos E., Thesis Bordeaux 1981
8. Winfree A., in "Biological and Biochemical oscillators" Ed. Chance, Pye, Gosh, Hess, N.Y. Acad. Press, p. 451, 1973

Electrically Coupled Belousov-Zhabotinsky Oscillators: A Potential Chaos Generator

Michael F. Crowley and Richard J. Field

Department of Chemistry, University of Montana
Missoula, MT 59812, USA

1. Introduction

A most important reason for the investigation of oscillating chemical reactions is their ability to demonstrate a wide variety of remarkable dynamic behaviors in relatively easily controlled experimental systems where the governing dynamic laws are sometimes reasonably well understood. The Belousov-Zhabotinsky (BZ) reaction^{1,2} (the metal-ion catalyzed oxidation and bromination of certain organic substrates by bromate ion in a strongly acidic aqueous medium), when run in a continuous-flow, stirred tank reactor (CSTR), is a prime example of such a chemical oscillator. It exhibits such phenomena as: both simple and complex waveform oscillations³, multiple steady states⁴, hysteresis phenomena⁵, excitability⁶ and quasi-periodic, apparently chaotic oscillations^{3,7}. A simple model of the BZ chemical kinetics, the Oregonator⁸, reproduces, at least qualitatively, all of these phenomena except the last, aperiodic or chaotic oscillations. However, experimental observations of aperiodic oscillations in the BZ reaction have been reported by several authors^{3,7}. It has not been entirely clear whether such aperiodic behavior is an intrinsic feature of the dynamic laws of the BZ reaction or whether it results from random environmental perturbations to the experimental system. The later experiments of HUDSON et al.³ seem to have been the best controlled to eliminate environmental perturbations. The concentrations of reactants in the feedstreams to the CSTR were kept constant in their experiments as the flowrate (which controls the residence time of species in the reactor) was the critical parameter varied. Aperiodic, apparently chaotic, oscillations appeared in a rather small range of residence times during which the system passed across a bifurcation between complex waveform limit cycles of quite noticeably different forms. The chaotic behavior⁹ was apparently a mixture of these complex waveform oscillations. SHOWALTER et al.⁹ and later GANAPATHISUBRAMANIAN AND NOYES¹⁰ attempted to reproduce the experimentally observed chaotic behavior using an extended version¹⁰ of the Oregonator model. They were unsuccessful. The transition between the two complex waveform oscillations observed by HUDSON et al.³ did indeed appear in their calculations, but it was very sharp with no apparent region of mixing. Thus it appears that the experimentally observed chaos resulted from either random environmental perturbations to the experimental system or from complexities of the BZ kinetics not modeled by the extended Oregonator. We believe the latter to be the case. In this regard, it is noteworthy that TURNER¹¹ has found chaotic oscillations using a model that, though overall somewhat simpler than the one used in [9] and [10], did, unlike [9] and [10], consider the step modeling Process C of the FKN mechanism¹ to be reversible. This suggests that the experimentally observed chaos may result from complexities in Process C. However, the details of this very complicated chemistry are not likely to ever be well enough understood to decide whether or not this is true or to carry out mathematical analysis relating the BZ dynamics to the appearance of chaos. Thus there is a need to develop a chemical system which may exhibit chaos under easily characterized and understood circumstances.

2. Electrically Coupled Belousov-Zhabotinsky Oscillators

ROSSLER¹² has shown that a chaos-generating machine may be created by coupling a limit cycle oscillator to a switching subsystem. The same author¹³ as well as KURAMOTO AND YAIHATA¹⁴ have shown that chaos can also occur in distributed systems of coupled oscillators. Thus we have undertaken an investigation of electrically coupled BZ oscillators. An important, but by no means the only, motivation for this work is a search for chaos. It is suggested that such a system will reflect mainly the gross limit cycle behavior of the BZ reaction and perhaps be less sensitive to the details of the BZ kinetics than a simple BZ-CSTR system.

Previous experiments have been carried out on coupled BZ oscillators¹⁵. However, in these experiments the coupling was effected by means of mass transfer between the two oscillators either by convection through an open port connecting them^{15a,b,c} or by pumping oscillating reagent between them^{15d}. Although the latter method is easier to quantitatively model than the former, both suffer from the fact that the coupling is carried out by transfer of reagent containing all reactants, products and intermediates. This problem is particularly difficult to deal with if the reactant concentrations are quite different in the two reactors as is often desired. The coupling of BZ oscillators by an electric current flow between large area Pt electrodes immersed in them offers the possibility of avoiding the mass-transfer problem. The circuit is completed by an ion bridge.

The redox potential of a cerium-catalyzed BZ oscillator is one of the principal oscillatory variables¹. Because the concentrations of Ce(III) and Ce(IV) are the highest of those expected to affect the redox potential of a BZ oscillator and because the form of the redox potential oscillations is very similar to the spectrophotometrically determined concentration of Ce(IV), we assume that the magnitude and sign of the redox potential between two electrically coupled BZ oscillators will depend primarily upon the difference between $[Ce(IV)]/[Ce(III)]$ in the two reactors. As a result of such a potential difference, a current will flow between the oscillators. The magnitude of this current will depend upon the amount of Ce(IV) reduced and Ce(III) oxidized in the respective oscillators. It is this chemical reaction which couples the oscillators. If it is assumed that the electrodes are reversible and that the reactions occurring at them mainly involve cerium ion, then the current, I , coupling the oscillators is given by the Nernst equation (1).

$$\frac{d[Ce(IV)]_1}{dt} = \frac{d[Ce(III)]_2}{dt} \text{ oc } I = \frac{E}{R} = \frac{0.0595}{R} \log \frac{[Ce(III)]_1 [Ce(IV)]_2}{[Ce(III)]_2 [Ce(IV)]_1} \quad (1)$$

In (1), R is the total resistance of the circuit and the subscripts refer to oscillators 1 and 2. The degree of coupling can easily be determined by measuring the current, I , and it can be controlled by varying the resistance. We note that electrical coupling of BZ oscillators introduces naturally a logarithmic term into the dynamic law of a real chemical system.

Preliminary experiments and calculations have been carried out to test the feasibility of carrying out experiments with electrically coupled BZ oscillators. The efficiency of coupling in such a system is expected to depend primarily on two factors. The first is how much current can flow between the oscillators and the second is the volume of the reactors; more current is required to couple larger than smaller reactors. The resistance of the circuit including the two oscillators is critical in this regard. Experiments have been carried out to determine the resistance of circuits composed of two cells containing concentration ratios of Ce(III) to Ce(IV) in at least 1M H₂SO₄ equivalent to those present at various phases of a BZ oscillation. These cells were coupled by large area Pt electrodes and an ion bridge. The solutions were rapidly stirred. It was quickly determined that most of the resistance of the circuit was in the ion bridge. Conventional Agar salt bridges had resistances of several hundred ohms. However, an ion bridge composed of two glass microfibre, 1-micron filter sheets (Whatman GF/C) gave circuit resistances as low as 20 ohms while allowing very little mass transfer. At the tenths

of a volt potential differences expected between out-of-phase BZ oscillators, about 10 ma will flow in such a circuit. This corresponds to about 10^{-7} moles of reaction per second at each electrode. In a one ml reactor changes in $[\text{Ce(IV)}]$ and $[\text{Ce(III)}]$ on the order of 10^{-4} M will occur. The concentration of cerium ion catalyst in a BZ oscillator is often of the order of 10^{-4} M. Thus it is expected that at experimentally accessible resistances the current flowing between reactors of about one ml volume should cause sufficient chemical reaction to substantially perturb both oscillators.

3. Numerical Simulations of Electrically-Coupled BZ Oscillators: Chaos

Simulations have been carried out of electrically coupled BZ oscillators running in one ml CSTRs. Flow reactors were used to obtain maximum control of the system. The extended Oregonator of SHOWALTER et al.⁹ was used as the basis of these simulations. This model involves seven species in each reactor (BrO_3^- , BrO_2^- , HBrO_2 , HOBr , Br^- , Ce(III) and Ce(IV)). Thus the simulations involved the numerical integration¹⁶ of a set of 14 differential equations. This complicated model was used in order to model the actual behavior of the BZ oscillators as closely as possible. The goal of the calculations was to guide in the construction of the experimental system rather than to carry out a systematic investigation of the properties of electrically coupled oscillators. For a mathematical analysis of the generalized dynamics of this system, it probably, would be appropriate to use the simple Oregonator⁸ perhaps in its stiffly coupled form, which could lead to a set of only four differential equations to describe the coupled system.

Figures 1-4 illustrate some of the various results obtained in these simulations. All calculations were carried out with an error parameter of at least 10^{-10} , and tightening it further did not affect the results of a calculation. Fig. 1 illustrates the suppression of one oscillator by the other when they are strongly coupled through a 5 ohm resistance. The plots show the variable Y (equivalent to $[\text{Br}^-]$) as a function of time. When the coupling was turned on at 500 s both oscillators went through a transition period before the oscillator with the shorter period (#1)

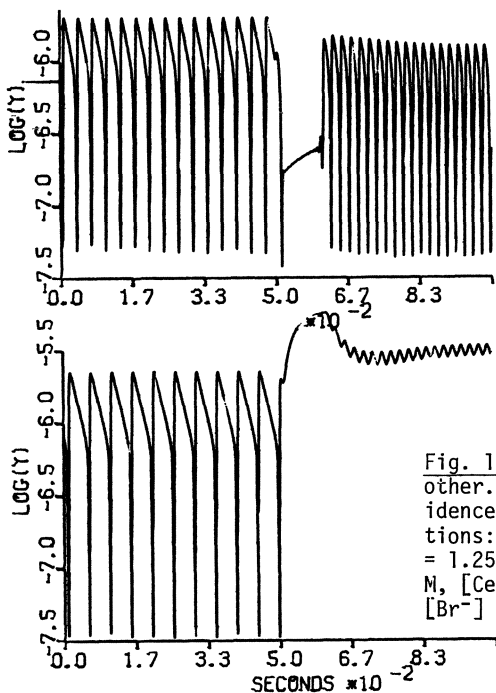


Fig. 1 Suppression of one oscillator by the other. $R = 5$ ohm. In both reactors the residence time = 167 s. Feedstream concentrations: Reactor 1 (top) $[\text{BrO}_3^-] = 0.14$ M, $[\text{Ce(III)}] = 1.25 \times 10^{-4}$; Reactor 2 (bottom) $[\text{BrO}_3^-] = 0.18$ M, $[\text{Ce(III)}] = 1.00 \times 10^{-4}$ M. Both reactors $[\text{Br}^-] = 0.0$ M. Coupling turned on at 500 s.

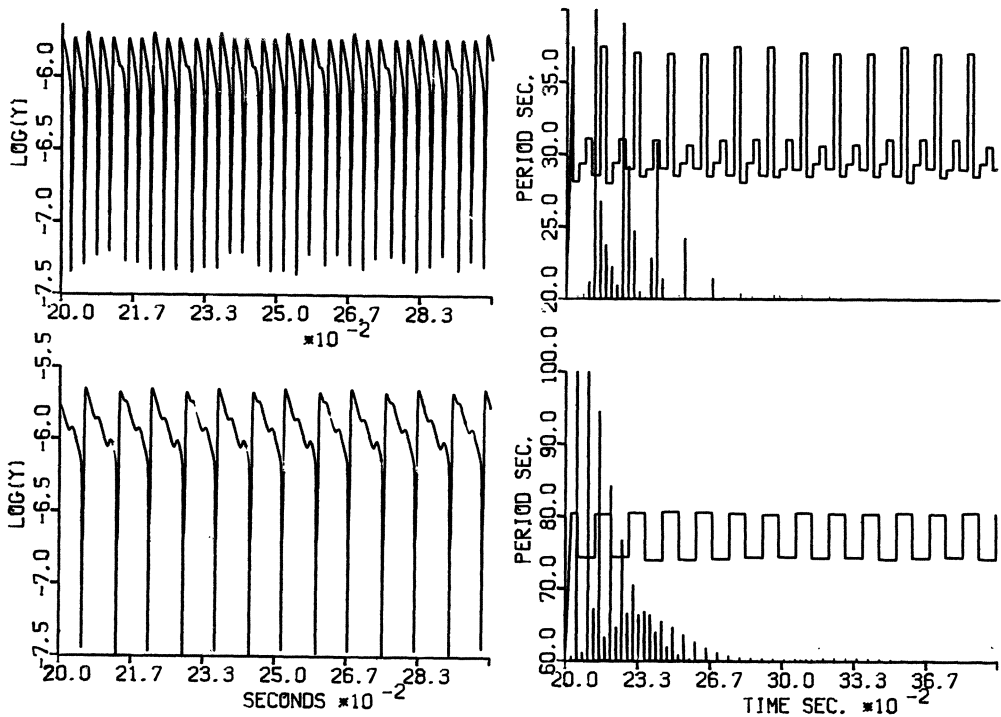


Fig. 2 Left side. Simple coupling of two oscillators. Right side. Successive period length and power spectrum of oscillations on the left side. $R = 10$ ohms. Other conditions the same as in Fig. 1

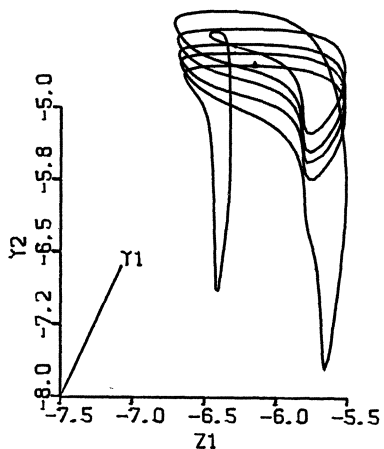


Fig. 3 Three-dimensional trajectory in Z_1, Y_1, Y_2 space of the calculation in Fig. 2

suppressed its mate. The mechanism of this suppression was that the faster oscillator kept $[Br^-]$ in the other high enough to keep it from ever entering the rapid oxidation phase of its oscillation. Fig. 2 (left) shows Y as a function of time for both oscillators when they are coupled to such a degree that both are perturbed but continue to exhibit periodic, complex wave-form oscillations. The conditions in Fig. 2 are the same as in Fig. 1 except that $R = 10$ ohm. Oscillator 1 repeats itself each 5 periods while oscillator 2 repeats itself each 2 periods. Fig. 2 (right) shows a plot of successive period lengths as well as the power spectra of the oscillators in Fig. 2 (left). The power spectra are exceedingly sharply spiked (reflecting the precision of the simulation) and evenly spaced. Fig. 3 is an orbit in $Y(\#1), Y(\#2), Z(\#1)$ space. The variable Z is equivalent to $[Ce(IV)]$.

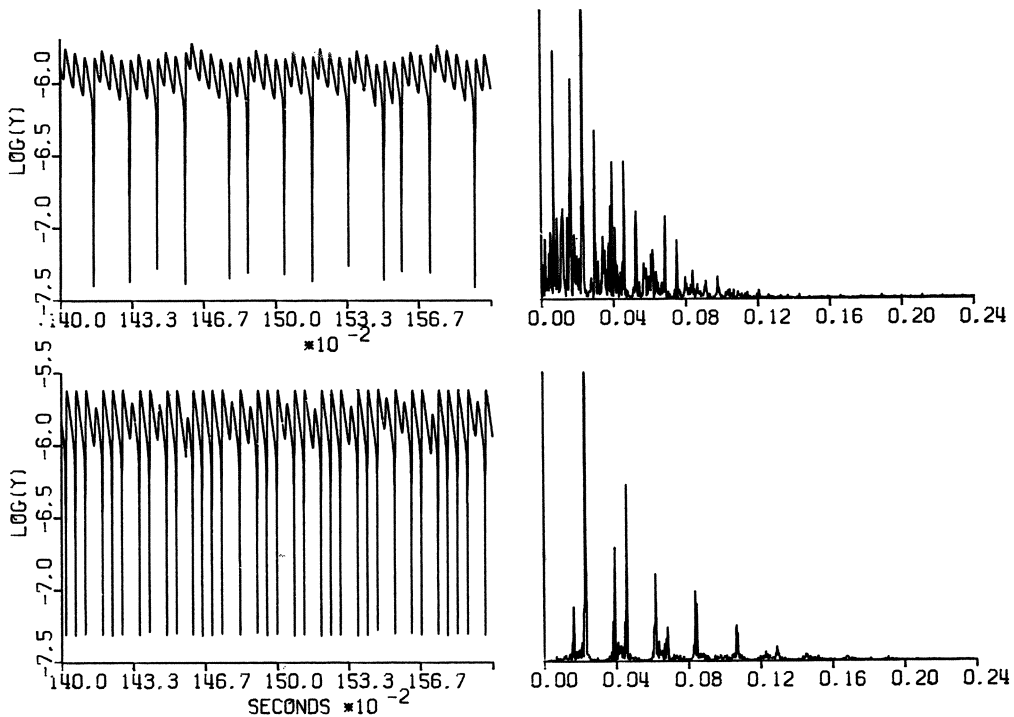


Fig. 4 Left side. Aperiodic oscillations. Right side. Power spectrum of left side oscillations. Reactor 1 (top): residence time= 25.6 m; Feedstream concentrations: $[\text{BrO}_3^-]= 0.14 \text{ M}$, $[\text{Ce(III)}]= 1.25 \times 10^{-4} \text{ M}$, $[\text{Br}^-]= 7.5 \times 10^{-6} \text{ M}$. Reactor 2 (bottom): Residence time= 20.9 m; Feedstream concentration: $[\text{BrO}_3^-]= 0.17 \text{ M}$, $[\text{Ce(III)}]= 1.5 \times 10^{-4} \text{ M}$, $[\text{Br}^-]= 7.5 \times 10^{-6} \text{ M}$

Figures 4 (left) shows a simulation which led to aperiodic, apparently chaotic, oscillations in oscillators coupled by a very low resistance of 2 ohm. The residence times in this simulation were much longer than in Fig. 2, and there was Br^- in the feedstreams. In general, Br^- in the feedstreams tends to enhance behaviors resulting from coupling. Similar, although somewhat less striking, aperiodic oscillations appear under other conditions at much higher resistances. The calculation in Fig. 5 was carried from 0 to 16000 s. The first 8000 s were ignored to assure that the oscillations had reached equilibrium with their feedstreams and each other. There is no detectable order in the remaining 8000 s of the calculation, only a fraction of which is shown in Fig. 4. This aperiodic behavior occurs near a transition point as did that observed by HUDSON et al.³ in a simple CSTR. As the ratio of $[\text{BrO}_3^-]$ in the two oscillators is varied, the system passes from a state of suppression of oscillator 1 by 2 through a periodic coupling to a state of suppression of oscillator 2 by 1. The aperiodic region is rather broad and dependent upon $[\text{Br}^-]$ in the feedstreams. Fig 4 (right) shows the power spectra of both oscillators calculated from the entire 8000 s range. These are very noisy, especially as compared to the power spectra in Fig. 2. There are, though, sharp peaks in the power spectra. We believe that these result from the fact that the coupling does not move the oscillators far from their unperturbed limit cycle; its chief effect is to simply introduce a large set of nested loops into the high Br^- phase of the uncoupled limit cycle. Fig. 5 shows the chaotic successive period maps resulting from the oscillators in Fig. 4. There appears to be some form to this plot including at least one crossing of the $P(N)=P(N+1)$ line^b and very steep areas. We are not sure that this plot is meaningful, however, as it probably is not single valued. That is, a period of length $P(N)$ may be followed by per-

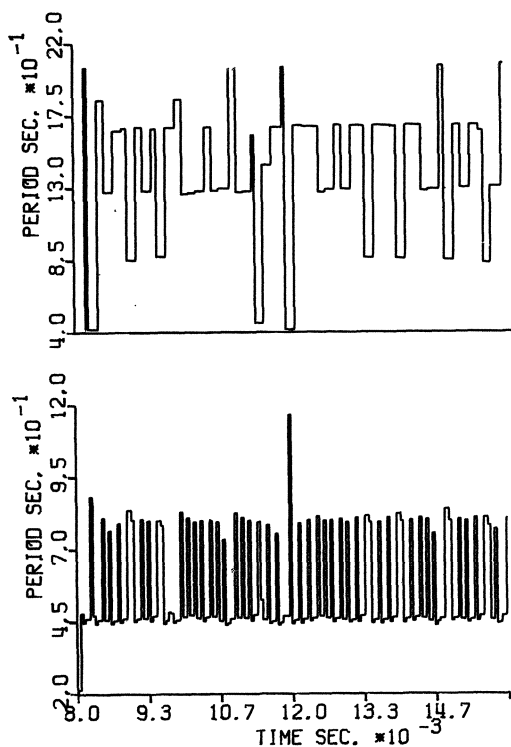


Fig. 5 Successive period lengths of oscillators of Fig. 4

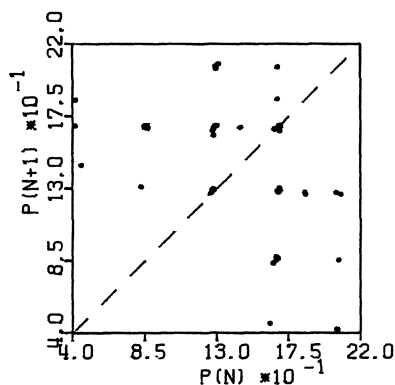


Fig. 6 Next period length map for oscillator 1 of Fig. 4

iods of lengths corresponding to a number of $P(N+1)$'s. This apparently results from the multi-dimensional nature of the system. A more meaningful next period or next amplitude map is being sought.

4. Conclusion

While we are not totally convinced that our calculations unambiguously show that chaos exists in electrically coupled BZ oscillators, we do believe that interesting dynamic phenomena will occur in such a system. We are continuing with our calculations and construction of an experimental prototype. It is possible to generate a bi-stable BZ system⁴, and we suggest that electrical coupling of such a system with a BZ oscillator may approximate more closely the chaos-generating machine of Rössler. This idea is also being investigated.

5. References

1. R.J. Field, E. Körös and R.M. Noyes, *J. Am. Chem. Soc.*, **94**, 8649 (1979).
2. R.J. Field in "Theoretical Chemistry: Advances and Perspectives," Vol. 4, Eds. H. Eyring and D. Henderson, Academic Press, New York (1978).
3. J.L. Hudson and J.C. Mankin, *J. Chem. Phys.*, **74**, 6171 (1981).
4. P. DeKepper and J. Boissonade, *J. Chem. Phys.*, **75**, 189 (1981).
5. R.D. Janz, D.J. Vanecek and R.J. Field, *J. Chem. Phys.*, **73**, 3132 (1980).
6. E.J. Reusser and R.J. Field, *J. Am. Chem. Soc.*, **101**, 1063 (1979).
7. a. R.A. Schmitz, K.R. Grazianai and J.L. Hudson, *J. Chem. Phys.*, **67**, 3040 (1977).
b. K. Wegman and O.E. Rössler, *Z. Naturforsch.*, **33a**, 1179 (1978).
c. J.L. Hudson, M. Hart and D. Marinko, *J. Chem. Phys.*, **71**, 1601 (1979).
d. J.L. Hudson, J. Mankin, J. McCullough and P. Lambda, "Experiments on Chaos in A Continuous Stirred Reactor," this volume.
8. R.J. Field and R.M. Noyes, *J. Chem. Phys.*, **60**, 1877 (1974).

9. K. Showalter, R.M. Noyes and K. Bar-Eli, *J. Chem. Phys.*, 69, 2514 (1978).
10. N. Ganapathisubramanian and R.M. Noyes, "Discrepancy Between Experimental and Computational Evidence for Chemical Chaos," preprint 1981.
11. J.S. Turner, "Bifurcation, Oscillations and Chaos in A Model of the Belousov-Zhabotinsky Reaction," this volume.
12. O.E. Rössler, *Z. Naturforsch.*, 31a, 259 (1976).
13. O.E. Rössler: in *Synergetics, A Workshop*, ed. by H. Haken (Springer, Berlin, Heidelberg, New York 1977) p.174
14. Y. Kuramoto and T. Yamada, *Progr. Theor. Phys.*, 55, 679 (1976).
15.
 - a. M. Marek and I. Stuchl, *Biophys. Chem.*, 3, 241 (1975).
 - b. H. Fujii and Y. Sawada, *J. Chem. Phys.*, 69, 3830 (1978).
 - c. K. Nakajima and Y. Sawada, *J. Chem. Phys.*, 72, 2231 (1980).
 - d. K. Bar-Eli and W. Geiseler, "Mixing and Relative Stabilities of Pumped States," preprint 1981.
16. A.C. Hindmarsh, "Gear: ordinary Differential Equation Solver," UCID-30001, Rev. 3

Part VI

Reaction-Diffusion Problems

The Rotor as a Phase Singularity of Reaction-Diffusion Problems and Its Possible Role in Sudden Cardiac Death

Arthur T. Winfree

Department of Biological Science, Purdue University,
West Lafayette, IN 47907, USA

1. Abstract

Some years ago a simple topological theorem enabled discovery of arrhythmic "singularities" in biological clocks, e.g., in the glycolytic oscillation of yeast cells (1). The context then was homogeneous chemical reaction, i.e., ordinary differential equations. It turns out now that the problem in spatially distributed context, i.e., the partial differential equation of reaction and diffusion, has the same topology. The singularity in this context appears to include the "ROTOR" or "REVERBERATOR". A heuristic extension of this theorem suggests a simple experimental procedure which may elicit rotors in a volume of oscillating reactants. This procedure resembles conditions which elicit fibrillation in oscillating heart muscle; the same singularity may underlie "SUDDEN CARDIAC DEATH".

2. Background

My purpose here is to exhibit a parallelism between certain aspects of heart physiology and corresponding aspects of physical chemistry in the Belousov-Zhabotinsky reagent. Its basic features have been noted before, but we can now additionally connect the earlier story to topological aspects of phase shifting in limit-cycle oscillators.

Krinskii (2), Troy (3), and Winfree (4,5) have drawn attention to the mathematical correspondence between Belousov-Zhabotinsky solution and other excitable media, e.g., neural membranes. In a nutshell, all exhibit a globally attracting steady state not far from a saddle-like region of flow beyond which trajectories execute a large excursion before inevitably returning to the steady state. In spontaneously oscillating excitable media, matters stand much the same except that trajectories only GRAZE the steady state and pass on to another excursion without assistance from any external stimulus (or, if you like, a chronic stimulus is built into the spontaneous dynamics).

3. Spatially Distributed Excitability

We now redirect our interest from the ordinary differential equations of spatially homogeneous kinetics in a stirred tank reactor to the partial differential equations of a spatially extended medium. The striking similarity between chemical excitability and neuroelectric excitability remains and is even enhanced. In the chemical case a Laplacian operator is added to the local kinetics to represent molecular diffusion. In the neuroelectric case the same operator is added to represent electric current flow along potential gradients.

4. Reflection of Action Potentials

We are accustomed to transfer sophisticated insight from the more fundamental sciences, such as physical chemistry, to the more phenomenological, such as neuro-

physiology. I believe there may be something to gain from carefully selected trans-fers in the opposite direction as well.

For example, many at this meeting have surely contemplated the faint prospects of REFLECTING a reaction-diffusion wave. Recent experiments in neurophysiology suggest against intuition (mine at least) that this may yet be possible. It has in fact been done both in the physiological laboratory (6) and by numerical simulations (7). The latter use the Hodgkin-Huxley model of excitable media, a parabolic partial differential equation similar in all essential respects to the equation governing excitable reactions spatially coupled by diffusion. The necessary trick seems to be to contrive a suitable parameter gradient to serve as a "mirror" at the boundary.

5. Phase Resetting of Neuroelectric Oscillators

A different example is better developed. It concerns rotating waves in an oscillatory excitable medium. We approach this subject through the topology of phase-resetting in pacemaker neurons.

Consider first a spatially homogeneous bioelectric membrane, spontaneously oscillating as in a pacemaker neuron. A discrete perturbation kicks its state point off the attracting limit cycle, to which it presently returns with some discrepancy of timing relative to an unperturbed control. For several years it has been recognized that this offset of timing depends on both the timing and the magnitude of the stimulus. This dependence is best described by a 3-dimensional plot that resembles a screw surface. Figure 1 shows the contour map of one such surface. This one was calculated from the Hodgkin-Huxley equations of rhythmically firing squid axon subjected to a current pulse (8,9).

6. Black Holes or Singularities on the Phase Map

The essential qualitative feature of this contour map for present purposes is the CONVERGENCE of contour lines to a BLACK HOLE in the half-plane of positive stimuli and to another in the complementary half-plane of negative stimuli. Each contour line joins the two BLACK HOLES. The BLACK HOLE may be arbitrarily small, even as small as an isolated point singularity bringing together all the contours lines. This curiosity is well understood theoretically – indeed, it was predicted from theory (10) – and is now also well established experimentally (11,12).

The topological analysis of attracting limit cycle kinetics leads to the inference (13) that the same qualitative pattern will be found when the corresponding measurements are carried out on the FKN model (14) or an actual Belousov-Zhabotinsky solution in a CSTR (e.g., using ultraviolet irradiation or bromide injections). This remains to be verified.

7. Phase Resetting in a Spatial Gradient

Now consider the implication for a spatially extended thin layer of excitable medium, subjected to a spatially graded stimulus. Imagine a train of parallel plane waves (ideally "pseudo-waves", i.e., phase gradients little affected by diffusion of molecules or electric potential [see (13) page 305]. Let each wavefront extend North-South, the wave proceeding from East to West. A perturbation falling on the medium (e.g., ultraviolet light or acetylcholine from a widely branching vagus nerve) finds volume elements at various phases in the cycle according to distance behind the nearest wavefront to the left – exactly as described by the horizontal axis in Fig.1. The vertical axis in Fig.1 represents stimulus magnitude, from zero to infinity in the upper half-plane. In the chemical analogue we might achieve that arrangement by grading the UV irradiance from zero upward to some extreme.

According to the scheme of Fig.1 this should result in resetting the phase of parochial oscillation in each volume element, according to its initial phase and the local exposure. The contour lines of Fig.1 then represent loci of uniform phase,

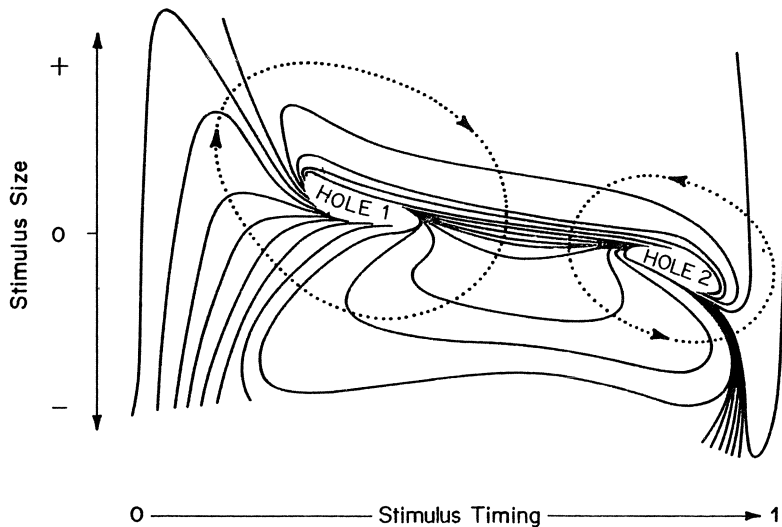


Fig.1. This contour map shows loci on the plane of stimulus size (zero in the middle, positive above, negative below) and stimulus timing (spanning one full cycle left to right) which result in resetting a Hodgkin-Huxley pacemaker to the same phase. Phase values on these contours vary through one full cycle clockwise around HOLE 1 and counterclockwise around HOLE 2. For details see (9,16,17)

i.e., of identical time until turning from red to blue or time until bioelectric discharge. They therefore represent the successive positions of a wavefront (specifically, of a "pseudo-wave"). This locus apparently rotates about an ambiguously phased pivot point once in every period of the spontaneous oscillation.

8. Spatial Coupling: Does it Affect the Topology of Wave Circulation?

This hand-waving argument ignores the spatial coupling of adjacent volume elements, blithely pretending that the autonomous ordinary differential equation is unaffected by molecular diffusion (in the case of the Belousov-Zhabotinsky reaction) or by electric currents (in the case of neural membranes). This might be an excellent approximation were the experiment conducted on a gargantuan scale with correspondingly shallow gradients of timing and of perturbation magnitude.

But even in this situation, contour lines AFTER perturbation converge to the boundary of a BLACK HOLE. Whether the latter be a finite disk or a mere point, contour lines approach infinite density there (15), so the gradients of phase AFTER perturbation exceed any pre-established limit. Consequently the Laplacian term MUST be reckoned with. Can it alter the TOPOLOGICAL configuration of the wave grandly rotating along the horizon? If not, then we have created a "reverberator", a "rotor". I know no mathematical proof but believe this to be the case.

9. Rotating Waves First Discovered in Excitable Cardiac Tissue

In the case of neural media, graded stimuli do commonly fall upon sheets of periodically firing cells, spatially graded in their timing. The heart is such an organ. Electric currents and vagal arborizations (in the atria) provide such stimuli. Perniciously stable rotating waves have been initiated in heart muscle by procedures similar to that idealized above (see 16, 17 for citations). There is some speculation that this constitutes one mode of SUDDEN CARDIAC DEATH, a mysteriously abrupt and lethally catastrophic onset of arrhythmia in the normal healthy heart (16,17).

Acknowledgements. This work has been supported by the U.S. National Science Foundation (Grant CHE-77-24649) and by the Institute for Natural Philosophy.

References

1. A.T. Winfree: Arch. Biochem. Biophys. *149*, 388 (1972)
2. V.I. Krinskii: Pharmac. Ther. B *3*, 539 (1978)
3. W.C. Troy: Theor. Chem. *4*, 133 (1978)
4. A.T. Winfree: Adv. Biol. Med. Phys. *16*, 115 (1977)
5. A.T. Winfree: Lecture Notes in Biomathematics *2*, 243 (1974)
6. F. Ramon, R.W. Joyner, J.W. Moore: Fed. Proc. *34*, 1357 (1975)
7. S. Goldstein, W. Rall: Biophys. J. *14*, 731 (1974)
8. E. Best: Biophys. J. *27*, 87 (1979)
9. A.T. Winfree: Lectures in Applied Mathematics *19*, 265 (1981)
10. A.T. Winfree: Science *197*, 761 (1977)
11. R. Guttman, S. Lewis, J. Rinzel: J. Physiol. (Lond.) *305*, 377 (1980)
12. J. Jalife, C. Antzelevitch: Science *206*, 695 (1979)
13. A.T. Winfree: *The Geometry of Biological Time* (Springer, Berlin, Heidelberg, New York 1980)
14. R.J. Field, E. Koros, R.M. Noyes: J. Amer. Chem. Soc. *94*, 8649 (1972)
15. J. Guckenheimer: J. Math. Biol. *1*, 259 (1976)
16. A.T. Winfree: In *Cardiac Rate and Rhythm*, ed. by H. Jongsma and L. Bouman (in press)
17. A.T. Winfree: Scientific American (in press)

Chemical Waves in the Iodate-Arsenous Acid System

Adel Hann, Alan Saul, and Kenneth Showalter

Department of Chemistry, West Virginia University
Morgantown, WV 26506, USA

1. Introduction

Chemical waves were observed in the iodate oxidation of arsenous acid over 25 years ago by EPIC and SHUB [1]. In a recent study [2], the existence of the waves was confirmed and a qualitative explanation was proposed. In addition, an electrochemical method for initiating waves in a thin film of solution was developed.

The chemical waves in the iodate-arsenous acid system differ significantly from the chemical waves exhibited by the Belousov-Zhabotinsky (BZ) reaction [3,4,5]. The iodate-arsenous acid reaction has the features of a clock reaction: a slow induction period followed by the onset of rapid reaction. The chemical wave in this system is a propagating *front*. The solution ahead and behind the front resembles the stirred reaction mixture during and following the induction period, respectively. The chemical wave in the excitable BZ reaction mixture is a propagating *pulse*. The pulse leaves the solution essentially unchanged after passing through it.

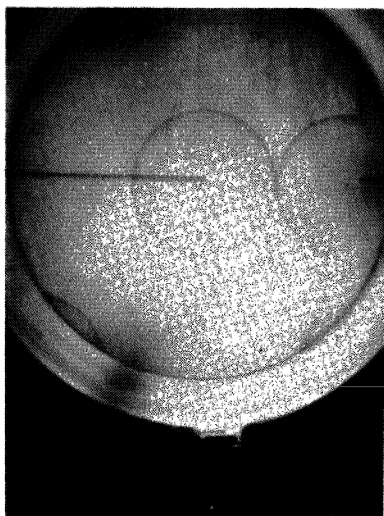
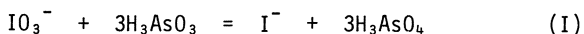
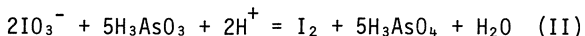


Figure 1

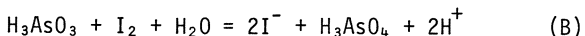
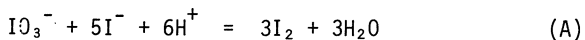
In the first systematic study of the iodate-arsenous acid reaction, EGGERT and SCHARNOW [6] reported autocatalysis in iodide. Net reaction (I) describes the system when arsenous acid is in stoichiometric excess to iodate ($[\text{As(III)}] > 3[\text{IO}_3^-]$):



When iodate is in stoichiometric excess to arsenous acid ($[\text{As(III)}] < 5/2[\text{IO}_3^-]$), the system is described by net reaction (II):



It is convenient to describe the reaction as a combination of two processes: the Dushman reaction [7] (process A) and the Roebuck reaction [8] (process B).



In solutions with $[\text{As(III)}] \geq 3[\text{IO}_3^-]$, the overall reaction is autocatalytic in iodide according to (A) + 3(B) or (I). Iodide accumulates until iodate is completely consumed. Chemical waves in these reaction mixtures (containing starch indicator) appear as thin blue bands. Figure 1 shows a typical wave at 17.6 min that was initiated at ca. 3.7 min after mixing reactants.

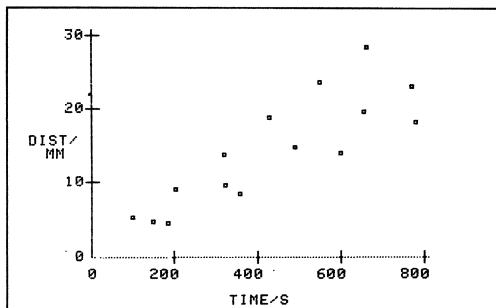


Figure 2

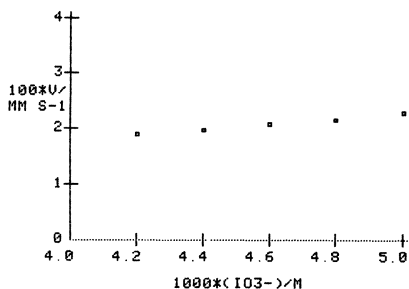


Figure 3

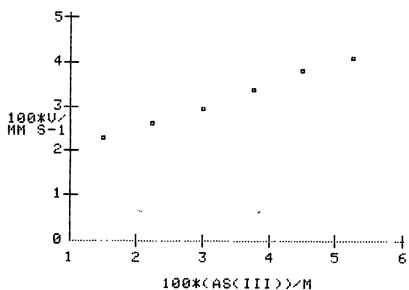


Figure 4

In this paper, we report on an investigation of chemical waves in the iodate-arsenous acid reaction. We confine this report to waves in reaction mixtures containing H_3AsO_3 in stoichiometric excess to IO_3^- . A more detailed account of our investigation, including experiments with $[\text{As(III)}] < 3[\text{IO}_3^-]$, can be found elsewhere [9].

2. Experimental

Chemical wave studies were carried out using a petri dish with a plate glass bottom, thermostated at $25.0 \pm 0.2^\circ\text{C}$ by a water jacket. Reaction mixtures were prepared by pipetting appropriate volumes of stock solutions. A buffer solution, prepared by mixing appropriate mole ratios of NaHSO_4 and Na_2SO_4 , was added to each reaction mixture to maintain constant acidity. The resulting solution was thoroughly mixed, spread over the bottom of the petri dish, and the electrodes were positioned. The 10.0 ml reaction mixture generated a solution depth of 0.8 mm in the petri dish. In all experiments, the reaction mixtures contained 0.04% starch indicator and 8×10^{-4} M sodium lauryl sulfate, which facilitated spreading of the solution in the petri dish. To investigate wave velocity dependence on reactant concentrations, one reactant concentration was varied while the other reactant concentrations were held constant ($[\text{NaIO}_3]_0 = 5.00 \times 10^{-3}$ M, $[\text{H}_3\text{AsO}_3]_0 = 1.55 \times 10^{-2}$ M, $[\text{H}^+]_0 = 7.1 \times 10^{-3}$ M).

Waves were initiated at a Pt electrode in the center of the dish negatively biased at -1.0 V with respect to a Pt electrode near the edge of the dish. The wave front position as a function of time was recorded by taking photographs at timed intervals.

Measurements of $[\text{I}^-]$ were made with an iodide selective microelectrode positioned 19.0 mm from the Pt initiation electrode. Iodide concentration was measured as a function of time as a wave passed through the electrode

position. Other measurements of iodide concentration in stirred reaction mixtures were made with the same microelectrode.

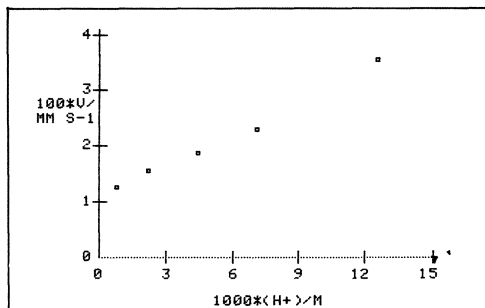


Figure 5

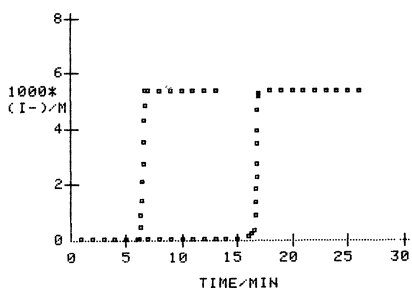


Figure 6

Table 1

Reactant (X) Varied	$\frac{dv/\text{mm s}^{-1}}{d[X]/\text{M}}$	$10^2 [X]_0 \left(\frac{dv}{d[X]} \right) / \text{mm s}^{-1}$
NaIO ₃	5.049	2.525
H ₃ AsO ₃	0.479	0.742
H ⁺	1.93	1.37

3.2 Iodide Concentration Measurements

Iodide concentration was measured as a function of time as a wave passed through an iodide selective microelectrode with a sensor diameter of about 0.4 mm. The curve in Fig.6 (left) shows iodide concentration as a function of time (standard reactant concentrations except $[H_3AsO_3]_0 = 5.43 \times 10^{-2} \text{ M}$). The wave velocity for this reaction mixture composition was $4.12 \times 10^{-2} \text{ mm s}^{-1}$. The increase in iodide concentration occurred almost entirely between 6.2 and 6.6 min; therefore, the wave front is about 1.0 mm wide. Photographs of waves in reaction mixtures with the same composition showed the width of the visible blue band to be about 0.4 mm.

3. Results

Plots of wave front position as a function of time were linear; therefore, waves propagate with a constant velocity. Figure 2 shows position as a function of time for three reaction mixtures differing only in initial $[H_3AsO_3]$.

3.1 Effect of Reactant Concentrations on Wave Propagation

Wave velocity dependence on initial reactant concentrations is shown in Figs.3-5. A linear dependence of wave velocity on initial $[IO_3^-]$ is shown in Fig.3. Only a narrow range of iodate concentrations could be studied in this series of experiments. At iodate concentrations lower than those in Fig.3, waves were not initiated at the Pt electrode; at higher concentrations, $[As(III)] < 3[IO_3^-]$ and wave velocity is no longer constant [9]. A linear velocity dependence on initial $[H_3AsO_3]$ is shown in Fig.4 and Fig.5 shows a linear velocity dependence on $[H^+]$. In the experiments for Fig.5, the NaHSO₄/Na₂SO₄ ratio of the buffer solution was varied to obtain different solution acidities. The $[H^+]$ of each reaction mixture was measured using a pH meter.

The least squares slopes for the data in Figs.3-5 are given in Table 1. Also given are the relative slopes, obtained by multiplying the slope in each case by the concentration at which the reactant was held constant in the other experiments. The relative slopes show that the wave velocity dependence on H^+ and IO_3^- is, respectively, about 2 and 3 times greater than the dependence on H_3AsO_3 .

According to (I), the iodide concentration should increase to a value given by the stoichiometric relation $[I^-]_{\max} = [IO_3^-]_0$. The measured $[I^-]_{\max}$ in Fig.6 is about 8% higher than the value of 5.0×10^{-3} M expected from stoichiometry. The discrepancy is apparently due to experimental error. Also shown in Fig.6 (right) is the iodide concentration as a function of time in a stirred reaction mixture with the same composition. The measured $[I^-]_{\max}$ for the stirred reaction mixture is also about 8% above the value expected from stoichiometry.

4. Discussion

The oxidation of arsenous acid by iodate can be expressed as a combination of the Dushman reaction [7] and the Roebuck reaction [8]. LIEBHAFSKY and ROE [10] have summarized the many studies of the Dushman reaction. They conclude that the kinetics of the reaction are best described by (1).

$$-\frac{d[I^-]}{dt} = (k_1 + k_2[I^-])[IO_3^-][H^+]^2[I^-] \quad (1)$$

The reaction is first order in iodide at $[I^-]$ less than about 10^{-6} M and second order in iodide at higher concentrations. Iodine generated by the Dushman reaction is reduced to iodide by As(III) in the Roebuck reaction. Process B is more rapid than process A and therefore the Dushman reaction is rate determining for the overall reaction. The regeneration of iodide by process B gives rise to autocatalysis in iodide at a rate given by (1).

In reaction mixtures containing H_3AsO_3 in stoichiometric excess, the iodine and oxyiodine intermediates never reach concentrations which are stoichiometrically significant. Therefore, the concentrations of iodate and iodide are related by $[IO_3^-] = [IO_3^-]_0 - [I^-]$ according to (I). Substituting this relation into (1) allows us to write the reaction-diffusion equation

$$\left(\frac{\partial C}{\partial t}\right)_x = D \left(\frac{\partial^2 C}{\partial x^2}\right)_t + (k_1 + k_2 C)([IO_3^-]_0 - C)[H^+]^2 C \quad (2)$$

where $C = [I^-]$. We now have a single variable model for the system with third-order kinetics. In (2) we must assume that I^- and IO_3^- have the same diffusion coefficients. The homogeneous steady states from (2) are $-k_1/k_2$, 0, and $[IO_3^-]_0$. A linear stability analysis shows that for the homogeneous system, the negative and positive roots are stable and the zero root is unstable to infinitesimal perturbation.

Figure 2 shows that waves propagate with a constant velocity. Substituting $v = (\partial x / \partial t)_C$ into (2) gives

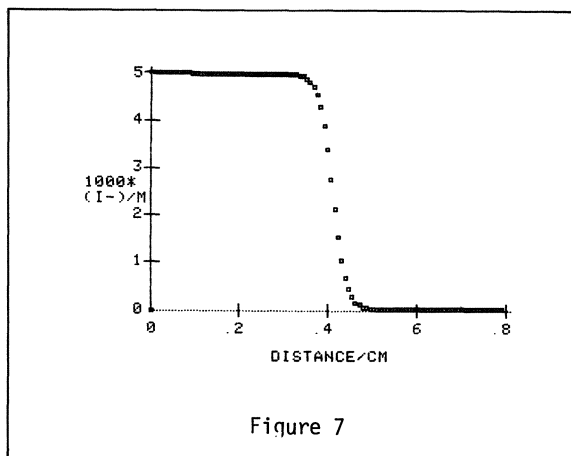
$$D \frac{d^2 C}{dx^2} + v \frac{dC}{dx} + (k_1 + k_2 C)([IO_3^-]_0 - C)[H^+]^2 C = 0 \quad (3)$$

A linear stability analysis of the two simultaneous first order differential equations derived from (3) shows that the zero root is an unstable node and that the positive root is a saddle point for $v < 0$. These reaction-diffusion stationary states correspond to a stable propagating front [12].

A particular analytical solution of (2) or (3) is given by:

$$C(x,t) = \frac{C_0}{1 + A e^{k(x-vt)}} \quad (4)$$

$$\text{where, } C_0 = \begin{cases} [IO_3^-]_0 \\ -k_1/k_2 \end{cases} \quad (5)$$



$$k = C_0[H^+](k_2/2D)^{1/2} \quad (6)$$

$$v = (k_1/k)[IO_3^-]_0[H^+]^2 + Dk \quad (7)$$

Figure 7 shows C as a function of distance for the arbitrary constant $A = 1.0$, $t = 100$ s, $D = 1.52 \times 10^{-5}$ cm² s⁻¹, $k_1 = 4.5 \times 10^3$ M⁻³ s⁻¹, $k_2 = 1.0 \times 10^9$ M⁻⁴ s⁻¹, $[H^+] = 7.1 \times 10^{-3}$ M, $C_0 = [IO_3^-]_0 = 5.0 \times 10^{-3}$ M, and the measured velocity for the reaction mixture composition in Fig.6. The values of k_1 and k_2 are from a study of kinetic bistability exhibited by this system in a CSTR [11]. From (5), (6) and (7), we calculate $v = 9.96 \times 10^{-3}$ mm s⁻¹. Therefore, the calculated velocity is low by a factor of 4

compared to the experimental velocity in Fig.6. Equations (2)-(7) do not take into account the effect of $[H_3AsO_3]$ on wave velocity. For the standard reaction mixture composition with $[H_3AsO_3]_0 = 1.55 \times 10^{-2}$ M, the experimental velocity ($v = 2.3 \times 10^{-2}$ mm s⁻¹) differs from the calculated velocity by a factor of only 2.3.

Equations (5)-(7) give the wave velocity dependence on reactant concentrations.

$$v = \alpha[H^+] + \beta[H^+][IO_3^-]_0 \quad (8)$$

where,
$$\alpha = k_1 \left(\frac{2D}{k_2} \right)^{1/2} = 2.48 \times 10^{-3} \text{ cm s}^{-1} \text{ M}^{-1}$$

$$\beta = \left(\frac{k_2 D}{2} \right)^{1/2} = 27.57 \text{ cm s}^{-1} \text{ M}^{-2}$$

For the standard reaction mixture, the first term in (8) accounts for less than 2% of the calculated velocity. The plot of v vs $[IO_3^-]$ with a constant $[H^+]$ in Fig.3 gives α and β values of -3.40×10^{-2} cm s⁻¹ M⁻¹ and 71.11 cm s⁻¹ M⁻², respectively. Disregarding the nonzero intercept of the plot of v vs $[H^+]$ in Fig.5, the slope gives $(\alpha + \beta[IO_3^-]_0) = 0.19$ cm s⁻¹ M⁻¹ compared to a value of 0.14 cm s⁻¹ M⁻¹ from (8). The reasonably good agreement with experiment indicates that the essential features of the traveling chemical wave are accounted for by (3) and (4).

References

1. Epik, P. A.; Shub, N. S. Dokl. Akad. Nauk SSSR 1955, 100, 503-506.
2. Gribschaw, T. A.; Showalter, K.; Banville, D. L.; Epstein, I. R. J. Phys. Chem. 1981, 85, 2152-2155.
3. Zaikin, A. N.; Zhabotinsky, A. M. Nature (London) 1970, 225, 535-537.
4. Field, R. J.; Noyes, R. M. J. Am. Chem. Soc. 1974, 96, 2001-2006.
5. Showalter, K.; Noyes, R. M.; Turner, H. J. Am. Chem. Soc. 1979, 101, 7463-7469.
6. Eggert, J.; Scharnow, B. Z. Elektrochem. 1921, 27, 455-470.
7. Dushman, S. J. Phys. Chem. 1904, 8, 453-482.

8. Roebuck, J. R. J. Phys. Chem. 1902, 6, 365-398.
9. Hanna, A.; Saul, A.; Showalter, K. J. Am. Chem. Soc., submitted.
10. Liebhaftsky, H. A.; Roe, G. M. Int. J. Chem. Kinet. 1979, 11, 663-685.
11. Papsin, G. A.; Hanna, A.; Showalter, K. J. Phys. Chem., in press.
12. Fife, P. C. "Mathematical Aspects of Reacting Diffusing Systems", Lecture Notes in Biomathematics, Vol. 28, Springer-Verlag, New York, 1979.

Mécanisme réactionnel fondé sur une étude expérimentale expliquant des instabilités interfaciales liées à des réactions chimiques

E. Nakache, M. Dupeyrat

Laboratoire de Chimie Physique de l'Université P. et M. Curie - L.A. 176 C.N.R.S. - 11, Rue P. et M. Curie
75 231 Paris Cedex 05 (France)

Les instabilités hydrodynamiques que nous étudions apparaissent dans un système à deux phases liquides non miscibles loin de l'équilibre. Elles se manifestent par exemple, lorsqu'on superpose une solution aqueuse d'un halogénure d'alkyltriméthylammonium (RCI), composé tensioactif hydrophobe, et une solution d'un composé hydrophile, l'acide picrique (HPi) dans le nitrobenzène. Lors de la mise en contact des phases chaque composé se trouve dissous dans la phase pour laquelle il a le moins d'affinité et le système est loin de l'équilibre thermodynamique. On observe des mouvements spontanés de l'interface lors de la relaxation du système. Ils se présentent sous la forme soit d'une vague qui apparaît le long d'une paroi de verre et déforme l'interface soit de contractions et d'expansions dans le plan de l'interface visibles grâce à une émulsion qui se produit spontanément peu après le contact des phases, mais qui n'est pas nécessaire à l'apparition des mouvements.

Ces deux types de mouvements sont liés à des variations locales de la tension interfaciale γ . Ce sont donc des effets "MARANGONI". Ils ne peuvent être attribués ni à un effet de densité lié au passage d'un soluté d'une phase dans l'autre ni à un transfert de chaleur, ni au transfert d'un soluté tensioactif entre les deux phases. Enfin ils n'obéissent pas aux critères de STERNLING et SCRIVEN [3]. Nous avons montré que l'existence d'une réaction chimique est nécessaire à l'apparition de ces instabilités et nous proposons maintenant un mécanisme réactionnel, basé sur l'expérience, pour justifier les phénomènes observés.

I. Méthodes Expérimentales

Nous avons corrélé visuellement les expansions et contractions de l'interface avec les variations de tension interfaciale γ , elles-mêmes couplées avec des modifications de la différence de potentiel ΔV de part et d'autre de l'interface [4]. Pour étudier les mouvements nous avons tracé la courbe de la variation de γ , mesurée par la méthode de l'étrier [5], en fonction du temps. La figure (1) représente à titre d'exemple les oscillations de relaxation obtenues avec HPi $1,25 \cdot 10^{-3}$ M (n) et $C_{12}Br$ $5 \cdot 10^{-3}$ M (e). Le mécanisme réactionnel proposé doit rendre compte de l'allure des oscillations.



Fig.1 Variation de la tension interfaciale du système HPi $1,25 \cdot 10^{-3}$ M(n) $C_{12}Br$ $5 \cdot 10^{-3}$ M (e) en fonction du temps.

4. Preuves Expérimentales de la Validité du Mécanisme Proposé

Si l'apport de Pi^- résulte d'une diffusion de HPI, l'augmentation de γ avec le temps dans la première partie d'une oscillation doit suivre une loi en \sqrt{t} . En effet, les données de la Fig.1 exprimées en \sqrt{t} donnent bien une droite lors de la partie ascendante de l'oscillation (Fig.2)

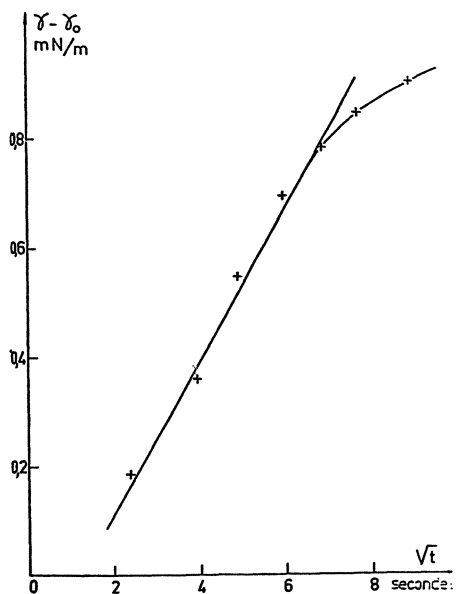


Fig.2 Variation de la tension interfaciale du système HPI $1,25 \cdot 10^{-3}$ M(n) C_{12}Br $5 \cdot 10^{-3}$ M(e) en fonction de la racine carrée du temps.

Si le mécanisme est correct, la suppression de la recombinaison des Pi^- doit empêcher le déclenchement des instabilités. Si l'on remplace HPI par un composé analogue mais dont la constante de formation dans le nitrobenzène est très faible, comme KPI par exemple, on supprime l'étape de rétroaction. Or l'expérience montre qu'on n'obtient pas d'instabilités dans ce cas, ce qui confirme notre hypothèse.

Par ailleurs le mécanisme n'explique pas la brutalité de la diminution de γ . En effet, le processus de recombinaison des Pi^- en HPI étant rapide, la diminution de tension en résultant devrait être progressive au fur et à mesure du transfert de RPI dans le nitrobenzène. En fait la recombinaison de Pi^- nécessite la présence de H^+ dans la phase organique, espèce qui ne peut provenir que de la phase aqueuse. Le transfert des ions H^+ , essentiellement sous forme acide halogéné HX, suppose un processus de diffusion et d'adsorption. S'il a lieu brusquement cela signifie que ces ions ne passent pas continuellement dans la phase organique par diffusion. Donc c'est l'adsorption - désorption qui est prédominant pour ces espèces.

Nous avons comparé cette situation à celle observée par DUPEYRAT et coll. [7] au cours de l'étude de la pénétration d'un alcool à chaîne courte dans un système eau-décane contenant un tensioactif dont les molécules "occupent" l'interface. Les conclusions de ce travail nous ont permis de supposer que l'adsorption - désorption des ions H^+ , dont l'adsorbabilité est très faible à l'interface "occupée" par les espèces tensioactives n'a lieu que lorsque leur concentration en phase aqueuse atteint un certain seuil. Si cette hypothèse est fondée, l'augmentation de la concentration d'HX dans la phase aqueuse doit permettre d'atteindre plus rapidement le seuil de concentration. Elle doit donc augmenter la fréquence des oscillations. La figure(3) montre en effet que la période des oscillations diminue après l'injection d'acide près de l'interface.

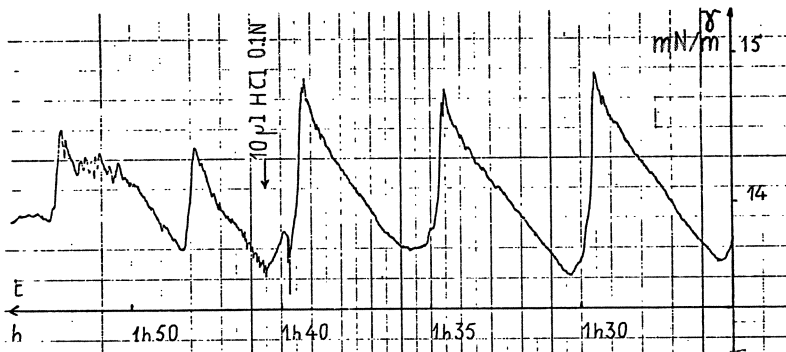


Fig.3 Effet de l'addition d'HCl sur le système $HP_{1,3,510}^{-4} M(n)/C_{16}Cl 410^{-4} M(e)$

5. Critique du Modèle

Cette interprétation peut sembler correspondre au modèle proposé par RUCKENSTEIN et BERBENTE [8] qui ont modifié l'approche théorique de STERNLING et SCRIVEN en y ajoutant une réaction chimique dans l'une des phases. Elle en diffère essentiellement par le fait que ces auteurs n'ont pas tenu compte de deux conditions essentielles sans lesquelles nous n'observons pas de mouvements. D'une part, un important déséquilibre de concentration est nécessaire pour déclencher le mouvement ; il est obtenu en dissolvant des composés de coefficients de partage très différents, dans la phase pour laquelle ils ont le moins d'affinité. D'autre part c'est la grande différence entre les coefficients de partage et l'adsorbabilité des composés intermédiaires, qui favorise le retour des espèces initiales dans leur phase d'origine et permet la formation et l'entretien des oscillations.

Par ailleurs SANFELD et coll. ont examiné le système que nous avons étudié d'un point de vue théorique, en tenant compte des mêmes processus de transport et d'une réaction interfaciale [9]. Or le phénomène peut être décrit par un mécanisme interfacial à condition que tous les composés s'adsorbent notablement à l'interface, ce qui n'est pas le cas ici. L'utilisation de ce modèle suppose donc une approche différente du problème relativement aux espèces non adsorbées.

Conclusion

Ce phénomène est un des rares exemples expérimentaux de structure dissipative d'énergie incluant des réactions chimiques dans un système biphasique. Il est remarquable que les réactions mises en jeu soient simples, contrairement aux réactions chimiques oscillantes en phase homogène. C'est que peut intervenir en système biphasique, une compétition entre diffusion et adsorption-désorption des diverses espèces. Par ailleurs il n'est pas nécessaire que les oscillations de concentration se manifestent par des mouvements pour qu'elles existent, ce qui autorise à élargir l'application de tels modèles par exemple à l'étude des réactions biochimiques oscillantes au voisinage des membranes.

- 1 - M. Dupeyrat, J. Michel, Exp. Suppl. 18, 269 (1971)
- 2 - E. Nakache, Thèse Paris (1981)
- 3 - C.V. Sternling, E.K. Scriven, A.I.Ch. E.J. 5, 514 (1959)
- 4 - M. Dupeyrat, E. Nakache, Proc. 19th Int. Meeting Soc. Chim. Phys. E. Roux ed., Elsevier Pub., Amsterdam (1977)
- 5 - J. Guastalla, J. Chim. Phys. 68, 822 (1971)
- 6 - M. Dupeyrat, E. Nakache, J. Coll. Sc. 73, 332 (1980)
- 7 - F. Billouet, M. Dupeyrat, 4th Int. Conf. Surf. Coll. Sc. I.U.P.A.C. abstract n°154 Jerusalem (1981)
- 8 - E. Ruckenstein, C. Berbente, Chem. Eng. Sc. 19, 329 (1964)
- 9 - M. Dalle Vedove, P.M. Bisch, A. Sanfeld, J. Non-Equ. Therm. 5, 35 (1980).

Part VII

Biochemical Processes

Complex Dynamic Structures

B. Hess, E.M. Chance⁺, A.R. Curtis⁺⁺ and A. Boiteux

Max-Planck-Institut für Ernährungsphysiologie, Rheinlanddamm 201
D-4600 Dortmund 1, Fed. Rep. of Germany

⁺ Dept. of Biochemistry, University College London, Gower St., London WC1 6BT, U.K.

⁺⁺ Computer Science and Systems Division, A.E.R.E. Harwell,
Didcot, Oxon OX11, ORA, U.K.

1. Introduction

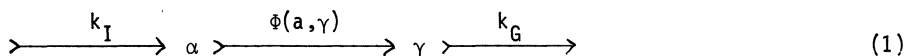
Pattern formation in reputedly homogeneous chemical systems has manifested itself in two characteristically quite different conditions: the BELOUSOV-ZHABOTINSKY reaction [1,2] as well as the glycolyzing cell-free extract of yeast [3,4,5] demonstrate time and space dependent concentration gradients. The common feature that these two systems share is their time-dependent coupling of the rate of chemical reaction and diffusion of reactants and products with the consequence that all components of the system are no longer homogeneously distributed in space. These features are maintained for given dynamic conditions.

We represent dynamic compartmentation by simultaneous differential equations for suitable geometry and boundary conditions, which incorporate the necessary terms for chemical reactions and diffusion. The properties of a two-dimensional representation of the solution of such a system of equations may be compared with patterns observed experimentally. We analyse numerically the influence of boundary conditions on the mathematical form of the waves produced. Standing waves are produced from discrete domain and steady state boundary conditions. Travelling waves are produced from boundary sink conditions, and the direction of the waves and velocity depends on the length of the boundary element. Theoretical and experimental results will be discussed.

2. Mathematical Analysis

In earlier studies [4,6] partial differential equations have been solved which were discretized in one dimension using linear increments in distance. Such a treatment would lead, in a two-dimensional representation, to a square mesh and results in artificial effects at the corners induced by the higher density of the mesh points. Furthermore, from an overhead perspective, the patterns observed experimentally in yeast appeared to be hexagonal in space, a geometry nearer to a circle than a square. Therefore, it was decided to discretise the one-dimensional equations in circular geometry linear in $\Delta(r^2)$ (the change in the square of radius at each mesh point) in order to obtain mesh cells of equal area.

Circular symmetry was thus assumed and the roughly hexagonal shape was approximated by an outer circular boundary, within which diffusion takes place. Catalysis is restricted to a smaller concentric region, consisting of a whole number of such cells. Consider the non-dimensional chemistry of an allosteric enzyme (for definitions see (6,7)) at a segment of a one-dimensional mesh



Let

$$L' = L(1+\epsilon)^2 \quad (2)$$

$$A = 2aD\epsilon \quad (3)$$

then

$$\phi = \frac{A (\epsilon+1+\alpha) (1+\gamma)^2}{L' (1+c\alpha)^2 + (\epsilon+1+\alpha)^2 (1+\gamma)^2} \quad (4)$$

to account for diffusion let

- n = total number of radial mesh cells
- m = number in which catalysis occurs
- b = outer radius
- r_i = outer radius of i th cell .

Then

$$r_i = b \sqrt{i/n}, \quad i = 1, 2, 3, \dots, n \quad (5)$$

(so that $r_n = b$) and the equations to be solved are

$$\frac{\delta\alpha}{\delta t} = k_I - \phi\alpha + \frac{1}{r} \frac{\delta}{\delta r} (r D_\alpha \frac{\delta\alpha}{\delta r}) \quad (6)$$

$$\frac{\delta\gamma}{\delta t} = \phi - k_G\gamma + \frac{1}{r} \frac{\delta}{\delta r} (r D_\gamma \frac{\delta\gamma}{\delta r}) \quad (7)$$

where D_α , D_γ are the diffusion constants for α and γ , respectively. Both equations are similar in structure, and we describe in detail the discretisation of equation (6) only.

Multiply equation (6) by $2r \, dr$ and integrate over the i th cell, from $r = r_{i-1}$ to $r = r_i$. Writing α_i for its mean value over this cell we obtain

$$\frac{\pi b^2}{n} \frac{d\alpha_i}{dt} = \frac{\pi b^2}{n} \left[(k_{I_i} - \phi_i \alpha_i) + 2\pi r D_\alpha \frac{\delta\alpha}{\delta r} \right]_{r_{i-1}}^{r_i} \quad (8)$$

In the last term of (8) we replace $r\delta\alpha/\delta r$ by $2r^2\delta\alpha/\delta(r^2)$, and approximate the derivative, at, for example, $r = r_i$, by

$$\left. \frac{\delta\alpha}{\delta(r^2)} \right|_{r_i} \approx \frac{\alpha_{i+1} - \alpha_i}{\Delta(r^2)} = \frac{\alpha_{i+1} - \alpha_i}{(b^2/n)} \quad (9)$$

With a similar approximation at $r = r_{i-1}$, (8) becomes, after dividing by $\pi b^2/n$,

$$\frac{\delta\alpha_i}{dt} = k_{I_i} - \phi_i \alpha_i + T_i (\alpha) \quad (10)$$

where

$$T_i(\alpha) = \frac{4nD_\alpha}{b^2} \left[i(\alpha_{i+1} - \alpha_i) - (i-1)(\alpha_i - \alpha_{i-1}) \right] . \quad (11)$$

The form of the last equation shows that we have exact conservation since the amount $4nD_\alpha i(\alpha_{i+1} - \alpha_i)/b^2$ entering cell i across r_i will, on replacing i by $(i+1)$ in (11) be exactly the amount leaving cell i across the same boundary. A precisely similar treatment of (7) leads to

$$\frac{d\gamma_i}{dt} = \phi_i \alpha_i - k_{Gi} \gamma_i + T_i(\gamma) \quad (12)$$

where

$$T_i(\gamma) = \frac{4nD_\gamma}{b^2} \left[i(\gamma_{i+1} - \gamma_i) - (i-1)(\gamma_i - \gamma_{i-1}) \right] . \quad (13)$$

Our choice of r_m as the outer boundary for catalysis imposes the conditions

$$k_{I_i} = \phi_i = k_{Gi} = 0 , \quad i = m+1, m+2, \dots, n . \quad (14)$$

Four types of boundary conditions were applied to the basic equations:

- I. No Flux - Reflective boundary at $r = b$.
- II. Discrete Domain - for value of $r > r_m$ catalysis and diffusion takes place. For values of $r_m < r \leq b$ only diffusion takes place.
- III. Boundary Sink - α and γ diffuses across $r = b$ into a boundary element whose area is V_b times the area of a mesh cell. If B_α, B_γ are the amounts in this element, the concentrations (in units corresponding to α, γ) are $B_\alpha/V_b, B_\gamma/V_b$. Thus, the term $i(\alpha_{i+1} - \alpha_i)$ in $T_i(\alpha)$ for $i=n$ is replaced by $n(B_\alpha/V_b - \alpha_n)$, and similarly for γ . Conservation then requires that

$$\frac{dB_\alpha}{dt} = \frac{4n^2 D_\alpha}{b^2} (\alpha_n - B_\alpha/V_b) \quad (15)$$

and similarly

$$\frac{dB_\gamma}{dt} = \frac{4n^2 D_\gamma}{b^2} (\gamma_n - B_\gamma/V_b) . \quad (16)$$

In this case we take $m = n$.

- IV. Steady State - the boundary element has constant steady-state values of α and γ (α_s and γ_s). This was achieved by setting

$$B_{\alpha} = \alpha_s \quad (17)$$

$$B_{\gamma} = \gamma_s \quad (18)$$

and V_b very large instead of (15) and (16). Here α_s and γ_s are obtained by solving the nonlinear steady-state equations with transport terms absent and $m = n$.

The global initial values are:

$$D_0 = 5 \times 10^{-3} \text{ [mM]} \quad (19)$$

$$a = 5 \times 10^5 \text{ [(mM s)}^{-1}] \quad (20)$$

$$c = 0.01 \quad (21)$$

$$L = 5 \times 10^6 \quad (22)$$

$$\varepsilon = 0.1 \quad (23)$$

$$\alpha_0 = \alpha_1 = \alpha_2 \dots = \alpha_n = \alpha_s \quad (24)$$

$$\gamma_0 = \gamma_1 = \gamma_2 \dots = \gamma_n = 0 \quad (25)$$

$$k_{G_i} = k_G^{(s)} = 0.15 \text{ [s}^{-1}], \quad i = 1 \text{ to } m \quad (26)$$

$$k_{I_i} = \gamma_s k_{G_i}, \quad i = 1 \text{ to } m, \quad (27)$$

where γ_s was chosen to be 1.5 and α_s was obtained by solving the steady-state equation

$$\phi_s \alpha_s = k_G^{(s)} \gamma_s. \quad (28)$$

The initial value of the boundary element in the boundary sink solutions are

$$B_{\alpha} = V_b \alpha_s \quad (29)$$

$$B_{\gamma} = V_b \gamma_s. \quad (30)$$

For Type I boundary condition $m = n = 40$, so that $b = r_n = r_m = 0.1 \text{ [cm]}$ and in all cases the radius r_m of the catalytic region was 0.1^n [cm]^m .

For Type II boundary condition, we have

$$b = r_n = r_m \sqrt{\frac{n}{m}} \quad (31)$$

and in this case we took (after some experimentation) $m = 40$, $n = 45$, giving $b = 0.1061 \text{ [cm]}$.

For Type III boundary condition we took $n = m = 40$, and values 1.0, 7.5, 20 for V_b . b in this case is given by

$$b = r_m \sqrt{1 + \frac{V_b}{m}}. \quad (32)$$

For Type IV boundary condition $m = n = 40$, $b = r_m = 0.1$ [cm] and $V_b = 10^6$.

The well-stirred bulk values of α and γ (α_t, γ_t), the normalized concentration term T_{r_i} , and the characteristic length λ_i are

$$\alpha_t = \frac{1}{n} \sum_i^n \alpha_i, \quad \gamma_t = \frac{1}{n} \sum_i^n \gamma_i \quad (33)$$

$$T_{r_i} = 100 \left[\frac{\gamma_{t_i}}{\alpha_{t_i} + \gamma_{t_i}} \right] \quad (34)$$

$$\lambda_t = \frac{1}{n} \sum_i^n \lambda_i \quad (35)$$

$$\lambda_i = \sqrt{\frac{D_\alpha}{\phi_i}} \quad (36)$$

for $D_\alpha = D_\gamma$.

The mean value of the characteristic length is calculated from

$$\bar{\lambda} = \frac{1}{m} \sum_i^n \lambda_i \quad (37)$$

and the normalized bulk concentration term T_r

$$T_r = \frac{1}{n} \sum_i^n T_{r_i} \quad (38)$$

The initial values of the concentrations of the various elements in the mesh were chosen so that the solution would reach the oscillatory steady state, from which the results were obtained in a reasonably short time. γ_s was chosen to be 1.5 which results in a value of 65.0775 for α_s and a period of about 10 minutes. The equations were solved on the Cambridge IBM 360/165 computer using the FACSIMILE program [8], and the oscillation was taken to have settled after 5 complete cycles, which required about 30 seconds of CPU time.

3. Results and Discussion

The effects of boundary conditions on the wave forms produced from numerical solution of the above equations are summarized in Table 1.

Steady-state boundary conditions produced travelling waves qualitatively similar to those obtained by Goldbeter [6], although the period in his study was about 3 times shorter. The direction of waves propagation were from boundary towards the center. For $V_b = 1$, the reverse was observed, and for $V_b = 7.5$, the two effects

Table 1 Effect of boundary conditions on spatial waves

Boundary Conditions	r_m [cm]	b [cm]	$\frac{b}{r_m}$	Wave Form
No Flux	0.1	0	0	None
Discrete Domain	0.1	0.1061	1.06	0
Boundary Sink ($V_b = 1$)	0.1	0.1012	1.01	-
Boundary Sink ($V_b = 7.5$)	0.1	0.1090	1.09	0
Boundary Sink ($V_b = 20$)	0.1	0.1225	1.225	+
Steady State	0.1	0	0	+

Wave Forms

- 0 = Standing Wave
- = Wave travelling from centre to boundary
- + = Wave travelling from boundary to centre

were balanced producing stable standing waves over a narrow range of V_b (7.5±0.5). Experimental studies on yeast [3,4,5] suggested a transition from one standing wave pattern to another during a cycle.

The boundary conditions which produced the best qualitative agreement with the experimental observation were the discrete domain conditions which produced standing wave patterns over a wide range of n , $42 < n < 50$, being tested. Therefore, we chose to do a more detailed analysis of the discrete domain case.

It can be seen from the inspection of equation (4) that the breakdown of α varies with γ^2 . From the bulk concentration plot (Fig.1) γ_t is significantly non-zero for only about 40% of the period, whereas α_t is always non-zero, indicating the domain in which the enzyme is inhibited and activated.

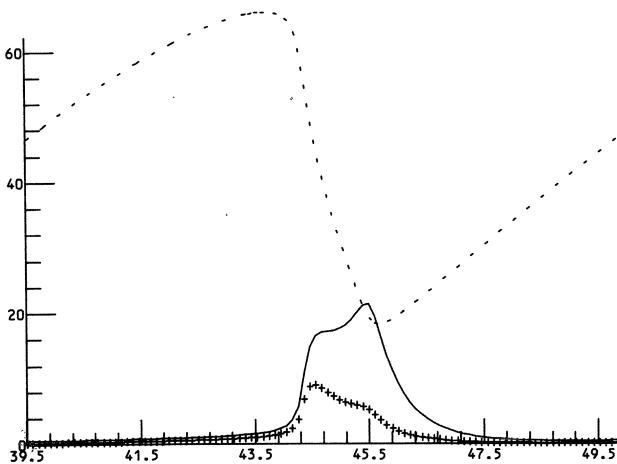


Fig.1 The dimensionless concentration parameters α_t (broken line), γ_t (plus sign), and T_r (solid line) are plotted against time in minutes.

The formation and subsequent decay of a complex three-dimensional structure in T_r is shown in (Fig. 2). T_r is plotted in x, y, z co-ordinate system making full use of the concentric circular symmetry implied in the discretization.

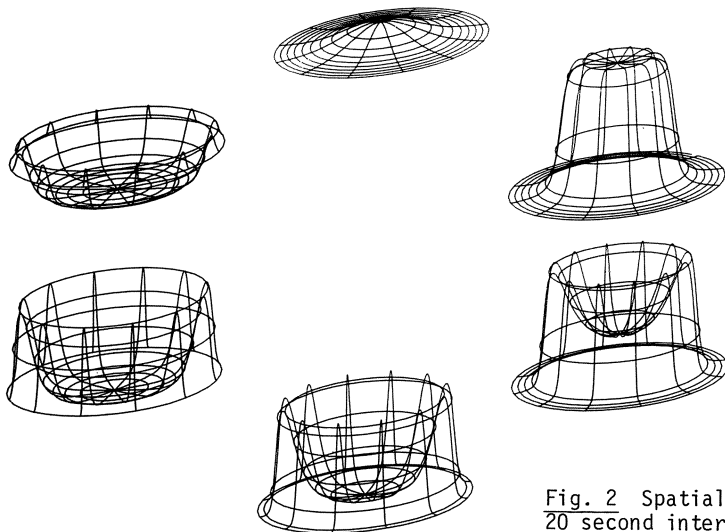


Fig. 2 Spatial Distribution of T_{r_i} at 20 second intervals (see text)

The diameter of the outer circular grid (see Fig.2) is $2b$ (0.212 [cm]) and the relative length of the x, y and z axes are 140:92:68 respectively. x and z represent distance and y concentration. The axes have not been plotted for the sake of clarity and the lines behind the surface which would not be normally visible from this perspective have not been removed. Circular grid lines are plotted every 5 mesh points and are not linearly spaced. The diameter of the second outer ring is $2r_1$ (0.2 [cm]). The distance between the grid points can be calculated from equation (5) for $i = 5, 10, 15, \dots, 45$. Six snap shots were taken at 20 second intervals from 2650 [s] (44.2 [min], Fig.1) and are displayed in a clockwise direction from the top to describe the formation of the complex structure and the beginning of its decay (Fig.2). The fully developed structure is snap shot 5 (lower left Fig.2) which occurs at 45.5 min, when the value of T_r is maximal.

The cycle may be divided into two parts, the resting portion in which $\gamma_t \approx 0$ and the active part $\gamma_t \gg 0$. In the resting portion of the cycle there are only small gradients in T_r reflected by a value of $\bar{\lambda} = 0.0310$ cm. In the active part of the cycle $\bar{\lambda}$ decreases to 0.0118 [cm] during maximum bifurcation.

The spatial distribution of λ is also of interest. The graph of λ vs. $\frac{d\alpha}{dt}$, $\frac{dy}{dt}$ vs. r yield parallel lines if no structure is present because ϕ is constant over r and $\frac{d\alpha}{dt} \neq \frac{dy}{dt}$. When a dynamic structure forms and decays, a large perturbation from parallel lines occurs. This perturbation is propagated outward from the center to the boundary as a travelling wave and when it reaches the boundary the complex structure has degenerated to its resting dish-shaped structure ready to form the complex structure in the next cycle.

These results show how allosteric enzyme kinetics can be coupled with diffusion processes to form very complex chemical structures without the need of physical compartments. In the course of evolution it is possible that rigorous chemical control could be exercised by an enzyme system before the complex physical organelles of the eukaryote cells were developed.

4. References

- 1 Belousov, B.P., Sborn. Referat. Radiats. Med. za 1958, 145, Medgiz, Moscow, (1959).
- 2 Zhabotinsky, A.M., Dokl. Akad. Nauk SSSR, 157, 392 (1964).
- 3 Boiteux, A. and Hess, B., Visualization of Dynamic Spatial Structures in Glycolytic Cell Free Extracts of Yeast. In: Dutton, P.L. and Scarpa, A., (eds) Frontiers of Biological Energetics, 789-798, Academic Press, New York (1974).
- 4 Hess, B., Boiteux, A. and Chance, E.M., Dynamic Compartmentation. In: Chapville, F. and Haenni, A.-L. (eds) Molecular Biology Biochemistry and Biophysics, 32, Chemical Recognition in Biology, 157-164, Springer Verlag Berlin, Heidelberg (1980).
- 5 Boiteux, A. and Hess, B. Spatial Dissipative Structures in Yeast Extracts Ber. Bunsenges. Phys. Chem. 84, 392-398 (1980).
- 6 Goldbeter, A., Patterns of Spatiotemporal Organization in an Allosteric Enzyme Model, Proc. Nat. Acad. Sci. USA, 70, 3255-3259 (1973).
- 7 Boiteux, A., Goldbeter, A. and Hess, B. Control of Oscillating Glycolysis of Yeast by Stochastic, Periodic and Steady Source of Substrate: A Model and Experimental Study, Proc. Nat. Acad. Sci. USA 72, 3829-3833 (1975).
- 8 Chance, E.M., Curtis, A.R., Jones, I.P. and Kirby, C.R., FACSIMILE: A Computer Program for Flow and Chemistry Simulation, and General Initial Value Problems, A.E.R.E. Harwell Report No. C.S.S. 54, H.M.S.O., London (1978).

Two Topics in Chemical Instabilities: I Periodic Precipitation Processes; II Resonances in Oscillatory Reactions and Glycolysis

John Ross

Department of Chemistry, Stanford University
Stanford, California 94305, USA

I. Periodic Precipitation Processes

In a series of experiments [1-4] we have investigated the periodic precipitation process known as Liesegang ring formation in which a sparingly soluble salt is precipitated in discontinuous bands during the diffusion of an electrolyte into a second electrolyte solution. We also performed experiments on instabilities in colloidal growth in which macroscopic structure arises from an electrolyte solution in the absence of concentration gradients. In our studies we were mainly concerned with the temporal development of Liesegang structures and the influence of the concentrations of the reagents on these spatial patterns.

A. Measurements of Temporal and Spatial Sequences of Events

We have chosen NH_4OH and MgSO_4 to form Liesegang rings of $\text{Mg}(\text{OH})_2$ precipitate in a gelatin gel, as well as KI and $\text{Pb}(\text{NO}_3)_2$ for periodic precipitation of PbI_2 in an agar gel. For the $\text{Mg}(\text{OH})_2$ system we determined a temporal sequence of events during the entire period from the start of a Liesegang experiment in a test tube to the completion of the final pattern at many locations in the tube by visual observations, and by measurements of transmitted light, of scattered light and of deflection of the transmitted light beam. By mixing the MgSO_4 with an indicator we observed and measured the motion of a pH front which corresponds approximately to an ion product three times that of the solubility product of the $\text{Mg}(\text{OH})_2$ salt. After a given interval of time following the pH front we detected the onset of a weak turbidity at any given location in the tube. Thus a broad turbidity region of colloid of $\text{Mg}(\text{OH})_2$ is established, the front of which travels along the tube and lags behind the pH front by a certain distance and time. After passage of these two fronts, which both obey a simple diffusion law, a strong change of the index of refraction occurs localized at the positions where visible rings form later.

The visual observations were reinforced by measurements with optical techniques. By combining measurements of the intensities of transmitted and scattered light as a function of time and space we confirmed that the formation of colloidal particles is continuous in space. The existence of colloidal particles is observed for a substantial interval of time prior to the next event, which is the onset of a substantial gradient of index of refraction. This gradient was measured by light deflection methods. It signals ring formation which occurs by a focussing mechanism in that the ring is formed in a space interval of a certain width which becomes narrower in time. The regions on either side of the ring become depleted in colloidal particles during the formation process as detected by light scattering. The light deflection technique also leads to the detection of the onset of homogeneous nucleation of colloidal particles. The colloid concentration close to the nucleation site is estimated to be 10^{-2} moles/liter. The particle number density ranges between 10^{15} and $10^{16}/\text{cm}^3$.

The measured sequence of events for Liesegang ring formation shows that as diffusion occurs nucleation takes place at any and all points in space where the ion product exceeds three times the value of the solubility product. Nucleation is followed in time by colloid formation, which again is continuous in space. Repeti-

tive ring formation comes about by a focussing mechanism which partially depletes the regions neighboring the ring of colloidal material and gives rise to the observed sharply defined rings of visible precipitate. We conclude that the ring formation is a post-nucleation phenomenon in that structure arises from a spatially homogeneous region of colloid a long time after nucleation has occurred. This conclusion is also supported by our experiments on the influence of gravity on the final location of PbI_2 rings in agar. The observed effect of gravity provides evidence for the existence of colloidal particles of several hundred angstroms in size for a substantial fraction of the time required for the formation of a visible structure. These experimental findings are contrary to the theories of Ostwald, Wagner, Prager and Keller in which nucleation, due to supersaturation, occurs discontinuously in space and the spatial pattern of nucleation determines the ring locations. We propose that the ring formation is associated with the autocatalytic growth of colloidal particles coupled with diffusion, as has been pointed out in connection with structures arising in the absence of macroscopic gradients.

B. Variation of Periodic Precipitation Processes with Concentration of Reactants

1. Dependence on Ion Product and Concentration Difference

We determined the influence of the variation of electrolyte concentrations (lead nitrate and potassium iodide) on the Liesegang patterns in several series of experiments with PbI_2 rings in agar gel. The concentration difference $\Delta = 1/2 [I^-] - [Pb^{++}]$ and the ion product $\sigma = [Pb^{++}] [I^-]^2$ or the quotient $S = \sigma/\sigma_0$, where σ_0 denotes the solubility product of PbI_2 , are determined to be important parameters. A simple ring spacing law is obeyed only when the number of rings is large. The experiments show the existence of a minimum value S^* , below which no ring formation takes place.

2. Spatial Bifurcation of Precipitation Bands and Stochastic Pattern Formation

Experiments on the early stages of pattern formation in a series of tubes with constant S (of the order of 10^3) and varying Δ (ranging from 0 to 0.03 M) show that after typically one day two rings appear in tubes with high Δ , one ring appears in tubes with intermediate Δ , while ring formation in the systems with lowest Δ values requires at least one week. The rings which have already formed after one day are surrounded by broad zones of PbI_2 colloid as determined by light transmission measurements. A comparison of the ring locations and the zones of colloid in tubes of different Δ suggests that an increase of Δ results in a broadening of the zones and a splitting of one ring into two well-separated rings (bifurcation of a precipitation band).

The reproducibility of Liesegang patterns is high for large Δ and S values and decreases with decreasing Δ or S . By preparing a large number of identical systems we determined the statistical distribution of ring locations. Within a set of identical systems the width of the distribution becomes larger when the ring number n increases from 1 to N . When Δ is close or equal to zero the location of rings appears to be nearly stochastic within a broad spatial region.

II. Resonances in Oscillatory Reactions and Glycolysis

Oscillatory reactions may occur in chemical and in biochemical systems sufficiently far from equilibrium [5-7]. The response of such systems to externally applied periodic perturbations produces entrainment of oscillations at the external period and higher multiples, quasi-periodic oscillations, and in certain cases chaotic motion [8]. There are a number of experimental studies on entrainment of biological and chemical oscillators. These studies include: entrainment of circadian rhythms by light and temperature cycles [9,10]; entrainment of neuronal oscillators in Aplysia by pulsed inhibitory synaptic inputs [11]; control of aggregation in Dictyostelium discoideum by an external periodic pulse of cyclic AMP [12]; resonance in the ATPase activity of insect fibrillar muscle by sinusoidal stretch and release [13,14]; entrainment of the Belousov-Zabotinsky reaction by a periodic UV irradiation [15].

In previous work [16-18], we have analyzed the entropy production, or dissipation in entrained oscillatory reaction systems below and above marginal stability. It was shown that large increases and decreases in dissipation (resonance phenomena) may occur in a very narrow range of the frequency of entrainment, which points to possible regulatory functions.

The purpose of the present article is to determine the role of this and other control features in glycolysis. We begin with a model for the glycolytic mechanism which is more comprehensive than previous ones in that it includes a larger number of known activations and inhibitions of enzymes by metabolites. We find resonance which in fact is established by a self-tuning mechanism. A more extensive presentation of our results can be found in [19-22].

A. Model

The model includes the phosphofructokinase (PFK) and pyruvate-kinase (PK) reactions, which are most irreversible steps in the pathway. The most important interactions of metabolites with enzymes are included in the model: ATP inhibition and AMP activation of PFK; FDP activation and ATP inhibition of PK. In deriving the scheme, we have lumped all the intermediate (reversible) reactions between FDP and PEP into an overall reversible reaction even though the intermediate phosphoglycerate-kinase reaction has a ΔG greater than RT.

The rate equations for the model are of the form:

input of glucose: $J_1 = J = \text{constant}$,

PFK reaction: $J_2 = v_2^m [F6P]^n / (K_2 + K_2 R_2 \frac{[ATP]^n}{[AMP]^n} + [F6P]^n)$,

FDP \rightarrow PEP reaction: $J_3 = k_3 [FDP]^\alpha - k_3^- [PEP]^\beta$,

PK reaction: $J_4 = v_4^m [PEP]^\gamma / (K_4 + K_4 R_4 \frac{[ATP]^m}{[FDP]^m} + [PEP]^\gamma)$, (1)

output of lactic acid: $J_5 = -k_5 [PYR]$,

ATP output: $J_6 = -k_6 [ATP]$.

We assume that the adenylate-kinase (AK) reaction is at equilibrium and that the total adenine nucleotide concentration remains constant. The values of the parameters appearing in the above kinetic equations can be extracted from experimental data [19]. There is substantial agreement of our calculated results with experimental findings in regard to the period of the oscillations, the periodic changes in the PFK activity, the ATP/ADP ratio as well as those in the concentrations of the intermediate metabolites. Phase shifts also are in agreement with experimental findings, except for the phase shift associated with the insufficiently represented GAPDH/PGK reactions.

B. Dissipation and Control Features in the Absence of Entrainment

The free energy dissipated in the glycolytic pathway in an oscillatory regime can be written

$$\overline{D}_{\text{osc}} = T^{-1} \int_0^T (2 J_3 + J_4 - J - J_2) (\mu_{\text{ADP}} - \mu_{\text{ATP}}) dt, \quad (2)$$

where we omit a part $J(\mu_{\text{GLU}} - \mu_{\text{LAC}})$ which is assumed constant. We analyze our model for different values of the parameter k_3 which represents the (lumped) forward rate constant for the FDP \rightarrow PEP reaction. For a range of k_3 values around the best estimates obtained from experimental data, we confirm oscillatory behavior. For a given k_3 , we further calculate the ATP/ADP ratio and the free energy dissipation (2) as a

function of the driving force for the glycolytic pathway, a measure of which is the total adenine nucleotide concentration. The model shows that the average ATP/ADP ratio is increased and the average free energy dissipation is decreased substantially in an oscillatory compared with a steady-state mode of operation [23,24]. Past marginal stability the period T_0 of the self-sustained oscillations approaches a plateau value which depends on k_3 .

We next inquire about the possibility of resonance response in glycolysis, as represented by the model system. In order to do this, we decompose the model into two coupled 2-variables subsystems (one for PFK and one for PK) and perform a linear stability analysis on each of them. The two variables necessary to describe the PFK subsystem are ATP and FDP, whereas those for the PK are FDP and PEP, the two subsystems being coupled through the variable FDP. Results obtained from our linear stability analysis of the PFK subsystem show [20] that sustained oscillations are indeed expected in the range of parameter values investigated above. In addition, the period T_{PK} of the oscillations obtained from our linear analysis is within 25% of the period T obtained by computer simulation of the full model. Thus, in agreement with previous work [25], our analysis indicates that the PFK reaction is the primary oscillophor in the glycolytic pathway. Our linear stability analysis of the PK reaction, on the other hand, shows an oscillatory relaxation (with period T_{PK}) in that, on perturbation, the reaction returns to its stable stationary state with damped oscillations. For values of k_3 around the best estimate, our analysis shows that the period of the PFK and that of PK oscillators are close and a typical ratio $T_0/T_{PK} \approx 0.72$ is observed at marginal stability. As the distance from marginal stability is slightly increased, the transitions observed in the dependence of dissipation and period on the pump parameter are seen to bring the period T_0 very close to T_{PK} . For lower values of k_3 , T_0 is much smaller than T_{PK} and no such transitions are observed.

Finally, we note that transitions similar to those observed above have been obtained for a substantial range of the other parameters. Hence, those results are not due to accidental choice of parameters. The sharp decrease in dissipation and increase in the (ATP/ADP) ratio immediately after the onset of oscillations are a result of the forced tuning of the PFK reaction by the PK reaction. The frequency of the primary oscillophor, the PFK reaction, is tuned by the PK reaction to resonance, which then allows control of dissipation and higher efficiency. Further analysis [20] shows that it is the coupling of the PFK and of the PK reactions via the FDP intermediate which leads to the resonance tuning of PFK by PK, precisely the coupling omitted in previous models.

C. Dissipation in the Presence of Entrainment

The dissipation $\overline{D_{osc}}$ in the presence of a sinusoidal variation (with period T) of the rate of glucose injection shows a large resonance effect in the fundamental entrainment band and smaller effects at higher harmonics and one subharmonic. The reduction in dissipation in the entrainment band is about 20% of the dissipation in the unstable steady state. Fundamental entrainment occurs in the range $0.85 \leq T_0/T \leq 1.25$ which agrees well with that found experimentally [26].

For small amplitudes of the external perturbation, the width of the fundamental entrainment band (on a T_0/T scale) is very small and our results on the dissipation show a single resonance peak inside that band. For larger amplitudes however, the width of the entrainment band increases and an additional resonance peak appears when T in the band reaches a value close to T_{PK} . Thus, a secondary resonance between the perturbation and the PK oscillator occurs. These secondary resonances are not observed for low values of k_3 at which the PK reaction loses its oscillatory behavior [22].

Acknowledgments

The work summarized here was done in collaboration with Drs. S. Kai, S.C. Müller and Y. Termonia. I thank them for helping in the preparation of this report.

This work was supported by the National Science Foundation and by the Air Force Office of Scientific Research.

References

1. Measurements of Temporal and Spatial Sequences of Events in Periodic Precipitation Processes. J. Chem. Phys., submitted for publication.
2. Variation of Periodic Precipitation Processes with Concentration of Reactants. Part I: Dependence on Ion Product and Concentration Difference. J. Phys. Chem., submitted for publication.
3. Variation of Periodic Precipitation Processes with Concentration of Reactants. Part II: Spatial Bifurcation of Precipitation Bands and Stochastic Pattern Formation, to be submitted to J. Phys. Chem.
4. Curiosities in Periodic Precipitation Patterns, to be submitted to Science.
5. A. Goldbeter and S.R. Caplan, Am. Rev. Biophys. Bioengin. 5, 449 (1976).
6. G. Nicolis and I. Prigogine, Self Organization in Non Equilibrium Systems, Wiley, New York (1977).
7. P.H. Richter, I. Procaccia and J. Ross, in Advances in Chemical Physics 43, 217 (1980).
8. N. Minorsky, Non Linear Oscillations, R. E. Krieger Publ. Company, Huntington, New York (1974).
9. V.G. Bruce, Cold Spring Harbor Symposium. Quantitative Biology, Biological Clocks 25, 29 (1960).
10. C.S. Pittendrigh and D.H. Minis, Amer. Natural. 98, 261 (1964).
11. H.M. Pinsker, J. Neurophysiol. 40, 527-544 (1977).
12. A. Robertson, D.J. Drage and M.H. Cohen, Science 175, 333 (1972).
13. G.J. Steiger and J.C. Regg, Pflügers Arch. 307, 1 (1969).
14. G.J. Steiger, in Insect Flight Muscle, Ed. R.T. Tregear, North Holland, p. 221 (1977).
15. A.N. Zaikin and A.M. Zhabotinsky, in Biological and Biochemical Oscillators, Eds. B. Chance, A.K. Gosh, E.K. Pye and B. Hess, Acad. Press, New York, p. 81 (1973).
16. P.H. Richter and J. Ross, J. Chem. Phys. 69, 5521 (1978).
17. P.H. Richter and J. Ross, Biophys. Chem. 12, 285 (1980).
18. Y. Termonia and J. Ross, J. Chem. Phys. 74, 2339 (1981).
19. Y. Termonia and J. Ross, Proc. Natl. Acad. Sci. 78, 2952 (1981).
20. Y. Termonia and J. Ross, Proc. Natl. Acad. Sci. 78, 3563 (1981).

21. P. Rehmus, Y. Termonia and J. Ross, Non Linear Kinetics and Dissipation with Application to Glycolysis, to appear in the Proceedings of the 10th annual meeting on Statistical Physics held in Morelos, Mexico (1981).
22. Y. Termonia and J. Ross, in preparation.
23. K. Tornheim, J. Theor. Biol. 79, 491 (1979).
24. P.H. Richter and J. Ross, Science 211, 715 (1981).
25. B. Hess and T. Plesser, Ann. N.Y. Acad. Sci. 316, 203 (1979).
26. A. Boiteux, A. Goldbeter and B. Hess, Proc. Natl. Acad. Sci. 72, 3829 (1975).

Part VIII

From Bistability to Oscillations

Bistability in a C.S.T.R.:

New Experimental Examples and Mathematical Modeling

I.R. Epstein, C.E. Dateo, P. De Kepper, K. Kustin and M. Orbán

Department of Chemistry, Brandeis University
Waltham, MA 02254, USA

1. Introduction

The ability of an open system to exhibit more than one stable state under the same set of external constraints is a classic illustration of the profound difference between open and closed systems. Until quite recently, however, the set of homogeneous systems reported to show multistability was limited to the Belousov-Zhabotinsky reaction [1] (and its cerium-bromate subsystem [2]), the Briggs-Rauscher reaction [3], and the reaction of bis(trichloromethyl)trisulfide with aniline in methanol [4].

Spurred by the fundamental connection between bistability and chemical oscillation [5], we have undertaken a search for new bistable systems, and we report here on a number of these. All of the experiments to be discussed were carried out in a continuous-flow stirred tank reactor (CSTR) thermostatted at 25°C with a range of residence times from 86 sec to infinity (batch), and in which the optical density at wavelengths between 350 and 700 nm and the potential from an ion-sensitive, pH or platinum redox electrode could be simultaneously monitored. Like chemical oscillation, predicting and understanding bistability provides a challenge to the theoretician attempting to model a chemical reaction, and we shall touch briefly on the mathematical modeling of bistable systems.

2. Bistable Systems

Thus far, six different reactions, all of them autocatalytic, have been found to exhibit bistability. We give below a brief description of each.

The reaction between arsenite and iodate is autocatalytic in the product iodide and forms part of the first systematically designed chemical oscillator [6], which was built by combining two bistable subsystems that share common intermediates. At low flow rates the system is found in a state (SSI) characterized by relatively high $[I^-]$ and $[I_2]$ in the reactor, while at higher flow rates, it undergoes a transition to a low $[I^-]$, low $[I_2]$ state SSII. For input concentrations $[IO_3^-]_0 = 1.33 \times 10^{-3} M$, $[H_3AsO_3]_0 = 2 \times 10^{-3} M$, the two states coexist over a range of residence times from about 100 to 4440 sec. DE KEPPER et al. [7] and PAPSIN et al. [8] have constructed simple models which are in excellent agreement with the experimental observations. In Fig. 1, we illustrate for both states the effects of sub- and supercritical perturbations which result, respectively,

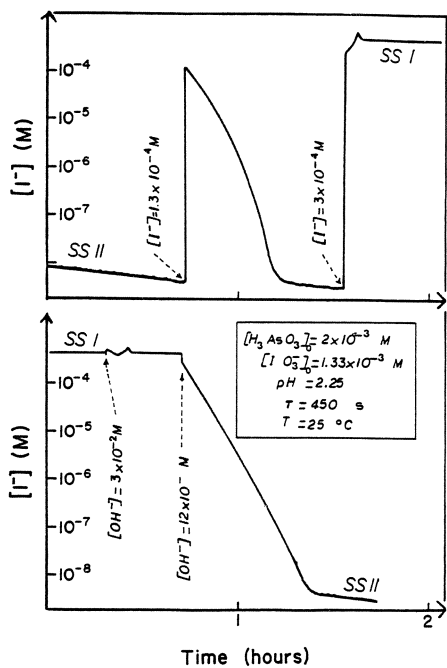


Fig. 1. Transitions between steady states of the iodate-arsenite system induced by single injections of the indicated species into the CSTR.

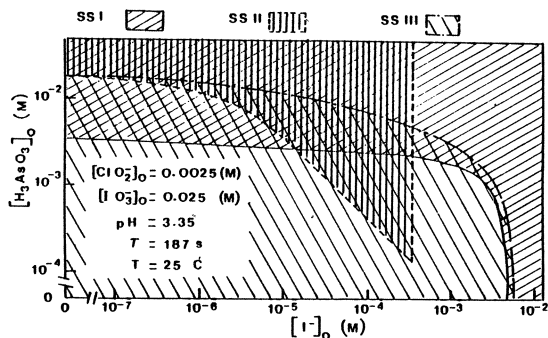


Fig. 3. Bi- and tristability in the arsenite-iodate-chlorite-iodide system.

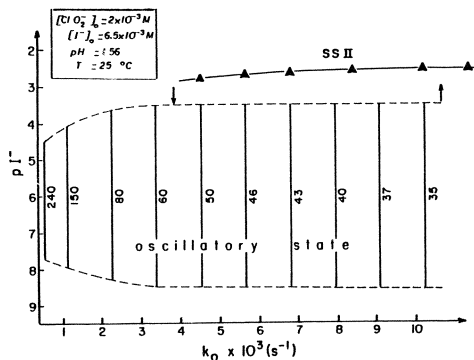


Fig. 2. Hysteresis in the transition between steady state SS II and the oscillating state of the chlorite-iodate reaction. Numbers next to vertical segments indicate period in sec.

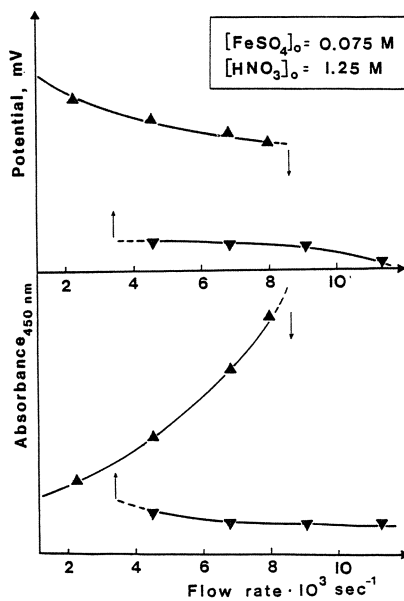


Fig. 4. Bistability in the absorbance of FeNO_2^+ and in the potential of a Pt redox electrode in the ferrous-nitrate system.

in a return to the initial steady state or in a transition to the other state.

The chlorite-iodide reaction constitutes the second half of the chlorite-iodate-arsenite oscillator [9], as well as serving as the basis for a large family of oscillators [10] involving chlorite, an iodine containing species (I^- , IO_3^- , I_2) and an appropriate oxidizing or reducing substrate. The reaction is autocatalytic in iodine. This system exhibits bistability both between two steady states and (Fig. 2) between a steady state and an oscillatory state.

A composite system containing AsO_3^{3-} , IO_3^- , I^- and ClO_2^- shows a rich variety of nonlinear behavior including oscillations and three different steady states, one resembling one of the states of the arsenite-iodate system, another similar to one of the chlorite-iodide steady states, and a third which appears to involve all of the species. As shown in Fig. 3, under appropriate values of the constraints any of the three states may be reached. We have tristability!

Chlorite and bromate undergo a clock reaction in batch and exhibit bistability in the CSTR with $[BrO_3^-] = 10^{-3}$ M, $[ClO_2^-] = 2 \times 10^{-3}$ M, pH = 0.80 for residence times between 86 and 440 sec.

At pH's between 4 and 6, chlorite and thiosulfate show bistability as a function either of pH or of flow rate. At pH 2-5 this system forms the first non-iodine containing chlorite based oscillator [11].

The reaction between Fe^{2+} and nitric acid is autocatalytic in NO. As Fig. 4 shows, bistability and hysteresis in the CSTR are easily seen by following the absorbance of the $FeNO^{2+}$ complex or the redox potential.

The permanganate-oxalate reaction, which is autocatalytic in Mn^{2+} [12], shows bistability as the residence time is varied between 187 and 374 sec for $[MnO_4^-]_0 = 0.0033$ M, $[C_2O_4H_2]_0 = 0.017$ M at a pH of about 1.

3. Mathematical Modeling

The requirement of showing bistability provides a stringent criterion for any model of a chemical reaction. To simulate a reaction in the CSTR, one must add appropriate flow terms. The rate equations then take the form

$$\frac{d\mathbf{X}}{dt} = \mathbf{F}(\mathbf{X}) + k_0(\mathbf{X}_0 - \mathbf{X}) \quad (1)$$

The vectors \mathbf{X} , \mathbf{X}_0 and \mathbf{F} contain, respectively, the species concentrations in the reactor, the input concentrations, and the chemical reaction rates, and k_0 is the reciprocal of the residence time.

The steady states can be found by equating the right hand side of (1) to zero and solving the resulting algebraic equations. A linear stability analysis can then be performed. Alternatively, one can solve the differential equations (1), which are often stiff, by an appropriate numerical method.

Ideally, the results of the calculation will agree in all respects with the experimental data. More realistically, we list some possible points of comparison with which one hopes for at least qualitative agreement:

1.) The existence and location of state to state transitions, i.e., the number of states and the values of the constraints at which the states become or cease to be stable. Such information can be conveniently represented by a "phase diagram" like that of Fig. 3.

2.) Steady state concentrations of whatever species can be monitored (e.g., Figs. 2 and 4).

3.) Sub- and supercritical perturbations. How big a change in a particular concentration is necessary to induce a transition between two states of a bistable system?

4.) Relaxation behavior. How and how rapidly does the system approach a steady state. Do we see undershoots, overshoots or critical slowing [13]? This is an area which deserves more attention and analysis.

4. Conclusion

With the recent rapid growth in the number of systems known to be bistable, we can expect bi- and multistability to become increasingly familiar phenomena to those with even a passing interest in chemical dynamics. If mechanical limitations on available flow rates can be overcome, the range of bistable systems should broaden still further. The success of a scheme [6] for designing chemical oscillators by adding a feedback to a bistable subsystem should further spur the search for more of these fascinating systems.

Acknowledgments

This work was supported by Grant No. CHE7905911 from the National Science Foundation.

1. P. De Kepper and J. Boissonade, *J. Chem. Phys.*, 75, 189 (1981).
2. W. Geiseler and H. H. Föllner, *Biophys. Chem.*, 6, 107 (1977).
3. P. De Kepper, A. Pacault and A. Rossi, *C. R. Acad. Sci. Paris*, 282C, 199 (1976).
4. J. Horak, F. Jiracek and L. Krausova, *Chem. Eng. Sc.*, 26, 1 (1971).
5. J. Boissonade and P. De Kepper, *J. Phys. Chem.*, 84, 501 (1980).
6. P. De Kepper, I. R. Epstein and K. Kustin, *J. Am. Chem. Soc.* 103, 2133 (1981).
7. P. De Kepper, I. R. Epstein and K. Kustin, *J. Am. Chem. Soc.*, in press.
8. G. Papsin, A. Hanna and K. Showalter, *J. Phys. Chem.*, in press.
9. C. E. Dateo, M. Orbán, P. De Kepper and I. R. Epstein, *J. Am. Chem. Soc.*, submitted.
10. M. Orbán, P. De Kepper, I. R. Epstein and K. Kustin, *Nature*, in press.
11. M. Orbán and I. R. Epstein, submitted for publication.
- 12.a) E. Abel, *Monatsh. Chem.*, 83, 695 (1952);
b) S. J. Adler and R. M. Noyes, *J. Am. Chem. Soc.*, 77, 2036 (1955).
13. M. Heinrichs and F. W. Schneider, *Ber. Bunsenges. Phys. Chem.*, 84, 857 (1980).

Chlorite Oscillators: A Result of the Cross-Shaped Phase Diagram Technique

P. De Kepper

Department of Chemistry, Brandeis University, Waltham, MA 02254, USA and
Centre de Recherche Paul Pascal (CNRS), 33405 Talence Cedex, France

1. Introduction

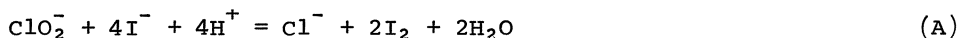
The number of fundamentally different known homogeneous isothermal chemical oscillating reactions is very small. In spite of intensive efforts in the last two decades to design new oscillators, only two nonbiological systems, both discovered by accident, have been well characterized: the Bray-Liebhascky [1] (B-L) and the Belousov-Zhabotinsky [2] (B-Z) reactions. The array of known oscillators has been augmented essentially by variation [3], and hybrids [4] of the above two reactions. The ability of chemists to test and develop general theories of chemical dissipative structures [5] has been somewhat hindered by this paucity of examples. Since no set of sufficient conditions to generate nonlinear oscillators is known, any practical method that can be used as a guideline in the discovery of new oscillators should be of considerable interest. We have recently presented such a systematic approach [6] and have successfully applied it to reveal a new family of chemical oscillators [7].

2. The Cross-Shaped Diagram Technique

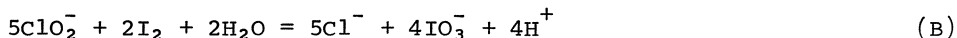
The method starts with the determination of bistability phenomena by studying autocatalytic reactions in a continuous stirred tank reactor (CSTR). The CSTR guarantees that the system is maintained far enough from equilibrium, a necessary condition for both bistability and sustained oscillations. Then, the results of a simple dynamical model developed by BOISSONADE and DE KEPPER [8] are used. They show that sustained oscillations can arise from the association of an intrinsically bistable system with a relatively slow feedback step which shifts the stability region of each branch of the bistable system and creates, as the amplitude of the feedback increases, a region of constraint where both branches become unstable. Sections of the phase diagram involving a constraint controlling the relative amplitude of the feedback will then exhibit a cross-shaped form [8] where the region of bistability gradually decreases and gives place to a domain of sustained oscillations. Referring to this characteristic topological feature, the experimenter can easily direct his search in the constraint space.

3. Application to Chlorite-Iodide Systems

The chlorite-iodide reaction is a spectacular clock reaction, the initial stage of which is characterized by process A:



This process is activated by its product I_2 (autocatalysis) and inhibited by iodide [9,10]. If chlorite is in excess, the iodine is further oxidized to iodate in the rapid process B:



3.1 CSTR results. In a CSTR the chlorite-iodide reaction exhibits bistability (Fig. 1) between a low (SSI) and a high (SSII) iodide state. Figure 2a shows a section of the bistable domain in the chlorite-iodide constraint space. Points P and P' terminate the bistable region respectively at high and low $[\text{ClO}_2^-]_0$ and $[\text{I}^-]_0$. Beyond P' only continuous changes from SSI and SSII are observed. Under these experimental conditions, point P could not be reached because of iodine precipitation perturbing the system. Applying the method, a feedback reaction was sought to modify the region of stability of SSI and/or SSII as a function of iodide. Iodate appeared to be the most natural species to introduce, since it reacts with iodide to produce iodine, a chemical species capable of destabilizing SSII. Figure 2b shows the

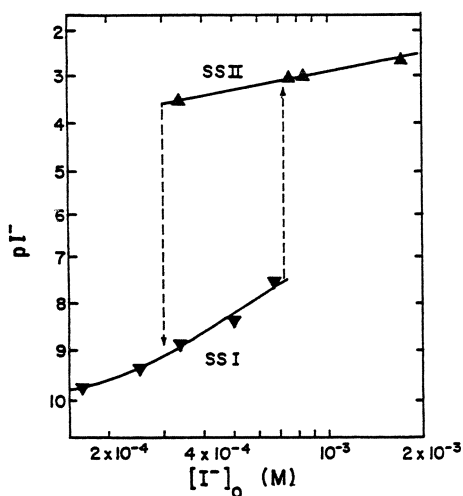


Fig. 1. Hysteresis phenomena in the iodide steady-state concentration as a function of the iodide inlet flux $[\text{I}^-]_0$. All other constraints are maintained constant: $[\text{ClO}_2^-]_0 = 2.5 \times 10^{-4} \text{ M}$, $\text{pH} = 3.35$, residence time 187 s and $T = 25^\circ\text{C}$.

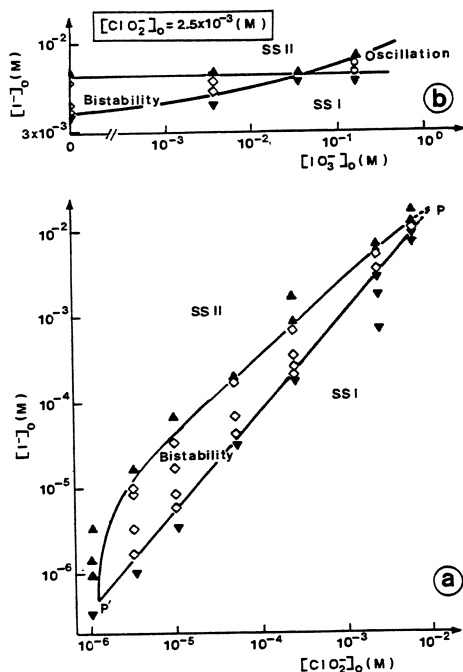


Fig. 2. (a) Section of the bistability domain in the $[\text{ClO}_2^-]_0$ - $[\text{I}^-]_0$ plane. (b) Cross shaped phase diagram obtained at fixed chlorite by addition of an iodate flow. All other constraints as in Fig. 1.

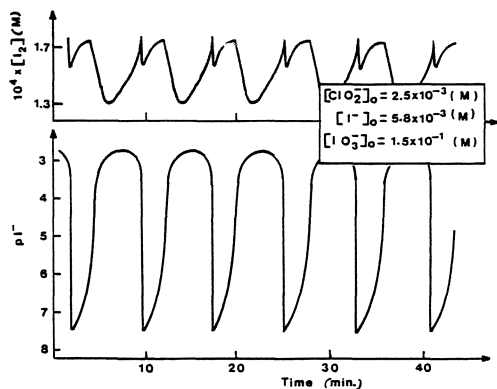


Fig. 3. Iodine and iodide concentrations vs. time in the oscillating state (Fig. 2b).

resulting phase diagram in the $[\text{IO}_3^-]_0$ - $[\text{I}^-]_0$ phase plane with fixed $[\text{ClO}_2]_0$. Beyond $[\text{IO}_3^-]_0 = 5 \times 10^{-3}$ M, the bistable region vanishes and gives place to a domain of large amplitude sustained oscillations as shown in Figure 3. This system constitutes the first methodically devised chemical oscillator. Remarkably, it involves only halogen species and seems to be a much "cleaner" system than many other known oscillators since it is not associated with any macroscopic gas evolution nor insoluble products.

Further studies of the phase diagram revealed that, for a lower pH and longer residence time than in Figure 2a, point P can be reached, and oscillations are also observed beyond this point in the absence of additional iodate input flow [11].

Many other oscillating variants of the chlorite-iodide-iodate system have been discovered. Iodide can be replaced by a number of one and two electron reducing substrates [6,7], such as: arsenite, thio-sulfate, sulfite, ascorbic acid or ferrocyanide ions, while iodate can be exchanged for other oxidizing species such as bichromate, peroxydisulfate or bromate.

3.2 Batch oscillations. All the previously enumerated systems only give rise to oscillations in a CSTR, i.e. oscillations cease as soon as the inlet flow is stopped. It was felt that in order to produce oscillations in batch, some chemical steps simulating a flux of iodine, in the oxidation state -1, 0 or +1, should be introduced. This was first achieved by adding a chlorite solution to a freshly prepared iodomalonic acid solution containing iodate (iodomalonic acid solutions readily decompose at room temperature). In a beaker, some of these compositions [12] can exhibit 50 or more rapid potential oscillations on a platinum electrode. The most dramatic results are obtained by mixing in a 10^{-2} M sulfuric acid solution $[\text{CH}_2(\text{COOH})_2] = 2.6 \times 10^{-3}$ M, $[\text{I}^-] = 6.6 \times 10^{-3}$ M and $[\text{ClO}_2] = 7 \times 10^{-3}$ M, in this order. In the presence of starch this composition exhibits, after a short induction, period a dozen orange-blue alterations.

3.3 Spatial structure. Since the iodide concentration varies by a factor of more than 10^5 during each oscillation, marked excitability phenomena could be expected and thus wave structure propagation should

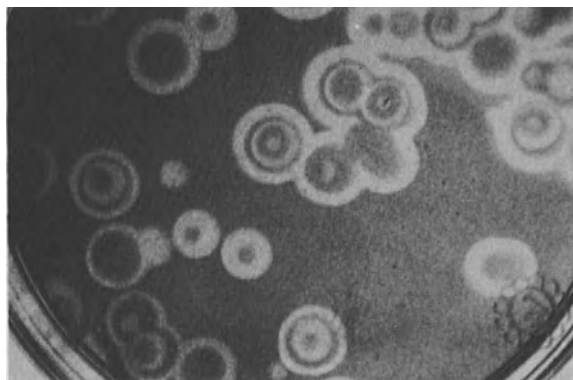


Fig.4. Spontaneous wave patterns observed at 5°C at a thin layer (2mm) of reaction solution with initial composition $[\text{CH}_2(\text{COOH})_2] = 0.0033 \text{ M}$, $[\text{I}^-] = 0.09 \text{ M}$, $[\text{ClO}_2] = 0.01 \text{ M}$, $[\text{H}_2\text{SO}_4] = 0.0056 \text{ M}$ and starch.

be observed in unstirred solution, as in the BZ reaction. Figure 4 shows the expected wave pattern triggered at many different pace-makers. Waves here appear as pale yellow rings migrating through a violet-blue solution [12]. These waves generally travel faster than their analogue in the BZ reaction, but the solution loses its propagation properties after only a few minutes.

4. Conclusion

It is hoped that the success of the cross-shaped phase diagram technique in devising a new family of chlorite oscillators and the increase in the number of bistable systems [13] will contribute to the multiplication of fundamentally different chemical oscillators. The method described here is probably not unique and more efforts should be devoted to practical approaches to chemical dissipative structures.

Acknowledgment

This work was carried out while the author was on sabbatical at Brandeis University, thanks to the Centre National de la Recherche Scientifique and to a grant (CHE 7905911) from the National Science Foundation. I would also like to thank C. Dateo and Dr. M. Orbán for their considerable assistance and Professors I. R. Epstein and K. Kustin for helpful discussions.

References

1. W. C. Bray, *J. Am. Chem. Soc.*, **43**, 1262 (1921); H. A. Liebhasky, W. C. Gavock, R. J. Reyes, G. M. Roe and L. S. Wu, *J. Am. Chem. Soc.*, **100**, 87 (1978).
2. J. J. Tyson, *Lecture Notes in Biomathematics No. 10* Springer-Verlag, Berlin, Heidelberg 1976.
3. R. M. Noyes, *J. Am. Chem. Soc.*, **102**, 4644 (1980).
4. T. S. Briggs and W. C. Rauscher, *J. Chem. Educ.*, **50**, 496 (1973).

5. G. Nicolis and I. Prigogine, *Self-organization in nonequilibrium systems*, Wiley-Interscience, New York (1977).
6. P. De Kepper, I. R. Epstein and K. Kustin, *J. Am. Chem. Soc.*, 103, 2133 (1981).
7. M. Orbán, P. De Kepper, I. R. Epstein and K. Kustin, *Nature*, in press.
8. J. Boissonade and P. De Kepper, *J. Phys. Chem.*, 84, 501 (1980).
9. D. M. Kern and C. H. Kim, *J. Am. Chem. Soc.*, 87, 5309 (1965).
10. J. De Meeus and J. Sigalla, *J. Chim. Phys.*, 63, 453 (1966).
11. C. E. Dateo, M. Orbán, P. De Kepper and I. R. Epstein, *J. Am. Chem. Soc.*, submitted.
12. P. De Kepper and I. R. Epstein, *J. Phys. Chem.*, submitted.
13. I. R. Epstein, C. E. Dateo, P. De Kepper, K. Kustin and M. Orbán
this volume.

A New Type of Chemical Oscillator: Potential Oscillation and Bistability on a Platinum Electrode in some Aqueous Hydrogen-Halogen (ATE) Pumped Systems

Miklós Orbán^{1a,b} and Irving R. Epstein^{1b}

Institute of Inorganic and Analytical Chemistry
aL. Eötvös University, H1443 Budapest and

bDepartment of Chemistry, Brandeis University, Waltham, MA 02254, USA

Introduction

Reviews on homogeneous [1], heterogeneous [2] and electrochemical[3] oscillating systems have emphasized the need to explore new classes of oscillators in order to learn more about the processes which govern oscillatory behavior.

In a recent paper [4] we reported on sustained oscillation and bistability in the potential of a platinum electrode immersed in an aqueous sulfuric acid solution of bromate, iodate or chlorite when a continuous stream of hydrogen gas is pumped through the solution. We report here that oscillation and bistability also occur if the halogenate solution is replaced by a flow of an acidic bromine or chlorine solution into a stirred tank reactor (CSTR).

Several examples of oscillatory reactions involving H₂ gas and platinum are known. BELYAEV et al. [5] and WICKE et al. [6] find oscillation in the gas-phase reaction between H₂ and O₂ in the presence of Pt wire, foil or pellets. THALINGER and VOLMER [7] describe current oscillations, while ARMSTRONG and BUTLER [8] observe oscillations in potential at bright Pt during the electrochemical oxidation of H₂ in a dilute H₂SO₄ solution.

The systems reported here represent a new type of oscillator because the halogen or halogenate plays an essential role in the oscillation and because the experimental conditions are rather different from those of known heterogeneous oscillators. No heterogeneous oscillations involving halogens at metal surfaces have previously been reported. Furthermore, these new oscillations proceed in aqueous solution at room temperature without the imposition of any external current or voltage on the platinum plate.

Experimental Results

The experiments involving halogenate solutions have been described in [4]. For the halogens, solutions were flowed into a stirred thermostated (25°C) CSTR of 30 cm³ volume by a peristaltic pump, while H₂ gas was bubbled in through a capillary tube. The potential change of a bright Pt plate electrode (surface area, 2 cm²) vs. Hg|HgSO₄|K₂SO₄ reference electrode was monitored by a high impedance chart recorder.

Depending upon the values of several constraints, the potential of the Pt electrode can take on (a) a steady high value near that of the pure halogen solution; (b) a steady low value slightly above that of a hydrogen electrode; (c) either potential (a) or (b) under the same constraints (bistability); or (d) sustained periodic oscillation, roughly between the potentials in (a) and (b). The most important constraints determining which state is reached are: concentration of halogen(ate), surface area of the Pt electrode, flow rate (residence time) in the reactor, intensity of the H₂ gas stream, and acidity of the solution. Less important constraints which may also influence the stability of the various states are temperature, stirring speed and rate of evaporation of volatile species.

Detailed results on the halogenate-H₂-Pt systems are presented in [4]. For the halogen systems only crude limits of bistability and oscillation have been established so far. However, even these preliminary results clearly show the existence of both phenomena with flow solutions containing either bromine or chlorine in a concentration range of about 10⁻⁴ M-10⁻² M in 1 M sulfuric acid. Figures 1a and 1b illustrate sustained oscillations in solutions containing bromine and chlorine, respectively. Bistability is found in these systems near the limits of concentration and residence times that give rise to oscillations. Transitions between the two bistable states can be induced by transient application of an appropriate potential to the Pt electrode. With iodine, oscillations and bistability have not been observed, even at very low [I₂] (<10⁻⁵M), presumably because of the extremely strong adsorption of iodine on platinum.

Discussion

Several models have been proposed for heterogeneous, isothermal oscillations and/or bistability in gas-solid systems. These models can easily be adapted to the experiments treated here, and we present some simple calculations after first pointing out the essential similarity of the principal models.

The three most successful schemes, the surface coverage dependent activation energy (SC) model, the vacant site (VS) model and the phase transition (PT) model, all involve the adsorption of the two reactive species onto the surface followed by reaction on the surface to form a product which rapidly desorbs. In the SC model [9], the rate of the reaction at temperature T is given by

$$V_r = k_r^0 \exp(-E^0/RT + u\theta_B) \theta_A^{n_A} \theta_B^{n_B} \quad (1)$$

where k_r^0 is a constant, E^0 is an activation energy, u is an inhomogeneity factor, θ_A and θ_B are the fractional coverages of the surface by adsorbed species A and B, respectively, and n_A and n_B are stoichiometric factors. The VS model [10] assumes that two neighboring empty sites are required in order for A and B to react, and thus replaces the exponential term in (1) by the term $(1-\theta_A-\theta_B)^2$. In the PT model [11] one postulates that above a certain threshold value of θ_B , the metal surface undergoes a transition to another form (e.g., an oxide) with an abrupt change in the rate constant for the reaction step and possibly for adsorption and desorption as well.

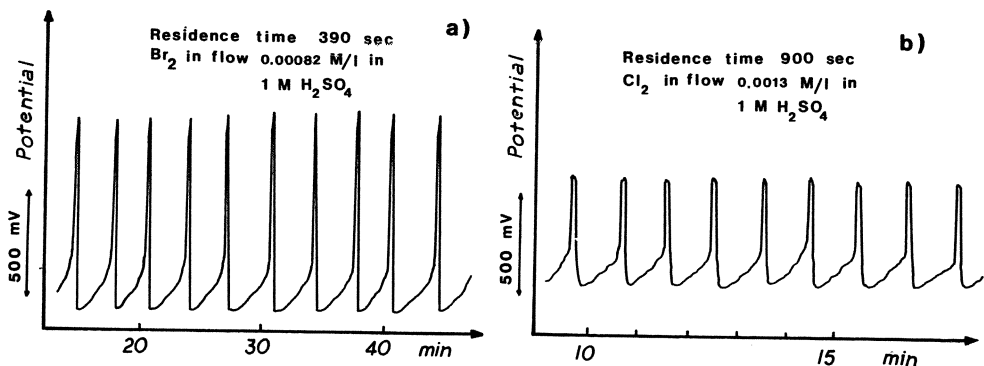


Fig. 1. Oscillations observed in the potential of a Pt electrode in (a) a Br₂-H₂ and (b) a Cl₂-H₂ pumped system.

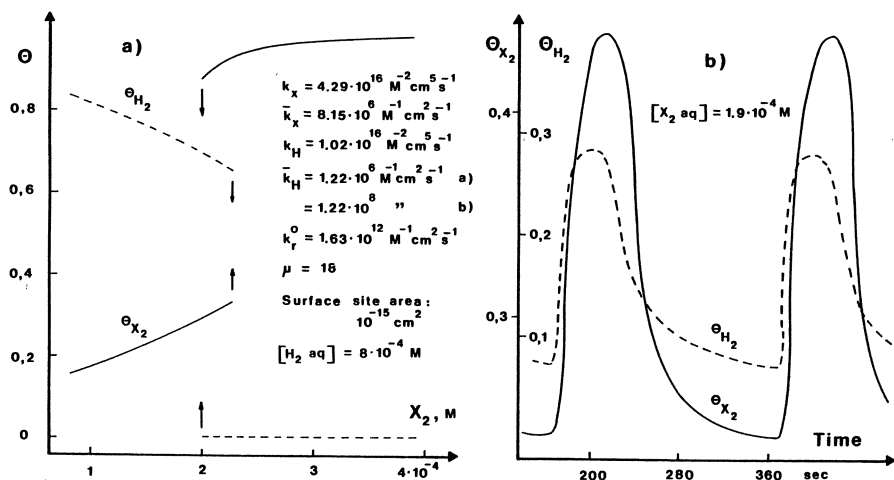
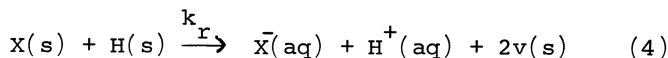


Fig. 2. Bistability (a) and oscillations (b) calculated using the SC model (1)-(4).

Thus, (1) contains no exponential or vacant site factor, but k_r is replaced by k_{r1} for $\theta_B < \theta_{crit}$ and by k_{r2} for $\theta_B > \theta_{crit}$.

On closer analysis, one observes that all three models generate oscillation by means of a common destabilizing element. In each case, the rate of reaction, and hence of removal of B from the surface, decreases as θ_B increases, thus providing an autocatalytic feedback on θ_B . We show in Figure 2 the results of a calculation using the following SC model for the X₂-H₂ (X = Br or Cl) system:



where (s) represents surface site, (aq) aqueous, v a vacant site, and k_r has the form given in (1) with $A = X_2$, $B = H_2$, $n_A = n_B = 1$. The aqueous concentrations of hydrogen and halogen are assumed constant. The value taken for μ , though high, appears consistent with similar "inhomogeneity factors" found for the adsorption of organic species on platinum surfaces by BAGOTZKY and VASSILIEV [12].

The model studied here can produce oscillations and/or bistability for any value of $u > 16$. High values of \bar{k}_H/\bar{k}_X appear to promote oscillation, while lower values tend to favor bistability. Similar results may be obtained for the other types of model. Unfortunately, establishing values for the parameters in our model or distinguishing among the models discussed above is not an easy task. Monitoring the state of a surface which has several adsorbed species and is in contact with a concentrated aqueous solution will not be straightforward, though application of rotating disk electrodes as well as recent advances in surface spectroscopic techniques may prove worthwhile.

Acknowledgments

This work was supported by National Science Foundation Grants CHE7905911 and PCM 7925375. We thank Dr. Patrick DeKepper and Prof. Richard M. Noyes for their helpful suggestions.

References

1. R. M. Noyes, J. Am. Chem. Soc., 102, 4644 (1980).
2. M. Sheintuch and R. A. Schmitz, Catal. Rev. - Sci. Eng., 15, 107 (1977).
3. J. Wojtowicz, in Modern Aspects of Electrochemistry, J. O'M. Bockris and B. Conway, eds. (Plenum: New York) 1973, vol. 8, pp 47-120.
4. M. Orbán and I. R. Epstein, J. Am. Chem. Soc., 103, 3723 (1981).
5. V. D. Belyaev, M. M. Slinko and M. G. Slinko, Proc. 6th Int. Congr. on Catalysis, London, 1976, Preprint B-15.
6. H. Beusch, P. Feiguth and E. Wicke, Adv. Am. Chem. Soc. Symp. 509, 615 (1972).
7. M. Thalinger and M. Volmer, Z. phys. Chem., 150, 401 (1930).
8. G. Armstrong and J. A. V. Butler, Disc. Faraday Soc., 1, 122(1947).
9. E. A. Ivanov, G. A. Chumakov, M. G. Slinko, D. D. Bruns and D. Luss, Chem. Eng. Sci., 35, 795 (1980).
10. C. G. Takoudis, L. D. Schmidt and R. Aris, Surface Sci., 105, 325 (1981).
11. L. Riekert, Ber. Bunsenges. Phys. Chem., 85, 297 (1981).
12. V. S. Bagotzky and Y. B. Vassiliev, Electrochim. Acta, 11, 1439 (1966).

Constrained and Continuously Pumped Chemical Systems with Emphasis on Conditions for Bistability

Richard M. Noyes

Department of Chemistry, University of Oregon
Eugene, OR 97403, USA

Science owes more to the steam engine
than the steam engine owes to science

Lawrence J. Henderson [1]

1. Introduction

This Conference is the second in three years at the Centre de Recherche Paul Pascal. The first was titled "Lois de l'Equilibre" and the second "Phénomènes non-linéaires". These excellent titles designate the major areas of theory as chemists attempt to develop general procedures for treating that most difficult of subjects - the living organism as a chemical system. We may get some guideposts for that attempt by looking briefly at the evolution of some of our ideas for treating simpler chemical systems.

The steam engine referred to above represents the first use of chemical change to perform useful¹ work. It was invented and developed by clever engineers before the concepts of thermodynamics existed. Only later did scientists recognize the utility of describing all interactions between a system and its surroundings in terms of the interchange of two conserved entities called matter and energy. Interchange of energy was further divided into mechanical work, electrical work, and heat flow².

¹ The first deliberate use of chemical change was probably to warm a cave. The first use to perform work was probably at the Battle of Crécy. It remains a value judgment as to whether the first uses of chemical (1346) and nuclear (1945) change to generate force were "useful".

² Emission or absorption of electromagnetic radiation can be treated as heat flow if only first law relations are involved. Second law relations are not relevant unless the spectral distribution coincides with that of black body radiation at the temperature of the system.

2. Constrained Chemical Systems

Chemical thermodynamics has developed almost entirely for systems that do not change their positions in any fields (gravitational, electrical, or magnetic), and those fields are assumed to remain invariant. We shall maintain those restrictions and the additional one that any mechanical work is associated with the interaction of a changing volume with an external force³.

It has also usually been assumed that in chemical systems each of the four possible types of interchange is either prohibited entirely or is restricted by the effects of a constant applied potential. Such a system is said to be constrained. The various types of constrained systems and the processes in them are summarized in Table I.

Table I
Classification of Chemical Systems (and Processes)
Associated with Possible Types of Constraints

Type of Interchange	Flux Prohibited	Constant Potential
Energy Flux		
Mechanical Work	Constant Volume ³ (isochoric)	Constant Pressure (isobaric)
Electrical Work	Electrically Insulated	Constant Voltage
Heat Flow	Thermally Insulated (adiabatic)	Constant Temperature (isothermal)
Matter Flux	Closed	Constant Chemical Potential ⁴
Matter <u>and</u> Energy Flux	Isolated	

If all of the possible flux types are constrained, a system will decay with time to a unique invariant state called chemical equilibrium. An important characteristic of the equilibrium state is that every phase is uniform and without gradients in composition. The path followed in the decay to equilibrium need not be unique, but one of the great conceptual advances in chemistry was the construction of

³A spring-driven watch is not a "chemical" system in this sense.

⁴Examples are an oxidation-reduction reaction in a solution saturated with air or a protolytic reaction in a system separated by an acid-permeable membrane from a large volume of buffer solution.

state functions like entropy and Gibbs free energy. Such a function can be developed in principle for any combination of the constraints of Table I. For any conceivable state of the system and for any possible path through that state, the sign of the change of such a state function unequivocally determines the direction in which change will occur. The state function acts as a potential that directs the system monotonically toward the ultimate equilibrium state. However, although thermodynamics⁵ is very valuable because it dictates the direction of change in any constrained system, it tells nothing about the rate of that change.

3. Pumped Chemical Systems

3.1 Nature of Pumped Systems

No living organism can be approximated for long as a constrained chemical system. We must include fluxes other than those associated with maintenance of the constraints of the right column of Table I. Chemical dynamics will no longer be irrelevant to direction of change, and rate of change of state functions will become a significant factor in our considerations. If such additional fluxes exist, we shall say the system is pumped.

Pumping may be associated with any of the four possible types of interchange in Table I. Often, but not necessarily, any flux of matter or energy entering the system will be balanced by an equal flux leaving it so that the total mass, energy, and elemental composition remain constant. Even when entering and leaving fluxes are thus equal in magnitude, they are not usually equal in kind.

3.2 Temporal Classification of Pumped Systems

One convenient classification is according to the variation of pumping with time. Such a classification recognizes pulsed, periodic, and continuous pumping.

Pulsed pumping can be illustrated with flash photolysis. A burst of matter or energy is introduced rapidly, and the subsequent evolution of the system is followed. Shock waves illustrate another type of pulse pumping.

Periodic pumping may involve successive pulses repeated at regular intervals. Input of pumped energy may also approximate a sine function. Periodically pumped systems need not be uniform in composition, and standing or traveling waves may develop.

⁵ Relations in constrained systems might better be called "thermostatics", but usage is too well established to try to change convention.

Continuous pumping maintains constant fluxes both entering and leaving the system. Periodic and continuous pumping need not be clearly differentiable, and the periodic nature of the pumping may be ignored if the period is short compared to any relaxation times of importance to the dynamics of the system.

3.3 Engines as Closed Energy-Pumped Systems

Often a convenient system to consider is one in which the excess flux is only matter or only energy while any flux of the other is subject to the constraints of Table I. The first major triumph of thermodynamics involved just such a system. The Carnot engine is a closed system for which the pumping energy flux is restricted to mechanical work and heat flow. The restrictions on relative values of those fluxes launched the whole subject of thermal efficiencies of heat engines.

3.4 The CSTR as an Energy-Constrained Matter-Pumped System

All living organisms are matter-pumped⁶ systems. We have already seen how the steam engine was an important technical device whose study provided the base from which came the whole subject of thermodynamics⁵ of closed chemical systems. Another technical device has been familiar to engineers for years but has been ignored by most scientists. That device is the continuously stirred tank reactor (CSTR).

In such a reactor, chemicals of high energy are added at a constant rate, and material is removed at the same rate from the homogenized contents of the reactor. Energy fluxes are determined by typical constraints of Table I which are usually electrically insulated⁷, constant temperature, and constant pressure.

Such a system eventually settles to a condition in which total mass, total energy, and elemental composition maintain constant time averages. However, that condition may or may not be invariant in time. If it is indeed invariant, the reactor is said to be in a stationary state whose free energy is clearly definable. However, the free energy is not a local minimum the way it is for the unique stationary state corresponding to equilibrium in the constrained system. In fact, stationary state composition in the CSTR need not be a unique function of pumping rate. If two stationary states do exist for the same pumping rate, the direction of spontaneous transition may involve either an increase or a decrease of system free energy [2] and may depend upon the way in which the system is perturbed [3]. The thermodynamic⁵ restrictions on constrained systems obviously do not apply.

⁶Of course green plants are also energy pumped.

⁷Potentiometric methods of analysis do not seriously perturb the constraint of assumed electrical insulation.

If the final condition is not time invariant, the composition of the reactor contents may vary through large amplitudes. Even when these variations are regularly periodic, the pattern may be very complicated. It does not yet seem to be established whether or not truly chaotic behavior is possible [4].

4. Possibilities for Bistability in a CSTR

This manuscript will conclude by considering a CSTR constrained to constant temperature and pressure and exhibiting a region of two different stationary states for the same pumping conditions. It is convenient to describe possible conditions with a $G-\phi$ phase plane as in Fig. 1. Here G is the Gibbs free energy per unit mass of reactor contents and ϕ is the pumping rate described as the reciprocal of average residence time of any material in the reactor. Although Fig. 1 implies that two parameters are sufficient to describe the system, reactor composition is not necessarily a unique function of G . Therefore, a full description of the system might require several dimensions.

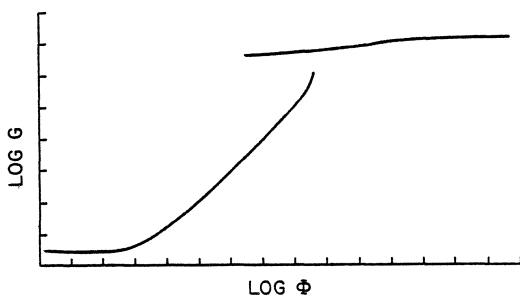


Fig. 1. Example of bistability in a CSTR. Abscissa is logarithm of pumping rate in volume per unit time, and ordinate is logarithm of free energy of reactor contents. Lower curve is equilibrium branch, and upper is rapidly pumped branch.

The minimum possible free energy in the system will be that of the equilibrium composition attained with zero pumping rate; no other state can persist in the unpumped system. The maximum possible free energy will be the stationary state corresponding to indefinitely large pumping rate and corresponding to reagents mixed without any reaction; as pumping rate increases, all system compositions must approach this state. Of the two curves in Fig. 1, the equilibrium branch extrapolates smoothly to zero pumping rate, and the rapidly pumped branch extrapolates to indefinitely large pumping rate.

Figure 1 is drawn so that for pumping rates at which two stationary states are possible the rapidly pumped branch has a larger free energy than the equilibrium branch. We have proved [5] that such a free energy difference will be found if the system can truly be described by the two dimensions of Fig. 1. Such a difference also seems to apply to all known experimental examples. Although we cannot prove the assertion, we anticipate that no exception will be found

just as we anticipate that nobody will ever find a liquid that freezes reversibly when its temperature is raised at constant pressure!

A corollary of that conclusion can be stated as follows: "If the pumping rate is varied indefinitely slowly and eventually returned to its original value, the trajectory in the Φ -G plane will either be a segment of a single curve or a loop traversed in the counter-clockwise direction." This assertion is similar to the familiar one for a closed isothermal system: "If any overall process eventually returns the system to its original state, any net fluxes will be such that electrical and/or mechanical work will have been done on the system and heat will have been evolved." The ultimate justification for that statement is only that nobody has ever found a statistically valid exception.

5. Concluding Remarks

The examination of constrained systems led in unanticipated ways to general principles of great value to understanding the behavior of closed chemical systems. Those thermodynamic⁵ principles are of only limited value for treating matter-pumped systems. However, there is at least a suggestion that some general principles do exist for matter-pumped systems. The further study of those principles may be very valuable for examining systems of greater complexity even though the extrapolation of a CSTR to a living bacterium must be at least as great as that from a Carnot engine to a fuel cell.

Acknowledgment. The development of these ideas was supported in part by a Grant from the United States National Science Foundation.

References

1. H. L. Burstyn: In "The History and Philosophy of Technology", ed. by G. Bugliarello and D. B. Doner, University of Illinois Press (1979), p. 62
2. R. M. Noyes: J. Chem. Phys. 71, 5144 (1979)
3. R. M. Noyes: J. Chem. Phys. 72, 3454 (1980)
4. N. Ganapathisubramanian, R. M. Noyes: J. Chem. Phys. (submitted)
5. R. M. Noyes: Proc. Nat. Acad. Sci. USA (manuscript in preparation)

Perturbation of Bromate Oscillators

Endre Körös, Margit Varga and Galina Putirskaya*

Institute of Inorganic and Analytical Chemistry
L. Eötvös University, Budapest

*Central Research Institute for Chemistry, Budapest, Hungary

1. Introduction

Bromate oscillators have been investigated from many aspects. One of the aims has been to reveal the chemical prerequisites of the oscillatory behaviour. Some quantitative results have been already published [1]. The bromate oscillators can be perturbed, e.g. by the addition of inhibitory property halides [2,3], by the supply of O₂ [3-6]; by keeping low the bromide concentration (addition of Ag⁺) [7]; or by γ -irradiation of the reacting system [8]. From the effect the perturbation exerts on a bromate oscillator, important information can be gained on the chemical mechanism of the oscillatory reaction.

Here we report briefly on some novel findings and quantitative data in respect to three different perturbations:

a/ irradiation with ⁶⁰Co γ -rays of some bromate oscillators of different catalysts. (A critical examination of [8].)

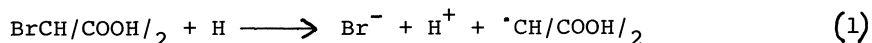
b/ addition of iodide to some catalyzed and uncatalyzed bromate oscillators. The main aim was to reveal the chemistry during the high frequency preoscillations.

c/ the addition of Tl/III/ ion. This ion forms soluble bromocomplexes of high stability and thus its presence in the reacting oscillatory system considerably influences the actual free bromide concentration and through this the course of the reaction.

2. Perturbations

2.1 Perturbation by γ -Irradiation

RAMA RAO and PRASAD [8] have investigated the effect of ⁶⁰Co γ -irradiation on the "classical" BZ system [bromate, malonic acid, sulphuric acid and Ce/III/] and found that depending on the composition of the reaction mixture, the oscillation terminated either immediately after the start of irradiation or only a certain period of time after it. They explained the oscillation-quenching effect by assuming that after the accumulation of a certain amount of bromomalonic acid (BrMA) one of the radiolysis products of water - the hydrogen atom - reacts with it, generating bromide ion.



and thus a higher-than-critical bromide concentration is sustained throughout the irradiation.

We doubted the important contribution of (1) to the overall process and therefore looked again at this problem also comparing the effect of γ -irradiation on BZ systems of different catalyst [Ce³⁺, Mn²⁺,

Fe/phen/ 2^+ , and Ru/dipy/ 3^+]. The oscillatory systems were irradiated from a ^{60}Co radiation source of 6×10^{13} Bq output at two dose rates: 2.74×10^{18} eV dm^{-3} s^{-1} and 1.37×10^{18} eV dm^{-3} s^{-1} , resp. The overall chemical reaction was followed by measuring the decrease of the total oxidation power of the reaction mixture. Fig. 1 shows typical experimental curves.

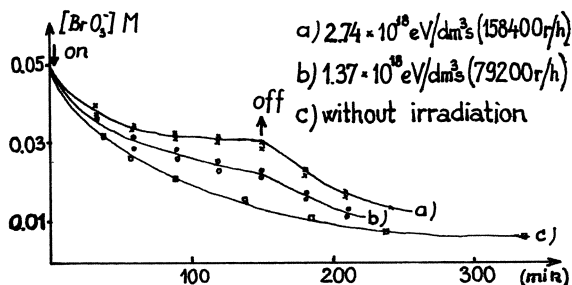


Fig. 1. The decrease of bromate concentration in time in a system with the composition: 0.05M KBrO_3 , 0.20M malonic acid, 1.0M H_2SO_4 and 0.002M $\text{Ce}/\text{IV}/$.

We also measured both the radiation-induced and the spontaneous hydrolytic decomposition of BrMA. The obtained values (0.9×10^{-7} and 2.0×10^{-7} M s^{-1} , resp.) are very close to each other.

The behaviour of a BZ reacting system on γ -irradiation depends also on the bromate concentration. At high initial bromate concentrations (above 0.1M) γ -irradiation has no effect on the chemical oscillation irrespectively of the catalyst used. At lower bromate concentrations the oscillation is either quenched or considerably decreased in frequency if Ce^{3+} or Mn^{2+} is the catalyst. However, BZ systems with Fe/phen/ 2^+ or Ru/dipy/ 3^+ are not affected by γ -irradiation. This difference in behaviour is shown on Fig. 2.

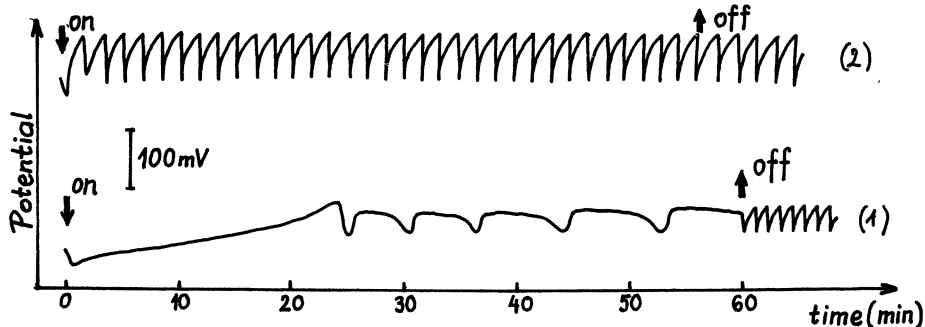


Fig. 2. The behaviour of two BZ systems during irradiation and without irradiation. Composition: 0.05M KBrO_3 , 0.20M malonic acid, 1.0M H_2SO_4 and (1) 4×10^{-4} M $\text{Ce}/\text{IV}/$; (2) 4×10^{-4} M $\text{Ru}/\text{dipy}/3^+$.

If a hydrogen atom scavenger (e.g. NO_3^-) is added to an otherwise radiation-sensitive BZ system, no change in the parameters of oscillation is observable. Since organic components of the complex BZ catalysts (i.e. phenanthroline or dipyrindine) do not function as hydrogen atom scavengers (proved in separate experiments), we assume that hydrogen atoms inhibit the autocatalytic oxidation by bromate of the catalyst if the catalyst is a labile complex (Ce- or Mn-sulphato), but exert no influence on inert complex catalysts Fe/phen/ 2^+ and Ru/dipy/ 3^+ . This probably can be attributed among other things to the difference in mechanisms by which the hydrogen atoms reach the metal ion center across a labile inorganic and an inert organic co-

ordination sphere. It can be concluded that γ -irradiation affects /if at all/ the BZ systems through its effect on the catalyst.

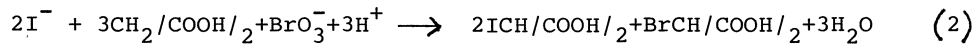
Uncatalyzed bromate oscillators studied so far /aromatics: phenol, 1,2,3-trihydroxybenzene, 1-(p-hydroxyphenyl)-2-methylamine-propane/ are not perturbed by γ -irradiation because the aromatics are rather effective hydrogen atom scavengers.

2.2 Perturbation by Iodide Ion

KANER and EPSTEIN have reported the effect of iodide ion added to an oscillator [3]. Among their findings the most fascinating was the observation of a high-frequency preoscillation in a rather narrow iodide concentration range: between $1 \times 10^{-3} \text{M}$ and $3 \times 10^{-3} \text{M}$.

We thought that this peculiar behaviour of the iodide-containing BZ systems deserves a more thorough investigation and extended our studies both to different bromate oscillators and also to BZ systems of different composition. Our main goal was to get an insight into the chemistry of the iodide-induced high-frequency oscillatory period of the reaction.

First we performed measurements at various concentrations of the BZ systems and used also Mn^{2+} as a catalyst (replacing Ce). The reaction was followed polarographically by measuring both the sum of the concentration of iodomalonic acid (IMA) and BrMA, and separately that of iodate. Thus the concentration of IMA could be calculated. The fate of iodide introduced into the BZ system is as follows: it is oxidized immediately by bromate to IMA with the simultaneous formation of BrMA:

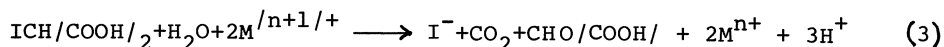


During the high-frequency oscillatory period, there is a low rate accumulation of BrMA and a low rate decomposition of IMA. (Iodine ends up in the system as iodate.) After termination of the high-frequency oscillatory period, a non-oscillatory period starts during which the rate of formation of BrMA is considerably higher /and equals with that measured in the iodine-free BZ system/, and finally the normal BZ oscillation begins and the rate of formation of BrMA drops somewhat. IMA added to a BZ system instead of iodide has the same effects. All these are shown in Fig. 3. It can also be seen that the high-frequency oscillatory period terminates when the concentration of IMA drops below a critical concentration value /here $1 \times 10^{-3} \text{M}$ /.

A change in catalyst or malonic acid concentration has practically no effect on the iodide concentration range where high-frequency oscillations occur. However, bromate and sulphuric acid concentration of the system and the nature of the catalyst do effect it. The higher is the bromate concentration, the wider is the iodide concentration range where high-frequency oscillation occurs. E.g. in a BZ system composed of 0.2M malonic acid, 1.0 H_2SO_4 and 0.001M $\text{Mn}/\text{II}/$ at 0.05M bromate the iodide-concentration range is 6×10^{-4} – $1.5 \times 10^{-3} \text{M}$, at 0.15M bromate it is 2.2×10^{-3} – $5.3 \times 10^{-3} \text{M}$. Beyond the upper concentration value, inhibition by iodide is observable. At sulphuric acid concentrations higher than 3M high-frequency oscillation cannot be initiated even at 10^{-2}M iodide, and neither is iodide an inhibitor. At high acid concentrations iodide is oxidized by bromate rapidly to iodate, the latter having only negligible effect on reacting BZ systems.

Our results do not preclude the formation of glyoxylic acid /GOA/ during the reaction, this compound, however, is not responsible for the high-frequency oscillation as assumed in [3]. This has been proved by adding to a BZ system IMA just below its critical (high-frequency-oscillation-inducing) concentration, BrMA (about half of the amount of IMA) and the IMA missing to the critical value was substituted by GOA. High-frequency oscillation was not observable in any of the experiments.

At Present what we know positively is that during the high-frequency oscillation, IMA is decomposed by its reaction with Ce/IV/ or Mn/III/:



and is regenerated in (2). Since some iodine is removed as iodate from this cycle after some time, the concentration of IMA drops below a critical value. At this time the concentration of BrMA is still below its crucial value to sustain the normal BZ oscillation /see Fig. 3/.

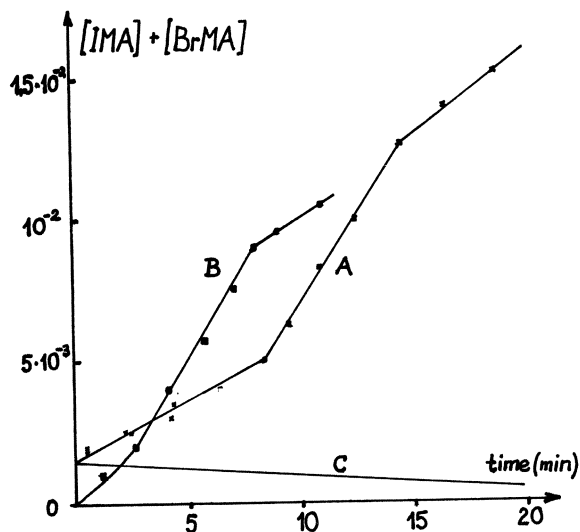


Fig. 3. Curve A: The accumulation of BrMA and decomposition of IMA in a BZ system with the composition 0.075M KBrO₃, 0.20M malonic acid, 1.0M H₂SO₄, 0.001M Ce and 0.002M IMA. Curve B: The accumulation of BrMA in the same BZ system without IMA. Curve C: Decrease in IMA concentration.

The effect of iodide on uncatalyzed bromate oscillators is rather diverse. In the case of systems containing 1-(p-hydroxyphenyl)-amino-propane derivatives, the effect manifests itself in an increase in the number of oscillations. For a system with the composition 0.025M 1-(p-hydroxyphenyl)-2-methylamino-propane, 0.075M KBrO₃ and 0.5M H₂SO₄, the following results were obtained:

[I ⁻] x 10 ³ M	0	1.0	2.0	3.0	3.5	4.0	8.0	10.0
No. of oscillations	10	14	30	38	43	32	4	0

The aromatics-portioning effect of iodide is now under thorough study in our laboratory.

2.3 Perturbation by Bromocomplex-Forming Ion: Tl/III/ or Hg/II/

In the reacting bromate oscillators Br⁻ has an essential role which has been discussed also lately in [9]. Bromide is the control intermediate in bromate oscillators since the kinetic state of the react-

ing system depends on its actual concentration. This means that any additive which influences in some way the concentration of Br⁻ results in a change in the behaviour of the oscillatory system [7].

We have been interested in how bromocomplex-forming ions [Tl/III/, Hg/II/] influence the course of the oscillatory reaction. Here we report mainly on our investigations with Tl/III/. This ion forms soluble bromocomplexes of high stability ($\lg \beta_1=9.62$, $\lg \beta_2=17.06$, $\lg \beta_3=22.59$ and $\lg \beta_4=26.73$). In addition, Tl/III/⁻ as has been proved in separate experiments - does not react either with the main components or with the intermediates /except Br⁻/ of the BZ system.

The addition of Tl/III/ in concentrations between 10⁻⁵ and 10⁻⁴M to any type of bromate oscillators - "classical" BZ, double substrate BZ /acetone-oxalic acid/, "heterogeneous" BZ /oxalic acid/, or uncatalyzed - causes a decrease in the frequency of oscillation and finally a total inhibition.

Table 1 Period-time-increasing effect of Tl/III/

[Tl ³⁺] x 10 ⁵ M	Relative period time of the 1. oscillation		
	System I.	System II.	System III.
0	1.0	1.0	1.0
1.0	1.7	1.4	1.2
4.0	3.6	6.8	2.8
6.0	7.1	10.5	3.3
8.0	no osc.	no osc.	3.6
10.0	no osc.	no osc.	4.9

System I: 0.05M KBrO₃, 0.1M malonic acid, 1.0M H₂SO₄ and 0.002M Ce/IV/

System II: instead of Ce/IV/ 0.002M Mn/II/

System III: 0.075M KBrO₃, 0.025M 1-(p-hydroxyphenyl)-2-methylamine-propane and 0.5M H₂SO₄

In System I. the effect of Hg/II/ is as follows:

[Hg ²⁺] x 10 ⁵ , M	0	6	8	10
Rel. period time	1.0	2.3	3.0	no osc.

At Tl/III/ concentrations above 5x10⁻³M a rather high-frequency potential oscillation can be recorded which is very strongly damped. A repeated addition of Tl/III/ induces this high-frequency oscillation again as shown in Fig. 4.

By the addition of Tl/III/ ($\sim 10^{-2}$ M) the amount of Br⁻ formed in a single oscillation can be determined, since Br⁻ is complexed by Tl/III/, and TlBr²⁺ reacts only very slowly with bromate. Bromide in the TlBr²⁺ complex is determined - after quenching the reaction with a pH 5 acetate puffer in the presence of EDTA - by titration with a 0.01M AgNO₃ solution applying potentiometric end-point detection. The amount of Br⁻ liberated during a single oscillation naturally depends on the composition of the reaction mixture. Under usual conditions /0.05M KBrO₃, 0.2M malonic acid, 1.0 H₂SO₄ and 0.002M catalyst/ it is in the order of 10⁻⁴M.

Our experimental results (the details to be reported in a subsequent paper) seem to clarify the much debated question on the role of Br⁻ in the bromate oscillators.

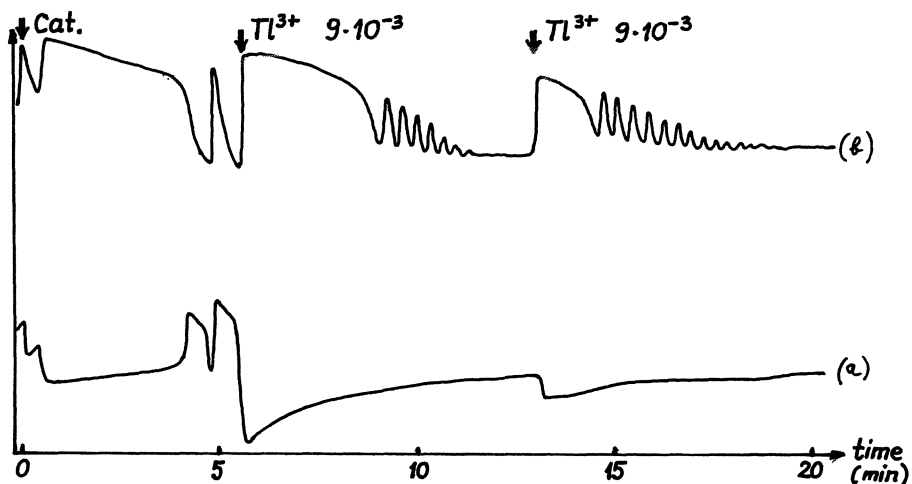


Fig. 4. The effect of $Tl(III)$ ($9 \times 10^{-3} M$) on a BZ system with the composition: 0.05M $KBrO_3$, 0.20M malonic acid, 1.0M H_2SO_4 and 0.002M $Ce(IV)$. (a) Bromide concentration trace; (b) redox potential trace.

References

1. M. Burger, E. Kőrös, J. Phys. Chem., 84, 496 /1980/; Ber. Bunsenges. Phys. Chem., 84, 363 /1980/.
2. S.S. Jacobs, J.R. Epstein, J. Am. Chem. Soc., 98, 1721 /1976/.
3. R.J. Kaner, J.R. Epstein, J. Am. Chem. Soc., 100, 4073 /1978/.
4. Z.Váradi, M.T. Beck, J. Chem. Soc. Chem. Comm., 1973, 30.
5. K. Bar-Eli, S. Haddad, J. Phys. Chem., 83, 2952 /1979/.
6. L. Treindl, P. Fabian, Coll. Czech. Chem. Comm., 45, 1168 /1980/.
7. Z. Noszticzius, J. Am. Chem. Soc., 57, 3660 /1979/.
8. K.V.S. Rama Rao, D. Prasad, "Kinetics of Physicochemical Oscillations", Vol. III. p. 724, Aachen, 1979.
9. R.M. Noyes, J. Am. Chem. Soc., 102, 4644 /1980/.

Periodic Reactions with Bromate II: Verification of Selection Criteria of Organic Radicals Oscillating Without Cagtalysts

J. Chopin-Dumas and P. Richetti
Centre de Recherches Paul Pascal
F-33405 Talence

1. Introduction

Most chemical oscillators are oxido-reductive reactions which can be understood through electrochemistry ; in 1977-1978, the publication of lists of reducing agents which oscillate with bromate alone incited us to investigate the anodic behaviour of these reducing agents [1] -in particular the anilines and the phenols- which was just becoming better known [2].

The compilation of anodic studies of anilines and phenols informs us, on the one hand, of the oxidizability of the reducing agent to a radical R ($S \rightarrow R + e^-$) the greater the oxidation potential, the weaker the reducing agent - and, on the other hand, the oxidizability of the radical. This last statement is indicated by the process by which the radical disappears : an oxidizable radical becomes oxidized ($R \rightarrow C + e^-$), a radical that is slightly oxidizable *is dimerized* ($2R \rightarrow D$), while a radical that is moderately oxidizable follows the above two processes simultaneously. The body of electrochemical data which brought us to this conclusion and the references of original publications have been outlined in a previous article [3].

The results obtained by RPE, which we have brought together in order to go deeper into the problem of the reactivity of radicals, have also produced two pieces of information. One concerns the exact values of hyperfine coupling constants of H^\bullet of the benzene cycle ; and the other, an approximate estimate of the radical half life -time. Only this last piece of information can be used. This has made it possible for us to note that *dimerization* was the process of the disappearance of the most unstable radicals, and oxidation that of the more stable radicals [3, annex 2]. As to spin densities which can be calculated from the coupling constants, these show, upon reflection, a static (thermodynamic) representation of the radical that is useless for the study of its kinetics. The few publications which suggest values of disappearance rates of radicals underline very well the absence of connection with those of spin densities. In practice, the most one can say is that high coupling constants are a condition necessary to, but not sufficient for, a great instability of the radical.

2. Selection criteria

Let us propose two rules for selecting organic reducing agents that oscillate with bromate. These compounds should:

- 1) Have an oxidation potential less than 1.1 V/SCE at pH = 1, that is to say, to be oxidized easily.

- 2) Supply an unstable radical, resistant to later anodic oxidation by dimerization from a carbon,

The excellent agreement observed between the oscillating property of a reducing agent and the great instability of its radical is at the very base of the above suggested selection criteria. Inversely, most of the nonoscillating reducing agents were found in connection with rather stable radicals. Statistically, once the nitro-anilines, because of their over-high oxidation potential, have been eliminated (as stipulated in the first criterion), we have :

out of twelve oscillating reducing agents examined :

- eleven dimerizable radicals
- one oxidizable radical (2,4-diaminodiphenylamine) but the oxidation product of the radical is hydrolysed by producing aniline having a dimerizable radical.

out of sixteen non-oscillating reducing agents examined :

- nine oxidizable radicals,
- three radicals oxidizable under conditions of pH and potential compatible with the oxidizing properties of bromate. These are the radicals of p-cresol, p-anisidine and guaiacol,
- four dimerizable radicals, those of o and m-toluidines and anisidines.

The list of *oscillating* and *non-oscillating* reducing agents do not have the same value. The first is irrefutable, while the second can be questioned. We are therefore going to reexamine the cases of o and m-toluidines and anisidines.

We refer you to our previous article [3] for further details concerning the subject of our summary. The anodic mechanisms are described in detail beyond the first two stages which we have cited (diagram 1 and annex 1). Tables 3, 4 and 5 show each reducing agent individually.

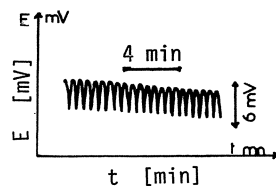
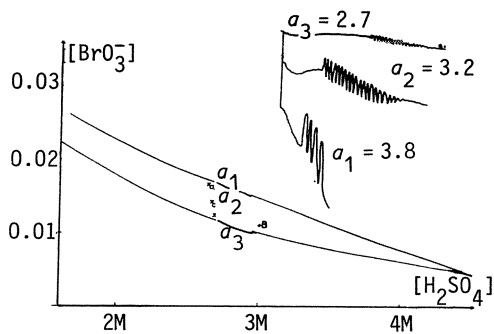
3. Experimental results

The simplest means of verifying the validity of the criteria is to prove the existence of the oscillations expected. The experiments carried out show encouraging results and raise new questions.

A) Study of o and m-Toluidines and Anisidines

Dimerizing anodically into substituted benzidine (Cp-Cp dimer) and/or 4-aminodiphenylamine (N-Cp dimer) [3], like aniline, these compounds ought to oscillate, according to the principles which we propose.

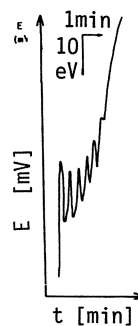
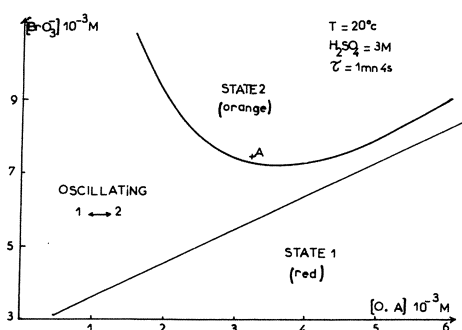
Ortho-toluidine oscillates in a closed reactor (Fig.1) as in an open one (point B, Fig.1) :



Point B

Fig.1 Diagram of oscillating states of ortho-toluidine in a CLOSED reactor, in space $[(H_2SO_4), (BrO_3^-)]$
Point B represents the composition in an OPEN reactor. Residence time $\tau = 8'40''$.

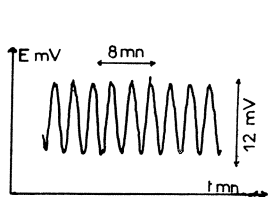
Ortho-anisidine oscillates in an open reactor (Fig.2) and in a closed reactor (point A in Fig.2) with colour change :



Point A

Fig.2 Diagram of oscillating states of ortho-anisidine in an OPEN reactor, in space $[(BrO_3^-), (O-A)]$
Point A represents a composition studied in a CLOSED environment. The oscillations are nearly instantaneous.

Meta-anisidine oscillates in an open reactor, for example :



$$|M.A| = 2 \times 10^{-3}M \quad \tau = 8'15''$$

$$|BrO_3^-| = 10^{-2}M \quad T = 20^\circ C$$

$$|H_2SO_4| = 3M$$

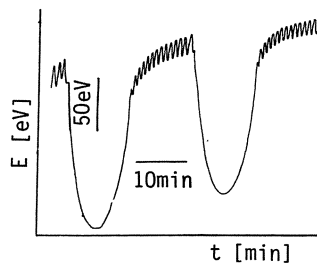
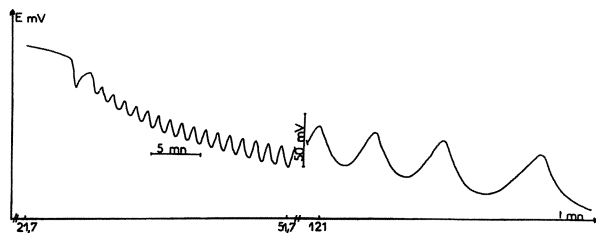
We were surprised not to find oscillations in a closed environment.

It seems that meta-toluidine oscillates neither in an open environment, no in a closed environment at ordinary temperature, in an aqueous solution.

Unlike aniline whose oscillating area covers a large ratio interval $[|\text{BrO}_3^-| / |\text{reducing agent}|]$, for example from 5 to 75, the oscillations of methyl- and methoxy-anilines take place within a very narrow ratio interval, for example, from 2,7 to 3,8 (cross section a_1 - a_3 of Fig.1).

B) Study of compounds having dimerizable radicals

Diphenylamine is dimerized into tetraphenylbenzidine [4]. Neither of these two products is very soluble, and we had to add a little acetonitrile in order to maintain a homogeneous solution. It oscillates in an open reactor :



In a closed reactor, the oscillations are numerous and hardly damped,

$$|\text{D.P.A.}| = 2,6 \times 10^{-3} \text{M}$$

$$|\text{BrO}_3^-| = 2,3 \times 10^{-3} \text{M}$$

Open reactor :

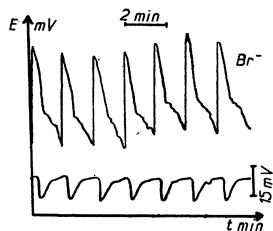
$$|\text{D.P.A.}| = 10^{-3} \text{M}$$

$$|\text{BrO}_3^-| = 3,5 \times 10^{-3} \text{M}$$

$$|\text{H}_2\text{SO}_4| = 3 \text{M} \quad \tau = 22'10'' \\ T = 20^\circ\text{C}$$

Ortho-bromoaniline dimerizes into dibrominated benzidine and 4-amino-diphenylamine [2b]. As these are not very soluble either in an aqueous acid environment, we had to add some acetonitrile.

It oscillates in an open reactor :



$$|\text{O.B.A.}| = 3,3 \times 10^{-3} \text{M}$$

$$|\text{BrO}_3^-| = 1,3 \times 10^{-2} \text{M}$$

$$|\text{H}_2\text{SO}_4| = 2,5 \text{M}$$

Acetonitrile 1,33%

$$\tau = 20'40''$$

$$T = 20^\circ\text{C}$$

It does not oscillate in a closed environment.

1 Naphtol can, like phenol, be oxidized to a dimer and to a monomer [5]. Acetonitrile is necessary to its solubility. We obtained oscillations in an open environment during a preliminary trial.

These results, which seem to confirm our rules for selection, raise other problems, however.

C) Duality between the closed and the open reactor. Study of sulfanilic acid

The verifications above stress the duality between the continuously supplied and the closed reactor. Reactions known up to the present, Bray, Belousov - Zhabotinsky, Briggs-Rauscher, showed of course different state diagrams, but with oscillations occurring for both reactors. We have just found for the compounds meta-anisidine and 2-bromoaniline conditions which are suitable for oscillations in an open environment, without being able to adapt these conditions to the case in which residence time $\tau \rightarrow \infty$; the closed environment is not therefore a simple borderline case of the open environment.

A study of sulfanilic acid made it possible for us to bring out an opposite case of a product which oscillates in a closed environment [1c], but which does not oscillate in a CSTR. In this last case, however, the reaction is bistable. We have studied the diagrams of the bistable states (Fig.3).

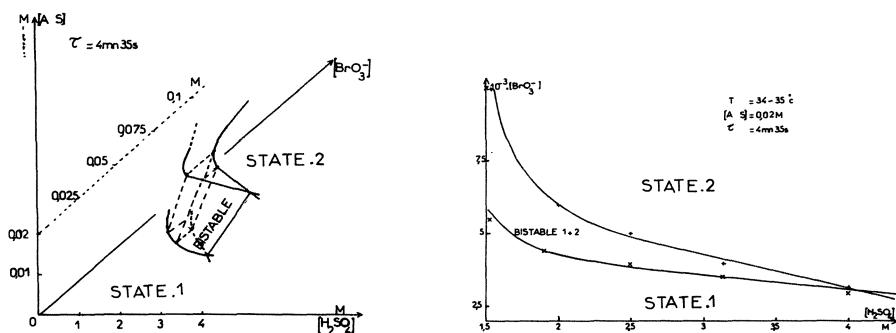


Fig.3

a) Diagram of bistable states of sulfanilic acid in an OPEN environment, in space $|(A-S); (H_2SO_4); (BrO_3^-)|$

b) Cross section of the state diagram, in space $|(BrO_3^-); (H_2SO_4)|$

Exploration of the temperature factor up to 75°C, the increase of $|H_2SO_4|$ over 4 M, according to the hypothesis that Fig.3b represents a crossed curve [6] — nothing made it possible to obtain oscillations. Subsequently, it is possible to consider this bistable bromate - sulfanilic acid as an element to which a *retroaction* should be added in order to obtain an oscillator.

D) Primary and Secondary radicals. Study of Catechol

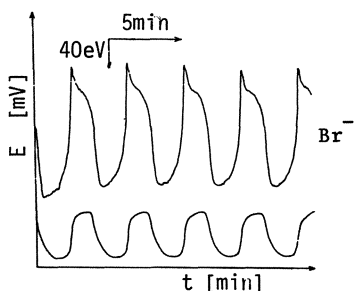
In the case of 2,4-diaminodiphenylamine, whose radical oxidizes, but which produces aniline by hydrolysis of its oxidation product, we imagined that the oscillating property could not be attributed to the primary radical stemming from the initial molecule, but rather to the aniline radical, described as secondary. Other diphenylamines parasubstituted by - OH, - NH₂, - OCH₃ are likely to be oxidized then hydrolysed [Ref.3, annex 11], and can have the properties of their secondary radicals.

We also cite the case of gallic acid, an oscillating reducing agent whose anodic mechanism is not known. The primary radical shows coupling constants so weak that its dimerization is most unlikely. On the other hand, a secondary radi-

cal is formed whose coupling constants are the highest that we recorded for the phenols [7] - the oscillating property of gallic acid is very likely due to its secondary radical. Pyrogallol and another of its derivatives show the same type of quinoid secondary radical [7].

Catechol [8], hydroquinone, p-aminophenol and p-phenylenediamine [9] are still examples of reducing agents having oxidizable primary radicals (m-quinones, imino-quinone or diimine), which are transformed more or less quickly in an oxidizing acid medium into a dimerizable secondary radical [8], that of the oscillating reducing agent called 1, 2, 4-trihydroxybenzene [1c].

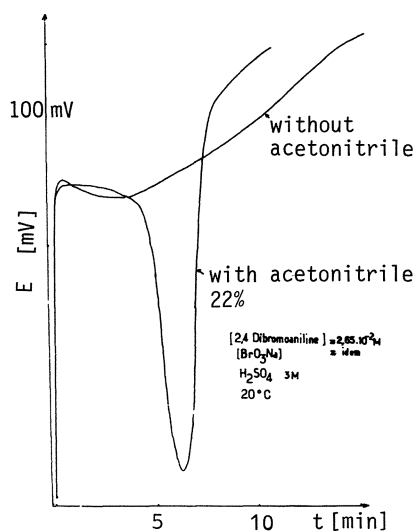
The compounds cited above can neither invalidate nor confirm our rules whatever their behaviour with bromate may be. The most one can say is that if they oscillate, the hydrolysis stage is taking place at a suitable speed ; and if they do not oscillate, hydrolysis is too slow for the secondary radical to do its job. We have, however, studied catechol. It oscillates in an open environment but not in a closed one, which agrees with NAIR'S [10] results for a stirred solution.



$|\text{Catechol}| = 10^{-2}\text{M}$
 $|\text{H}_2\text{SO}_4| = 2\text{M}$
 $|\text{BrO}^-| = 9,5 \times 10^{-3}\text{M}$
 $\tau = 2' 44''$
 $T = 20^\circ\text{C}$

E) Role of solvent

We had to add acetonitrile to some reactors in order to make the reducing agent soluble or to maintain a homogeneous medium. The figure opposite is an example of the change brought about in the kinetics of the reaction. The effect of acetonitrile is far less than that of methanol.



4. Discussion

The problem of the validity of our rules for selection can be approached in two ways. The first is a statistical verification, an experimental evaluation of the percentage of exceptions to the rules. The second is the justification of these rules by means of a theoretical approach supported experimentally.

The justification of criteria is more difficult than their verification. We have suggested - since this happens in an anodic medium for parabrominated radicals - that the dimerization stage be the stage when bromide is free [3]. By experiment, it would be necessary to characterize the dimers, which are transitory forms, easily oxidized, then hydrolysed (with the exception of the benzidines). We have only been able to note that the oxidation of sulfanilic acid by bromate or by means of a potentiostat produce in both cases a growing peak which afterwards disappears, at the 530-nm absorption region of the 4-aminodiphenylamines.

Only the verification of our selection rules has been taken up in the preceding paragraph. On the whole, the balance sheet appears to be satisfactory : we were able to obtain oscillations with six reducing agents out of the seven which were tried because of their adequate characteristics. However, this work raises the question of experimental conditions : closed or open reactor, use of organic solvent, stirring of the solution. These factors have a real importance, generally little known ; their influence can become primordial in borderline cases where oscillating state diagrams are of small dimensions.

5. References

1. a) L. Kuhnert and H. Linde, *Z. Chem.*, 17, 19 (1977)
b) E. Koros and M. Orban, *Nature*, 273 (I), 371 (1978)
c) M. Orban and E. Koros, *J. Phys. Chem.*, 82 (14), 1372 (1978)
d) M. Orban and E. Koros, *React. Kinet. Catal. Lett.*, 8 (2), 273 (1978)
e) M. Orban and E. Koros, *Synergetics, Far From equilibrium*, Eds A. PACAULT et C. VIDAL, Springer Verlag, Berlin 1979, 43-46
f) L. Kuhnert, *Z. Chem.*, 19 (2), 63 (1979)
2. a) R.L. Hand and R.F. Nelson, *J. Am. Chem. Soc.*, 96 (3), 850 (1974)
b) R.L. Hand and R.F. Nelson, *J. Electrochem. Soc.*, 125 (7), 1059 (1978)
3. J. Chopin-Dumas, *J. Chim. Phys.*, 78, 461-9 (1981)
4. R.F. Nelson, Anodic oxidation pathway of aliphatic and aromatics Nitrogen functions, Chap. 5 (535-792) de "Techniques of electroorganic synthesis" od. N.L. Weinberg, Wiley 1974
5. L. Papouchado, R.W. Sandford, G. Petrie et R.N. Adams, *J. Electroanal. Chem.*, 65, 275 (1975)
6. J. Boissonade and P. De Kepper, *J. Phys. Chem.* 84, 501 (1980)
7. W.T. Dixon and D. Murphy, *J.C.S. Perkin II*, 850 (1975)
8. L. Pajouchado, G. Petrie et R.N. Adams, *J. Electroanal. Chem.*, 38, 389 (1972)
9. R.N. Adams, *Electrochemistry at solid electrodes*, Dakar 1969
10. Punnappillil K.R. Nair and coll., *Bull. Chem. Soc. JPN.*, 54, 317-318 (1981)

Part IX

Mathematical Modeling

On Scaling the Oregonator Equations

John J. Tyson

Department of Biology, Virginia Polytechnic Institute
Blacksburg, VA 24061, USA

1. Introduction

The Oregonator is a system of three ordinary differential equations suggested by FIELD & NOYES [1] as a model of the FIELD, KÖRÖS & NOYES [2] mechanism of the BELOUSOV-ZHABOTINSKII reaction. The equations are

$$\dot{X} = k_1 AY - k_2 XY + k_3 AX - 2k_4 X^2, \quad (1a)$$

$$\dot{Y} = k_1 AY - k_2 XY + fk_5 Z, \quad (1b)$$

$$\dot{Z} = k_3 AX - k_5 Z, \quad (1c)$$

where the dot notation indicates a time derivative, $A = [\text{BrO}_3^-]$, $X = [\text{HBrO}_2]$, $Y = [\text{Br}^-]$, $Z = 2[\text{Ce}^{4+}]$, f is a stoichiometric parameter and k_1, \dots, k_5 are rate constants. FIELD & NOYES [1] cast this system of equations into dimensionless form by defining

$$x = (k_2/k_1 A)X, \quad y = (k_2/k_3 A)Y, \quad (2a)$$

$$z = (k_2 k_5/k_1 k_3 A^2)Z, \quad t = (k_1 k_3)^{1/2} A \text{ (time)}, \quad (2b)$$

$$s = (k_3/k_1)^{1/2}, \quad w = k_5/A(k_1 k_3)^{1/2}, \quad (2c)$$

$$q = 2k_1 k_4/k_2 k_3. \quad (2d)$$

In these terms (1) becomes

$$\dot{x} = s(y - xy + x - qx^2), \quad (3a)$$

$$\dot{y} = s^{-1}(-y - xy + fz), \quad (3b)$$

$$\dot{z} = w(x - z). \quad (3c)$$

From known values of rate constants in the FKN mechanism of the BZ reaction, FIELD & NOYES estimated that $s \cong 80$, $q \cong 10^{-5}$, $w \cong 0.1$, and $f \cong 1$. They realized that, for $s \gg 1$, x would change very rapidly (since $|\dot{x}| \gg 1$) except near the "slow manifold" defined by $y - xy + x - qx^2 = 0$. They suggested that the full system (3) could be approximated by (3b), (3c) and

$$x = \{(1-y) + [(1-y)^2 + 4qy]^{1/2}\}/2q. \quad (4)$$

This is, of course, the start of an analysis of (3) by singular perturbation theory: the complete matched asymptotic expansion was derived by STANSHINE & HOWARD [3] who set $q = Qs^{-2}$, $Q = O(1)$, $f = 1$, and solved (3) in the limit $s \rightarrow \infty$.

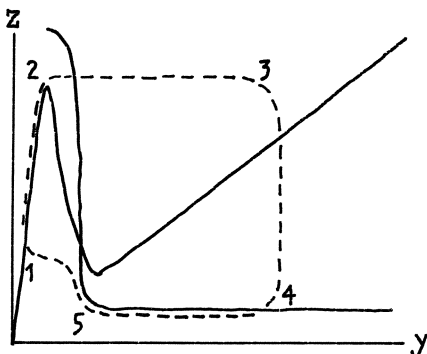


Fig.1 The nullclines (—) and a limit cycle solution (---) of system (3b), (3c) and (4).

Figure 1 illustrates a limit cycle solution of (3) in the y - z phase plane. The limit cycle has been divided into five sections. In section 1 \rightarrow 2, y is small, x is large, and $\dot{z} \approx wx$, so z increases rapidly. In section 2 \rightarrow 3, $z \approx x \approx q^{-1}$, and $\dot{y} = O(fs^2/Q) \gg 1$; thus, y increases very rapidly at approximately constant z . In section 3 \rightarrow 4, $y = O(q^{-1})$, \dot{y} is small, and $\dot{z} = w(1 - z)$, i.e. $z \rightarrow 1$ exponentially with time constant w . In section 4 \rightarrow 5, $z \approx x \approx 1$ and $\dot{y} = s^{-1}(f - 2y) < 0$, so y decreases very slowly. Finally, section 5 \rightarrow 1, which brings us back to where we started, is difficult to describe analytically (it took STANSHINE & HOWARD six different scaling regions to match the expansion at point 5 with the expansion at point 1).

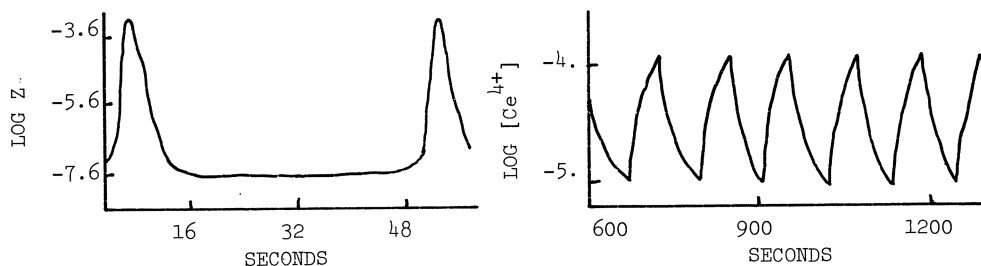


Fig.2 Waveform for Ce^{4+} oscillations: left, as predicted by the Oregonator [1], and right, as observed in the BZ reaction [2]. The observed period of oscillation is about 2 minutes.

Figure 2 shows the waveform for Z predicted by this analysis in comparison with the observed waveform for $[Ce^{4+}]$. Notice that the Oregonator oscillation does not agree with the observed oscillation in amplitude and waveform. The model predicts $[Ce^{4+}]_{max}/[Ce^{4+}]_{min}$ too large by 10^3 , and it predicts $[Ce^{4+}] = [Ce^{4+}]_{min}$ for most of the oscillation, which is not usually the case experimentally. The analysis of STANSHINE & HOWARD [3] shows that

$$[Ce^{4+}]_{max}/[Ce^{4+}]_{min} \approx (4q)^{-1}, \quad (5a)$$

$$\text{Period} \approx -\ln(4q(ws-2))/2k_1A. \quad (5b)$$

Thus the amplitude and period of the model could be brought in line with observations if q were chosen significantly larger than 10^{-5} , but the whole asymptotic analysis would have to be redone (with $q = Qs^{-1}$, say) and it is not clear how this would change the waveform of $[Ce^{4+}]$ oscillations.

In the next section I will show that asymptotic analysis of the Oregonator equations can be greatly simplified by scaling them differently and that, indeed, the waveform of $[Ce^{IV}]$ oscillations comes out right when q is taken to be $O(10^{-3})$.

2. An Alternative Scaling of the Equations

Let us replace the definitions in (2) by

$$x = (2k_4/k_3A)X, \quad y = (k_2/k_3A)Y, \quad (6a)$$

$$z = (2k_4k_5/(k_3A)^2)Z, \quad t = k_3A(\text{time}), \quad (6b)$$

$$= 2k_4/k_2, \quad p = k_3A/k_5, \quad q = 2k_1k_4/k_2k_3. \quad (6c)$$

Then (1) becomes

$$\dot{x} = qy - xy + x - x^2, \quad (7a)$$

$$\epsilon \dot{y} = -qy - xy + fz, \quad (7b)$$

$$p \dot{z} = x - z. \quad (7c)$$

From rate constants in the FKN mechanism we estimate that $\epsilon \approx 0.05$ and $p \approx 500$ (where I have used $k_5 = 1 \text{ sec}^{-1}$, in line with the value chosen by FIELD & NOYES [1]). This suggests a singular perturbation analysis with $\epsilon \rightarrow 0$ and $p \rightarrow \infty$. In chemical terms, y (bromide ion) changes on the fastest time scale and z (cerium IV ion) changes on the slowest time scale.

For $\epsilon \ll 1$, (7) can be approximated by [4]

$$\dot{x} = x(1-x) - fz(x-q)/(x+q), \quad (8a)$$

$$p \dot{z} = x - z, \quad (8b)$$

and

$$y = fz/(x+q). \quad (9)$$

The phase plane of system (8) is illustrated in Fig.3. In section 1 \rightarrow 2, $x = O(1)$ and $p \dot{z} \approx 1 - z > 0$, so z increases slowly, rate = $O(p^{-1})$, and during this time x is given by $x(1-x) = fz$. In section 2 \rightarrow 3, $z = z.\text{max} \approx 1/4f$ and x decreases very rapidly, rate = $O(1)$, to $x = x.\text{min} \approx q$. In section 3 \rightarrow 4, $x = O(q)$ and $p \dot{z} \approx -z$, so z decreases exponentially, half-life = $0.7 p$, from $z.\text{max}$ to

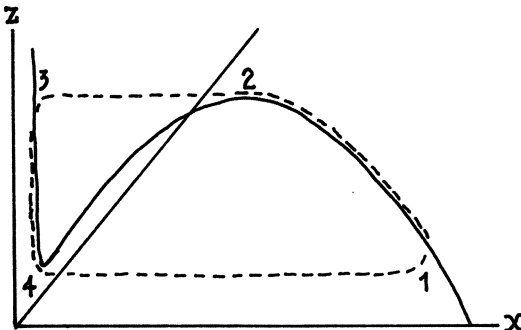


Fig.3 The nullclines (—) and a limit cycle solution (---) of system (8) for $p \gg 1$.

$z_{\min} = 0(q)$. Finally, in section 4 \rightarrow 1, $z = z_{\min}$ and x increases rapidly from x_{\min} to $x_{\max} \approx 1$. Obviously, the waveform of $[Ce^{4+}]$ oscillations is similar to the observed waveform (Fig.2 (right)), and does not have the long flat section in Fig.2 (left). The amplitude and period of the oscillation are given by [4]

$$[Ce^{4+}]_{\max} / [Ce^{4+}]_{\min} \approx (24q)^{-1}, \quad (10a)$$

$$\text{Period} \approx -\ln(24q) / k_5. \quad (10b)$$

The amplitude is too large if $q \approx 10^{-5}$ but can be brought in line with experiment [4] by choosing $q = 4 \times 10^{-5}$. In that case, the period is correct if $k_5 = 0.02$ sec⁻¹.

The analysis I have just sketched is valid only if the time scales on which x , y and z change are such that y changes most rapidly, x changes moderately rapidly, and z changes slowly during all phases of the limit cycle. This will be the case if the right-hand sides of (7) are all of the same order at each point around the limit cycle. Examining (7) at positions 1 through 4 in Fig.3, we see that the right-hand sides are all $O(1)$ at 2, $O(1)$ at 3, and $O(q)$ at 4, but at position 1 we find that

$$\dot{x} = O(1), \quad \epsilon \dot{y} = O(q), \quad p \dot{z} = O(1). \quad (11)$$

In order that $|\dot{y}| \gg |\dot{x}|$, we must insist that $\epsilon \ll q$. If $q \ll \epsilon = 5 \times 10^{-2}$, then our description of the limit cycle breaks down in the vicinity of position 1, but this does not greatly change the qualitative and quantitative results given above until q becomes smaller than ϵ/p . If $q \ll \epsilon/p = 10^{-4}$, then $|\dot{y}| \ll |\dot{z}|$ and this changes the picture drastically.

This conclusion has been confirmed numerically by John RINZEL [private communication], who integrated system (7) with a Gear-type algorithm for $\epsilon = 0.05$, $p = 500$, $f = 1$, and $q = 10^{-3}$, 10^{-4} , and 10^{-5} and compared these results with the numerical integration of the second-order subsystems obtained from (7) by making a pseudo-steady-state hypothesis (pssh) for x or y . He found that the pssh for x gives a good approximation to (7) for all values of q , but the pssh for y gives a good, fair, and poor approximation to (7) for $q = 10^{-3}$, 10^{-4} , and 10^{-5} , respectively.

3. Discussion

The Oregonator, though derived from a reasonable mechanism of the BZ reaction, was not intended by its authors to be a quantitative model of the BZ reaction, but rather to be an abstract model of oscillatory chemical kinetics, akin to and, perhaps, more realistic than the Brusselator [5]. What I have shown here, and previously [4], is that the Oregonator can give a quantitatively accurate description of oscillations in the BZ reaction if q is taken to be considerably larger and k_5 is taken to be considerably smaller than the values estimated by FIELD & NOYES [1].

Are the values that I use for q (10^{-3}) and k_5 (10^{-2}) more or less reasonable than the values used by FIELD & NOYES? First, consider k_5 . In the experiments of ZHABOTINSKII, ZAIKIN, KORZUKHIN & KREITSER [6], bromomalonic acid replaced malonic acid as the organic substrate for the BZ reaction. This considerably simplifies the estimation of k_5 , since KASPEREK & BRUCE [7] have determined that the oxidation of bromomalonic acid by Ce^{4+} follows the kinetics



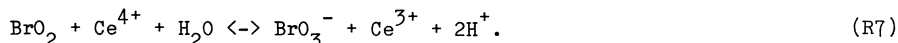
where $k = 0.07$ sec⁻¹ and $K = 0.20$ M. For $[BrMA] \approx 0.01$ M, as in the experiments

of ZHABOTINSKII *et al.* [6],

$$-d[\text{Ce}^{4+}]/dt = k_5[\text{Ce}^{4+}], \quad k_5 = 3.5 \times 10^{-3} \text{ sec}^{-1}, \quad (13)$$

which is within a factor of 2 of the value used in [4]. With malonic acid present, as well, in the reaction mixture, k_5 should be somewhat larger; in the neighborhood of 0.02 sec^{-1} estimated above.

The parameter $q = 2k_4k_1/k_2k_3$ was estimated by FIELD & NOYES [1] from rate constants given by FIELD *et al.* [2]. FÜRSTERLING, LAMBERZ & SCHREIBER [8] have studied the kinetics of the $\text{HBrO}_2/\text{BrO}_3^-$ reaction and concluded that the ratio k_4/k_3 should be 50 times larger than the value used by FIELD & NOYES, which implies that $q \approx 4 \times 10^{-4}$. Furthermore, the term k_2AX in the Oregonator equations is meant to represent the combined kinetics of at least three reactions [2]



FIELD *et al.* [2] have shown that the kinetics of these three reactions (neglecting the reverse of reaction R5) can be represented by

$$dX/dt = k_3AXF(A,C,Z) \quad (14)$$

where A, X, Z have their usual meanings, $C = [\text{Ce}]_{\text{total}}$, and F is a rather complicated function of its arguments and the rate constants of reactions (R5) - (R7). From the data given in EDELSON, FIELD & NOYES [9] one can estimate that $F \approx 0.1$ during that phase of the oscillation when $[\text{HBrO}_2]$ is small (this is the phase when q plays an important role). Thus, the effective value of k_3 should be taken at least ten times smaller, and q at least ten times larger, i.e. $q \approx 4 \times 10^{-3}$ as suggested above.

These arguments suggest that k_3 should be taken 50-500 times smaller than $10^4 \text{ M}^{-2} \text{ sec}^{-1}$, the value estimated by FIELD *et al.* [2]. Not only does this provide much better agreement with the observed period and amplitude of oscillations in the well-stirred batch reactor, but it also clears up a long standing discrepancy between the observed and predicted speed of trigger-wave propagation in unstirred thin layers of Z reagent. FIELD & NOYES [10] showed that waves of oxidation should propagate with speed

$$c = (4k_3D[\text{H}^+][\text{BrO}_3^-])^{1/2}, \quad (15)$$

where D is the diffusion constant for HBrO_2 . Taking $k_3 = 10^2 \text{ M}^{-2} \text{ sec}^{-1}$ and $D = 10^{-5} \text{ cm}^2 \text{ sec}^{-1}$, we find that

$$c = 38 \text{ mm min}^{-1} \text{ M}^{-1} ([\text{H}^+][\text{BrO}_3^-])^{1/2}, \quad (16)$$

which compares favorably with the experimental results of FIELD & NOYES [10] and SHOWALTER [11].

Finally, let me make a few comments about scaling conventions and pseudo-steady-state hypotheses (pssh's). If systems (3) and (7) are integrated numerically for the same values of the parameters A, f , and k_1, \dots, k_5 , then we must get exactly the same limit cycle solutions, since the scaling conventions, (2) and (6), are arbitrary definitions. However, whether we make a pssh for HBrO_2 or Br^- is not arbitrary: the two hypotheses lead to two different approximations to the exact solution of the full third-order system. As mentioned earlier, a pssh for Br^- is not uniformly valid for $q < \epsilon/p = 0(10^{-4})$, but it is a good approximation for

larger values of q . Since experiments suggest that $q = 0(10^{-3})$, it is equally valid to make a pssh for HBrO_2 or Br^- . Indeed, for $q = 0(10^{-3})$ both $[\text{HBrO}_2]$ and $[\text{Br}^-]$ change rapidly with respect to $[\text{Ce}^{4+}]$, and it is valid to make pssh's for both variables (except, of course, during the short periods, twice per cycle, when $[\text{HBrO}_2]$ and $[\text{Br}^-]$ make rapid jumps).

I am indebted to John Rinzel for many helpful discussions about the Oregonator and for permission to quote his unpublished results on numerical integration of system (7) and its subsystems. My research on chemical dynamics is supported by the National Science Foundation, Grant MCS-7919787.

4. References

1. R. J. Field, R. M. Noyes: J. Chem. Phys. 60, 1877-1884 (1974)
2. R. J. Field, E. Koros, R. M. Noyes: J. Am. Chem. Soc. 94, 8649-8664 (1972)
3. J. A. Stanshine, L. N. Howard: Stud. Appl. Math. 55, 129-165 (1976)
4. J. J. Tyson: Ann. N.Y. Acad. Sci. 316, 279-295 (1979)
5. G. Nicolis, I. Prigogine: Self-Organization in Nonequilibrium Systems (Wiley, New York 1977)
6. A. M. Zhabotinskii, A. N. Zaikin, M. D. Korzukhin, G. P. Kreitser: Kinet. & Catal. 12, 516-521 (1971)
7. G. J. Kasperek, T. C. Bruice: Inorg. Chem. 10, 382-386 (1971)
8. H. D. Forsterling, H. J. Lamberz, H. Schreiber: Z. Naturforsch. 35a, 1354-1360 (1980)
9. D. Edelson, R. J. Field, R. M. Noyes: Internat. J. Chem. Kinet. 7, 417-432 (1975)
10. R. J. Field, R. M. Noyes: J. Am. Chem. Soc. 96, 2001-2006 (1974)
11. K. Showalter: J. Phys. Chem. 85, 440-447 (1981)

The Behavior of a Multistable Chemical System Near the Critical Point

Kedma Bar-Eli

Department of Chemistry, Tel-Aviv University
Tel Aviv 69978, Israel

Abstract

The bistability of the cerium-bromate-bromide system in an open flow (CSTR) system was investigated near the critical point where the bistability disappears. The critical point is approached via a "cusp" catastrophe. The behaviour of the Jacobian in this region is discussed. Due to the appearance of complex eigenvalues, certain SS became unstable without changing the regularity of the Jacobian matrix. Beyond the critical point a region with only one unstable SS was found. In this small region, oscillations occur around the SS.

Introduction

The oxidation of cerous ions by bromate in sulfuric acid medium was investigated earlier, both in a closed system [1] and in an open system [2,3,4] of a continuous stirred tank reactor (CSTR). It was shown first by GEISELER and FOLLNER [2] that the above system in CSTR shows bistability and can transfer from one steady state to the other via a hysteresis cycle. BAR-ELI and NOYES [3,4] using a mechanism devised by NOYES, FIELD and THOMPSON [5] (NFT mechanism) calculated the various steady states and the kinetic approach to them. Recently GEISELER and BAR-ELI [6] calculated and measured the hysteresis limits under a variety of constraints, thus confirming the NFT mechanism and giving accuracy limits to the various rate constants.

The multistability is limited, of course, to a certain region of the constraints space, and beyond this region only one stable steady state exists. In this work we have investigated the behaviour of the system near the critical point where the bistable system becomes monostable. We have limited ourselves mainly to the bromate-bromide subspace of constraints, while keeping all other constraints constant. As it turns out, due to the high degree of nonlinearity of the system, the approach to the critical point is quite complicated. The stability of the various steady states changes, certain stable steady states become unstable and the possibility of oscillations appears to be feasible. This region of possible oscillations, although small, may be tested experimentally.

Calculations and Results

The NFT mechanism is made up of the following seven chemical reactions, the rate constants of which are shown. These rate constants are partly measured [7], partly estimated [8] and slightly corrected to agree with kinetic data [1b].



$$k_1 = 2.1 \text{ M}^{-3} \text{ s}^{-1} \quad k_{-1} = 1 \times 10^4 \text{ M}^{-1} \text{ s}^{-1}$$



$$k_2 = 2 \times 10^9 \text{ M}^{-2} \text{ s}^{-1} \quad k_{-2} = 5 \times 10^{-5} \text{ M}^{-1} \text{ s}^{-1}$$



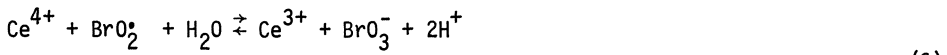
$$k_3 = 8 \times 10^9 \text{ M}^{-2} \text{ s}^{-1} \quad k_{-3} = 110 \text{ s}^{-1}$$



$$k_4 = 1 \times 10^4 \text{ M}^{-2} \text{ s}^{-1} \quad k_{-4} = 2 \times 10^7 \text{ M}^{-1} \text{ s}^{-1}$$



$$k_5 = 6.5 \times 10^5 \text{ M}^{-2} \text{ s}^{-1} \quad k_{-5} = 2.4 \times 10^7 \text{ M}^{-1} \text{ s}^{-1}$$



$$k_6 = 9.6 \text{ M}^{-1} \text{ s}^{-1} \quad k_{-6} = 1.3 \times 10^{-4} \text{ M}^{-3} \text{ s}^{-1}$$



$$k_7 = 4 \times 10^7 \text{ M}^{-1} \text{ s}^{-1} \quad k_{-7} = 2.1 \times 10^{-10} \text{ M}^{-2} \text{ s}^{-1}$$

The rate constants are used with the assumption that the concentration of water is constant at unit activity, thus making the total number of chemical species - 9.

To the rate equations formed from the seven reactions (1-7), the terms $k_0(C_{oi} - C_i)$ are added, where C_i is the concentration of species i , C_{oi} is the concentration of this species in the feed flow, and k_0 is the ratio between the flow rate V and the volume of the reaction vessel V_R . Its reciprocal is sometimes called the "retention time".

The equations thus obtained are

$$\frac{dC_i}{dt} = F_i(C) + k_0(C_{oi} - C_i) \quad (8)$$

where $F_i(C)$ describes the chemical mass action rates derived from (1-7). Eq. (8) was solved by Newton's method for a steady state, i.e. for $\dot{C} = 0$. The fact that there are only 5 independent concentrations was, of course, taken care of (see appendix).

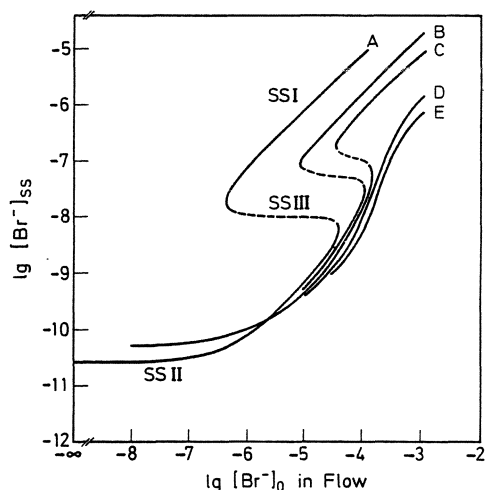


Fig. 1 Dependence of steady state bromide concentration $[Br^-]_{SS}$ on bromide concentration in the inflow $[Br^-]_0$ for different bromate flows. Values of $[BrO_3^-]_0$ are A- $2 \times 10^{-3}M$, B- $10 \times 10^{-3}M$, C- $20 \times 10^{-3}M$, D- $100 \times 10^{-3}M$ and E- $200 \times 10^{-3}M$. Constant constraints: $[Ce^{+3}]_0 = 1.5 \times 10^{-4}M$ $[H^+]_0 = 1.5M$ $k_0 = 4 \times 10^{-3} sec^{-1}$

In Fig.1, the general behaviour of the system is shown. At low bromide ion concentrations, the system can, in a certain range of bromide ion concentrations, exist in three steady states [4,5]: SS I - having relatively high concentration of bromide and low concentration of ceric ions, SS II - having relatively low concentration of bromide and high concentration of ceric ions. This steady state is the one which will go over smoothly to equilibrium as k_0 becomes zero, i.e. when the system is closed. Between these two stable steady states, a third unstable one SS III exists - shown in dashed lines. Being unstable, it cannot, of course, be attained experimentally. The transition between the physically attainable SS I and SS II can be achieved by changing slowly bromide ion concentration and tracing a hysteresis cycle.

As bromate ion concentration is changed, the region of multistability is changed too. Increasing bromate concentration narrows the limits of the multistability, until finally a point will be reached where only one steady state exists. A smooth transition between high and low bromide (or ceric) ion concentrations without hysteresis will occur. This is clearly shown by the different plots of Fig.1. At low bromate concentrations, (Plots A,B,C), the three steady states, with the possibility of hysteresis, are contrasted with the high bromate concentrations (Plots D,E), where a smooth transition between high and low bromide is observed. These predictions and hysteresis limits were calculated and tested experimentally by GEISLER and BAR-ELI [6]. Typical results for $[BrO_3^-]_0 - [Br^-]_0$ subspace are shown in Fig.2. The comparison between the experimental and calculated data in this as well as in other subspaces was used by the above authors to obtain accuracy limits for the various rate constants.

The three steady states are characterized by the Eqs. $\dot{C}_i = 0$ where C_i are the concentrations of the various species in the reaction cell. The Jacobian matrix $\partial \dot{C}_i / \partial C_j$ has only negative eigenvalues for SS I and SS II, while SS III must have at least one positive eigenvalue.

If we assume that this is indeed the case, namely, that the Jacobian matrix of SS III has only one positive eigenvalue, then the Jacobian, which is equal to the product of all the eigenvalues, will have three values in the region of coexistence of the three SS: (one positive and two negative, whereas it will be single

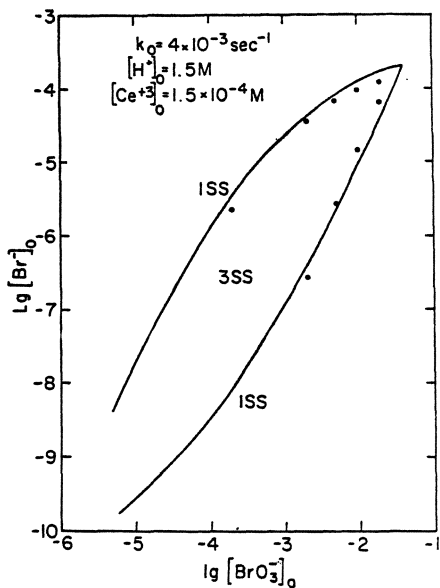


Fig.2 Hysteresis limits in $[\text{BrO}_3^-]_0 - [\text{Br}^-]_0$ subspace of constraints. Constant constraints: $[\text{Ce}^{+3}]_0 = 1.5 \times 10^{-4} \text{M}$, $[\text{H}^+]_0 = 1.5 \text{M}$, $k_0 = 4 \times 10^{-3} \text{sec}^{-1}$. (—) calculated, experimental (\cdot)

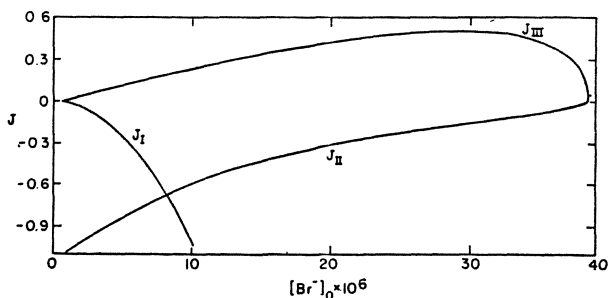


Fig.3 The Jacobian determinant as a function of $[\text{Br}^-]_0$ in the flow. Constant constraints: $[\text{BrO}_3^-]_0 = 2 \times 10^{-3} \text{M}$, $[\text{Ce}^{+3}]_0 = 1.5 \times 10^{-4} \text{M}$, $[\text{H}^+]_0 = 1.5 \text{M}$, $k_0 = 4 \times 10^{-3} \text{sec}^{-1}$. J_I , J_{II} and J_{III} correspond to the Jacobian of SSI , SSII and SSIII , respectively

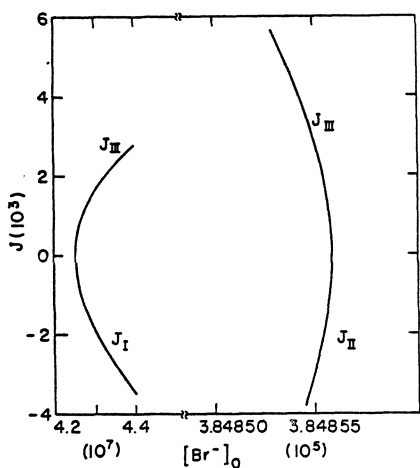


Fig.4 A detailed view of Fig.3 near the upper and lower hysteresis limits

values and negative in all other regions. The sign of the Jacobian will, of course, change if the number variables is even instead of odd, as in our case.

Figure 3 shows that this is indeed the case. At low and high values of $[\text{Br}^-]_0$ the Jacobian J has only one negative value, in certain intermediate values, the Jacobian has two negative values, corresponding to SSI and SSII , and one positive value, corresponding to SSIII . Since $J > 0$, this steady state cannot be stable and SSIII cannot be physically attained.

At the hysteresis limits, $J=0$ and it passes through this point with infinite slope. Fig.4, which is a magnification of Fig.3 near the upper and lower hysteresis limits, stresses this point.

Since J is a continuous function of $[\text{Br}^-]_0$, J must have a maximum with a zero slope at some point between the upper and the lower hysteresis limits.

As the other constraint, namely $[\text{BrO}_3^-]_0$, increases, the region of multistability changes. This was shown already in Figs.1 and 2 and is shown again with a different view point in Fig.5. Here the Jacobian of SSIII- J_{III} is plotted as a function of $[\text{Br}^-]_0$ for different values of $[\text{BrO}_3^-]_0$. As bromate concentration increases, the region of multistability increases and then decreases and finally disappears at the critical point. Following this change there is a parallel change in the maximum value of J_{III} . The rather strange values given in Fig.5 were obtained in the following way.

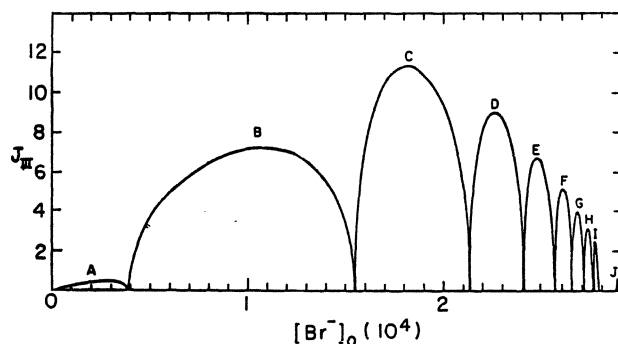


Fig.5 The Jacobian of SSIII- J_{III} vs. $[\text{Br}^-]_0$ for the different following values of $[\text{BrO}_3^-]_0$: A - $2 \times 10^{-3}\text{M}$, B - $20.225894 \times 10^{-3}\text{M}$, C - $40.85939 \times 10^{-3}\text{M}$, D - $48.11639 \times 10^{-3}\text{M}$, E - $51.23639 \times 10^{-3}\text{M}$, F - $52.92939 \times 10^{-3}\text{M}$, G - $53.94523 \times 10^{-3}\text{M}$, H - $54.60423 \times 10^{-3}\text{M}$, I - $55.05812 \times 10^{-3}\text{M}$, J - $56.405924 \times 10^{-3}\text{M}$
Constant constraints: $[\text{Ce}^{+3}]_0 = 1.5 \times 10^{-4}\text{M}$ $[\text{H}^+]_0 = 1.5\text{M}$ $k_0 = 4 \times 10^{-3} \text{ sec}^{-1}$

A point $[\text{BrO}_3^-]_0$ and $[\text{Br}^-]_0$, between the upper and lower hysteresis limits at SSIII was taken. Newton method was used to calculate other points of $\dot{C}=0$ at SSIII at constant $[\text{BrO}_3^-]_0$ and increasing values of $[\text{Br}^-]_0$ until the point of the upper hysteresis limit was reached. This point was recognized by the failure of Newton's method, due to the singularity of the Jacobian matrix at this point. The increase of $[\text{Br}^-]_0$ was stopped and an increase of $[\text{BrO}_3^-]_0$ started until a further singularity was reached. Thus, by alternately changing $[\text{BrO}_3^-]_0$ increase and $[\text{Br}^-]_0$ increase, the limits of SSIII region were traced.

Same limits are obtained by starting from any point at SSI, decreasing $[\text{Br}^-]_0$ and reaching $J=0$; repeating such calculations for different $[\text{BrO}_3^-]_0$ gives the lower limits of the bistability region. Starting at a point at SSII and increasing $[\text{Br}^-]_0$ will end at the other points of $J=0$ - the upper limit of the region. The same results are obtained regardless of the method of calculation. Thus, the obtained limits are certainly reliable inasmuch as the NFT mechanism is correct. The experimental verification is shown in Fig.2 and in the work of GEISELER and BAR-ELI [6] for the other subspaces.

The critical point, namely the point at which SSIII disappears, is slowly approached through a "cusp" catastrophe [9].

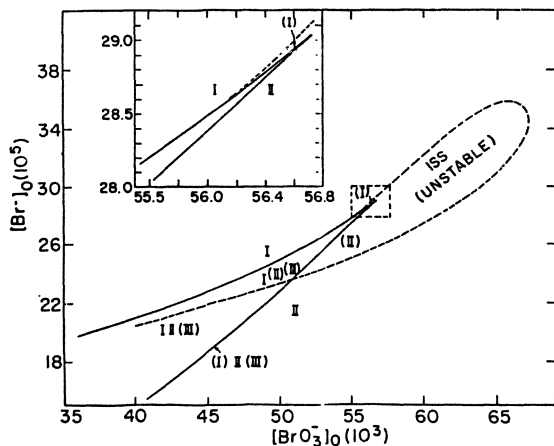


Fig.6 $[\text{Br}^-]_0 - [\text{BrO}_3^-]_0$ subspace near the critical point. Regions of the various SS are shown. When the symbol of the SS is shown in parentheses, the SS is unstable. (----) region of unstable one SS

In Fig.6 and especially in the insert, this "cusp" catastrophe is clearly shown. The critical point occurs at $[\text{BrO}_3^-]_0 = 56.7283 \times 10^{-3} \text{M}$, $[\text{Br}^-]_0 = 29.037 \times 10^{-5} \text{M}$ at the constant constraints $[\text{Ce}^{+3}]_0 = 1.5 \times 10^{-4} \text{M}$, $[\text{H}^+]_0 = 1.5 \text{M}$ and $k_0 = 4 \times 10^{-3} \text{sec}^{-1}$. Obviously the critical point will change with the change of the constant constraints.

This figure is, of course, a detailed enlargement of Fig.2 near the critical point where SSIII disappears.

At this critical point, the three points, namely $\frac{dJ}{d[\text{Br}^-]_0} = +\infty$, $\frac{dJ}{d[\text{Br}^-]_0} = 0$ and $\frac{dJ}{d[\text{Br}^-]_0} = -\infty$, will coalesce as is evidenced from Figs.7 and 8, which are very similar to Fig.3 except that they correspond to $[\text{BrO}_3^-]_0$ slightly smaller and slightly larger than the critical value.

In Fig.8, both the dependence of the Jacobian and that of $[\text{Br}^-]_{\text{SS}}$ are shown. It is seen that the Jacobian is negative and single valued throughout, and has a maximum, i.e. $\frac{dJ}{d[\text{Br}^-]_0} = 0$ at a certain point. The two points where the Jacobian

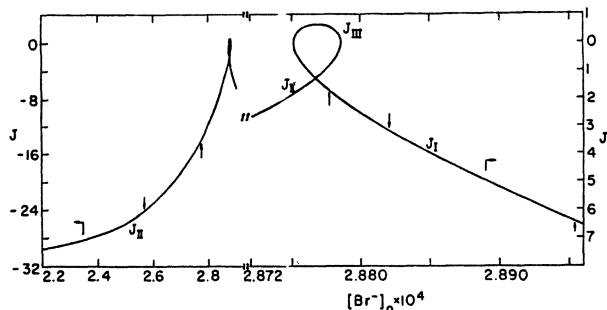


Fig.7 The Jacobian of the various SS vs. $[\text{Br}^-]_0$ at $[\text{BrO}_3^-]_0 = 56.4059 \times 10^{-3} \text{M}$, $[\text{Ce}^{+3}]_0 = 1.5 \times 10^{-4} \text{M}$, $[\text{H}^+]_0 = 1.5 \text{M}$ and $k_0 = 4 \times 10^{-3} \text{sec}^{-1}$, just before the critical point. Upward arrow - Hopf bifurcation points, Downward arrow - real part of a conjugate pair of eigenvalues becomes zero.

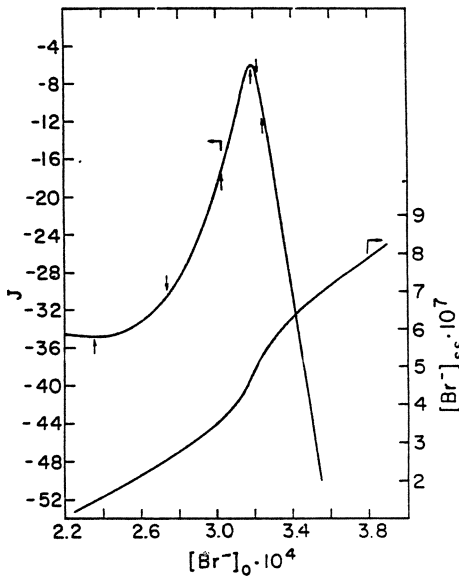


Fig.8

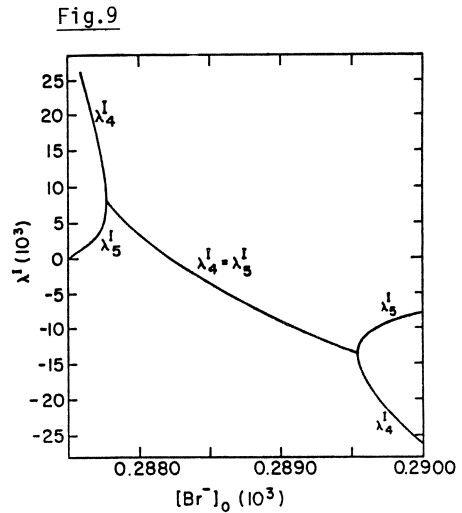


Fig.9

Fig.8 The Jacobian of the SS and $[\text{Br}^-]_{\text{SS}}$ vs. $[\text{Br}_3^-]_0 = 60 \times 10^{-3} \text{M}$, $[\text{Ce}^{+3}]_0 = 1.5 \times 10^{-4} \text{M}$, $[\text{H}^+]_0 = 1.5$ and $k_0 = 4 \times 10^{-3} \text{sec}^{-1}$, slightly after the critical point. Note the existence of only one SS. Upward arrow - Hopf bifurcation points. Downward arrow - real part of a conjugate pair of eigenvalues becomes zero

Fig.9 The change of two eigen values of SSI which become a conjugate pair vs. $[\text{Br}^-]_0$. Only the real part of the pair is shown. Constant constraints: $[\text{BrO}_3^-]_0 = 56.405924 \times 10^{-3} \text{M}$, $[\text{Ce}^{+3}]_0 = 1.5 \times 10^{-3} \text{M}$, $[\text{H}^+]_0 = 1.5 \text{M}$, $k = 4 \times 10^{-3} \text{sec}^{-1}$. Hopf bifurcation points at $[\text{Br}^-]_0 = 2.8954 \times 10^{-4} \text{M}$ and $[\text{Br}^-]_0 = 2.8777 \times 10^{-4} \text{M}$. Real part of eigenvalues equal zero at $[\text{Br}^-]_0 = 2.8821 \times 10^{-4} \text{M}$

changes its sign with infinite slope has disappeared beyond the critical point. The behaviour of $[\text{Br}^-]_{\text{SS}}$ changes accordingly. Whereas before the critical point $[\text{Br}^-]_{\text{SS}}$ has three possible values, as shown in Fig.1 (plots A,B,C), after the critical point it is single valued only. It changes smoothly from low to high values of $[\text{Br}^-]$ without hysteresis. It will be noted from Fig.8 that the maximum of the Jacobian corresponds exactly to the maximum slope of $[\text{Br}^-]_{\text{SS}}$.

When the system is far away from the critical point, all its eigenvalues are real and $J = \prod_i \lambda_i$. As the system approaches the critical point, a Hopf bifurcation occurs and two real eigenvalues coincide to become a conjugate pair, as shown in Fig.9 for the pair belonging to SSI. Similar phenomenon happens for SSII. The limits of existence of the conjugate pair is shown by upward arrows in Figs.7 and 8. When the real part of two such conjugate eigen values changes its sign, the sign of the Jacobian determinant remains negative as before, and the previous plots, such as Figs. 7 and 8, are unaffected. The Jacobian does not become zero at this point since the imaginary part will contribute its share. In other words, the

Jacobian matrix remains regular at this point. The steady state in question will, however, become unstable despite the Jacobian being negative.

As a consequence, the steady states I and II may lose their stability and become unstable even in regions where hitherto they were considered stable. Fig.6 shows this delicate and rather unexpected phenomenon. For instance, SSI is unstable in a narrow region above the upper and lower hysteresis limits. SSII is unstable in a region well below the critical point; SSIII is, of course, unstable at all times. It will be noted that the instability of SSIII results from one eigenvalue being positive, while the instability of SSI and SSII results from two eigenvalues (conjugate pair or not) being positive.

As seen from Fig.8, the possibility of two eigenvalues being positive exists even beyond the critical point - where only one SS exists. In fact, we see in Fig. 6 a whole region where only one unstable state exists. This implies that in this region the system must oscillate around the steady state. In fact, the solution of the differential equations in this region [10] does oscillate in a simple periodic manner while in all other regions the solution will go very fast, as expected, to the same SS as is found by Newton's method.

Table I shows the period, at various points in this region, as a function of bromate, bromide and flow rates. It is seen that the period increases with bromide concentration, decreases with bromate concentration and increases also with the flow rate.

Table 1. Constant constraints: $[Ce^{+3}]_0 = 1.5 \times 10^{-4} M$ $[H^+]_0 = 1.5 M$

Period (sec)	$[Br^-]_0 \times 10^{+5} M$	$[BrO_3^-]_0 \times 10^{+3} M$	$k_0 \cdot 10^3 \text{ (sec}^{-1}\text{)}$
135	31	65	4
130	32	65	4
150	33	65	4
180	34	65	4
230	35	65	4
160	28	60	4
170	29	60	4
205	30	60	4
265	31	60	4
510	32	60	4
185	27	58	4
210	28	58	4
270	29	58	4
455	30	58	4
290	26	55	4
stable SS	31	65	3.8
190	31	60	3.8
155	29	60	3.8

The range of existence of this unique unstable steady state is rather small, as can be seen from Fig.6. Moreover, the flow rates limits are also very small, e.g. at the point $[\text{BrO}_3^-]_0 = 60 \times 10^{-3} \text{M}$ and $[\text{Br}^-]_0 = 31 \cdot 10^{-5} \text{M}$ the positive eigenvalues exist only between $k_0 = 3.425 \times 10^{-3} \text{ sec}^{-1}$ and $k_0 = 4.165 \times 10^{-3} \text{ sec}^{-1}$.

The bromide ion concentration changes during the oscillation by at most one order of magnitude, while that of the cerium ions changes by not more than 30%. These values become smaller as the period is shortened.

All these factors may contribute to the difficulties of observing oscillations experimentally.

Our oscillating system differs in one important aspect from the other well-known homogeneous oscillating reactions [11]. In the BELOUSOV-ZHABOTINSKII [12] reaction, to take an example, the cerium ions serve as an intermediate. They are oxidized by the bromate ions, while the malonic acid (or some other reducing organic species [13]) reduces them. Oscillations arise when these two processes occur alternately as described in detail by FIELD, KÖRÖS and NOYES [7] (FKN mechanism). In the present system, which contains all the ingredients of the Belousov-Zhabotinskii system apart from the malonic acid, no reducing species exists. The cerous ions are the only species which can reduce the bromate ions.

In the closed system, i.e. $k_0=0$, the species concentration will approach equilibrium in kinetics which is well documented in the literature [1,14]. The open system, i.e. $k_0 \neq 0$ stabilizes generally, under certain sets of constraints is rather surprising because of the lack of malonic acid. The experimental verification of these oscillations seems therefore to be of utmost importance and deserves the effort in spite of the above-mentioned difficulties.

APPENDIX A

There are $N=9$ chemical species (not counting the water) and $R'=7$ chemical reactions. Since reactions 4,5 and 6 and 1, -2 and 7 sum up to null reactions, it turns out that there are only $R=5$ independent reactions. In other words, the stoichiometric matrix has only five independent columns and its rank is thus five and not seven:

<u>Reaction</u>	1	2	3	4	5	6	7
Species							
1 (BrO_3^-)	1	0	0	1	0	-1	-1
2 (HBrO_2)	-1	1	0	1	-1	0	2
3 (HOBr)	-1	-2	1	0	0	0	-1
4 (BrO_2^-)	0	0	0	-2	1	1	0
$v =$							
5 (Br^-)	1	1	1	0	0	0	0
6 (H^+)	2	1	1	1	1	-2	-1
7 (Ce^{+4})	0	0	0	0	-1	1	0

(A.1)

$$\begin{array}{cccccccc} 8 (\text{Br}_2) & & 0 & 0 & -1 & 0 & 0 & 0 & 0 \\ 9 (\text{Ce}^{+3}) & & 0 & 0 & 0 & 0 & 1 & -1 & 0 \end{array}$$

Greek characters are used to denote matrices, and Latin ones to denote vectors. The matrix γ' multiplied by v will give zero. γ' is of course:

$$\gamma'^T = \begin{array}{ccccccc} 0 & 0 & 0 & 1 & 1 & 1 & 0 \\ 1 & -1 & 0 & 0 & 0 & 0 & 1 \end{array} \quad (\text{A.2})$$

$$v\gamma' = 0. \quad (\text{A.3})$$

A matrix β exists of N-R = 9-5 = 4 rows and N = 9 columns which will annul the matrix v

$$\beta v = 0. \quad (\text{A.4})$$

The matrix β is found to be:

$$\beta = \begin{array}{cccccccc} 1 & 1 & 1 & 1 & 1 & 0 & 0 & 2 & 0 \\ 0 & 0 & 0 & 0 & 0 & 0 & 1 & 0 & 1 \\ 6 & 1 & -1 & 2 & 0 & -3 & -1 & -4 & 1 \\ -38 & 452 & -32 & -212 & 322 & -234 & -147 & 56 & 147 \end{array} \quad (\text{A.5})$$

and its rank is obviously four.

We realized immediately that the first two rows of β express the conservation of bromine and cerium atoms, respectively, while the two bottom lines were chosen so as to be orthogonal to both the first two rows and to the columns of v . Since water concentration is considered constant (its value is already included in the rate constants), no conservation of hydrogen or oxygen atoms is applicable.

There are, therefore, only five independent concentrations (C_{ind}), while the other four (C_{dep}) can be expressed as a linear combination of the independent ones. C_{ind} can be arbitrarily chosen as the first five and C_{dep} as the last four concentrations. Introducing the functions "f" which are the mass action rates of the individual reactions 1-7, Eq. (8) will be written in matrix form as:

$$\dot{C} = v f + k_0 (C_0 - C). \quad (\text{A.6})$$

k_0 is, of course, a scalar. The functions F of Eq. (8) is relate to f by $F = v f$.

Multiplying Eq. (A.6) by β one obtains:

$$\beta \dot{C} = \beta v f + k_0 \beta (C_0 - C) = k_0 \beta (C_0 - C). \quad (\text{A.7})$$

The last equality is the result of Eq. (A.4).

At a steady state $C=0$ and one obtains:

$$\beta C_0 = B = \beta C, \quad (\text{A.8})$$

where the vector B (of dimension nine) is a constant for a particular set of constraints. Define β_{ind} and β_{dep} as the first five and last four columns of matrix β , respectively. Eq. (A.8) can be rewritten:

$$B - \beta_{\text{ind}} C_{\text{ind}} = \beta_{\text{dep}} C_{\text{dep}} \quad (\text{A.9})$$

As the rank of matrix β is four β_{dep} must have an inverse and thus

$$\beta_{\text{dep}}^{-1} B - \beta_{\text{dep}}^{-1} \beta_{\text{ind}} C_{\text{ind}} = C_{\text{dep}} \quad \text{or} \quad (\text{A.10})$$

$$C_{\text{dep}} = \alpha C_{\text{ind}} - \alpha C_{0\text{ind}} + C_{0\text{dep}}, \quad (\text{A.11})$$

where the matrix $\alpha = -\beta_{\text{dep}}^{-1} \beta_{\text{ind}}$ is computed to be

$$\alpha = \begin{array}{ccccc} 6 & 3 & 1 & 4 & 0 \\ -5 & -3 & -1 & -4 & 1 \\ -\frac{1}{2} & -\frac{1}{2} & \frac{1}{2} & -\frac{1}{2} & -\frac{1}{2} \\ 5 & 3 & 1 & 4 & -1 \end{array} \quad (\text{A.12})$$

In this way the computations via Newton's method are done only on the five independent concentrations.

As is reported in the text, the region of oscillations associated with the unique unstable steady state is rather small and depends strongly on the external constraints. A check was made regarding the possible influence of the variation of water concentration on the existence and extent of this region. Addition of water as one of the variables may cause slight changes in the rates of those reactions where water participates, namely (3), (4) and (6). The number of variables increases from 9 to 10 and thus the number of dependent variables will increase to 5. The algebraic calculations are facilitated by the fact that conservation laws can be used throughout. The appearance of water in the equations causes the conservation of bromine, cerium, hydrogen and oxygen atoms to hold. In addition to these four, conservation of charge gives the necessary five rows of the matrix β . The fifth row of matrix α is thus calculated to be -3, -2, -1, -2, 0, while the first four rows are the same as given in Eq. (A.12).

When the calculations are repeated with the possible variation of water, the same results are obtained as reported above. Thus no error is introduced when water is considered constant and its concentration absorbed directly into the appropriate rate constants.

REFERENCES

1. a. G.J. Kasperek and T.C. Bruice, *Inorg. Chem.* **10**, 382 (1971).
b. S. Barkin, M. Bixon, R.M. Noyes and K. Bar-Eli, *Int. J. Chem. Kinet.* **11**, 841 (1977).
2. W. Geiseler and H. Föllner, *Biophys. Chem.* **6**, 107 (1977).
3. K. Bar-Eli and R.M. Noyes, *J. Phys. Chem.* **81**, 1988 (1977).
4. K. Bar-Eli and R.M. Noyes, *J. Phys. Chem.* **82**, 1352 (1978).
5. R.M. Noyes, R.J. Field and R.C. Thompson, *J. Am. Chem. Soc.* **93**, 7315 (1971).

6. W. Geiseler and K. Bar-Eli, J. Phys. Chem. (in press).
7. R.J. Field, E. Körös and R.M. Noyes, J. Am. Chem. Soc. 94, 8649 (1972).
8. W.M. Latimer, "Oxidation Potentials", 2nd ed., Prentice Hall, New York, N.Y. (1952).
9. R. Poston and I.N. Stewart, "Taylor Expansions and Catastrophes", Pitman Publishing, London (1976).
10. a. C.W. Gear, "Numerical Initial Value Problems in Ordinary Differential Equations", Prentice Hall, Englewood Cliffs, N.J., 1971, p. 209-229.
b. A.C. Hindmarsh, "Gear: Ordinary Differential Equation System Solver", VCID 2001, rev. 3, Dec. 1974.
11. R.M. Noyes and R.J. Field, Acc. Chem. Res. 10, 273 (1977), and references therein.
12. a. B.P. Belousov, Sbornik Referat Radiats. Med. Medgiz Moscow 1950, p. 145.
b. A.M. Zhabotinskii, Dokl. Akad. Nauk. SSSR 157, 392 (1964).
c. A.M. Zhabotinskii, Biofizika 9, 306 (1964).
13. P.G. Bowers, K.E. Caldwell and D.F. Prendergast, J. Phys. Chem. 76, 2185 (1972).
14. K. Bar-Eli and E. Geiseler (in press).

Recent Developments in the Theory of Stoichiometric Networks and Application to the Belousov-Zhabotinsky System

Bruce L. Clarke

Department of Chemistry, University of Alberta
Edmonton, Alberta, Canada T6G 2G2

1. Introduction

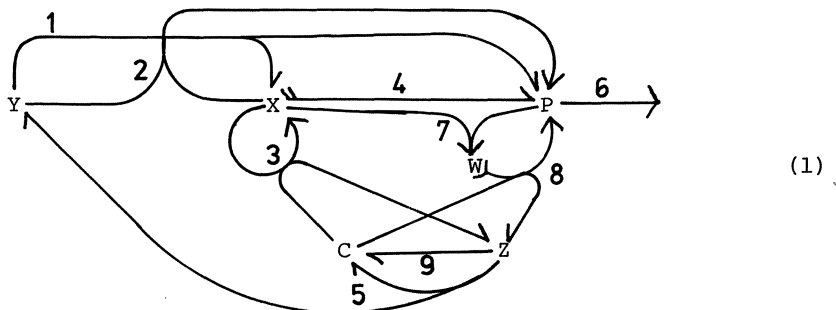
The term "stoichiometric network" refers to a set of processes (such as chemical reactions) which proceed according to rate laws having a particular mathematical form and rate constants in the range $0 \leq k_i < \infty$. Networks whose rate laws are products of concentrations are best understood [1]. These "power law" networks are specified by a matrix ν giving the net reaction stoichiometries and a matrix κ giving the orders of kinetics.

A typical question is whether a particular network can have chaotic dynamics for any possible choices of nonnegative rate constants. Other questions concern the existence of oscillations, multiple steady states or explosions. The ideal answer to such questions is an algorithm which answers the question for the general network starting from the network specification -- usually ν and κ .

The aim of this paper is to illustrate what can be said about a typical network using the current state of the theory and corresponding computer algorithms which test ν and κ . The network used is a model of the Belousov-Zhabotinski system which should be of interest from a purely chemical standpoint.

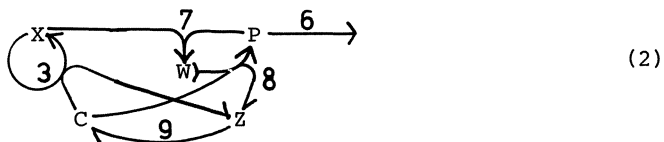
2. Motivation for the Model

Oscillations have been observed [2,3] in a BZ system using oxalic acid and acetone instead of malonic acid. NOSZTICZIUS believes that Br^- does not play a role in these oscillations and has proposed new reactions to explain the oscillations [4]. The model we study is essentially the Oregonator after modification to include the dynamics of HOBr and the reactions proposed by NOSZTICZIUS. The model is (see [1] for notation)

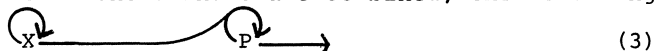


Reactions 1,2,3,4,5 and species X,Y, and Z are the Oregonator with P made explicit. Instead of using variable stoichiometry in reaction 5, I used reaction 9 to achieve the same effect.

The model which NOSZTICZIUS used to explain oscillations in the absence of Br⁻ is roughly the following subnetwork of our model but without cerium



where reaction 9 represents the oxidation of oxalic acid by cerium. If cerium is omitted and reactions 7 and 8 are combined, the resulting network



is the Lotka-Volterra (LV) oscillator whose dynamics are a structurally unstable centre. If the reaction $X+P \rightarrow 2P$ in (3) is replaced by $X+P \rightarrow 2W \rightarrow 2P$, the system has a limit cycle instead of a centre. Thus model (1) has two distinct oscillators -- an Oregonator oscillator and a modified Lotka-Volterra (MLV) oscillator. In this paper we study how these oscillators interact with each other.

As justification for the important new reactions 7 and 8, note that these reactions represent the autocatalytic reproduction of HOBr by a mechanism precisely analogous to the reproduction of $HBrO_2$. Such reactions were seriously considered by FIELD and NOYES prior to the original development of the Oregonator [5].

A network which combines two separate oscillators or sources of instability is a good candidate for chaotic dynamics. For example, take the LV oscillator (3) and combine it with the network



which is an unstable competition between X and Z. The resulting network



has been shown by WILLAMOWSKI and ROSSLER [6] to have chaotic dynamics if the reactions are reversible. Model (1) is essentially this chaotic model with an Oregonator replacing the XZ competition. The possibility of chaos in our model is a second reason for studying it.

3. Analysis of the Model

Model (1) has 6 species which will be taken in alphabetical order. It has 18 reactions, 9 forward and 9 reverse. The stoichiometric matrix v and the kinetic matrix κ appear below and on the next page. Rows correspond to species and columns to reactions.

$$v = \begin{pmatrix} 0 & 0 & -1 & 0 & 1 & 0 & 0 & -1 & 1 & 0 & 0 & 1 & 0 & -1 & 0 & 0 & 1 & -1 \\ 1 & 2 & 0 & 1 & 0 & -1 & -1 & 2 & 0 & -1 & -2 & 0 & -1 & 0 & 1 & 1 & -2 & 0 \\ 0 & 0 & 0 & 0 & 0 & 0 & 2 & -2 & 0 & 0 & 0 & 0 & 0 & 0 & 0 & -2 & 2 & 0 \\ 1 & -1 & 1 & -2 & 0 & 0 & -1 & 0 & 0 & -1 & 1 & -1 & 2 & 0 & 0 & 1 & 0 & 0 \\ -1 & -1 & 0 & 0 & 1 & 0 & 0 & 0 & 0 & 1 & 1 & 0 & 0 & -1 & 0 & 0 & 0 & 0 \\ 0 & 0 & 1 & 0 & -1 & 0 & 0 & 1 & -1 & 0 & 0 & -1 & 0 & 1 & 0 & 0 & -1 & 1 \end{pmatrix}$$

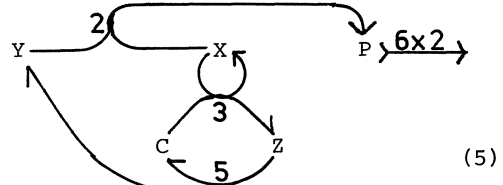
From v we first determine an "extreme current" matrix E using the algorithm CURRENTS [7]. E has 59 columns but only 12 of them are given

below. Each column of E represents an extreme steady state flow or current on the network. The entries in the columns are the weight factors that the stoichiometries must be multiplied by to obtain a set of reactions which

$$K = \begin{pmatrix} 0 & 0 & 1 & 0 & 0 & 0 & 0 & 1 & 0 & 0 & 0 & 0 & 0 & 1 & 0 & 0 & 0 & 1 \\ 0 & 0 & 0 & 0 & 0 & 1 & 1 & 0 & 0 & 1 & 2 & 0 & 1 & 0 & 0 & 0 & 1 & 0 \\ 0 & 0 & 0 & 0 & 0 & 0 & 0 & 1 & 0 & 0 & 0 & 0 & 0 & 0 & 0 & 2 & 0 & 0 \\ 0 & 1 & 1 & 2 & 0 & 0 & 1 & 0 & 0 & 1 & 0 & 2 & 0 & 0 & 0 & 0 & 0 & 0 \\ 1 & 1 & 0 & 0 & 0 & 0 & 0 & 0 & 0 & 0 & 0 & 0 & 0 & 1 & 0 & 0 & 0 & 0 \\ 0 & 0 & 0 & 0 & 1 & 0 & 0 & 0 & 1 & 0 & 0 & 1 & 0 & 0 & 0 & 0 & 1 & 0 \end{pmatrix}$$

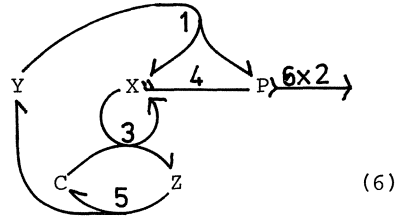
$$E = \begin{pmatrix} 0 & 1 & 0 & 1 & 0 & 0 & 0 & 0 & 0 & 0 & 0 & 0 & 0 & 0 & 0 & 0 & 0 & 0 \\ 1 & 0 & 0 & 0 & 1 & 0 & 0 & 0 & 0 & 0 & 0 & 0 & 0 & 0 & 0 & 0 & 0 & 0 \\ 1 & 1 & 1 & 0 & 0 & 1 & 0 & 0 & 0 & 0 & 0 & 0 & 0 & 0 & 0 & 0 & 0 & 0 \\ 0 & 1 & 0 & 0 & 0 & 0 & 1 & 0 & 0 & 0 & 0 & 0 & 0 & 0 & 0 & 0 & 0 & 0 \\ 1 & 1 & 0 & 0 & 0 & 0 & 0 & 1 & 0 & 0 & 0 & 0 & 0 & 0 & 0 & 0 & 0 & 0 \\ 2 & 2 & 1 & 0 & 0 & 0 & 0 & 0 & 0 & 1 & 0 & 0 & 0 & 0 & 0 & 0 & 0 & 0 \\ 0 & 0 & 1 & 0 & 0 & 0 & 0 & 0 & 0 & 0 & 1 & 0 & 0 & 0 & 0 & 0 & 0 & 0 \\ 0 & 0 & 1 & 0 & 0 & 0 & 0 & 0 & 0 & 0 & 0 & 0 & 1 & 0 & 0 & 0 & 0 & 0 \\ 0 & 0 & 2 & 0 & 0 & 0 & 0 & 0 & 0 & 0 & 0 & 0 & 0 & 0 & 1 & 0 & 0 & 0 \\ 0 & 0 & 0 & 1 & 0 & 0 & 0 & 0 & 0 & 0 & 0 & 0 & 0 & 0 & 0 & 0 & 0 & 0 \\ 0 & 0 & 0 & 0 & 1 & 0 & 0 & 0 & 0 & 0 & 0 & 0 & 0 & 0 & 0 & 0 & 0 & 0 \\ 0 & 0 & 0 & 0 & 0 & 1 & 0 & 0 & 0 & 0 & 0 & 0 & 0 & 0 & 0 & 0 & 0 & 0 \\ 0 & 0 & 0 & 0 & 0 & 0 & 1 & 0 & 0 & 0 & 0 & 0 & 0 & 0 & 0 & 0 & 0 & 0 \\ 0 & 0 & 0 & 0 & 0 & 0 & 0 & 1 & 0 & 0 & 0 & 0 & 0 & 0 & 0 & 0 & 0 & 0 \\ 0 & 0 & 0 & 0 & 0 & 0 & 0 & 0 & 1 & 0 & 0 & 0 & 0 & 0 & 0 & 0 & 0 & 0 \\ 0 & 0 & 0 & 0 & 0 & 0 & 0 & 0 & 0 & 1 & 0 & 0 & 0 & 0 & 0 & 0 & 0 & 0 \\ 0 & 0 & 0 & 0 & 0 & 0 & 0 & 0 & 0 & 0 & 1 & 0 & 0 & 0 & 0 & 0 & 0 & 0 \\ 0 & 0 & 0 & 0 & 0 & 0 & 0 & 0 & 0 & 0 & 0 & 1 & 0 & 0 & 0 & 0 & 0 & 0 \\ 0 & 0 & 0 & 0 & 0 & 0 & 0 & 0 & 0 & 0 & 0 & 0 & 1 & 0 & 0 & 0 & 0 & 0 \\ 0 & 0 & 0 & 0 & 0 & 0 & 0 & 0 & 0 & 0 & 0 & 0 & 0 & 1 & 0 & 0 & 0 & 0 \\ 0 & 0 & 0 & 0 & 0 & 0 & 0 & 0 & 0 & 0 & 0 & 0 & 0 & 0 & 1 & 0 & 0 & 0 \\ 0 & 0 & 0 & 0 & 0 & 0 & 0 & 0 & 0 & 0 & 0 & 0 & 0 & 0 & 0 & 1 & 0 & 0 \\ 0 & 0 & 0 & 0 & 0 & 0 & 0 & 0 & 0 & 0 & 0 & 0 & 0 & 0 & 0 & 0 & 1 & 0 \\ 0 & 0 & 0 & 0 & 0 & 0 & 0 & 0 & 0 & 0 & 0 & 0 & 0 & 0 & 0 & 0 & 0 & 1 \end{pmatrix}$$

will sum to the null reaction. These reactions represent a steady state. For example, column 1 is a steady state combining reactions 2,3, and 5 with the original stoichiometry and reaction 6 with the stoichiometry doubled. Drawing these reactions as a network gives

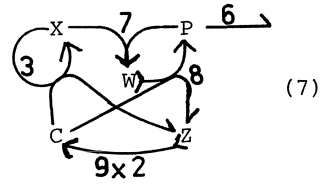


This "extreme current" of model (1) is also found in the Oregonator and

is the unstable steady state which leads to oscillation. The Oregonator with forward reactions only has only two extreme currents. In addition to (5) the current shown at the right is an extreme current of the Oregonator. It appears as column 2 in E for our model. Steady states involving this current are stable provided this current is the main contribution to the steady state.



The network proposed by NOSZTICZIUS appears as column 3 in E and has the diagram shown at the right. This subnetwork has unstable steady states and is a modified Lotka-Volterra oscillator.



4. All Steady States

All steady states of the general network for concentrations $X_i \geq 0$ and rate constants $k_i \geq 0$ can be found for any rate laws [7]. The complete set of steady states of model (1) on the open domain $X_i > 0, k_i > 0$ are

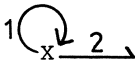
$$X_i = 1/h_i \quad i = 1, \dots, 6 \quad (8)$$

$$k_i = \sum_{\ell=1}^{59} E_{i\ell} j_\ell \prod_{m=1}^6 h_m^{K_{mi}} \quad i = 1, \dots, 18 \quad (9)$$

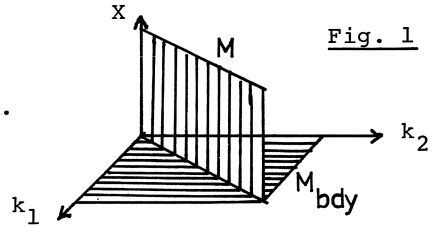
where the parameters $h = (h_1, \dots, h_6)$ and $j = (j_1, \dots, j_{59})$ take all values in the open orthants R_+^6 and R_+^{59} . This set of steady states is a simply connected 19-dimensional differentiable manifold imbedded in the

24-dimensional space of X and k .

Most reaction networks have a complicated set of steady states in the boundary of the set $\{X \in R_+^n, k \in R_+^r\}$. As an illustration consider the network



whose steady states are shown in Fig. 1. For $X > 0$ the steady state manifold M satisfies $k_1 = k_2$. For $X = 0$ the entire $k_1 - k_2$ plane is a steady state manifold called M_{bdy} .



The steady states (8)-(9) are analogous to M in Fig. 1. If h and j take values on the closed domains \bar{R}_+^6 and \bar{R}_+^9 , then (8) and (9) can also give some of the steady states on the boundary. Of interest are the steady states where all components of j vanish except j_1, j_2 and j_3 . These boundary steady states involve only the first three columns of E diagrammed in (5), (6) and (7). Since these steady states tell us how the Oregonator interacts with the oscillator proposed by NOSZTICZIUS, we will later consider them in more detail.

The complete set of steady states can be found with the algorithm ALLSS given in [7]. This algorithm divides $X-k$ space into 2^n domains, where $n = \text{number of species} = 6$. For each domain enough information is given to construct equations analogous to (8) and (9) for the manifold of steady states in the boundary.

Only one of the 64 cases will be discussed. Suppose cerium (C and Z) is absent. ALLSS says that the boundary steady states with $C = Z = 0$ form an 18-dimensional manifold. Thus if cerium is missing, the system will probably be in a stable steady state at some point in this boundary manifold M_{bdy} . If a small ("infinitesimal") amount of cerium is now added, the system will probably evolve to a stable steady state in the interior ($X_i > 0, k_i > 0$). The interior manifold M is 19 dimensional and intersects the boundary $C=Z=0$ in a manifold having at most 17 dimensions. Little of the 18-dimensional manifold of steady states with $C=Z=0$ can be near this 17-dimensional manifold. Hence it is improbable that the original steady state in M_{bdy} lies near where M intersects $C=Z=0$. Therefore the addition of a small amount of cerium must usually cause the system to make a large jump between the initial stable steady state in M_{bdy} and a second distant stable steady state of M near $C = Z = 0$. For the general network, it frequently happens that the introduction of a very small amount of some species can cause a very large change in the steady state.

5. Geometry of the Interior Steady State Manifold M

From the explicit form of M some simple tests [8] can be made to determine some features of its geometry.

In order for multiple steady states to exist the characteristic equation must have a zero "relevant" eigenvalue. Multiple steady states are possible for model (1) only if the fifth coefficient of the characteristic equation α_5 can vanish for some h and j . This coefficient is a polynomial in h and j which was constructed by computer. It has no negative terms and thus is always positive. Hence no folding of M occurs. This means that each set of positive rate constants has at most one positive steady state.

A closely related question is whether some steady state with $X_i > 0$

exists for every set of positive rate constants. The network in Fig. 1 is an example where steady states only exist if $k_1=k_2$. This question may now be answered for the general network [8]. The test uses a complicated algorithm which is currently being programmed.

6. M and Thermodynamic Equilibrium

The 19-dimensional manifold of interior steady states M is in a one to one correspondence with a 19-dimensional convex polyhedral cone C. This correspondence is a diffeomorphism. The thermodynamic equilibrium states form a 15-dimensional submanifold M^O of M and these correspond to a 15-dimensional subcone C^O of C. These cones can be expressed

$$C = R_+^6 \times C_V \qquad C^O = R_+^6 \times C_V^O$$

where C_V and C_V^O have 13 and 9 dimensions, respectively. C_V^O is a subcone of C and corresponds to the equilibrium steady states.

The 9-dimensional equilibrium cone C_V^O is spanned by columns 4 to 12 of E as given. These are the 9 extreme currents which satisfy detailed balancing. A suitable slice through C_V yields a 12-dimensional polytope P_V and within it lies an 8-dimensional equilibrium simplex P_V^O whose vertices are these detailed balanced columns of E (suitably scaled). Figure 2 gives the idea. This cube represents a 3-dimensional P_V and its diagonal represents a 1-dimensional P_V^O . For model (1) P_V has 59 vertices and P_V^O has 9 vertices.

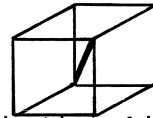


Fig. 2

One way to draw a polytope is to choose a projection which projects P_V^O into a point. Since P_V for model (1) has 4 more dimensions than P_V^O , this projection gives a 4-dimensional result. The same technique applied to Fig. 2 gives Fig. 3. All equilibrium steady states have been projected into the point in the centre. The rest of the hexagon consists entirely of nonequilibrium steady states.

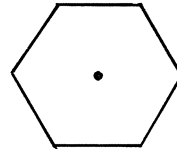


Fig. 3

7. A Global Lyapunov Function

The Gibbs free energy function for an ideal mixture is called a Lyapunov function when it has certain properties. Having these properties (for some steady state) implies the steady state is globally asymptotically stable. One can prove that if the Gibbs function is a Lyapunov function for a set of subnetworks corresponding to some columns of E, then all steady states in the cone spanned by these vectors are globally asymptotically stable and have the same Lyapunov function [8].

The reversible Oregonator is a good example. The polytopes P_V and P_V^O are similar to those in Fig. 3. There are 6 nonequilibrium extreme currents. Numerical studies show that the Gibbs function is a global Lyapunov function for four of these non-equilibrium extreme subnetworks. It follows that the shaded region in Fig. 4 consists of globally attracting steady states. The two remaining regions are unstable. One corresponds to (5) and the other to the reverse of this subnetwork.

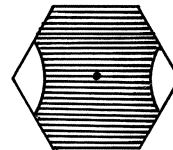


Fig. 4

The Gibbs function was shown to be a Lyapunov function for "zero deficiency networks" by HORN, FEINBERG and JACKSON (HFJ)[9]. "Zero deficiency" means the steady states are "complex balanced" and more generally HJF proved complex balanced steady states are globally

attracting. The only steady states of the Oregonator that are complex balanced are those in P_V , i.e. those which correspond to the dot in the centre of Fig. 4. Hence the set of networks that have the Gibbs function as a Lyapunov function is very much larger than the zero-deficiency networks. HJF's proof was analytical while my result is numerical. For model (1) the conservation condition ($C+Z=$ constant) makes the Gibbs function fail as a Lyapunov function; however, there is hope this weakness can be overcome.

8. Stability Analysis

The stability of any steady state depends only on the steady state concentrations and the weights (j) of the extreme subnetworks. The range of concentrations for which instability occurs is given by systems of inequalities which can be approximated quite well by other systems of inequalities which specify extreme polyhedral cones in the space of the logarithms of the parameters. For mathematical details see [1,10,11,12].

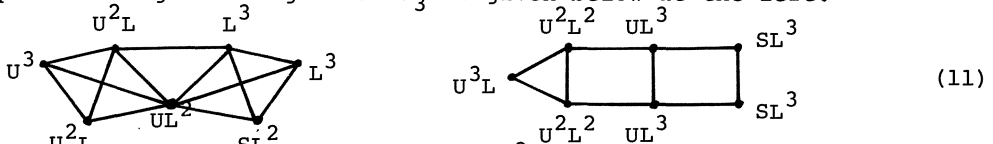
Stability analysis tells us how these cones of instability are connected to each other and associates each cone with various extreme subnetworks. Our results will be summarized using diagrams in which a dot represents a cone and a line between two dots means the cones touch each other facet to facet. Hence, connected regions of these diagrams correspond to connected regions in parameter space where the network is unstable due to particular functions being negative.

Since our purpose is to understand the interaction between extreme subnetworks (5), (6), and (7), only these have been included. Contributions from all other extreme subnetworks must be sufficiently small for this analysis to be valid. The contributions are marked thus: (5) = U = unstable Oregonator, (6) = S = stable Oregonator, (7) = L = modified Lotka-Volterra.

The network is unstable if any of the coefficients α_i of the characteristic equation are negative. Both α_1 and α_5 are always positive. The topology of the negative region of α_2 is

$$U^2 \bullet \qquad \bullet L^2 \qquad (10)$$

Thus it has two disconnected regions, one for the unstable Oregonator current (5) and the other for the unstable MLV current (7). The topology of the negative region of α_3 is given below at the left.



Thus the Oregonator unstable region (U^3) is simply connected to the MLV unstable region (L^3). The topology of the negative region of α_4 is given above at the right. This region is also simply connected. The two sets of cones above occupy roughly the same region of parameter space and the two cones (10) lie in the same region. Thus the whole region of instability is simply connected. The Oregonator limit cycle can thus be continuously changed into a MLV limit cycle by continuously changing the rate constants.

Each vertex in (10) and (11) is a system of 15 to 20 inequalities. The inequalities describing the negative region of α_2 , where the Oregonator is predominant, say that P, C, and Z must be large:

$$P > X \qquad Z > X \qquad PZ > XY \qquad C > 2Y \qquad C > 2X \qquad (12)$$

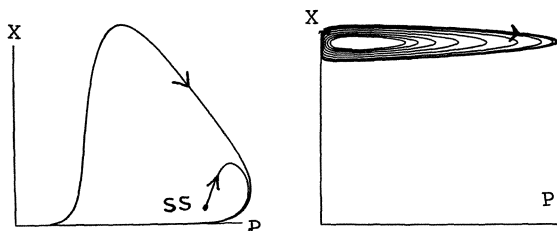
In addition, there are 15 inequalities giving lower bounds on j_1/j_2 and j_1/j_3 . The main region of α_2 instability of the MLV current is given by the cone L^2 in (10) which says C , W , and Z are large:

$$C > 4X \quad CW > 2PX \quad C > P \quad Z > 4X \quad ZW > 4PX \quad (13)$$

and in addition j_3/j_1 and j_3/j_2 have certain lower bounds.

9. Bifurcation Theory and Dynamics

Throughout the unstable region two eigenvalues have $\text{Re}(\lambda) > 0$. A Hopf bifurcation occurs on the boundary. The limit cycles which occur are shown at the left. The leftmost cycle is in the Oregonator region (12) while the rightmost cycle is in the MLV region (13).



10. Possibilities for Chaos

So far, efforts to find chaos by computer integration of realistic models of the BZ system have failed, although complicated limit cycles have been found in flow system models [13]. Extreme sensitivity to the flow rate in these models [14] suggests that the experimentally observed chaos could be due to flow rate fluctuations. In this paper we have examined a model which appeared more likely than the Oregonator to have chaos but chaos was not found. Perhaps extension to a flow system will give chaos.

11. Generality of the Method of Analysis

Starting with reactions typed as ' $X+Y=Z$ ' the computer constructs v , κ and E . It finds all steady states, if multiple steady states occur, and if some rate constants have no steady states. The computer finds the unstable region, optimal solutions to these inequalities, and integrates the dynamics in any cone of instability. The 20 second analysis given here can easily be repeated for any model of similar complexity.

References

1. B. L. Clarke: *Advances in Chem. Phys.* 43 (I Prigogine and S. A. Rice, Eds.) (Wiley, New York, 1980) pp. 1-215.
2. Z. Noszticzius: *J. Bodiss, J. Am. Chem. Soc.* 3177-3182 (1979)
3. Z. Noszticzius: *J. Am. Chem. Soc.* 3660-3663 (1979)
4. Z. Noszticzius: H. Farkas: preprint
5. R. J. Field: private communication
6. K. D. Willamowski, O. E. Rossler: in *Kinetics of Physicochemical Oscillators, Preprints of Submitted Papers, (Aachen 1979)* pp. 505-513
7. B. L. Clarke: *J. Chem. Phys.*, in press, Nov 1981
8. B. L. Clarke: in preparation
9. M. Feinberg, F. J. M. Horn: *Chem. Eng. Sci.* 29, 775-787 (1974)
10. B. L. Clarke: *J. Chem. Phys.* 64, 4165-4178 (1976)
11. B. L. Clarke: *J. Chem. Phys.* 64, 4179-4191 (1976)
12. B. L. Clarke: *SIAM J. Appl. Math.* 35, 755-786 (1978)
13. K. Showalter, R. M. Noyes, K Bar-Eli: *J. Chem. Phys.* 69, 2514-2564 (1978)
14. N. Ganapathisubramian, R. M. Noyes: preprint, 1981

Part X

Poster Abstracts

Stratification Phenomena in Corrosion Scales: Towards a Nonlinear Interpretation

G. Bertrand, J.-M. Chaix, K. Jarraya, J.-P. Larpin

Laboratoire de Réactivité des Solides, (LA. 23)
Université de Dijon, Faculté des Sciences Mirande
BP 138, 21004 Dijon Cédex, France

This study is part of a work we have undertaken on dissipative structures in solid-gas reactions in order to explain some self-organization phenomena in the solid as the result of a coupling between diffusional and chemical processes.

The stratification phenomenon. High temperature oxidation of several metals and alloys give rise to multilayered corrosion scales. The oxidation of titanium in oxygen and the sulfidation of a Fe-22Cr-5.5Al alloy in H_2S have been chosen for an experimental study.

Non-equilibrium : time evolution. The multilayered state is not a stable equilibrium state of the system : it disappears with time by recrystallisation, sintering, diffusion and/or phase transition processes, finally leading to an homogeneous TiO_2 layer (Fig. 2a, 2b) and a duplex sulfide scale (Fig. 1a, 1b).

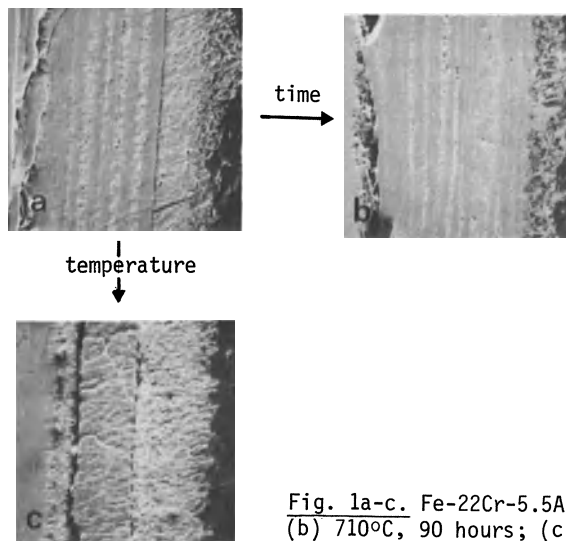


Fig. 1a-c. Fe-22Cr-5.5Al/ H_2S . (a) 710°C, 30 hours;
(b) 710°C, 90 hours; (c) 1000°C

Nonlinear phenomena : experimental critical values. Temperature : the sulfide scale is multilayered below 740°C ; in this range, the thickness of the layers increases with temperature. The sulfide scale is a duplex scale above 740°C (Fig. 1c).

Sample thickness : when the Ti sample is completely oxidized, a core in the middle of the sample always remains unstratified (Fig. 2b) ; below a critical value of the initial sample thickness, no stratification can be obtained (Fig. 2c).

Modelling approach. Corrosion scales self-organization phenomena are studied on models involving the growth of a scale on a solid substrate by the coupling of diffu-

sion processes through the scale and nonlinear interface chemical processes. A first simple model, used in an heuristic purpose, is able to find the existence of a critical scale thickness and a critical temperature for transition between multisteady states.

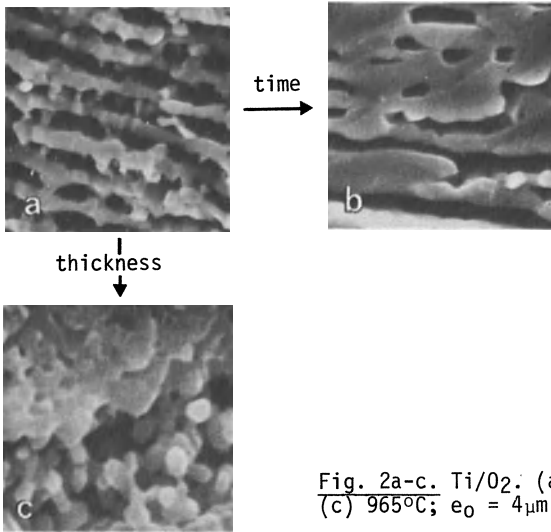


Fig. 2a-c. Ti/O₂: (a) 965°C, 27h, 250 μ m; (b) 965°C, 140h;
(c) 965°C; $e_0 = 4\mu$ m

Nucleation Process in the Two-Dimensional X^3 Schlögl Model

A. Blanché and P. Hanusse

Centre de Recherche Paul Pascal (C.N.R.S.), Domaine Universitaire
F-33405 Talence Cédex, France

We have performed Monte Carlo calculations of birth and death dynamics of the one and two-dimensional X^3 Schlögl model ($A + 2X \xrightarrow{\lambda} 3X$, $X \xrightarrow{\mu} B$) using a technique described elsewhere [1]. Following the study of the critical behavior near $\delta = \delta' = 0$ [2] we have explored the bistable region ($\delta, \delta' < 0$). First we have determined an "experimental" bistable domain using the following procedure. For a given point in the (δ, δ') parameter space we perform two separate simulations with an initial state corresponding to each stationary state predicted by the deterministic theory. We let the system evolve for a given fixed time t_f , large in comparison to any characteristic time in the system, typically 5×10^7 processes. We then record the nature of the final state and so determine three distinct regions in the plane: A, high-concentration state at t_f whatever initial state is considered; B, the initial state determines which state is reached at t_f (bistable region); C, low-concentration state at t_f whatever initial state is considered. A cusp-like diagram is obtained [3]. Border lines between A and B regions and between B and C regions are accurately determined. A change of parameter smaller than 0.01 is enough to switch from one regime to the other. The cusp so determined is narrower than that given by the deterministic theory, and narrower in one dimension than in two dimensions. This is consistent with the idea that the higher the dimensionality the stronger the mean field effect. These calculations were achieved with $A = 20$, $D = 20$ (see [2] for definitions). With these values no nucleation process was observed. The transition between two states occurs usually rapidly and looks rather like a spinodal decomposition. However, it was possible to observe a nucleation process for different parameter values ($A = 40$, $D = 3$, $\delta = -1$, $\delta' = -0.622$). Starting with $X = 0$ particles in the system, the lower state is reached in a few time units and is maintained for 75 units when a rapid transition occurs through the formation of a local nucleus of large concentration that grows and fill up the system. The upper state is then reached. Now a more careful examination reveals a very interesting pretransitional phenomenon, which is observable on mean and variance plots. Namely, an intermediate state is stabilized for about 10 time units, which means that the transition occurs in two stages through a metastable state. In some instances this intermediate state can be observed temporarily, well before the transition. It turns out that this intermediate state is just at the position of the unstable state predicted by the global deterministic theory! This state seems to be stabilized in some sense by local fluctuations. This very peculiar feature seems to be specific of this kind of nonequilibrium dynamical system. Nothing equivalent seems to exist in equilibrium transitions. It is reminiscent of observations reported some time ago on the effect of local fluctuations on a limit cycle bifurcation [4].

References

- ¹P. Hanusse and A. Blanché, J. Chem. Phys. 74, 6148-6153 (1981)
- ²P. Hanusse, in the present proceedings
- ³to be published and A. Blanché, thesis Bordeaux I, 1981
- ⁴P. Hanusse, J. Chem. Phys. 67, 1282 (1977)

From Bistability to Oscillations: A Phase Diagram Approach. Application to the Belousov-Zhabotinsky Reaction

J. Boissonade and P. De Kepper

Centre de Recherche Paul Pascal (C.N.R.S.), Domaine Universitaire
F-33405 Talence, France

During the last years, we have developed a simple theory which shows that many chemical oscillations can be described by the association of a bistable system and a feedback with suitable time scale ratios. The cross shaped topology of the phase diagram is very characteristic and furnishes a very convenient experimental tool to discuss the mechanism of a reaction [1] and a practical guide to create new oscillating systems [2]. The theoretical and experimental application to the BZ case, presented on the poster, is extensively expounded in Ref.1.

References

1. P. De Kepper, J. Boissonade, J. Chem. Phys., 75, 189 (1981)
2. P. De Kepper, this issue

Previous References on this approach

J. Boissonade : "*Non-linear dynamics and fluctuations in non equilibrium chemical systems*", Thesis, Bordeaux (1980)

J. Boissonade, P. De Kepper, J. Phys. Chem. 84, 501 (1980)

Numerical Simulations of Surface Reactions *

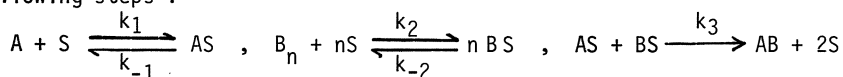
M. Bouillon, R. Dagonnier, P. Dufour and Martine Dumont**

Falultê des Science, Université de l'Etat
B-7000 Mons, Belgium

The nonlinear kinetics of isothermal surface reactions of the type



is investigated by means of Monte Carlo simulations. The simulation includes the following steps :



where S denotes an active site. When the surface distribution of the components is quasi uniform (i.e. when the clustering is weak) we may tentatively propose coverage functions for the various steps included in the reaction. The resulting kinetic equations should be profitably compared to the corresponding model equations.

First example : the CO oxidation on Pt at atmospheric pressure (i.e. $A = CO$, $B_2 = O_2$, case = 2). The average fractional coverages are noted $x = \theta_{CO}$, $y = \theta_O$. We assume $k_{-1} = 0$ and $k_1(2) \sim \exp[-\mu(x-y)]$ where x, y denote the local coverages. The simulated dimensionless ($\alpha_1 = k_1/k_3$, $\tau = k_3 t$) kinetic equations are represented by

$$\frac{dx}{d\tau} = \frac{\alpha_1}{2} e^{-\mu(x-y)}(1-x-y) - (xy)^{1/2} e^{-\mu(x-y)} \quad (2a)$$

$$\frac{dy}{d\tau} = \alpha_2 e^{\mu(x-y)}(1-x-y)^2/xy - (xy)^{1/2} e^{-\mu(x-y)} \quad (2b)$$

Notice that the reaction mechanism contribution is not simply proportional to xy .

Second example : the TSA model [1], i.e. the case $n = 1$ but with a reaction mechanism requiring two adjacent vacant sites. With TSA parameter values the simulated kinetic equations are ($x = \theta_A$, $y = \theta_B$) :

$$\frac{dx}{d\tau} = 4\alpha_1 xy(1-x-y) - \frac{\alpha_1}{2} x^2 y^2 - 4xy^2(1-x-y)^2 \quad (3a)$$

$$\frac{dy}{d\tau} = \frac{\alpha_2}{2} (1-x-y) - \alpha_2 x^2 y^2 - 4xy^2(1-x-y)^2 \quad (3b)$$

which should be compared to those proposed by TSA [1].

These two examples show that Monte Carlo simulations of surface reactions can provide coverage functions rather different than those involved in usual model with, as a result, possible changes in the stability features of these systems.

1 C.G. Takoudis, L.D. Schmidt and R. Aris, Surface Sci. 105, 325 (1981)

* Work partly supported by the IRIS Program sponsored by the Belgian Ministry for Science Policy.

**Chargé de Recherches au F.N.R.S. de Belgique.

On the Preoscillatory Period of the Belousov-Zhabotinsky Reaction: A Search for Intermediates

Maria Burger and Krisztina Rácz

Institute of Inorganic and Analytical Chemistry
L. Eötvös University
Budapest, Hungary

In the Belousov-Zhabotinsky systems, where the catalytic oxidative bromination of malonic acid [MA] takes place with bromate, oscillations start only after a pre-oscillatory period. Intermediates formed during this part of the reaction initiate the transition from the non-oscillatory to the oscillatory state of the system.

Our previous results concerning the investigation of the preoscillatory period have shown that the bromomalonic acid [BrMA] concentration grows during this time and reaches a crucial concentration value $[BrMA]_{cru}$ at the onset of the oscillation. Having determined the $[BrMA]_{cru}$ values in the MA-bromate-manganese-nitric acid [5M] system, in order to clarify whether BrMA alone was responsible for the start of the oscillation or other organic intermediates played also an important role, the effect of the BrMA addition on the preoscillatory period was studied.

The addition of BrMA to the reaction mixture shortens the preoscillatory period, but oscillation does not start when [BrMA] added is equal to $[BrMA]_{cru}$. Generally, the value of the [BrMA] added has to exceed the crucial value to get prompt oscillation. However, the preoscillatory period always disappears when the reaction mixture contains about 0.001 M glyoxylic acid [GOA] or oxalic acid [OA] beside the crucial BrMA concentration. It should be noted that at this low concentration neither GOA alone nor OA alone show an oscillating character with bromate and manganese.

The literature data do not rule out the formation of GOA and OA during the pre-oscillatory period. OA reacts with manganese [III] very quickly, probably it can not accumulate in detectable concentration. The rate of the GOA-manganese [III] reaction is slower than that of OA, therefore GOA can be present in the reacting system.

By devising an analytical method, GOA was determined during the preoscillatory period of the MA-bromate-manganese-nitric acid [5M] system in the order of 0.0001M concentration range. Its concentration showed a maximum during the preoscillatory period, a typical behaviour of intermediates.

Our results show that during the preoscillatory period, another reaction besides the BrMA accumulation takes place too: BrMA reduces the catalyst. In this reaction intermediates are formed which react with manganese [III] faster than BrMA, and these compounds are important in the initiation of the oscillation. If we add BrMA to the reacting system, then a certain time has to elapse to produce these intermediates. Probably this is the reason why oscillation does not start adding the $[BrMA]_{cru}$ to the reaction mixture.

Non-Equilibrium Phase Transition of the Intercalation Process

T. Butz and A. Hübler

Physik-Department, Technische Universität München,
D-8046 Garching, Fed. Rep. of Germany

and

A. Lerf

Zentralinstitut für Tieftemperaturforschung der Bayerischen Akademie der Wissenschaften,
D-8046 Garching, Fed. Rep. of Germany

We have observed a non-equilibrium phase transition during the process of electrochemical lithium intercalation into 2H-TaS_2 , the prism surface current density being the control parameter. Information on the lithium distribution was obtained via the observation of the Ta nuclear quadrupole interaction by means of time differential perturbed angular correlations. The electric field gradient at the Ta nucleus was found to depend very sensitively on the lithium concentration [1].

For a surface current density $j \leq 50 \mu\text{A}/\text{cm}^2$ the intercalation proceeds as follows. In pristine 2H-TaS_2 a threshold lithium concentration of $x=0.22$ is required to force the phase boundary empty/intercalated lattice to propagate towards the crystal center (ashtray thickness profile). When this phase boundary reached the center, the average $x \approx 0.33$, and further intercalation proceeds via a continuous and homogenous filling up of empty lattice sites (single phase).

For a surface current density $j \geq 175 \mu\text{A}/\text{cm}^2$ the intercalation proceeds in a different way: superimposed onto the low concentrated phase ($x=0.22$ to 0.33) new phases with limiting concentrations $x=0.67$ and $x=1$ build up (coexistence of up to three phases). The $x=0.33$ and $x=0.67$ phases disappear as the average x approaches unity. This behaviour is quite analogous to the chemical intercalation via *n*-butyllithium, where the initial surface current density is calculated to be $j=200 \mu\text{A}/\text{cm}^2$ [1]. We thus estimate the critical surface current density to be $j_{\text{critical}}=100 \mu\text{A}/\text{cm}^2$.

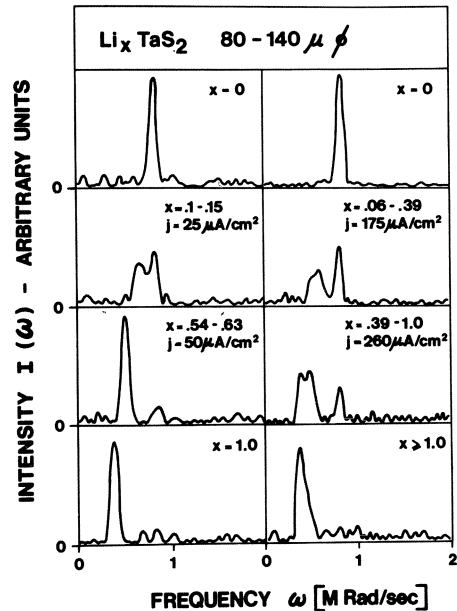


Fig.1. Nuclear quadrupole frequencies observed during lithiation of 2H-TaS_2 . (Left) Low surface current density yields two phases until $x=0.33$, then single phase. (Right) High current density yields up to three coexisting phases

Reference: 1. R. Mühlberger, T. Butz, A.Lerf: Physica 105B, 218 (1981)

Pseudo-Steady States in Solid-Liquid Systems

M. Cournil, P. Galtier, and F. Conrad

Ecole Nationale Supérieure des Mines, 158, Cours Fauriel
F-42023 Saint-Etienne, France

The behaviour of a closed system consisting of a solid phase with uniform granulometry and its aqueous solution is described by three equations :

- a condition expressing thermodynamical equilibrium
- a stability - or self-evolution - condition for the system
- the mass balance .

Where as for an open system every equilibrium state is unstable, we show that our closed system may meet two equilibrium states during its evolution : an unstable one corresponding to VOLLMER's critical nucleus and a stable one.

The hydration mechanism of a solid-like plaster involves a dissolution step (for the anhydrous) and a nucleation-growth step (for the hydrate). Experiment establishes that as soon as water comes into contact with plaster, the concentration of the solution first increases rapidly to some value which is kept constant for a certain time, then decreases to reach the equilibrium value of the hydrate.

It is possible to describe quantitatively the kinetics of the different stages ; nucleation is genuinely nonlinear, dissolution and growth of the grains are autocatalytic. The evolution of the system has been predicted by computer ; we notice that the supersaturated state is a pseudo-stationary one. It seems that the end of this state is not only determined by the exhaustion of the plaster.

It will be important, for applications, to get a good understanding of the status of the pseudo-stationary states. In particular they govern the setting of some solids like plasters and cements.

$A + 2B = 3B$ Kinetics Producing all of Flip or None Stimulus Response in a Cell Model, and Strategies for a Chemical Implementation of such Kinetics

Peter Decker and Oemer Saygin

Chemical Institute, Veterinary School
D-3000 Hannover, Fed. Rep. of Germany

Autocatalysis second order in products, $A+2B=3B$ (ASOP), the nonlinear reaction in the classical Brusselator model, may cause nontrivial behaviour in open systems: oscillations, morphogenesis (1) or the production of optically active compounds (2).

A cell model with ASOP, a first order shunt $A \rightarrow B$ and diffusion of A and B through a cell membrane (mathematically equivalent to a stirred reactor with inflow and overflow of A and B) can exhibit up to three steady states. Among the phase topologies of such systems we found a remarkable model of an excitable cell exhibiting a novel "all or flip or none" stimulus response. Depending on stimulus size we have three response qualities: i. spiking; ii. switching into another state; and iii. no response.

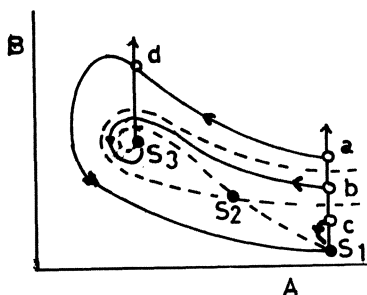
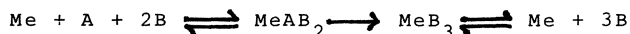


Fig.1 Phase portrait of a cell model with bimodal stimulus response to a sudden input of the product B: input a causes spiking around state S_3 , b produces switching into S_3 , c produces no reaction. d returns the system from state S_3 back to S_1 (3)

Since in real nonlinear systems chemical analysis represents a bottleneck, there is a need for a chemical implementation of the so far unknown class of simple ASOP reactions. Weak octahedral complexes where $MeXB_2$ or $MeAB_2$ catalyzes the formation of B from A should afford Michaelis-Menten-like approximate ASOP kinetics, a challenging goal for researchers in the vast field of metal ion catalysis (4)



- 1) Decker, P., (1979), Ann. New York Acad. Sci. 316, 236.
- 2) Decker, P., (1979), In: D.C.Walker Ed., Origins of Optical Activity in Nature, pp. 109-124, Elsevier, Amsterdam.
- 3) Decker, P. and Saygin, Oe., (1979), Z.Naturforsch. 34c, 649.
- 4) Decker, P., (1975), Origins of Life 6, 211.

Topological Order in 2D Chemical Systems

G. Dewel*, D. Walgraef*, and P. Borckmans*

Faculté des Sciences de Université Libre de Bruxelles
Campus Plaine, C.P. 231
B-1050 Bruxelles

Depending on the values of the external constraints, the "Brusselator" nonlinear chemical prototype [1] exhibits either a transition to chemical oscillations (HOPF bifurcation) or to spatial patterns (TURING bifurcation). These instabilities are characterized by the spontaneous breakdown of a continuous symmetry, respectively that of phase or translation and rotation. Near those instabilities the behaviour of the system is dominated by its slow mode dynamics that leads to a TDGL description which is used to analyze the fluctuations in analogy with equilibrium phase transitions [2].

In both cases, for large 2d systems (thin layers), the strong phase fluctuations preclude the existence of long range order. The systems therefore exhibit power law decay (quasi-long-range order) of the correlations of the order parameter and are characterized by the presence of pairs of topological (phase) excitations, the unbinding of which mediate the instabilities leading to short-range order [3].

Above the HOPF bifurcation, the system therefore desynchronises spontaneously creating excitations such as target patterns or pair of Archimedian spirals. The characteristics of these spatio-temporal structures and their statistics are found to be different and present strong analogies with the observations [4].

The spatial patterns arising at Turing's instability also spontaneously develop topological defects [5] (dislocations, disclinations,...) of which the dynamics may be invoked to explain not only the Turing bifurcation but also the fusion of these structures at higher amplitudes first by formation of grain boundaries and crystallites and thereafter the melting of the crystallites themselves in analogy with certain instabilities in liquid crystals [6].

References :

1. G. Nicolis, I. Prigogine : Self-Organization in Nonequilibrium Systems (Wiley, New York, 1977).
2. D. Walgraef, G. Dewel and P. Borckmans : Adv. in Chem. Phys. to appear 1981.
3. J.K. Kosterlitz, D. Thouless, J. Phys. C.6, 1181 (1973).
4. A.T. Winfree : Science 175, 634 (1972).
M.L. Smoes : Dynamics of Synergetic Systems, ed. by H. Haken (Springer, Berlin, Heidelberg, New York, 1980), page 80.
5. G. Dewel, D. Walgraef and P. Borckmans : J. Physique-Lett. 42, L-361 (1981).
6. E. Guazzelli, E. Guyon : C.R. Hebd. Sean. Acad. Sci. 292 II, 141 (1981).

* Chercheur Qualifié F.N.R.S.

Bifurcation of Multiple Limit Cycles in Plane Quadratic Mass-Action Systems

C. Escher

Institut für Theoretische Physik, Technische Hochschule Aachen
D-5100 Aachen, Fed. Rep. of Germany

1. Models Under Consideration

We consider homogeneous open two-variable mass-action systems with quadratic rate equations:

$$\dot{x} = a_1x^2 + a_2xy + a_3y^2 + a_4x + a_5y + a_6, \quad \dot{y} = b_1x^2 + b_2xy + b_3y^2 + b_4x + b_5y + b_6.$$

If these equations are to account for elementary processes between particle or species - as is the case in chemistry, biochemistry, ecology and semiconductors - it is necessary that

$$\bar{a}_3, \bar{a}_5, \bar{a}_6, \bar{b}_1, \bar{b}_4, \bar{b}_6 \geq 0.$$

2. Questions to be Answered

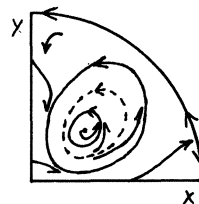
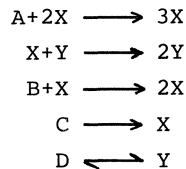
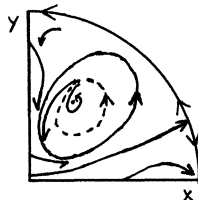
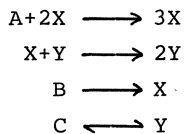
We raise the question if these simple nonlinear rate equations can account for such a complex behaviour as bistability of two limit cycles or of a limit cycle and a stationary point.

3. Method to Tackle the Problem¹

By the aid of nonlinear stability theory we show that it is indeed possible that up to three limit cycles appear from multiple foci in the considered models.

4. Results

We affirmatively answer the questions raised above and give some examples of chemical reaction systems with the desired properties. Two of them lead to reaction schemes and phase portraits (Poincaré plots of the positive quadrant) shown below (Q [•]): stable [unstable] limit cycle).



¹ A detailed paper will appear in Chem. Phys.

Belousov-Zhabotinsky System: Mechanism of the Ce^{3+} /Bromate Reaction

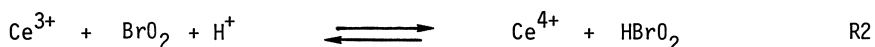
H.D. Försterling, H.J. Lamberz, and H. Schreiber

Fachbereich Physikalische Chemie, Universität Marburg
D-3550 Marburg, Fed. Rep. of Germany

The overall reaction



was analysed by studying the set of elementary reactions



Proof of formation of BrO_2 :

Reaction R3: a solution of NaBrO_2 in NaOH was injected into a solution of NaBrO_3 in sulfuric acid. The formation of an intermediate was monitored spectroscopically using the dual wavelength technique. The absorption spectrum of the intermediate was found to be identical with the BrO_2 spectrum. The same results were obtained for the reaction of Ce^{4+} with HBrO_2 (R2) and for the reaction of Ce^{3+} with HBrO_3 (R1, formation of BrO_2 in steps R2-R4).

Proof of the stoichiometry of the reactions:

By decreasing the initial concentration of NaBrO_2 in R2, R3 and Ce^{3+} in R1 from 10^{-3} M to 10^{-7} M, the yield of the reaction products (Ce^{3+} in R2, BrO_2 in R3 and R1) was increased drastically and reached nearly the value predicted by stoichiometry. In these experiments it is clearly to be seen that the competitive reaction R5 is playing a serious role at high HBrO_2 concentrations.

Computer simulation of the overall reaction:

On the basis of the results obtained in the case of the elementary reactions, new values of the rate constants for (R2) - (R6) were obtained. Computer simulations on the basis of these new rate constants are in good agreement with experimental results for the overall reaction R1.

References:

H.D.Försterling, H.Schreiber, W.Zittlau, Z.Naturforsch. 33a, 1552 (1978)

H.D.Försterling, H.J.Lamberz, H.Schreiber, Z.Naturforsch. 35a, 329 (1979);
35a, 1354 (1980)

H.D.Försterling, H.J.Lamberz, H.Schreiber, W.Zittlau, Acta Chimica Acad.Sc. Hungaricae, in press.

The Legitimacy of the Quasi-Steady State Approximation in Enzyme Kinetics: A Singular Perturbation Approach

G. Fritzsich and M.S. Seshadri

Max-Planck-Institut für Biophysik, Kennedy-Allee 70
D-6000 Frankfurt 70, Fed. Rep. of Germany

Although the quasi-steady state hypothesis is frequently employed in enzyme kinetics, its legitimacy and domain of validity have not been properly defined. We address ourselves to this question in the context of one substrate - one enzyme sequential reactions.

It is pointed out that the existence of a well-defined quasi-steady state implies a small parameter (some function of the initial concentrations and rate constants). The method of singular perturbation takes cognisance of the existence of two time scales in the evolution of the system. The transients are contained in the short-time description. The system runs to the quasi-steady state after the transients die out. This treatment imposes weaker restrictions than those used in MICHAELIS-MENTEN kinetics.

Incidentally, it turns out that in sequential reactions in a closed system (with neither autocatalysis nor feed-back regulation), damped oscillations may occur about the quasi-steady state for a certain range of the parameters.

References

1. Van Dyke, M. (1975). Perturbation Methods in Fluid Mechanics. Stanford: Parabolic Press.
2. Seshadri, M.S. & Fritzsich, G. (1981). J. theor. Biol., in press.

Nonlinear Phenomena in Stirred Flow Systems of Mn²⁺ and Acidic Bromate

W. Geiseler

Institute of Technical Chemistry, Technical University
D-1000 Berlin 12, Fed. Rep. of Germany

The oxidation of Mn²⁺ ions by acidic bromate in the presence of bromide inhibitor was studied experimentally in isothermal flow systems (single and coupled CSTRs). The reaction is closely related to the oscillatory BELOUSOV-ZHABOTINSKII reaction [1] and exhibits peculiar nonlinear phenomena which were investigated in some detail. The set of experimental conditions used generally was: [KBrO₃]₀ = 0.002 M, [KBr]₀ = 0.00001 M, [MnSO₄]₀ = 0.00015 M, [H₂SO₄]₀ = 1.5 M, k₀ = 0.004 s⁻¹, T = 32.0°C.

In a single CSTR two different locally stable steady states (SSI and SSII) could be attained for identical flow conditions (bistability). The concentrations of intermediate species differed considerably in each steady state. After a perturbation introduced to the CSTR in SSII by temporarily increasing the inflow concentration of the inhibitor, the system either returned to its previous steady state (SSII) or moved to the other one (SSI) depending on how long the perturbation persisted. The critical period of perturbation was measured for various enhanced inhibitor inflows. The data described a hyperbola-like curve which was found to be fitted reasonably well by a relationship analogous to BLAIR's law [2]. If any constraint (inflow concentration, residence time) was varied slowly within certain ranges while the others remained constant, the steady state once established followed a hysteresis curve. Such curves were observed for each input reactant and residence time. The hysteresis loop limits which define the region of bistability for a certain set of constraints were measured systematically. As a result we obtained some two-dimensional domains of bistability, which are quite similar to those of the cerous flow system [3]. Oscillations, although predicted recently [4], were not detected under the tested flow conditions.

Inspired by the papers of SMALE [5] and TYSON [6] we coupled two identical CSTRs in series configuration in order to generate oscillations. However, instead of oscillations the system exhibited quite different behavior, namely switching phenomena and hysteresis effects. The different steady states which could be established in the CSTRs were subjected to increasing coupling (mixing the reactor contents by means of a pump) and to varying the inhibitor inflow concentration, respectively. The system either switched to two similar steady states (increasing the coupling) or followed two separate hysteresis loops, the limits of which collapsed for sufficiently large couplings (increasing the inhibitor inflow concentration).

The observations and data reported here are quite similar to those of cerous flow systems [3,7], although some slight deviations were noticed. In spite of these minor deviations the data of the Mn²⁺ systems appear to be fitted reasonably well by the same model [3,7,8]. The results add considerably to our confidence in the NFT mechanism [9] checked here with Mn²⁺ as the weak one-electron reducing agent.

References

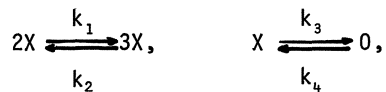
1. P.B. Belousov, Sb. Ref. Radiats. Med., 1958, 145 (1959); A.M. Zhabotinskii, Dokl. Akad. Nauk SSSR, 157, 392 (1964); R.J. Field, E. Körös, and R.M. Noyes, J. Am. Chem. Soc., 94, 8649 (1972)
2. H.A. Blair, J. gen. Physiology, 15, 709 (1932)
3. W. Geiseler and K. Bar-Eli, J. Phys. Chem., 85, 908 (1981)
4. K. Bar-Eli, this conference
5. S. Smale, in: Lectures in Mathematics in Life Sciences, Vol. 6, p. 17 (1974)
6. J.J. Tyson, Ann. New York Acad. Sci., 316, 279 (1979)
7. K. Bar-Eli and W. Geiseler, J. Phys. Chem., in press
8. K. Bar-Eli and R.M. Noyes, J. Phys. Chem., 81, 1988 (1977); *ibid.*, 82, 1352 (1978)
9. R.M. Noyes, R.J. Field, and R.C. Thompson, J. Am. Chem. Soc., 93, 7315 (1971)

On Phase Transitions in Schlögl's Second Model

P. Grassberger

Physics Department, University of Wuppertal,
D-5600 Wuppertal, Fed. Rep. of Germany

We study Schlögl's second model, characterized by chemical reactions



in d -dimensional space. The reactions are assumed to be local ; local fluctuations are fully taken into account, and particle transport occurs via diffusion.

In contrast to previous investigations, we find no phase transition when $k_4 \neq 0$ and $d < 4$. For $k_4 = 0$, $k_3 \neq 0$, and $1 \leq d < 4$, we find a second-order phase transition which is in the same universality class as the transition in Schlögl's first model. Only for $d \geq 4$ we do find the first-order transition found also by previous authors.

These claims are supported by extensive Monte Carlo calculations for various realizations of this process on discrete space-time lattices.

A Nonlinear Phenomenon of Chemical Dynamics in Geology: The Case of Skarns

Bernard Guy

Département Géologie, Ecole des Mines
F-42023 St. Etienne, Cedex, France

In our poster, we wish to draw the attention of the chemists to certain transformations met in geology. They are observed in the rocks called skarns: these are the result of the transformation of various rocks, particularly limestones, by the operation of aqueous fluids in strong disequilibrium with them. These waters percolate through the mass of the rock that they progressively transform. They may originate from a granitic mass under crystallization and/or they may be waters moved by convection at the vicinity of a hot granitic intrusion. These phenomena occur at depths of 4-5 km or more, at temperatures of the magnitude 400-600°C and pressures of the magnitude 1-2 kb. The transformations may affect several m³ of rocks. Such rocks may be observed today (their formation having ended several millions years ago) thanks to orogenic movements and erosion.

One of the conspicuous features of skarns is the frequent existence of zones of ABCD and so on which seem to indicate that the starting material was transformed by steps. Each zone is defined by a group of minerals (at centimetric or metric scale) and is separated from the adjacent zones (before and after) by sharp limits. More rarely, recurrent zonations constituted by "strata" ABAB and so on may be observed, also in the same context.

We do not propose to achieve an analysis of these phenomena. Let us simply mention that several features of these transformations should be of interest to a conference such as the present one:

- the chemical reactions are in competition with transport phenomena (convection and also diffusion).
- these may produce components in competition with one another, and this starting from the affrontement of other components of composition maintained constant at the boundaries: the input fluid on one hand, the starting rock on the other.
- the modeling, already classical among the geologists, proposed by the russian author Korzhinskii, makes a nonlinearity appear: it is responsible for the "shocks" or fronts which may be seen in these phenomena. The nonlinearity lies in the exchange term between the fluid and the solid.

It is not certain that this appraisal, which is based on the hypothesis of a chemical equilibrium between the solid and the fluid, may explain all the observed cases, and notably the recurrent alternations that one would be tempted to reappraise to the chemical dissipative structures.

The Prepattern Theory of Mitosis: Spatial Dissipative Structures in the 3-Dimensional Sphere

Axel Hunding

Institute for Chemistry, University of Copenhagen
Raadmandsgade 71, DK-2200 Copenhagen N

Spontaneous pattern formation in biology may arise through bifurcations in nonlinear biochemical reaction-diffusion systems. Numerical simulations have been carried out for the 3-dimensional sphere, and primary and secondary bifurcations are studied. The algorithm is 470 times faster than non-stiff methods, exploiting the sparseness and stiff structure of the equations. Series of patterns are obtained, and their change-over studied numerically and by analytical bifurcation theory to reveal the proper selection rules. The theoretical pattern series corresponds to previously experimentally recorded chromosome distributions in spindle-free nuclear division in certain protozoans. This is evidence that Turing structures do play a governing role in biology. The proof is based on experimentally observed chromosome distributions of more than 1000 chromosomes, being confined to a 3-dimensional form resembling a highly buckled circular plate not explainable by conventional spindle forces. The structure is identified as the null region of the pattern $j_1Y_{10} + j_2Y_{22}$ which shows up numerically. This pattern experimentally breaks up into two parallel 'horseshoes' with their openings in the same direction, and the same happens numerically. Among the stable patterns arising is the bipolar 'mitosis' prepattern j_2Y_{20} , also observed experimentally. Asymmetrically placed live chromosomes in trivalents (i.e. with 2 microtubules toward one pole, and 1 to the other) are shown to be in force balance, if the 'mitosis' prepattern governs the spindle forces. Subsequently, a 'cytokinesis' prepattern $j_2Y_{20} + j_0$ appears. The numerically recorded spatial dissipative structures should be an ideal series of prepatterns for the process of mitosis. It is suggested that the evolutionary origin of the governing principles in mitosis was such prepatterns, later to be supplemented by centriolar structures.

References

1. G.D. Billing & A. Hunding, Bifurcation analysis of nonlinear reaction-diffusion systems: Dissipative structures in a sphere, *J.Chem.Phys.* 69 (1978) 3603.
2. A. Hunding & G.D. Billing, Secondary bifurcations in spherical reaction-diffusion systems, *Chem.Phys.* 45 (1980) 359.
3. A. Hunding, Dissipative structures in reaction-diffusion systems: Numerical determination of bifurcations in the sphere, *J.Chem.Phys.* 72 (1980) 5241.
4. A. Hunding, Possible prepatterns governing mitosis: The mechanism of spindle-free chromosome movement in *Aulacantha Scolymantha*, *J.Theor.Biol.* 89 (1981) 353.
5. A. Hunding & G.D. Billing, Spontaneous pattern formation in spherical nonlinear reaction-diffusion systems: Selection rules favor the bipolar 'mitosis' pattern, *J.Chem.Phys.* 75 (1981) 486.

Mechanistic Study of the Briggs-Rauscher Reaction

Patrick De Kepper and Irving R. Epstein

Department of Chemistry, Brandeis University
Waltham, MA 02254, USA

The Briggs-Rauscher reaction involving iodate, hydrogen peroxide, malonic acid and Mn(II) in acid solution exhibits bistability and oscillation in a CSTR as well as batch oscillation. We have developed a mechanism for this reaction which reproduces these and other dynamic features. Astonishingly, our model is qualitatively identical to, though quantitatively different from, that derived independently by NOYES and FURROW [1].

In Fig. 1, we show that the model is in excellent qualitative agreement with the observed "cross-shaped phase diagram" [2] in which bistability and oscillations appear as the flows of IO_3^- and I_2 into the reactor are varied. The observed steady state iodine concentration undergoes hysteresis with "inverse regulation" as a function of I_2 flow, jumping from a high to a low iodine state as $[\text{I}_2]_0$ is increased [2]. The model predicts this surprising behavior as well as the batch oscillations and the experimentally observed increase in the period of oscillation when parameters corresponding to methylmalonic acid are employed. These results suggest that the scheme does indeed account for the kinetic skeleton of the reaction.

This work was supported by NSF Grant CHE 7905911.

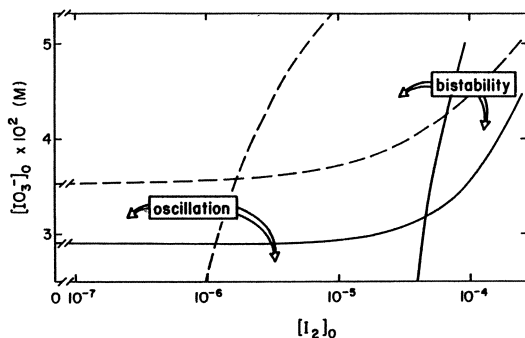


Fig. 1. Experimental (—) and calculated (---) "cross-shaped phase diagram" in the $[\text{IO}_3^-]_0$ - $[\text{I}_2]_0$ constraint space. $[\text{H}_2\text{O}_2]_0 = 3.3 \text{ M}$, $[\text{MA}]_0 = 0.0015 \text{ M}$, $[\text{H}^+]_0 = 0.056 \text{ M}$, $[\text{Mn}^{+2}] = 0.004 \text{ M}$, residence time 156 s.

References

1. R. M. Noyes and S. D. Furrow, J. Am. Chem. Soc., to be published.
2. P. De Kepper and A. Pacault, C. R. Acad. Sc. 286C, 437-441 (1978).

Multiwavelength Analysis of Linear and Nonlinear Kinetics in the CSTR

H. Lachmann

Institut für Physikalische Chemie der Universität Würzburg, Marcusstraße 9-11
D-8700 Würzburg, Fed. Rep. of Germany

By measuring the reaction spectra (i.e. the time-dependent spectra $A(\lambda)_{t_1, t_2, \dots, t_m}$ of a reaction mixture) and/or the absorbance-time curves $A(\lambda)_{\lambda_1, \lambda_2, \dots, \lambda_n}$ at several selected wavelengths, it is possible to get more specific information about a chemical reaction system than by analyzing a single progress curve. First of all the number of linear independent reaction steps is determined by graphical matrix rank analysis (A-, AD-, ADQ-diagrams) [1-4].

Subsequently, a number of new evaluation methods are used for kinetic analysis. In contrast to other methods, absorbance-time curves at different wavelengths are combined for evaluation. Initial concentrations, A_{∞} -values, molar absorptivities, etc. do not need to be known [2-6]. Therefore the whole reaction system can be analyzed with high precision and significance.

All these methods, which have been developed originally for closed reaction systems, may be extended to open systems, too. They may be applied to different spectroscopic techniques, if there exists an equation corresponding to Beer-Lambert's law (for example in VIS-UV absorption and fluorescence; CD, ORD, IR spectrometry). The advantages of these new methods are demonstrated by some bio-organic reaction systems in the continuous stirred tank reactor (CSTR) and by the autocatalytic conversion of trypsinogen to trypsin, which is a first realistic example of "critical slowing down" in the CSTR [7].

The application of multiwavelength analysis to chemical oscillations is discussed.

References

1. H.Mauser, Z. Naturforsch. 23b (1968) 1021, 1025
2. H.Lachmann, H.Mauser, F.Schneider, H.Wenck, Z. Naturforsch. 26b (1971) 629
3. H.Mauser, Formale Kinetik, Bertelsmann Universitätsverlag, Düsseldorf (1974)
4. G.Lachmann, H.Lachmann, Fresenius Z. Anal. Chem. 290 (1978) 118
5. G.Lachmann, H.Lachmann, H.Mauser, Z. Phys. Chem. NF 110 (1978) 237
6. G.Lachmann, H.Lachmann, H.Mauser, Z. Phys. Chem. NF 120 (1980) 9,19
7. H.Lachmann, H.Schraut, M.Heinrichs, F.W.Schneider, Kolloquium der Deutschen Gesellschaft für Biophysik, Hünfeld (1981)

Inhomogeneous Fluctuations and Bifurcations in Nonlinear Chemical Systems

H. Lemarchand

Laboratoire de Chimie Générale, Université Pierre et Marie Curie
75 230 Paris Cedex 05, France and

G. Nicolis

Faculté des Science de l'Université Libre de Bruxelles
C.P. 226 1050 Bruxelles, Belgique

Nonlinear systems far from equilibrium undergo a variety of bifurcations leading to multiple steady states, limit cycles, space structures, or propagating waves. The understanding of these transition phenomena necessitates the explicit consideration of thermodynamic fluctuations. At present, fluctuations are studied primarily at the stochastic level and the approaches used are the *Master Equation* and the *Langevin Equation*. The latter is motivated by the analogies between nonequilibrium bifurcations and equilibrium critical phenomena. As we do not wish to take such analogies for granted, but rather deduce them from the analysis, we here adopt the Master Equation approach.

For a reaction-diffusion system this equation has the form [1,2]:

$$\frac{d}{dt} P(\{X_i\}; t) = \sum_{\mathbf{x}} L_{ch}(\mathbf{x}) P + \sum_{\mathbf{x}, \mathbf{z}} L_d(\mathbf{x}, \mathbf{z}) P. \quad (1)$$

The chemical operator L_{ch} and the diffusion operator L_d are both extensive, i.e. proportional to the volume V of each cell within our macroscopic system. Most of the methods of solution of (1) are based on this property. We may mention VAN KAMPEN's expansion [3], the cumulant method [4], the KUBO-MATSUO-KITAHARA method [5], and the singular perturbation method of NICOLIS, MALEK-MANSOUR and TURNER [2,6].

In the present communication we extend the KUBO-MATSUO-KITAHARA method to systems involving inhomogeneous fluctuations. We set

$$P \sim \exp(VU) \quad (2)$$

and develop U around an extremum. By solving the equations for the expansion coefficients we find an explicit representation of the stationary probability distribution in the following situations [8]:

(i) One variable systems near a cusp bifurcation. For a cubic nonlinearity we recover previous results displaying the exponential of the LANDAU-GINZBURG functional [2,7].

(ii) Multivariable systems near a bifurcation leading to steady state spatial dissipative structures. We show that, in general, the "stochastic potential" U has cubic terms in the deviation from the extremum.

Some comments on the structure of P in the region of multiple solutions [9] are finally presented.

References

- 1 G. Nicolis, I. Prigogine, *Self-Organization in Nonequilibrium Systems* (Wiley, New York 1977)
- 2 M. Malek-Mansour, C. Van den Broek, G. Nicolis, J.W. Turner, *Annals of Physics*, **131**, 283 (1981)
- 3 N.G. Van Kampen, *Advan. Chem. Phys.* **34**, 245 (1976)
- 4 H. Lemarchand, G. Nicolis, *Physica* **82A**, 251 (1976)
- 5 R. Kubo, K. Matsuo, K. Kitahara, *J. Stat. Phys.* **9**, 51 (1973)
- 6 G. Nicolis, J.W. Turner, *Physica* **89A**, 326 (1977)
- 7 G. Dewel, P. Borckmans, D. Walgraef, *Z. Physik* **B28** 235 (1977)
- 8 H. Lemarchand, *Bull. Acad. Roy. Belg.* to be published
- 9 H. Lemarchand, *Physica* **107A**, 518 (1980)

Temperature-Compensated Epigenetic Oscillations: Timing of Cell Division Cycles and Circadian Rhythms?

David Lloyd and Steven W. Edwards

Department of Microbiology, University College
Newport Road, Cardiff, Wales, UK

An extensive literature describes biological oscillations with periods of the order of minutes (metabolic oscillations) or of about a day (circadian oscillations). The former have no well-established function and may simply represent an inevitable consequence of feedback control in an open system. The latter are of paramount importance in all eukaryotes for accurate timekeeping. It is widely believed that long period circadian oscillations must be derived from a high frequency rhythm; no metabolic oscillation that has been tested fulfils the criterion of temperature-compensated frequency. We have observed another class of oscillators in *Acanthamoeba castellanii*, and in several other protozoa. These have a period of about 1 h, and are thus in the epigenetic time domain. Respiration and adenine nucleotide pools show these oscillations, but the fundamental oscillator appears to be in a transcriptional or translational feedback loop. Thus total cellular protein and RNA contents oscillate and these systems slave the system of mitochondrial energy supply. The coupled oscillators are revealed in synchronous cultures established by a method which causes no measurable perturbation. Lowering the temperature from 30° to 20° increases the cell cycle time from 8 to 16 h, but does not influence the period of the rhythm. It is suggested that these epigenetic oscillations may serve the dual role of cell cycle and circadian timekeeping (Fig. 1).

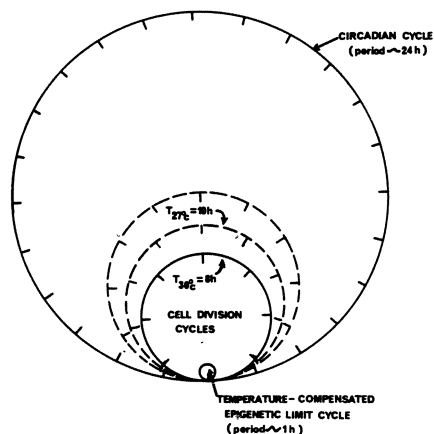


Fig. 1. Epigenetic-cell division cycle-circadian interaction in *A. castellanii*: a hypothetical scheme. An epigenetic oscillator with a period of approximately 1 h is temperature compensated. Frequency reduction by an unknown mechanism generates quantized cell division cycle times which may have values between 8 h (under optimal growth conditions) and the circadian value.

Chaotic Behavior of E.H.D. Instability for an Insulating Liquid Subjected to Unipolar Injection

B. Malraison and P. Atten

C.N.R.S. Laboratoire d'Electrostatique - 166 X
F-38042 Grenoble, Cédex

A plane layer of an insulating liquid is subjected to strong injection of ions from one of the electrodes. The bulk Coulomb force due to the space charge plays a destabilizing role balanced by viscosity; thus an electrohydrodynamical instability appears above a critical voltage. Despite the analogy with the Rayleigh-Bernard problem, this instability exhibits particular features, such as the nature of the transport mechanism (ion migration and not diffusion), the existence of two instability criteria (linear and not linear, associated with an hysteresis loop, and the three-dimensional pattern of hexagonal convective cells (1).

Transition to chaotic régime of motion in this system has been investigated through the study of the fluctuations of the total current induced by the time-dependent convection. The onset of unsteady convection coincides with the instability threshold. There are different routes leading to chaos which depend mainly on the aspect ratio Γ (i.e., successively periodic, biperiodic and chaotic for small Γ , always chaotic for large Γ); in all cases a fundamental oscillation mechanism can be recognized with a frequency f_1 varying with U as the mean quadratic velocity of the liquid (2).

We examine the characteristics of power law spectra of current fluctuations in the chaotic régime. We can distinguish two régimes of motion, one dominated by viscous effect ($U < U_T$), the other by inertial effect ($U > U_T$). In the viscous domain the spectra beyond the oscillation peak exhibit an exponential decay $\exp(-f/f_c)$ with a characteristic frequency $f_c \approx 0.6 f_1$ (3).

In the inertial régime this exponential decay is observed only in a frequency interval of relative width decreasing as U is increased. In the high frequency part of the spectra a power law is obtained with an exponent in the range 6 to 8. As suggested by a recent theory (4) the exponential decay may be related to intermittency phenomena which has been observed in the viscous régime.

References

1. P. Atten, J.C. Lacroix: *J. Mécan.* 18, 469 (1979)
2. P. Atten, J.C. Lacroix, B. Malraison: *Phys. Lett.* 79A, 255 (1980)
3. B. Malraison, P. Atten: *C.R. Acad. Sci. (Paris)* 292, 267 (1981)
4. U. Frisch, R. Morf: *Phys. Rev. A* 23, 2673 (1981)

Effect of Light Intensity Fluctuations on a Real Photochemical Reaction: The Thermoluminescence of Fluorescein in Boric Acid Glass

J.C. Micheau, W. Horsthemke and R. Lefever
Chimie Physique II - Campus Plaine C.P. 231
Université Libre de Bruxelles
B-1050 Bruxelles

The thermoluminescence of fluorescein in boric acid glass is a photochemical biphotonic reaction. Its nonlinear behaviour against incident light intensity has allowed us to approach an experimental investigation of light intensity fluctuations using a well-known real system. For this purpose an optical noise generator delivering a quasi-gaussian real noise was put into shape.

The steady state values of thermoluminescence are sensitive to light intensity fluctuations :

1 - even if the overall light dose was kept strickly constant and,
2 - even in the limit where the noise is rapid as compared with the relaxation time of the system ($\tau_{cor} \ll \tau_{macro}$), fluctuations are able to deeply modify the yield of the photochemical process. Particularly, the saturation into the energy-rich species (i.e. photoionized dye) is reached for lower mean light intensities.

This phenomenon corresponds to a significant bias between deterministic and fluctuating steady state values as illustrated in Figure 1.

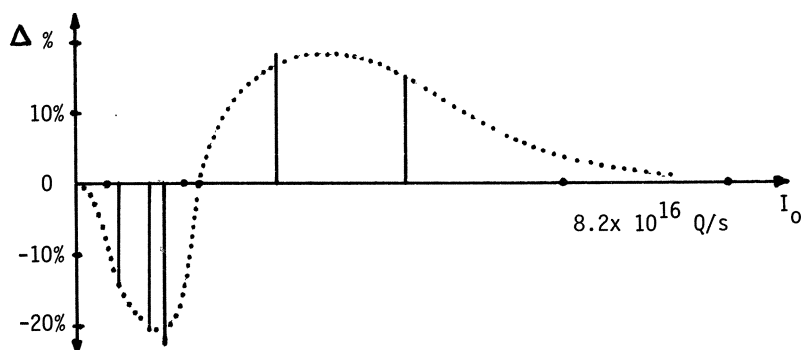


Fig. 1 - Experimental relative bias between deterministic (full line) and fluctuating (dotted line) steady state values of thermoluminescence as a function of mean light intensity

The nature of such bias is fully consistent with our previous theoretical predictions.

Bifurcation Theoretic Approach for Strong Field Photodissociation Phenomenon

N.K. Rahman

Istituto di Chimica Quantistica ED Energetica Molecolare Del C.N.R.
Via Risorgimento 35, I-56100 Pisa and

Service de Physique des Atomes et des Surfaces, CEN/SACLAY
F-91191 Gif-sur-Yvette, Cedex

Photodissociation problems of molecules are usually limited to the linear regime of the coupling constant which arises from the coupling of the electromagnetic field to the transition dipole moment of the molecule between the relevant electronic states. When the electromagnetic field is strong (high powered lasers), it is possible to encounter the situation where the exponential depopulation of the discrete state is replaced by a generalized Rabi-like oscillation. Another way of looking at this physical situation is to regard this as a "return from the continuum." We shall see, in what follows, that the process lies in the realm of bifurcation theory.

Consider a discrete state $|i\rangle$ coupled to the continuum $|\alpha, E\rangle$, where α is the set of quantum numbers needed to describe the continuum and E is the energy. Let the total Hamiltonian be $H = H_0 + \lambda V$ and the coupling matrix element $v(\alpha, E) = \langle i|V|\alpha, E\rangle$. Then, the amplitude of the evolution of the state $|i\rangle$ is given by

$$U_i(t) = \lim_{\epsilon \rightarrow 0} \int dE e^{iEt} [G_i(E + i\epsilon) - G_i(E - i\epsilon)]$$

with

$$G_i(E) = \frac{1}{E - E_i - \lambda^2 \int \frac{|v(\alpha, E')|^2 d\alpha dE'}{E - E'}}$$

The function

$$F(E) = \lim_{\epsilon \rightarrow 0} [G_i(E + i\epsilon) - G_i(E - i\epsilon)]$$

is real, and since the Fourier transform of this function determines the time evolution, it behooves one to examine this function. Under quite relaxed conditions on $v(\alpha, E)$, the maxima of $F(E)$ show qualitative changes of behaviour with increase of λ . It is seen that normally, (a) for weak λ , $F(E)$ has a single maximum; (b) for critical $\lambda = \lambda_C$, a maximum appears at negative energy; (c) for above this critical value and beyond certain particular value λ_0 , three extrema arise, two of which are maxima, while one is a minimum [1,2].

It is quite easy to see that for a large class of functions $|v(\alpha, E)|^2$, this qualitative change of behaviour is best described by the bifurcation theory. This allows one a deeper analysis of the dissociation phenomena than the usual one, and at the same time, permits the description with a small number of parameters (instead of the knowledge of in general complex valued function over a semiinfinite domain of energy, which is usually not available).

Recent developments on imperfect bifurcations appear to offer further assistance in this regard [3].

References

1. A. Lami, N.K. Rahman: *Il Nuovo Cimento* 63, 253 (1981); *Chem. Phys. Lett.* 79, 63 (1981)
2. C. Cohen-Tannoudji: *Cours du Collège de France*, 1975-1976 (unpublished)
3. M. Golubitsky, D. Schaffer: *Comm. Pure and Appl. Math.* 31, 21 (1979)

A Linear Method to Analyze a Nonlinear Oscillator: Driving the Glycolytic Oscillator by Sinusoidal Temperature Cycles

K. Rinast, R. Heringer, R. Joerres, T. Kreuels, W. Martin, K. Brinkmann
Botanisches Institut der Universität Bonn, Kirschallee 1,
D-5300 Bonn, Fed. Rep. of Germany

The well-known glycolytic oscillator has been investigated with respect to temperature responses. The examination of the NADH oscillations driven by sinusoidal temperature cycles should give new aspects for a more general system description and improve existing models.

Fluorescence signals and temperature were recorded on tape punch from 40-ml yeast suspensions kept under temperature program by means of Peltier elements. Amplitude and phase of the signals were calculated using the program system TIMESDIA (W. MARTIN, 1977) which includes spectral analysis, calculation of average signals and complex demodulation. The fluorescence signals must be corrected by the temperature dependence of the NADH fluorescence, which can be done by means of a multiplicative model.

Typical runs are partitioned into three sections sequential in time: A) Anaerobic glycolysis without substrate, B) Oscillating glycolysis induced by adding excess of substrate and C) Stationary non-oscillating glycolysis. The behaviour of the system in these three sections is examined under driving temperature cycles.

The temperature responses differ drastically in part B and C. Part B responded with an unstable amplitude and phase, indicating a complex interaction of the temperature cycle with the temperature-dependent eigenfrequency of the system. In Part C synchronous oscillations of the fluorescence are seen with stable amplitudes and phases, which both depend on the frequency of the driving temperature cycle. Some preliminary data are presented towards a BODE diagram.

Releasing the system from the driving temperature cycle in part B causes the oscillation to switch back to its eigenfrequency and normal damping behaviour. After releasing in part C however, the oscillation will stop immediately suggesting different internal states of the glycolysis in part B and C.

Reference

W. Martin, U. Kipry, K. Brinkmann: TIMESDIA - ein interaktives System zur Analyse periodischer Zeitreihen. EDV in Medizin und Biologie 8, 90-96 (1977)

Bursting Phenomena in the Belousov-Zhabotinsky Reaction

John Rinzel
National Institutes of Health, Bethesda, MD 20205, USA

and

William C. Troy
University of Pittsburgh, Pittsburgh, PA 15260, USA

We [1] have investigated a model for the Belousov-Zhabotinskii reaction in a continuous flow, stirred tank reactor. The model consists of a system of three ordinary differential equations derived from a more complicated five-variable, Oregonator [2] model proposed by JANZ, VANECEK, and FIELD [3]. Over an appropriate range of physical parameters (e.g., lower flow rates) the system exhibits *bursts* of oscillations. As in some experiments (e.g., MAREK and SVOBODOVA [4]), the observer sees several spikes followed by an interval of quiescence (IQ) which is subsequently followed by a resumption of the spikes, etc. The bursting phenomenon results from a hysteresis loop in which the solution alternates between a stable periodic solution, during the oscillatory phase, and a stable steady state of low oxidation, during the IQ, of a two-variable batch-reactor sub-system. This bistable behavior is due to a subcritical Hopf bifurcation (hard-oscillation) in the two variable system. We have estimated analytically the IQ duration and its dependence on parameter values. For other parameter ranges we find qualitatively different bursting phenomena. In one example the CSTR system is excitable; there is a stable steady state and the response to an adequate perturbation is an excitation burst of several pulses and then a return to the steady state. At considerably higher flow rates, there are repetitive, single-spike bursts with IQ's of high oxidation; such patterns resemble those calculated by SCHOWALTER, NOYES, and BAR-ELI [5] and observed experimentally by SCHMITZ, GRAZIANI, and HUDSON [6].

References

1. J. Rinzel, W.C. Troy: J. Chem. Phys. (to appear 1981)
2. R.J. Field, E. Koros, R.M. Noyes: J. Am. Chem. Soc. *94*, 8649 (1972)
3. D. Janz, D. Vanecek, R.J. Field: J. Chem. Phys. *73*, 3132 (1980)
4. M. Marek, E. Svobodova: Biophys. Chem. *3*, 263 (1975)
5. K. Schowalter, R. Noyes, K. Bar-Eli: J. Chem. Phys. *69*, 2514 (1978)
6. R.A. Schmitz, K.R. Graziani, J.L. Hudson: J. Chem. Phys. *67*, 3040 (1977)

Experimental Investigations and Model Simulations for Studying the Influence of Noise and External Disturbances on the Behavior of the Belousov-Zhabotinsky Reaction

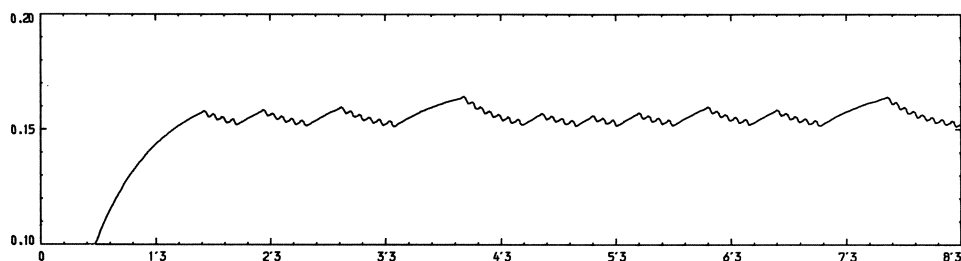
P. Graae Sørensen

Department of Chemistry, H.C. Ørsted Institute
University of Copenhagen, Universitetsparken 5
DK-2100 Copenhagen

Abstract

The homogeneity of concentration variations for the Belousov-Zhabotinskii (BZ) reaction in a CSTR has been investigated by simultaneous measurements of light absorption at two different positions in the cell. By varying the distance between the examined volumes and the propeller, information about the spatial coherence properties of the reaction can be obtained.

The results are compared with numeric integrations of an Oregonator based model for the BZ reaction. The model use 5 variables and show burst oscillations which agree with the experimental bifurcation pattern, when the total flow rate is used as bifurcation parameter. To simulate the behavior of stirred systems the model has been integrated with random perturbations of the rate constants. Results from perturbation free behavior is compared with the behavior at two different perturbation levels. Fig(1) show the variations in the concentration of bromo-malonic acid during burst oscillations in a typical run with initial concentration zero.



Fig(1) Variations in the concentration of bromo-malonic acid.
Time unit 1 sec.

Linearization Procedure and Nonlinear Systems of Differential and Difference Equations

W.-H. Steeb

Universität Paderborn, Theoretische Physik
D-7490 Paderborn, Fed. Rep. of Germany

Carleman [1] showed that an autonomous finite dimensional nonlinear system of differential equations $\dot{x}=f(x)$ can be embedded into an infinite linear system of differential equations, where the f_i are polynomial in x . Recently, several authors [2-7] have taken up this idea and solved nonlinear differential equations within this approach. Steeb and Wilhelm [4] have written the original system with the help of the Kronecker product \otimes as: $\dot{x}=Ax+B(x\otimes x)+\dots+Z(x\otimes x\otimes\dots\otimes x)$, where A, B, \dots, Z are matrices with constant coefficients. They calculated the time evolution of $x\otimes x$, $x\otimes x\otimes x$ and so on and obtained an infinite system with simple block structure, whereas the infinite system obtained from Carleman linearization has no simple block structure and must be rearranged before this can be obtained. The infinite system can easily be expressed with the help of Bose operators. The infinite system and the finite system are not equivalent, because the infinite system admits solutions which are not solutions of the finite system. However, if we restrict ourselves to analytical solutions, then the two approaches are equivalent. When we solve the infinite system by Laplace transformation or an exponential ansatz, we are forced to consider carefully the problem of convergence. When we cut off the infinite system at some finite dimension, we do not, in general, find a good approximation, in particular for large times. However, when the original system admits only asymptotically stable stationary solutions, such an approximation can be carried out. Recently, Steeb [7] applied the approach to nonlinear difference equations. The solution of the logistic equation $x(t+1)=ax(t)(1-x(t))$ ($t=1,2,\dots$) for $a=4$ can be determined. The ansatz $x_n(t):=(x(t))^n$ leads to the linear infinite system

$$x_n(t+1) = a^n \sum_{r=0}^n (-1)^r \binom{n}{r} x_{n+r}(t) \quad .$$

The solution $x_1(t)=x(t)$ is given by $x(t)=1/2-1/2\cos(2^t \arccos(1-2x_0))$ (white noise behaviour).

References:

1. T. Carleman, Acta Math. 59 (1932) 63.
2. R. Bellman and J.M. Richardson, Quart. Appl. Math. 20 (1963) 333.
3. E. Montroll and R. Helleman, AIP Conf. Proc. 27 (1976) 75.
4. W.-H. Steeb and F. Wilhelm, J. Math. Anal. Appl. 77 (1980) 601.
5. R. Andrade and A. Rauh, Phys. Lett. 82A (1981) 276.
6. L. Brenig and V. Fairen, J. Math. Phys. 22 (1981) 643.
7. W.-H. Steeb, Talk presented at the "Dynamic Days Twente" (Enschede, 1981).

Reversible and Non-Reversible Modifications of Enzyme Systems Activity by Electric Fields

J.M. Valleton, E. Selegny, and J.C. Vincent

Laboratory of Macromolecular Chemistry
ERA 471, CNRS, F-76130 Mont-Saint-Aignan

In the past, multiple steady states have been theoretically pointed out in enzyme diffusion-reaction systems [1][2]. In particular, the existence of two stable steady states leads to hysteresis phenomena, experimentally observed with urease and uricase [3], for example. The introduction of imposed electric fields in these multiple steady states systems was first applied theoretically and experimentally to kinetics with inhibition by an excess of an ionic substrate [4].

An analytical treatment, supported by a convenient graphical interpretation was carried out by defining a unidimensional compartmented model (the chemical reaction is limited to a central cell separated from two reservoirs by electrically and chemically inert films). Assuming the presence of a high concentration of electrolyte, the electric field E , perpendicular to the films, was considered constant. Calculations led to the fundamental equation:

$$\lambda^{\circ} = 2(s_{\circ} - s^{\circ}) / \psi .$$

λ is the substrate dependence of the enzyme activity (here λ is the only parameter of the activity) and ψ is the dimensionless transport-reaction parameter:

$$\psi = \sigma / (e / 1 + |z\zeta| / 2) ,$$

where σ is the diffusion-reaction parameter [5] modulated by the electrical parameter ζ [6] which is proportional to the electric field. Superscript $^{\circ}$ corresponds to steady state values and subscript $_{\circ}$ to boundary values of a variable.

Five typical solutions $\lambda^{\circ}(E)$ of the fundamental equation exist: three correspond to continuous variations of enzyme activity: activation, deactivation and activation followed by deactivation, and two correspond to discontinuous phenomena: hysteresis and electrically non-reversible modifications of activity. The activity surface $\lambda^{\circ}(s_{\circ}, E)$ is a typical "frence" catastrophe surface. The projection of this surface on the (s_{\circ}, E) plane corresponds to a cusp, which can also be obtained by a linear analysis of stability. A similar (analytical and graphical) treatment can be applied to reactions inducing pH changes, by the use of a symbolic species: $(H^+) - (OH^-) D_{\text{oh}} / D_{\text{h}}$.

The case of electrically non-reversible modifications of activity, experimentally observed with uricase, can be considered as a binary memorization of information (the electric field itself). This memory is protected from any new electrical action but it is, however, possible to erase it by chemical potential variations on the boundaries. We can also point out that an electrically non-reversible modification of activity is possible with a bienzyme system, leading, with adequate assumptions, to an active transport induction from a global zero activity system.

REFERENCES

- 1 A. KATCHALSKY and A. OPLATKA (1966), *Neurosciences Res. Symp.*, 1, 352.
- 2 D. THOMAS, (1976) in "Analysis and control of immobilized enzyme systems."
- 3 A. NAPARSTEK, J.L. ROMETTE, J.P. KERNEVEZ and D. THOMAS (1974) *Nature* 249, 490.
- 4 J.M. VALLETON, E. SELEGNY and J.C. VINCENT, submitted.
- 5 E. SELEGNY (1974) in "Polyelectrolytes", E. SELEGNY, M. MANDEL and U.P. STRAUSS Ed. Reidel, Dordrecht, Holland, p419.
- 6 J.M. VALLETON (1980) Thesis of Docteur-ingénieur, Rouen, France.

A Dynamic Regime with Structured Fourier Spectrum

C. Vidal and A. Rossi

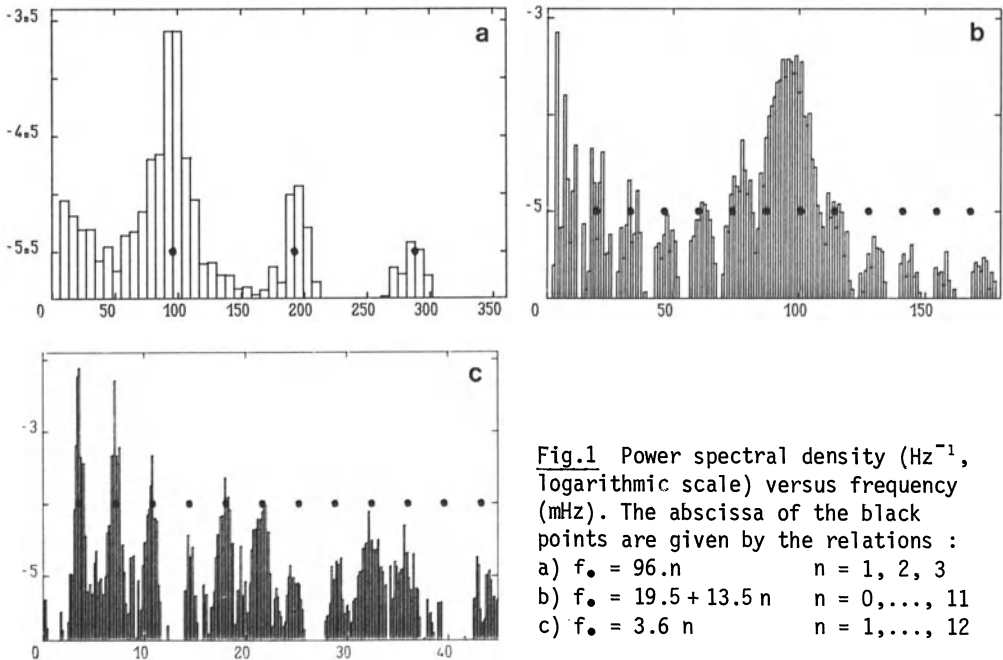
Centre de Recherches Paul Pascal
F-33405 Talence

The Belousov-Zhabotinsky reaction carried out in a CSTR is well known to display different kinds of dynamic regimes (for a review, see in this volume the paper titled "*Chemical kinetics as an experimental field for studying the onset of turbulence*", by C. VIDAL). With the following set of experimental conditions :

$$\begin{aligned} \left[\text{CH}_2(\text{COOH})_2 \right]_0 &= 0.33 \text{ mole l}^{-1} & \left[\text{Ce}_2(\text{SO}_4)_3 \right]_0 &= 0.00025 \text{ mole l}^{-1} \\ \left[\text{Na BrO}_3 \right]_0 &= 0.036 \text{ mole l}^{-1} & \left[\text{H}_2 \text{SO}_4 \right]_0 &= 1.5 \text{ mole l}^{-1} \end{aligned} \quad T = 40^\circ\text{C}$$

we have observed three dynamic regimes, depending on the flow rate at which the CSTR is fed with reagents. Two of them are periodic, but the third one exhibits a Fourier spectrum whose shape is very peculiar. Three sets of well-ordered peaks appear in this spectrum, depending on the frequency resolution of the plot PSD versus frequency, as shown in Fig.1. Although a parallel may be drawn with some theoretical predictions made in the field of solid state physics [1], the interpretation of our observation remains an open problem.

1. S. Aubry, private communication



Index of Contributors

- Atten, P. 269
Baras, F. 104
Bar-Eli, K. 228
Bertrand, G. 248
Blanché, A. 250
Boissonade, J. 134,251
Boiteux, A. 172
Borckmans, P. 257
Bouillon, M. 252
Brinkmann, K. 272
Burger, M. 253
Butz, T. 254
Carmona, F. 5
Chaix, J.-M. 248
Chance, E.M. 172
Chopin-Dumas, J. 213
Clarke, B.L. 240
Conrad, F. 255
Cournil, M. 255
Crowley, M.F. 147
Curtis, A.R. 172
Dagonnier, R. 252
Dateo, C.E. 188
Decker, P. 256
De Kepper, P. 188,192,
251,265
Dewel, C. 257
Dufour, P. 252
Dulos, E. 140
Dumont, M. 252
Dupeyrat, M. 166
Edwards, S.W. 268
Epstein, I.R. 188,197
265
Escher, C. 258
Feigenbaum, M.J. 95
Field, R.J. 147
Försterling, H.D. 259
Fritzsche, G. 260
Galtier, P. 255
Geiseler, W. 261
Glandsdorff, P. 2
Grassberger, P. 262
Gray, P. 20
Griffiths, J.F. 20
Guy, B. 263
Haken, H. 15
Hanna, A. 160
Hanusse, P. 115,250
Hasko, S.M. 20
Heringer, R. 272
Hess, B. 172
Horsthemke, W. 120,270
Hudson, J.L. 44
Hübner, A. 254
Hunding, A. 264
Iooss, G. 71
Jarraya, K. 248
Joerres, R. 272
Körös, E. 207
Kreuels, T. 272
Kustin, K. 188
Lachmann, H. 266
Lamba, P. 44
Lamberz, H.J. 259
Larpin, J.-P. 248
Lefever, R. 120,270
Lemarchand, H. 267
Lerf, A. 254
Lloyd, D. 268
Lobry, C. 67
Lozi, R. 67
Malek Mansour, M. 104
Malraison, B. 269
Mankin, J. 44
Martin, W. 272
McCullough, J. 44
Micheau, J.C. 270
Mori, H. 88
Nakache, E. 166
Nicolis, G. 104,267
Noyes, R.M. 201
Orbán, M. 188,197
Pacault, A. 5
Piaud, J.J. 5
Pomeau, Y. 63
Procaccia, I. 128
Putirskaya, G. 207
Rącz, K. 253
Rahman, N.K. 271
Richetti, P. 213
Rinast, K.A. 272
Rinzel, J. 273
Rössler, O.E. 79
Ross, J. 180
Rossi, A. 277
Roux, J.C. 38
Ruelle, D. 30

Saul, A. 160	Sørensen, P.G. 274	Varga, M. 207
Saygin, O. 256	Steeb, W.-H. 275	Vidal, C. 49,277
Schreiber, H. 259	Swinney, H.L. 38	Vincent, J.C. 276
Selegny, E. 276	Troy, W.C. 273	Walgraef, D. 257
Seshadri, M.S. 260	Tyson, J.J. 222	Winfree, A.T. 156
Shówalter, K. 160	Valleton, J.M. 276	Wunderlin, A. 15

Hydrodynamic Instabilities and the Transition to Turbulence

Editors: H. L. Swinney, J. P. Gollub
With contributions by numerous experts

1981. 81 figures. XII, 292 pages
(Topics in Applied Physics, Volume 45)
ISBN 3-540-10390-2

Contents: *H. L. Swinney, J. P. Gollub:* Introduction. – *O. E. Lanford:* Strange Attractors and Turbulence. – *D. D. Joseph:* Hydrodynamic Stability and Bifurcation. – *J. A. Yorke, E. D. Yorke:* Chaotic Behavior and Fluid Dynamics. – *F. H. Busse:* Transition to Turbulence in Rayleigh-Bénard Convection. – *R. C. DiPrima, H. L. Swinney:* Instabilities and Transition in Flow Between Concentric Rotating Cylinders. – *S. A. Maslowe:* Shear Flow Instabilities and Transition. – *D. J. Tritton, P. A. Davies:* Instabilities in Geophysical Fluid Dynamics. – *J. M. Guckenheimer:* Instabilities and Chaos in Nonhydrodynamic Systems.

Modelling of Chemical Reaction Systems

Proceedings of an International Workshop,
Heidelberg, Federal Republic of Germany,
September 1–5, 1980
Editors: K. H. Ebert, P. Deuflhard, W. Jäger

1981. 163 figures. X, 389 pages
(Springer Series in Chemical Physics, Volume 18)
ISBN 3-540-10983-8

The purpose of the workshop from which the proceedings resulted was to bring together engineers, mathematicians and chemists on the problems of chemical reactions. Numerical-mathematical and analytical-mathematical methods for chemical reaction systems are discussed, and are given for these methods in science and engineering. New methods for the description of the dynamical behaviour of chemical reaction systems are given. The problems of large and very stiff differential equations, which result from chemical systems, are treated. The proceedings give a survey of the most modern methods for treating chemical reaction systems, the problems which are now being studied by scientists all over the world and the future aspects of this field of research.

J. Schnakenberg

Thermodynamic Network Analysis of Biological Systems

Universitext

2nd corrected and updated edition 1981.
14 figures. X, 149 pages
ISBN 3-540-10612-X

Contents: Introduction. – Models. – Thermodynamics. – Networks. – Networks for Transport Across Membranes. – Feedback Networks. – Stability. – References. – Subject Index.

Turbulent Reacting Flows

Editors: P. A. Libby, F. A. Williams
With contributions by numerous experts

1980. 38 figures, 3 tables. XI, 243 pages
(Topics in Applied Physics, Volume 44)
ISBN 3-540-10192-6

Contents: *P. A. Libby, F. A. Williams:* Fundamental Aspects. – *A. M. Mellor, C. R. Ferguson:* Practical Problems in Turbulent Reacting Flows. – *R. W. Bilger:* Turbulent Flows with Nonpremixed Reactants. – *K. N. C. Bray:* Turbulent Flows with Premixed Reactants. – *E. E. O'Brien:* The Probability Density Function (pdf) Approach to Reacting Turbulent Flows. – *P. A. Libby, F. A. Williams:* Perspective and Research Topics.

Springer-Verlag
Berlin
Heidelberg
New York



G. Eilenberger

Solitons

Mathematical Methods for Physicists

1981. 31 figures. VIII, 192 pages
(Springer Series in Solid-State Sciences,
Volume 19)
ISBN 3-540-10223-X

Contents: Introduction. - The Korteweg-de Vries Equation (KdV-Equation). - The Inverse Scattering Transformation (IST) as Illustrated with the KdV. - Inverse Scattering Theory for Other Evolution Equations. - The Classical Sine-Gordon Equation (SGE). - Statistical Mechanics of the Sine-Gordon System. - Difference Equations: The Toda Lattice. - Appendix: Mathematical Details. - References. - Subject Index.

Relaxation of Elementary Excitations

Proceedings of the Taniguchi International Symposium, Susono-shi, Japan, October 12-16, 1979

Editors: R. Kubo, E. Hanamura

1980. 117 figures, 15 tables. XII, 285 pages
(Springer Series in Solid-State Sciences,
Volume 18)
ISBN 3-540-10129-2

Contents: Lattice Relaxation. - Intermediate State Interaction. - Nonlinear Optical Phenomena. - Molecular Crystal and Biological System. - Molecular System. - Index of Contributors.

Solitons

Editors: R. K. Bullough, P. J. Caudrey
With contributions by numerous experts

1980. 20 figures. XVIII, 389 pages
(Topics in Current Physics, Volume 17)
ISBN 3-540-09962-X

Contents: *R. K. Bullough, P. J. Caudrey:* The Soliton and Its History. - *G. L. Lamb, Jr., D. W. McLaughlin:* Aspects of Soliton Physics. - *R. K. Bullough, P. J. Caudrey, H. M. Gibbs:* The Double Sine-Gordon Equations: A Physically Applicable System of Equations. - *M. Toda:* On a Nonlinear Lattice (The Toda Lattice). - *R. Hirota:* Direct Methods in Soliton Theory. - *A. C. Newell:* The Inverse Scattering Transform. -

V. E. Zakharov: The Inverse Scattering Method. - *M. Wadati:* Generalized Matrix Form of the Inverse Scattering Method. - *F. Calogero, A. Degasperis:* Nonlinear Evolution Equations Solvable by the Inverse Spectral Transform Associated with the Matrix Schrödinger Equation. - *S. P. Novikov:* A Method of Solving the Periodic Problem for the KdV Equation and Its Generalizations. - *L. D. Faddeev:* A Hamiltonian Interpretation of the Inverse Scattering Method. - *A. H. Luther:* Quantum Solitons in Statistical Physics. - Further Remarks on John Scott Russel and on the Early History of His Solitary Wave. - Note Added in Proof. - Additional References with Titles. - Subject Index.

Solitons and Condensed Matter Physics

Proceedings of the Symposium on Nonlinear (Soliton) Structure and Dynamics in Condensed Matter, Oxford, England, June 27-29, 1978

Editors: A. R. Bishop, T. Schneider

Revised 2nd printing. 1981. 120 figures.
XI, 342 pages
(Springer Series in Solid-State Sciences,
Volume 8)
ISBN 3-540-09138-6

Contents: Introduction. - Mathematical Aspects. - Statistical Mechanics and Solid-State Physics. - Summary. - Index of Contributors. - Subject Index.

Springer-Verlag
Berlin
Heidelberg
New York

